

41 0628842 4



426318

PHD/2005 NG

ProQuest Number: 10183125

All rights reserved

INFORMATION TO ALL USERS

The quality of this reproduction is dependent upon the quality of the copy submitted.

In the unlikely event that the author did not send a complete manuscript and there are missing pages, these will be noted. Also, if material had to be removed, a note will indicate the deletion.



ProQuest 10183125

Published by ProQuest LLC (2017). Copyright of the Dissertation is held by the Author.

All rights reserved.

This work is protected against unauthorized copying under Title 17, United States Code  
Microform Edition © ProQuest LLC.

ProQuest LLC.  
789 East Eisenhower Parkway  
P.O. Box 1346  
Ann Arbor, MI 48106 – 1346

**Application of Conventional Machining  
Techniques for Green Ceramic Compacts**

**Produced by  
Powder Reaction Moulding**

**Siak Hong NG**

**B.Eng. M.Phil.**

*A thesis submitted in partial fulfilment of the requirements of the  
Nottingham Trent University for the degree of Doctor of Philosophy.*

2005

---

To my Dad, Mum, brothers, sisters and my girlfriend  
for their love, support and encouragement.

No words can express my deepest gratitude to them.

谨以此文，献给我的父母，  
以及爱护，关心我的人们。

---

This thesis has been supplied on condition that anyone who consults it is understood to recognise that its copyright rests with the author and that no information derived from it may be published without the author's prior written consent.

## **Abstract**

The study of the green machining of a new ceramic material is important for the future development and application of that material, since this is a common manufacturing process in many industries. Following a previous research project at Nottingham Trent University that led to the development of a novel alumina/cyanoacrylate material produced by Powder Reaction Injection Moulding Engineering (PRIME), this research programme has been designed to investigate the application of conventional machining techniques for the green ceramic compacts.

In order to produce a high quality machinable novel green compact, experimental investigation of a number of processing parameters and conditions for producing the green compacts was undertaken. Various cyanoacrylates were investigated for their suitability as a binder for the alumina powder. A series of experiments have been performed to establish the effects of the relevant parameters, such as inhibition, initiation and mixing condition on product integrity and process efficiency, since the cyanoacrylate was an exceedingly reactive binder, which posed problems when mixing the feedstock. Para-toluene-sulphonic acid has been determined as an effective inhibitor, and caffeine as an effective initiator, for the alumina/cyanoacrylate feedstock.

The moulded green compacts were investigated to establish their machinability using conventional machining operations: turning, milling and drilling. The green compacts could be machined exceptionally well using these conventional methods. The results indicated that the green compacts have

adequate mechanical strength to withstand the shearing action produced by the tool during the machining operations.

In order to gain a better appreciation of how the material behaved during the machining processes, a finite element analysis (FEA) was used to simulate the machining of the alumina/cyanoacrylate compact. The turning of the green compact was simulated in 2D using DEFORM 2D.

The moulded and the machined alumina/cyanoacrylate compacts were then investigated to establish their debinding and sinterability using conventional thermal equipment.

The main thrust of this research was focused on green machining of the novel material, from both the practical and modelling viewpoints, to develop a detailed understanding of the nature of the processes involved.

## **Acknowledgements**

First of all, I would like to pay tribute and extend my sincere gratitude to my supervisors, Prof. Hull and Prof. Henshall, for providing the opportunity to conduct this research, and for their tremendous advice and help throughout the research. They have spent countless hours reading my documents including conference papers, transfer report and especially this thesis.

My sincere thanks are also given to all technicians at Nottingham Trent University for their technical support. I am particularly grateful to Judith Kipling and Ralph James for their technical support and also sharing knowledge of their expertise.

Also, I would like to thanks all my seniors and friends for their support, encouragement and all those joyful moments that we have spent together.

Last but not least, I would like to dedicate this thesis to my family and my girlfriend, Voon, for their continuous support. No words can express my deepest gratitude to them.



## List of Figures

- Figure 2.1: Typical ceramic processing flow diagram [Source: Reed, 1995]. 9
- Figure 2.2: The Bayer process for chemically refining bauxite into alumina [Source: Reed, 1995]. 13
- Figure 2.3: Schematic diagram of material removal during machining [Trent and Wright, 2000]. 18
- Figure 2.4: Categories of swarf types [Source: Engineering Fundamentals, 2005]. 19
- Figure 2.5: (a) Types of wear observed in cutting tools. The thermal cracks shown are usually observed in interrupted cutting operations, such as in milling, (b) Catastrophic failure of tools, and (c) Features of tool wear in a turning operation. The VB indicates average flank wear [Source: Kalpakjian 1997]. 21
- Figure 2.6: Stages of binder removal by evaporation. (a) Evaporate from the compact surface. (b) Binder liquid being driven to surface by a capillary pressure. (c) Forming a 'network' of interconnected pores. (d) Final stage of evaporation with complete evaporation [Source: Ridgway, 2000]. 32
- Figure 2.7: Physical changes during initial stage of sintering. (a) Starting particles arrangement. (b) Rearrangement. (c) Bonding/Neck formation [Source: Richerson, 1992]. 34
- Figure 2.8: Physical changes during intermediate stage of sintering. (a) Neck growth and compact volume shrinkage. (b) Lengthening of grain boundaries. (c) Further neck and grain growth, and volume shrinkage [Source: Richerson, 1992]. 35
- Figure 2.9: Physical changes during the final stage of sintering. (a) and (b) Continuous grain growth and porosity reduction. (c) Porosity eliminated [Source: Richerson, 1992]. 36
- Figure 2.10: Schematic diagram of PIM [Jeffrey and David, 1996]. 37
- Figure 2.11: PRIME processes [Hull and Ridgway, 2001]. 40
- Figure 2.12: Cyanoacrylate adhesive monomer formulations [Source: Courtney and Verosky, 1999]. 42
- Figure 2.13: Cyanoacrylate anionic polymerisation [Source: Courtney and Verosky, 1999]. 42
- Figure 3.1: Examples of blooming in pure cyanoacrylate (99.9%) compacts. 52

|  |    |
|--|----|
| Figure 3.2: SEM image of the alumina powders. (a) MA2LS. (b) RAC45B.   | 54 |
| Figure 3.3: Steam Cooker used for Initiation.  | 60 |
| Figure 3.4: Thermocouple Data Logger   | 65 |
| Figure 3.5: Variation of temperature ( $^{\circ}\text{C}$ ) with time (sec) after mixing and cooling to room temperature for para-toluene-sulphonic acid inhibited alkoxy-ethyl cyanoacrylate/alumina initiated with caffeine (all concentrations are the same).       | 66 |
| Figure 3.6: The variation of compact hardness with time.   | 69 |
| Figure 4.1: Continuous swarf was formed when cutting pure cyanoacrylate compacts with cutting speed 2000 rpm, cut depth 1.0 mm, and feed rate 0.1 mm/rev using a carbide tool.   | 75 |
| Figure 4.2: Bridgeford Interact 720X Computer Numerical Control (CNC) machine.   | 78 |
| Figure 4.3: Comparison of new and used drills. Note all the drills are approximately 4 mm in diameter.   | 80 |
| Figure 4.4: Swarf stuck to the masonry drill surface   | 82 |
| Figure 4.5: METASERV 30 mm (left) and 40mm (right) diameter cylindrical polyethylene moulds  | 84 |
| Figure 4.6: (a) Schematic diagram of the machined compact, in which those holes labelled as Group 1 was machined at 1000 rpm, Group 2 was machined at 1500 rpm and Group 3 at 2000 rpm (b) Actual drilled compact.   | 85 |
| Figure 4.7: Colchester Student 1800 Series lathe   | 86 |
| Figure 4.8: Geometry of coated carbide cutting tool insert.  | 88 |
| Figure 4.9: Production of continuous swarf during turning.   | 90 |
| Figure 4.10: SEM image on machined surface shows the particles were still bonded together by the cyanoacrylate after machining at a cutting speed of 1800 rpm, feed rate of 0.2 mm/rev, and depth of cut of 1.0 mm.  | 90 |
| Figure 4.11: Microscope images on the used and unused cutting edges. (a) Side view (b) End view, (c) and (d) Top view. The cutting edge used to turn the compact for $\sim 100$ m, at a cutting speed of 1800 rpm, feed rate of 0.2 mm/rev and depth of cut of 1.0 mm. | 91 |

- Figure 4.12: Collected swarf from turning operation with a cutting speed of 1800 rpm, feed rate of 0.2 mm/rev, and depth of cut of 1.0 mm. (a) Continuous swarf (b) SEM image on the swarf from the turning of a compact. 92
- Figure 4.13: Milled green compact. (Note: the large scale porosity that can be seen on some of the surfaces was present prior to the machining trials) 94
- Figure 4.14: Tool coating analysis (a) SEM image of the insert (b,c) Tool substrate material: Tungsten carbide (d) Inner coating: TiN (e, f) Outer coating:  $Al_2O_3$ . 96
- Figure 4.15: Bench vice used to hold the compact for sawing for preparation of samples. 98
- Figure 4.16: Collet fixed on the CNC table to hold the compact for drilling. 98
- Figure 5.1: Insert geometry (All dimensions in mm). 102
- Figure 5.2: Boundary conditions for simulations. 103
- Figure 5.3: Initial position of the work piece together with the cutting insert. 104
- Figure 5.4: Comparison of temperature and equivalent stress results for different mesh densities: (a) 500 elements (b) 1000 elements and (c) 1500 elements. 106
- Figure 5.5: Schematic diagram of the coated carbide tool. 108
- Figure 5.6: Temperature contours in work piece, tool and swarf for three different tool materials (a) AISI-D3HSS (b) 15% cobalt carbide (c) Coated carbide (15% cobalt). 109
- Figure 5.7: Comparison of the temperature distributions for the different values of Young's modulus. 114
- Figure 5.8: Comparison of the calculated temperature distributions for the different values in thermal conductivity. 115
- Figure 5.9: Swarf formation in the simulation at cutting speed of 85 m/min. 119
- Figure 5.10: Primary shear zone in the machining simulation. 120
- Figure 6.1: Thermogravimetric analysis of degradation of cyanoacrylate in the compact [Birkinshaw, 2003]. 125
- Figure 6.2: DSC analysis of degradation of cyanoacrylate in the compact [Birkinshaw, 2003]. 126

|   |            |
|---|------------|
| <i>Figure 6.3: Debinding oven with PC programmable temperature control and extractor fan facility.</i>  | <i>127</i> |
| <i>Figure 6.4: Bubbled effect in the bottom surface of the compact that were debonded on a metal plate (a) and vitreosil basin (b).</i>                               | <i>129</i> |
| <i>Figure 6.5: Distortion in the bottom surface of the compact that was debonded on a metal net (a) and defect free compact that was debonded on a firebrick (b).</i> | <i>129</i> |
| <i>Figure 6.6: Percentage debonded vs temperature profile for sample DebII- E.</i>  | <i>133</i> |
| <i>Figure 6.7: Digital weighing machine used to weigh the compact with the firebrick.</i>   | <i>134</i> |
| <i>Figure 6.8: Debinding profile of cyanoacrylate.</i>  | <i>135</i> |
| <i>Figure 6.9: Microstructure of a debonded compact.</i>  | <i>136</i> |
| <i>Figure 6.10: A hollow cylindrical alumina debonded compact placed in a bed of loose boron nitride powder in a two part hollow cylindrical graphite die.</i>        | <i>138</i> |
| <i>Figure 6.11: Analogue to digital data logger used for temperature reading.</i>   | <i>138</i> |
| <i>Figure 6.12: Arrangement used for sintering</i>  | <i>139</i> |
| <i>Figure 6.13: Induction coil covered with thermal insulating tape.</i>  | <i>140</i> |
| <i>Figure 6.14: SEM image of a sintered compact fractured surface.</i>  | <i>142</i> |
| <i>Figure 6.15: The sintered machined compact.</i>  | <i>143</i> |

## Table of Contents

|  |             |
|--|-------------|
| <b>Abstract</b>  | <b>I</b>    |
| <b>Acknowledgements</b>  | <b>III</b>  |
| <b>List of Figures</b>   | <b>IV</b>   |
| <b>Table of Contents</b>   | <b>VIII</b> |
| <b>Chapter 1 Introduction</b>                                      | <b>1</b>    |
| <b>1.1 Background</b>  | <b>1</b>    |
| <b>1.2 Project Aim</b>   | <b>2</b>    |
| <b>1.3 Project Objectives</b>                                      | <b>2</b>    |
| <b>1.4 Report Structure</b>  | <b>4</b>    |
| <b>1.5 Publications and Presentations Related to this Research</b> | <b>5</b>    |
| <b>Chapter 2 Literature Review</b>                                 | <b>6</b>    |
| <b>2.1 Ceramics</b>  | <b>6</b>    |
| 2.1.1 High Performance Engineering Ceramics                        | 7           |
| <b>2.2 Ceramics Processing</b>                                     | <b>8</b>    |
| <b>2.3 Ceramic Powders</b>   | <b>10</b>   |
| 2.3.1 Aluminium Oxide ( $Al_2O_3$ )                                | 11          |
| 2.3.2 Zirconium Oxide ( $ZrO_2$ )                                  | 15          |
| <b>2.4 Machining</b>   | <b>17</b>   |
| 2.4.1 Mechanisms of Machining                                      | 18          |
| 2.4.2 Swarf/Chip Formation   | 19          |
| 2.4.3 Tool Wear  | 20          |
| 2.4.4 Finite Element Analysis (FEA) of Machining Operations        | 22          |
| <b>2.5 Ceramics Machining</b>                                      | <b>24</b>   |
| <b>2.6 Green Ceramics Machining</b>                                | <b>26</b>   |
| 2.6.1 Advantages of Green Machining                                | 28          |
| 2.6.2 Problems Associated with Green Machining                     | 29          |

|                  |  |           |
|------------------|--|-----------|
| <b>2.7</b>       | <b>Debinding</b>                                       | <b>30</b> |
| <b>2.8</b>       | <b>Sintering</b>                                       | <b>32</b> |
| 2.8.1            | Polymorphic Transformation                             | 33        |
| 2.8.2            | Sintering stages                                       | 33        |
| <b>2.9</b>       | <b>Powder Injection Moulding (PIM)</b>                 | <b>36</b> |
| 2.9.1            | Ceramics Injection Moulding (CIM)                      | 37        |
| 2.9.2            | Metal Injection Moulding (MIM)                         | 38        |
| 2.9.3            | Feedstock  | 39        |
| <b>2.10</b>      | <b>Powder Reaction Injection Moulding Engineering</b>  | <b>39</b> |
| 2.10.1           | Cyanoacrylate as Binder                                | 41        |
| 2.10.2           | Inhibition and Initiation of Polymerisation            | 43        |
| 2.10.3           | Key Properties of Cyanoacrylate as Reactive Binder     | 44        |
| <b>2.11</b>      | <b>Summary</b>   | <b>44</b> |
| <b>Chapter 3</b> | <b>Compact Moulding Techniques</b>                     | <b>45</b> |
| <b>3.1</b>       | <b>Introduction</b>                                    | <b>45</b> |
| <b>3.2</b>       | <b>Selection of Binder</b>                             | <b>47</b> |
| 3.2.1            | Blooming   | 50        |
| <b>3.3</b>       | <b>Selection of Ceramic Powder</b>                     | <b>52</b> |
| <b>3.4</b>       | <b>Mixing</b>  | <b>56</b> |
| 3.4.1            | Inhibition   | 57        |
| 3.4.2            | Initiation   | 59        |
| <b>3.5</b>       | <b>Mould materials</b>                                 | <b>63</b> |
| <b>3.6</b>       | <b>Material properties</b>                             | <b>64</b> |
| 3.6.1            | Reproducibility  | 64        |
| 3.6.2            | Hardness   | 67        |
| 3.6.3            | Summary  | 69        |
| <b>Chapter 4</b> | <b>Green Machining</b>                                 | <b>71</b> |
| <b>4.1</b>       | <b>Introduction</b>                                    | <b>71</b> |
| <b>4.2</b>       | <b>Machinability of Alumina/Cyanoacrylate compacts</b> | <b>72</b> |
| 4.2.1            | Preliminary Machining Exercises                        | 73        |
| 4.2.2            | Machining of Cyanoacrylate Binder                      | 74        |

|                  |   |            |
|------------------|---|------------|
| <b>4.3</b>       | <b>Tool Materials</b>   | <b>76</b>  |
| 4.3.1            | Tool Material Trials  | 77         |
| <b>4.4</b>       | <b>Drilling</b>   | <b>83</b>  |
| <b>4.5</b>       | <b>Turning</b>  | <b>85</b>  |
| <b>4.6</b>       | <b>Milling</b>  | <b>92</b>  |
| <b>4.7</b>       | <b>Tool Wear</b>  | <b>94</b>  |
| <b>4.8</b>       | <b>Handling of the Green Compact for Machining</b>                              | <b>97</b>  |
| <b>4.9</b>       | <b>Summary</b>  | <b>99</b>  |
| <b>Chapter 5</b> | <b>Finite Element Analysis of Green Machining</b>                               | <b>100</b> |
| <b>5.1</b>       | <b>Introduction</b>   | <b>100</b> |
| <b>5.2</b>       | <b>Creation of Models</b>   | <b>101</b> |
| <b>5.3</b>       | <b>Boundary Conditions</b>  | <b>102</b> |
| <b>5.4</b>       | <b>Model of Tool/Work Piece Contact Interface</b>                               | <b>103</b> |
| <b>5.5</b>       | <b>Object Meshing</b>   | <b>103</b> |
| <b>5.6</b>       | <b>Tool Materials</b>   | <b>107</b> |
| <b>5.7</b>       | <b>Material Properties of the Alumina/cyanoacrylate</b>                         | <b>110</b> |
| <b>5.8</b>       | <b>Flow Stress Model for the Composite</b>                                      | <b>116</b> |
| <b>5.9</b>       | <b>Cutting speeds</b>   | <b>118</b> |
| <b>5.10</b>      | <b>Swarf Formation</b>  | <b>119</b> |
| <b>5.11</b>      | <b>Summary</b>  | <b>120</b> |
| <b>Chapter 6</b> | <b>Debinding and Sintering</b>  | <b>122</b> |
| <b>6.1</b>       | <b>Introduction</b>   | <b>122</b> |
| <b>6.2</b>       | <b>Debinding</b>  | <b>123</b> |
| 6.2.1            | Differential Scanning Calorimeter (DSC) and<br>Thermogravimetric Analyser (TGA) | 124        |
| 6.2.2            | Debinding of Alumina/Cyanoacrylate compacts                                     | 126        |
| 6.2.3            | Handling Methods for Debinding  | 128        |
| 6.2.4            | Heating Rate  | 130        |
| 6.2.5            | Debinding of Machined Compact   | 136        |
| <b>6.3</b>       | <b>Sintering</b>  | <b>137</b> |
| 6.3.1            | Sintering Procedure   | 137        |

|   |  |            |
|---|--|------------|
| 6.3.2                                   | Microstructure of the Sintered Compacts          | 142        |
| 6.3.3                                   | Sintering of Machined Compact                    | 143        |
| 6.3.4                                   | Hardness of the Sintered Compact                 | 143        |
| 6.4                                     | <b>Summary</b>                                   | <b>144</b> |
| <b>Chapter 7 Summary and Discussion</b> |  | <b>145</b> |
| 7.1                                     | <b>Introduction</b>                              | <b>145</b> |
| 7.1.1                                   | Compact Moulding Techniques                      | 146        |
| 7.1.2                                   | Green Machining                                  | 148        |
| 7.1.3                                   | FEA of the Green Machining                       | 150        |
| 7.1.4                                   | Debinding and Sintering                          | 152        |
| 7.2                                     | <b>Discussion</b>                                | <b>153</b> |
| 7.2.1                                   | Compact Manufacturing Techniques                 | 154        |
| 7.2.2                                   | Green Machining                                  | 156        |
| 7.2.3                                   | Debinding  | 157        |
| 7.2.4                                   | Sintering  | 158        |
| 7.3                                     | <b>Summary</b>                                   | <b>158</b> |
| <b>Chapter 8 Conclusions</b>            |  | <b>159</b> |
| 8.1                                     | <b>Compact Moulding Techniques</b>               | <b>159</b> |
| 8.2                                     | <b>Green Machining</b>                           | <b>160</b> |
| 8.3                                     | <b>FEA of the Green Machining</b>                | <b>161</b> |
| 8.4                                     | <b>Debinding and Sintering</b>                   | <b>161</b> |
| <b>Chapter 9 Further work</b>           |  | <b>162</b> |
| 9.1                                     | <b>Improvement in the Reactive Binder System</b> | <b>162</b> |
| 9.2                                     | <b>Mixing and Moulding System</b>                | <b>162</b> |
| 9.3                                     | <b>Computational Analysis</b>                    | <b>163</b> |
| 9.4                                     | <b>Analysis of Green Machining Parameters</b>    | <b>163</b> |
| 9.5                                     | <b>Sintering Process</b>                         | <b>163</b> |
| 9.6                                     | <b>Application of the Technique</b>              | <b>163</b> |
| <b>References</b>                       |  | <b>164</b> |



|                   |  |             |
|-------------------|--|-------------|
| <b>Appendix A</b> | <b>Technical Data Sheet of Loctite 408</b>                               | <b>i</b>    |
| <b>Appendix B</b> | <b>Technical Data Sheet of Loctite 460</b>                               | <b>iii</b>  |
| <b>Appendix C</b> | <b>Technical Data Sheet of Loctite 403</b>                               | <b>v</b>    |
| <b>Appendix D</b> | <b>Technical Data Sheet of Loctite 4062</b>                              | <b>vii</b>  |
| <b>Appendix E</b> | <b>Technical Data Sheet of Alcan Reactive Grade<br/>Calcined Alumina</b> | <b>ix</b>   |
| <b>Appendix F</b> | <b>Technical Data Sheet of Alcan Low Soda Grade<br/>Calcined Alumina</b> | <b>xi</b>   |
| <b>Appendix G</b> | <b>Programmes for CNC Machining</b>                                      | <b>xiii</b> |
| <b>Appendix H</b> | <b>Finite Element Model of Turning of PRIME<br/>Compact</b>              | <b>xvi</b>  |

## **Chapter 1 Introduction**

### **1.1 Background**

Advanced or engineering ceramics are used in significant quantities in the production of engineering components and biomedical prosthetics. The increased use of such materials is directly related to the superior properties of ceramics, such as resistance to wear, high temperature strength, and resistance to corrosion. Applications that take advantage of these attributes in major industries such as automotive, aerospace and medical instruments industries include valves, valve seats, turbine blades, liners, cutting tools, electronic components, artificial hip joints, dental prosthetics and artificial heart valves [Freitag and Richerson, 1998].

Powder Reaction Injection Moulding Engineering (PRIME) is a technique that involves mixing a reactive binder with a particulate ceramic powder, moulding, debinding and finally sintering to near net density. This process has proved to be successful for developing conduit articles out of ceramics [Hull et al., 1996]. Components produced by this method appeared to have good mechanical properties in the 'green' unfired state. It seemed that the binder could provide adequate strength for green machining, which would provide the possibility of making parts to a high tolerance before being sintered. For articles where surface finish is a prime concern, such as the heart valve, this method is of significant benefit.

This research programme has been designed to investigate the application of conventional machining techniques for ceramic compacts in the green unfired state, produced by PRIME.

## **1.2 Project Aim**

- **To investigate conventional machining of green ceramic powder compacts produced by Powder Reaction Injection Moulding Engineering (PRIME).**

## **1.3 Project Objectives**

The specific objectives of the proposed research can be stated as follows:

- **To establish the effects of the following materials parameters on product integrity:**
  - Powder- particle size, chemical composition.
  - Binder- blooming level, types (methyl-, ethyl-, butyl-, alkoxy-ethyl).
- **To establish the interaction of parameters and conditions to produce high quality of ceramic products:**
  - Generally concerned with the properties of the compact, and hence the preparation processes for the compact, i.e. inhibition, initiation, mixing, moulding and the selection of materials are key aspects.
  - The investigation of the reproducibility and properties of the green compact.
- **To establish the parameters and conditions for machining of green compacts by conventional techniques. This involves:**

- Investigation of the machinability of the green compact using various conventional machining operations, such as drilling, turning, and milling.
  - Investigation of the influence of machining feed rate and cutting speed on the machined surface.
  - Investigation of the handling method for machining of the green compact.
  - Investigation of swarf formation.
- 
- **To analyse and model the complex machining process in order to produce the most efficient and effective manufacturing techniques for part production.**
    - Development of a FEA model to analyse the machining of the green compact.
    - The validation of these models by comparing the FEA results to the observations from the experimental study, e.g. formation of the swarf and work piece/tool interface temperature(s).
    - The investigation of temperature distribution and maximum work piece/tool interface temperatures.
- 
- **To investigate the debinding and sintering parameters of the compact, i.e. shape/ size, shape/ distortion, surface finish etc.**
    - The investigation of effective debinding and sintering temperatures and times for the compact.

- The investigation of handling methods for debinding and sintering the compact.

## **1.4 Report Structure**

This report is organized into nine chapters:

- **Chapter 1** presents a general introduction and the research aim and objectives.
- **Chapter 2** discusses the existing literature in the relevant fields.
- **Chapter 3** discusses the material properties, mixing and moulding methods used to produce the green compacts.
- **Chapter 4** discusses the machinability of the green compacts.
- **Chapter 5** discusses a numerical analysis of the green compact turning process using a Finite Element Method.
- **Chapter 6** discusses the debinding and sintering processes that have successfully been applied to the green compact.
- **Chapter 7** presents a general summary and discussion of this study.
- **Chapter 8** concludes the report.
- **Chapter 9** presents suggestions for future work for further development of the technique and the material.

**Chapters 3, 4 and 6** detail a complete ceramic process involving mixing of the reactive binder with the ceramic powder, moulding, debinding and finally sintering.

## 1.5 Publications and Presentations Related to this Research

- **Ng S. H., Hull J. B. and Henshall J. L.**, “*Manufacture of a Novel Alumina/Cyanoacrylate Advanced Ceramic Material*”, 3<sup>rd</sup> Materials Research Conference, London, UK, 22 June 2004.
- **Ng S. H., Hull J. B. and Henshall J. L.**, “*Machining of a Novel Alumina/Cyanoacrylate Green Ceramic Compact*”, Britain's Younger Scientists, Engineers and Technologists Poster Presentations, UK National Science Week 2004, the House of Commons, London, UK, 15 March 2004.
- **Ng S. H., Hull J. B. and Henshall J. L.**, “*Machining of Novel Alumina/Cyanoacrylate Green Ceramic Compacts*”, Journal of Materials Processing Technology, awaiting publication.
- **Ng S. H., Hull J. B. and Henshall J. L.**, “*Machining of a Novel Alumina/Cyanoacrylate Green Ceramic Compact*”, Proceeding of the 12<sup>th</sup> International Scientific Conference- Achievements in Mechanical & Material Engineering, Zakopane, Poland, 7-10 December 2003.

## **Chapter 2 Literature Review**

### **2.1 Ceramics**

The ceramics industry is a multibillion-pound international industry that is concerned with converting raw materials taken directly from the earth (clay, sand, etc.) into many useful products such as: porcelain and pottery vessels, glass, tableware, sanitary ware, tiles and cement, which are among the more familiar.

The most exciting recent innovation in the ceramic materials was the development of a range of high performance engineering ceramics. These ceramic parts can replace and greatly improve on the performance of metals in many demanding applications. Engineering ceramics are generally highly wear resistant. For example, cutting tools made of dense alumina can cut faster and last longer than the best metal tools; they are used in the manufacture of engines, turbines and turbochargers because they can stand much higher temperatures than metals. Ceramics are also used in various applications, such as magnets in television, optical fibres for telecommunication, insulators for high speed trains, automobile spark plugs, ceramic engines, abrasives, bearing components, and even rocket components [Campbell, 1997, Sōmiya, 1984].

Ceramics hold a unique position in nuclear fission power and also play an important role as neutron absorbers in nuclear control systems [Roberts, 1979]. In bioceramics, they are used for artificial teeth [Filser et al., 1998], bones and heart valves [Ridgway, 2000 & 2001]. They are also widely used in electronic components, heating elements, substrates for integrated circuits, dielectric components, underwater transducers etc [Fujishima, 2000]. Coatings are another important ceramics option. In this case, a thin surface layer of ceramic deposited

onto metal imparts favourable ceramic characteristics such as corrosion resistance or wear resistance, while retaining the durability and structural benefits of the metal [Wachtman, 1993]. Ceramic filters are well proven for hot gas filtration because of their excellent thermal and chemical stability as well as their high filtration efficiency and their long-term durability. Filtration at very high temperatures and pressures, as well as under aggressive chemical conditions, is possible when using ceramic filter elements [Newby et al., 1999].

King [2002] has stated that ceramics is considered a technology and not a science, in that most properties of ceramic materials are predictable only from experience and not from theory. Ceramics are generally characterized by a crystalline structure and covalent and/or ionic bonding between the atoms. The difference in the atomic bonding distinguishes them from metals, and their inorganic nature from organic materials (plastics, rubbers and wood). Most ceramics are metal oxides [Richerson, 1992].

In general they are very stiff, hard but brittle, have low densities, high melting temperatures, high thermal resistance, high electrical insulation, and are chemical and ageing resistant. The great stiffness and hardness of ceramics can be combined with the toughness of polymers or metals by making composites [Ashby and Jones, 1998].

### **2.1.1 High Performance Engineering Ceramics**

Engineering ceramics are used for their hardness, wear resistance, corrosion resistance, high temperature strength and capacity for heat insulation. Nevertheless, these advantageous properties are accompanied by disadvantages,



including low ductility and a tendency to cracking that limit the processing methods. A new class of fully dense, high strength ceramics is emerging, which combine a higher toughness with a narrower distribution of smaller micro-cracks. Although they are relatively expensive, their properties make them competitive with metals, cermets, and even diamond, for tools, dies, implants and engine parts. Some examples are listed in *Table 2.1*.

*Table 2.1: High Performance Engineering Ceramics*

| <b><i>Ceramic</i></b>                  | <b><i>Typical composition</i></b> | <b><i>Typical uses</i></b>  |
|--|-----------------------------------|---|
| <b><i>Dense alumina</i></b>            | $Al_2O_3$                         | Cutting tools, dies; wear-resistant surfaces, bearings; medical implants; engine and turbine parts; armour. |
| <b><i>Silicon carbide, nitride</i></b> | $SiC, Si_3N_4$                    |   |
| <b><i>Sialons</i></b>                  | $Si_2AlON_3$                      |   |
| <b><i>Cubic zirconia</i></b>           | $ZrO_2 + 5wt\% MgO$               |   |

## 2.2 Ceramics Processing

Ceramics processing technology is used to produce commercial products that are diverse in size, shape, complexity, material composition and particle structure. The functions of ceramic products depend on their chemical composition, which determines their properties. The basic composition for engineering ceramics can vary over a fair range in which oxide, nitride and carbide materials are used.

These days, the structure of particles and the distribution of pores are more carefully investigated to achieve better quality and reliability in ceramic products. In the research and development of advanced ceramics, scientific control of the materials and processes is required to minimise structural defects in the products.

Ceramics processing typically begins with one or more ceramic materials and one or more liquids as binder. Additives or processing aids are also used in some cases. A typical ceramic processing flow chart indicating the sequences of operations used in forming a ceramic product is shown in *Figure 2.1*.

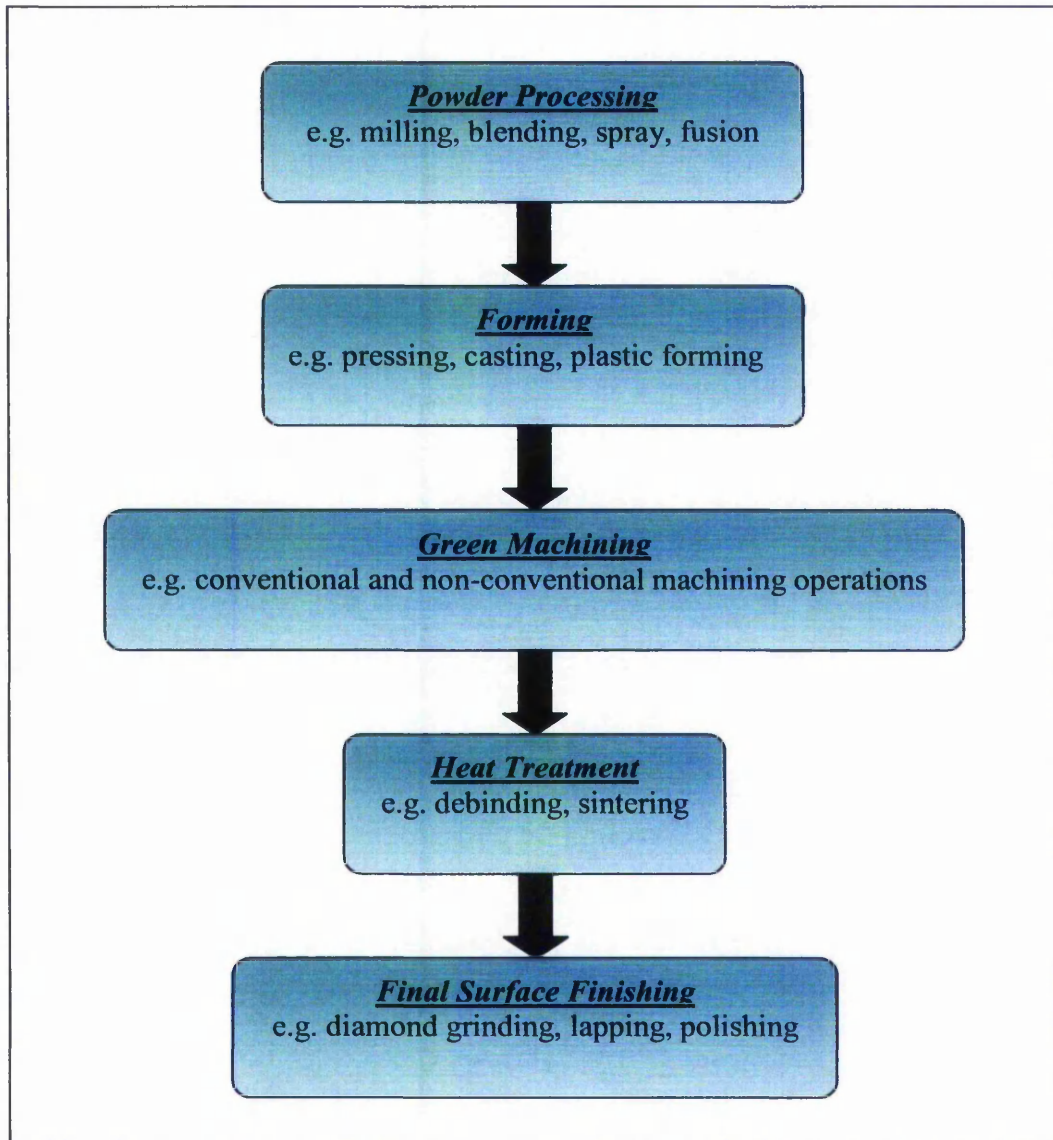


*Figure 2.1: Typical ceramic processing flow diagram [Source: Reed, 1995].*

## **2.3 Ceramic Powders**

Ceramic powders are generally the fundamental raw material for the manufacture of ceramic compacts for both monolithic and composite ceramics. Traditionally, powder preparation for traditional ceramics, e.g. glass and porcelain, was primarily by the extraction, cleaning and filtration of natural minerals such as clay, silica sand, quartz and limestone. However, because of the rapid development of engineering ceramic technology, the need for fine and homogeneous ceramic powders has increased. Thus, the advanced ceramics require more chemical processing in the preparation of the ceramic powder. By comparison with traditional powder preparation methods, where usually a crushing or a milling step is compulsory, the advanced synthesis methods aim to produce directly, by controlled chemical processes, very fine powders having a high degree of consistency in their main characteristics [Tirlocq and Cambier, 1989].

The nature of the raw material has a key effect on the final properties of a ceramic compact. The choice of raw material for a particular product is dependent on purity, particle size distribution, reactivity, cost and technical processing considerations to achieve the optimum properties for the intended applications. For example, advanced ceramics require very fine particles (typically  $<1 \mu\text{m}$ ) to achieve a fine grain microstructure with minimum flaw size [Richerson, 1992].

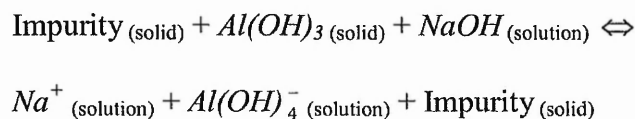
Important industrial ceramics powders include calcined alumina, stabilised zirconia, magnesium oxide, silicon carbide and silicon nitride. Extensive chemical refinement reduces the content of impurity minerals, and thus may increase the purity to  $>99.5\%$  [Reed, 1995].

In traditional ceramics processing, ceramics powders are usually formed into an initial shape using a processing method such a dry pressing, hot pressing, isostatic pressing, casting, extrusion or injection moulding. The powder particles are often mixed with a liquid base binder and are transported by the binder during the shaping process.

### 2.3.1 Aluminium Oxide ( $Al_2O_3$ )

Aluminium oxide ( $Al_2O_3$ ), also known as alumina, is the most commonly used advanced engineering ceramic. Some useful properties of alumina are its resistance to wear, high temperature strength, and resistance to corrosion. Alumina is the most widely used oxide advanced ceramic, either in pure form or as raw material to be mixed with other oxides. It is also known as sapphire, or corundum. Alumina powder is produced relatively cheaply in massive quantities for the ceramics industry using the Bayer process. It is manufactured synthetically, therefore its quality can be well controlled [Lee and Rainforth, 1994].

The principal operation in the Bayer process is the physical beneficiation of the bauxite, dissolution (in the presence of caustic soda  $NaOH$  at an elevated temperature and pressure), clarification, precipitation and calcination, followed by crushing, milling and sizing, see *Figure 2.2*. During the dissolution, most of the hydrated alumina goes into solution as sodium aluminate:



Settling and filtration remove insoluble compounds of iron, silicon and titanium. After cooling, the filtered sodium aluminate solution is seeded with fine gibbsite  $Al(OH)_3$ , and at a lower temperature, the aluminium hydroxide reforms as the stable phase. The agitation time and temperature are carefully controlled to obtain a consistent gibbsite precipitate. The gibbsite is continuously classified, washed to reduce the sodium content, and then calcined. Material calcined at  $1100^{\circ}C$  to  $1200^{\circ}C$  is crushed and ground to obtain a range of sizes. Tabular alumina is obtained by calcining at a higher temperature, around  $1650^{\circ}C$  [Reed, 1995].

Alumina ( $Al_2O_3$ ) has mechanical and physical properties particularly suitable for electrical and thermal insulation and also for cutting tools and abrasives. It has very good anti-corrosion properties. It can be found in different degrees of purity and crystal structures, with different properties and costs (very high for very pure grades). High purity aluminium oxide allows transparency of sintered pieces, which are used for optical applications.

Alumina is highly biocompatible and bio-stable, besides having potentially a long operational life. These properties make it suitable for the manufacture of prostheses such as the head cup for hip prosthesis and artificial heart valves [Ridgway, 2000].

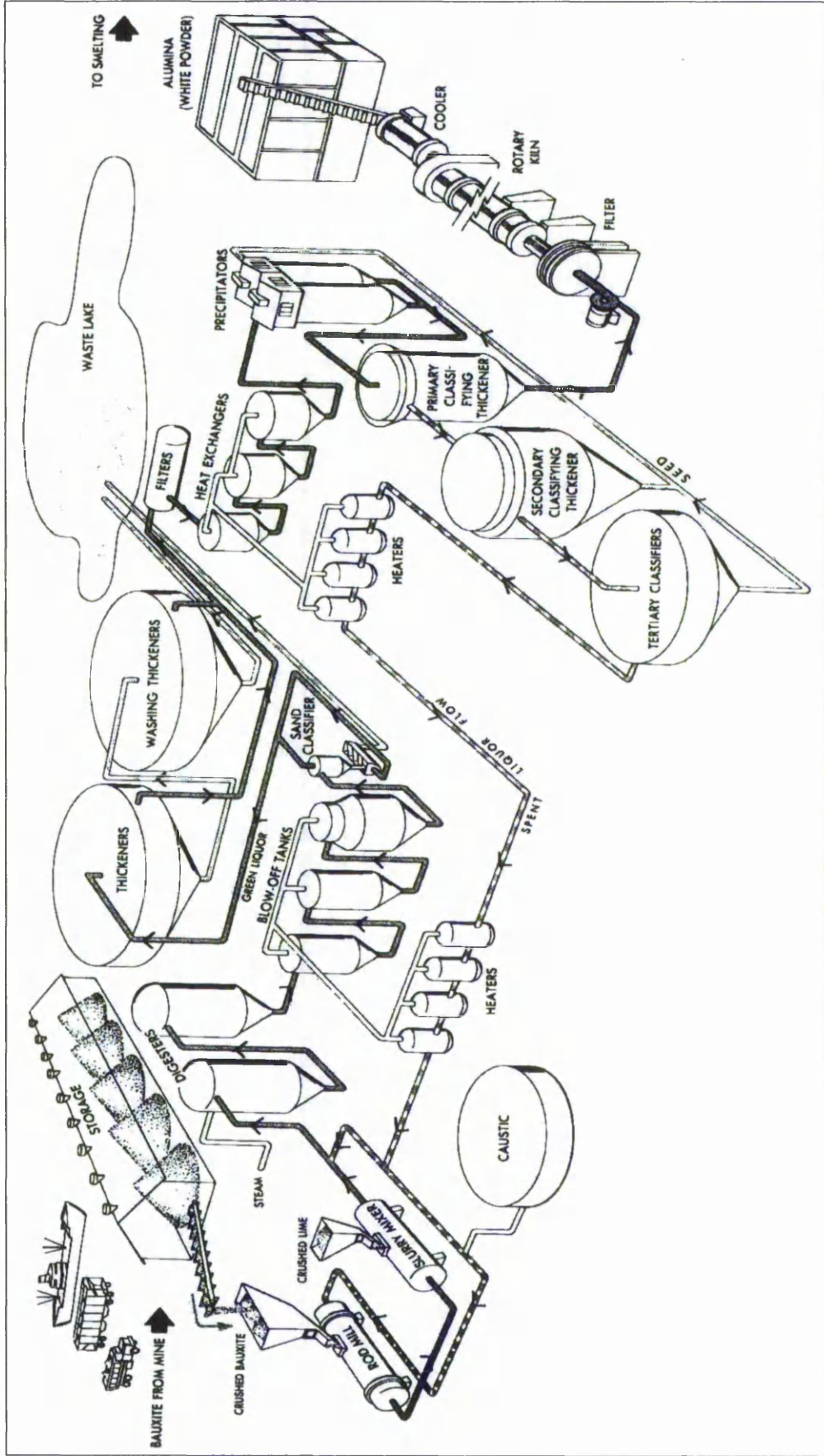


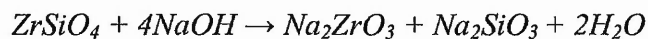
Figure 2.2: The Bayer process for chemically refining bauxite into alumina [Source: Reed, 1995].

### 2.3.2 Zirconium Oxide ( $ZrO_2$ )

Zirconium oxide, also known as zirconia or zirconium dioxide, is used as a high temperature refractory material, and for cutting blades. It has a very high melting point (about  $2700^{\circ}C$ ). It has received considerable interest because of its application as thermal insulation and as oxygen sensors, in addition to its high room temperature toughness [Stevens, 1986].

Zirconia is commercially available in two basic forms: naturally, from the mineral Baddeleyite; synthetically, derived from zircon sand ( $ZrSiO_4$ ). Zirconia can exist in three different polymorphs: the monoclinic, tetragonal and cubic phases. The monoclinic phase is the natural room temperature form and it is stable up to around  $1170^{\circ}C$ . At this temperature it transforms into the tetragonal phase, which is then stable up to around  $2370^{\circ}C$ . At this temperature it transforms into the cubic phase, which exists up to the melting point of zirconia  $2880^{\circ}C$  [Reed, 1995]. Because of its properties, zirconia is an advanced material that has been used in a wide variety of applications. These include high temperature refractories, electronic components, technical ceramic components, colour pigments, thermal barrier coatings and many more. It can be also found in industries ranging from glass production to jet engine manufacture [Russo and Partis, 2000]. The high temperature crystal structures, cubic and tetragonal, can be stabilised by the addition of calcium, magnesium, yttrium, or cerium oxides. The compositions are normally adjusted to give a stable cubic structure at room temperature (fully stabilised); a mixture of cubic and metastable tetragonal phases (partially stabilised, *PSZ*); or entirely metastable tetragonal phase (*TZP*). The metastable tetragonal phase transforms to the stable monoclinic phase under

stress, which results in a very tough ceramic, i.e.  $K_{IC} > 10 \text{ MPam}^{1/2}$  [Hannink et al., 1989]. The addition of *MgO* yields partially stabilised zirconia (*PSZ*), with a relatively coarse microstructure (50-100  $\mu\text{m}$ ), which can be used as a refractory material (e.g. thermal barriers for high efficiency heat engines), as it retains its properties up to 1100°C. Additions of yttria ( $\text{Y}_2\text{O}_3$ ) yield tetragonal zirconia polycrystal (*TZP*), a fine-grained microstructure (less than 1  $\mu\text{m}$ ) with high strength, toughness, and temperature capability (up to 500°C), used as a structural material or for durable cutting blades. Zirconia of 99% purity is obtained by the caustic fusion of zircon  $\text{ZrSiO}_4$  :



Chemical dissolution of the silicate in water simultaneously hydrolyses the sodium zirconia to hydrated zirconia [Reed, 1995].

Monoclinic zirconia plays an important role as a constituent for ceramic colours and electronic components. It is also used as an additive to enhance the properties of other oxide ceramics by promoting sintering. Due to zirconia's wear and corrosion resistance, it is a good refractory material for handling molten metals; for example, crucibles for manufacturing aircraft alloys and nozzles, and slide gates used in the continuous casting of steels. Zirconia ceramics' high strength and toughness make them an excellent choice for applications such as extrusion dies, grinding media, ceramic liners, cutting tools, valve seat guides, engine parts and medical implants.



Honeycomb components used within the aerospace industry have been coated with zirconium oxide by plasma spraying in order to give them good thermal insulation. This combines lightness and mechanical resistance.

## **2.4 Machining**

Machining is an operation in which a thin layer of component, the chip or swarf, is removed by a tool, often wedge shaped, from a larger body. There is no hard and fast line separating swarf-forming operations from others such as shearing of sheet metal, punching of holes, or cropping of lengths from a bar. These can also be considered as machining, but the action of the tools and the process of the operation of separation into two parts are so different from those encountered in swarf forming operations, that the subject requires a different treatment [Trent and Wright, 2000].

Machining is commonly associated with big industries which manufacture large sized products, such as automotive, aerospace, home appliance etc. The machining of metals and alloys plays a crucial role in a range of manufacturing activities, including the ultra precision machining of extremely delicate components [Trent and Wright, 2000].

In the engineering industry, the term machining is used to cover swarf-forming operations, and this definition appears in many dictionaries. Most machining operations today are carried out to shape metals, alloys, plastics and ceramics.

### 2.4.1 Mechanisms of Machining

The initial explanations of the mechanism of machining was formulated in the late 19<sup>th</sup> century and the proposed theories were based on a ‘splitting’ of the work piece material ahead of the cutting tool [Mills and Redford, 1983].

In practical machining, the included angle of the tool edge varies between 55° and 90°, so that the removed layer, the swarf, is diverted through an angle of at least 60° as it moves away from the work piece, across the rake face of the tool. In this process, the whole volume of metal removal is plastically deformed, and thus a large amount of energy is required to form the swarf.

In the machining process, two new surfaces are formed, the new surface of work piece (*OA* in *Figure 2.3*) and the under surface of the swarf (*BC* in *Figure 2.3*).

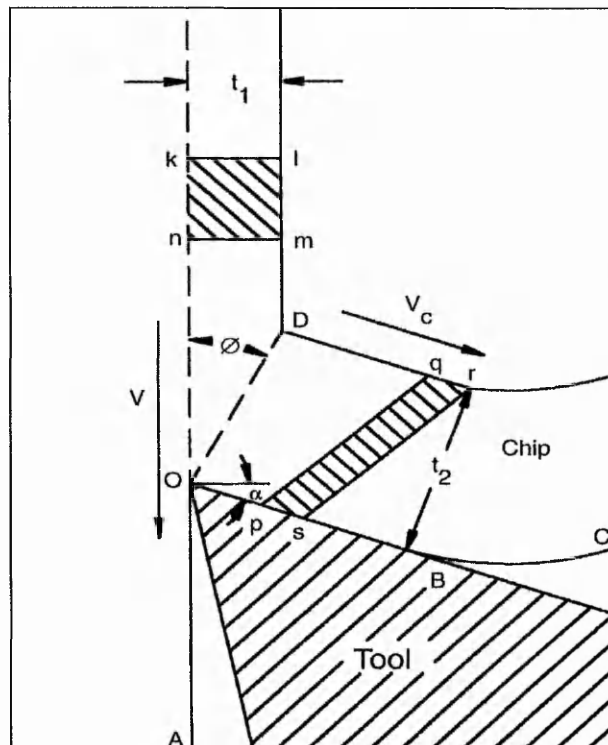


Figure 2.3: Schematic diagram of material removal during machining [Trent and Wright, 2000].

### 2.4.2 Swarf/Chip Formation

Based on shear plane theory, the swarf is formed during machining by fracture along successive shear planes that are inclined to the direction of cutting [Mills and Redford, 1983]. The swarf from machining are very variable in shape and size in industrial machining operations.

Figure 2.4 illustrates different categories of swarf types. The formation of all types of swarf involves a shearing of the work piece material in the region of a plane extending from the tool edge to the position where the upper surface of the swarf leaves the work piece surface (*OD* in Figure 2.3). A very large strain occurs in this region in a very short interval of time, and not all materials can withstand this strain without fracture.

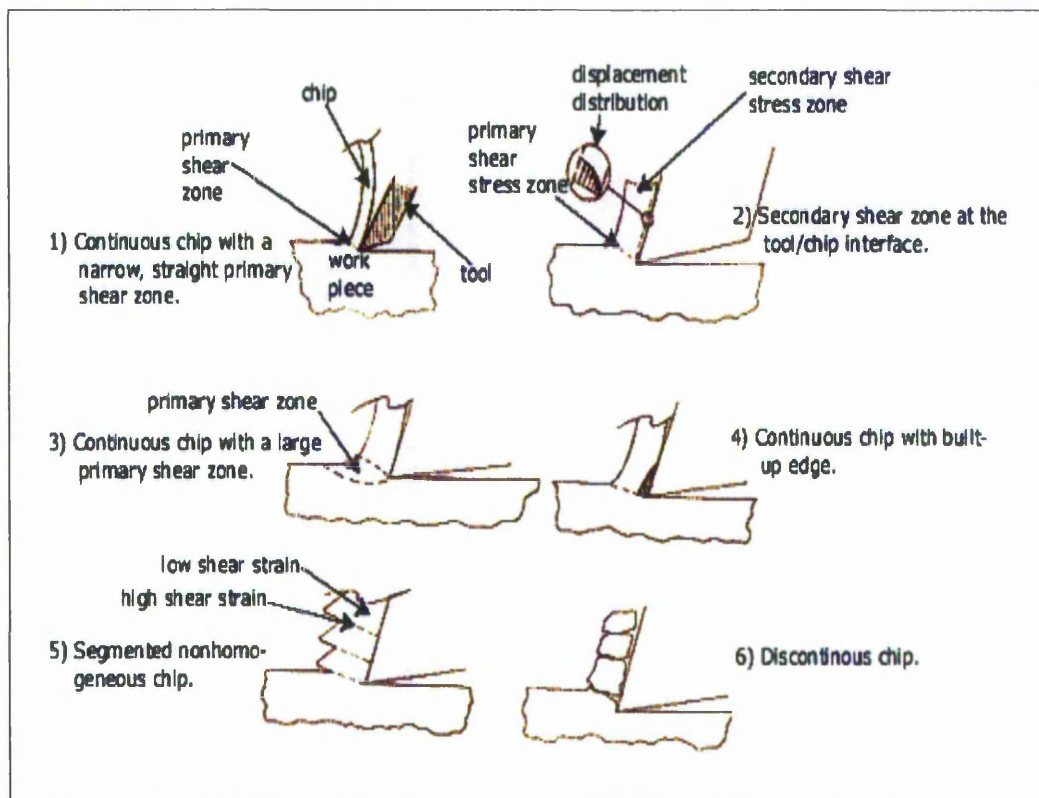


Figure 2.4: Categories of swarf types [Source: Engineering Fundamentals, 2005].

### **2.4.3 Tool Wear**

In nearly all machining processes, the action of cutting results in wear of the tool, so that the shape of the tool edge progressively changes with time and the tool ceases to cut efficiently or fails completely. The geometrical change of the tool surface is induced by forces, temperature and sliding during the cutting process [Kalpakjian, 1997]. The criteria for the end of the tool life are varied, and would include such parameters as: when the temperature rises and fumes are generated: when substantial noise is produced: when excessive vibrations occur: or when the dimensions or surface finish of the work piece change too much, etc. The skill of the operator is required to detect symptoms of the end of the tool life to avoid damage to the part being machined. Cutting tool materials and their appropriate selection are also crucial factors in most machining operations. During the machining operation, a tool is subjected to high contact stresses and rubbing on the work piece surface, as well as by the swarf climbing up the rake face of the tool, often accompanied by significant temperature increases.

Indeed, tool wear affects the quality of the surface finish and the economics of machining. It is one of the most crucial and complex aspects of machining operations. Although cutting speed is an independent variable, the forces and temperatures generated are dependent variables and are functions of numerous parameters. In the same way, tool wear also depends on the physical, mechanical and chemical properties of both the tool and work piece materials. Analytical predictions for tool wear, which is based on a large number of parameters, are considered difficult and therefore knowledge of tool wear on the machining of a new material is normally based mainly on experimental data [Kalpakjian, 1997].

The basic wear behaviour of a tool is shown in *Figure 2.5*. The various regions of wear are identified as flank, crater wear, nose wear and chipping of the cutting edge. Tool geometry can be changed by these various wear processes, and as a whole, these directly influence the cutting operation. In addition to these wear processes, plastic deformation of the tool can also take place to some extent, such as in softer tools at elevated temperatures. Gross chipping of the tool is called catastrophic failure, whereas wear is usually a gradual process [Kalpakjian, 1997].

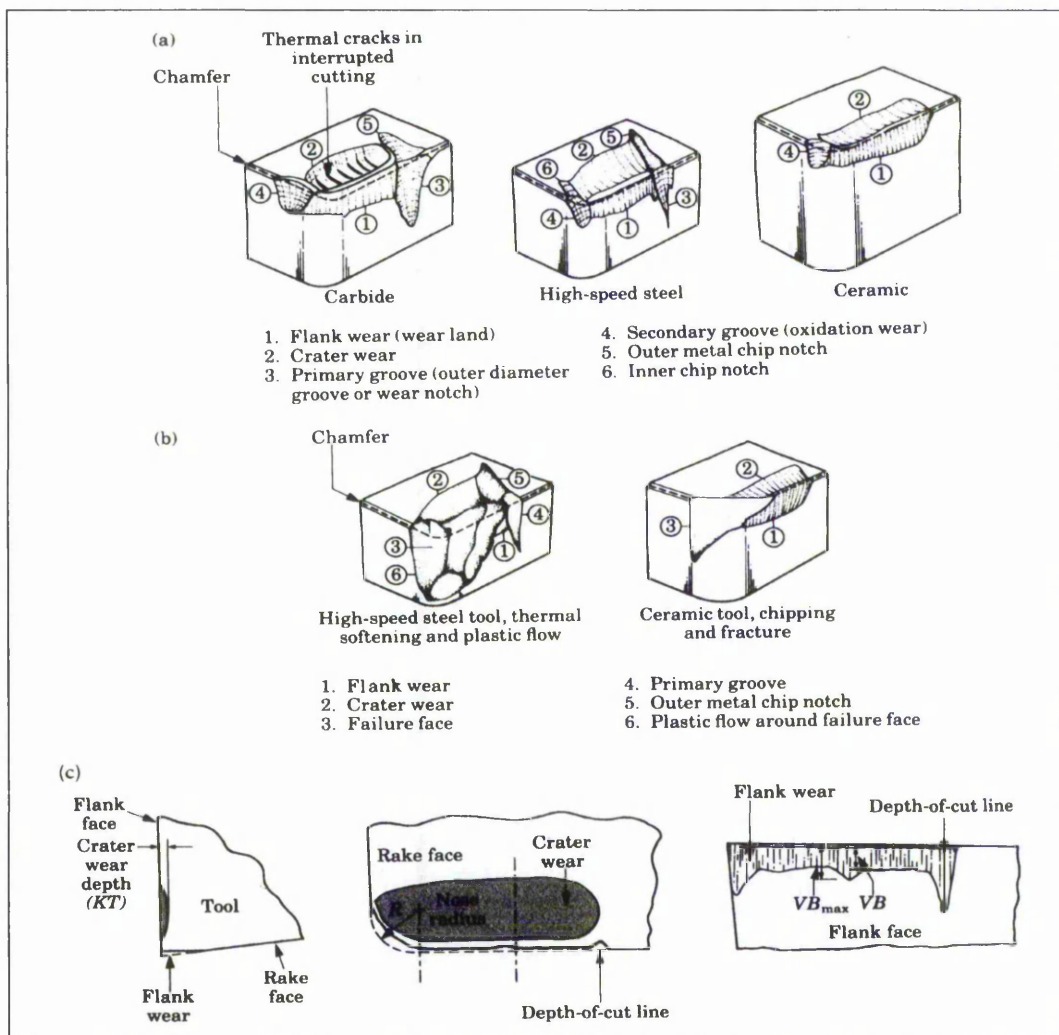


*Figure 2.5: (a) Types of wear observed in cutting tools. The thermal cracks shown are usually observed in interrupted cutting operations, such as in milling, (b) Catastrophic failure of tools, and (c) Features of tool wear in a turning operation. The  $VB$  indicates average flank wear [Source: Kalpakjian 1997].*

#### **2.4.4 Finite Element Analysis (FEA) of Machining Operations**

The finite element method was developed in the 1950s by a group of aerospace engineers when they tried to analyse the complex structural problem of an aeroplane [Pao, 1986]. The method has been developed simultaneously with the increasing use of high-speed computers and with the growing emphasis on numerical methods for engineering analysis. Today, super-high-speed computers have enabled engineers to employ various theories and formulations, which have been progressively refined and generalised, to analyse various complex problems in foundation engineering, structural engineering, aerospace engineering, heat conduction, hydrodynamics, nuclear engineering and many other fields.

However, it is difficult to obtain analytical solutions for many engineering problems, including conventional machining operations. An analytical solution is a mathematical expression that gives the value of the desired unknown quality at any location in a body, and as a consequence it is valid for an infinite number of the locations in the body [Desai and Abel, 1972]. Analytical solutions can be obtained only for certain simplified situations. For problems involving complex material properties, e.g. machining operations, the numerical methods are alternative ways that provide approximate and acceptable solutions.

The Finite Element Method (FEM) has been developed to simulate complex orthogonal machining operations since the early 1970s [Okushima and Kakino, 1971, Tay et al., 1974]. These pioneering works triggered a flurry of interest from the machining fraternity. This can be confirmed by the large number of publications on the subject in the last three decades [e.g. Tay et al., 1974, Oxley, 1989, Lin and Lin, 1992, Arola and Ramulu, 1997]. However, up until the mid-1990s, over 70% of researchers used finite element codes that were

developed by the researchers themselves [Ng, 2002]. The use of commercial packages has only increased dramatically over the past few years. Products on offer that are capable of modelling the machining process include DEFORM, NIKE2, ABAQUS/Standard, MARC, FORGE, ALGOR, FLUENT, ABAQUS/Explicit and LS DYNA. With the continuous improvement in computing power, the ability and efficiency of FEA for evaluating bigger and more complex problems can be achieved.

The main advantage of using FEM compared to other empirical methods is its ability to represent work piece material properties as a function of temperature, stress and strain rate. Correspondingly, the tool/swarf and tool/work piece interface can be idealised with sticking and sliding function conditions [Ng and Aspinwall, 2002].

Early FEM publications focused primarily on continuous swarf formation. However, several researchers have developed 2D models that simulate segmented swarf since the mid 1990s. Ceretti [1998] used an implicit finite element code, DEFORM 2D, to model the segmented swarf formed when turning a low carbon free cutting steel AISI 1045. Hua and Shivpuri [2002] also used DEFORM 2D to simulate swarf segmentation when machining titanium alloy *Ti-6Al-4V* over a range of cutting parameters. Other studies concerning segmented and discontinuous swarf have been published by Baker et al. [2002], Obikawa et al. [1997] and Marusich [1995].

Much literature on FEM in machining operations was mainly 2D in nature up to the early 1990s. Cutting is essentially a swarf formation process; and one of the most important considerations when modelling is the method by which elements of the work piece material separate as the cutting tool advances. For

Lagrangian based models, these have included node separation [Shet, 2000], element deletion [Ceretti, 1998], and adaptive remeshing [Marusich, 1995]. Thus, elements of the work piece material flow around the cutting edge and replace themselves to form the swarf and machined surface.

More recently, the emphasis has shifted towards 3D modelling simulations involving cutting operations other than turning. The transition from 2D to 3D simulation in term of computing time and model complexity (contact conditions between models and geometry of models) is significantly more tedious, although development in computing technology has improved some of these aspects. Ceretti et al. [2000] developed a 3D turning model using DEFORM 3D to predict cutting forces, temperature, stress distributions and swarf flow, when machining aluminium alloy under orthogonal conditions, and also low carbon steel with an oblique cutting configuration. Sohner et al. [2001] employed the same programme to produce a 3D simulation of a face milling operation of AISI 1045 medium carbon steel.

DEFORM is a versatile system with the opportunity to include a user's own constitutive models. It has been used to simulate various engineering machining situations, e.g. tool wear prediction [Yen, 2003] and machining speed optimisation [Fischer and Chigurupati, 2003].

## **2.5 Ceramics Machining**

Advances in space science and electronics technology have led to increasingly stringent requirements for ceramic parts with a high degree of precision. Most of these ceramic parts are formed from a powder, sintered at high temperature, and then machined to the required dimensions [Kobayashi, 1986].



However, the properties of ceramics have drawbacks with respect to this engineering fabrication. High hardness and low toughness present difficulties when machining fully sintered monolithic ceramics and bulk material removal is normally carried out by the traditional approach of diamond grinding [Kobayashi, 1989]. Nevertheless, although diamond grinding is used for more than 80% of all machining performed on advanced ceramics [Allor and Jahanmir, 1996], it results in induced damage in these ceramics [Zhang et al., 2002] and it is limited in the complexity of shapes that can be produced.

Consequently, new Physical and Chemical (P&C) machining techniques have been introduced to try and overcome these factors. Solid ceramic particles can be removed by non-conventional methods such as Ultrasonic Machining (USM) [Deng and Lee, 2002], Electrical Discharge Machining (EDM) [Puertas and Luis, 2004], Laser Beam Machining (LBM) [Glaw et al., 1997, Tsai et al., 2004], Electro Chemical Machining (ECM), Abrasive Jet Machining (AJM) [Wakuda et al., 2003], or combined techniques such as combination of USM and EDM [Thoe et al., 1999]. These techniques are able to machine some ceramic compacts without a problem. However, the main limitations to the use of these techniques are the high initial investment cost and restrictions on the types of material that can be machined [Ridgway et al., 1999]. The cost of ceramic machining could be as high as 90% of the total price of the ceramic compact, depending on the requirements for the surface finish and geometric tolerance [Allor and Jahanmir, 1996]. Diamond grinding and P&C are best suited to machining dense, sintered ceramics. Conversely, the design of complicated ceramics is often inhibited by the limitations of these techniques.

## **2.6 Green Ceramics Machining**

An alternative approach to the forming of ceramics is to mould the component to form an intermediate shape, known as the 'green compact'. The traditional methods used to form such green compacts are slip casting (which uses a water-based slurry), dry-pressing, or injection moulding of a thermoplastic/ceramic powder feedstock. These green compacts can be machined using a simple conventional technique, such as turning with a lathe, before sintering [Ridgway et al., 1999]. This is known as 'green ceramics machining', which occurs by particle abrasion, and is typically used for the production of spark plug insulators [Reed, 1995].

In many cases, green machining of the original shaped compact prior to debinding and sintering within the guide of near-net-shape production can be an economic alternative, in order to reduce costs in prototype processing and fabrication at a sufficient quality level. Therefore, the study of green machining of a new ceramic material is important for the future development and application of the material. Green machining offers considerable advantages in term of quality, economic efficiency and flexibility.

Green machining separates the two steps of consolidation and shaping. For example, a lump of ceramic can be isostatically pressed (or isopressed) and then green machined to shape [King, 2002]. Green machining can be performed using a conventional or a non-conventional machining method. It depends on the material and complexity of the geometry. Practical limitations of applying non-conventional methods on green ceramic compact are high initial investment costs and restrictions on the types of material that can be machined. Non-conventional

machining methods are also distinguished from traditional techniques by their higher power consumption with lower material removal rates.

Green machining can only be applied to green compacts that have adequate mechanical strength to withstand the shearing action produced by a tool. The most crucial parameter of the ceramic part being machined is its fracture strength. The work piece must be strong enough to resist the induced stresses involved with machining and clamping without fracture. Fracture is often the case if the strength of a green material is less than 2 MPa [Reed, 1995]. Conventional feedstock designed for powder injection moulding normally consists of a binder that contains a wax or polymer mixture, which has low mechanical strength and may not be effortlessly machined. Furthermore, the material's mechanical strength depends on the strength of the binder and the volume fraction of ceramic powder to binder, e.g. higher loading equates to lower fracture strength, because of the reduction in binder adhesion between the powder particles.

Some approaches have made use of a thermoplastic as a binder for the ceramic, but this created two different major problems to green machining: (1) the mixture is very viscous and considerable wear to the dies etc. occurs, which means that only relatively small components can be made ( $\sim 1 \text{ cm}^3$ ), and (2) porosity introduced during the removal of the polymer binder by heating, can reduce the strength significantly [Mutsuddy and Ford, 1995].

There is a need to develop green compacts with sufficient mechanical strength to allow precise mechanical shaping, which do not have debinding problems. This will concentrate on the key issue identified in the Material Panel Foresight report for advanced structural ceramics, which recommends, "Future

efforts should be devoted to improved cost-effectiveness". [Foresight report, 2000].

The reduction in green machining costs that would be achieved by having effective green compacts able to withstand complex machining operations would be a significant step in the direction of reducing final costs. Key factors for the optimisation of green machining are:

- Hardness, toughness, strength
- Grain size
- Porosity
- Thermal properties
- Elastic properties

### **2.6.1 Advantages of Green Machining**

There are several advantages to green machining:

- Does not require expensive tooling
- Can obtain a uniform high density packing
- Can shape the part to precise dimensions

One commercial example of green machining is the manufacture of spark plugs. A blank is isopressed and then ground by a form-grinding wheel. This process is very effective and produces an accurate and uniform dense body [King, 2002].

### **2.6.2 Problems Associated with Green Machining**

Green ceramics components are usually characterized by a lower level of inherent strength than sintered parts, thus posing a variety of problems. Unfired green ceramics are relatively fragile and great care is necessary in the design and fabrication of machining and handling, so that the parts can be accurately and uniformly held during the various machining operations. In addition, the machining parameters must be carefully controlled to avoid overstressing the fragile material and producing cracks, breakage or poor surface finish.

Clamping or holding of a ceramic compact for machining is typically a problem because of its fragility. For machining, however, the work piece must be held rigidly and without distortion or stress concentration. Once a ceramic part has been secured rigidly in a fixture, machining can be conducted by a variety of operations, such as turning, milling, drilling, form wheel grinding, and profile grinding. Difficulties arise not only in connection with clamping and handling, but also with regard to the measurement of surface quality.

Green machining can be either dry or wet, depending on the binder present. In both cases, the compact is abrasive and will result in a tool wear. A wear on the cutting edge as little as 0.1 mm wide can cause a build up of cutting pressure and thus damage to the ceramic part [Richerson, 1992]. It is possible to machine compacts with high-speed steel (HSS) or cemented carbide cutting tools, but this is not recommended for all green materials. In some cases, the tool dulls so rapidly that extreme care is necessary to avoid damage to the work piece.

The abrasive nature of the swarf from ceramic materials, not only results in a high level of tool wear, but also necessitates modifications to the machine design to allow green ceramic machining to take place. When green ceramics are

machined, dust-like particles are produced instead of the long swarf that is usually associated with metal machining operations. These particles can stick to the work piece surface, resulting in increased tool wear. Moreover, the particles that settle on the slideways and bearings have a highly abrasive affect and cause wear damage, adversely affecting the accuracy of the machine tool and ultimately resulting in the destruction of bearings and slideways. It is observed that only a few reports [Kumar et al., 2000, Maier et al., 1997 and Wang et al., 2003] have been presented on green machining using conventional methods.

## **2.7 Debinding**

Debinding is a process for the removal of the binder from a green ceramic compact after moulding, and any other operation such as green machining. The main purpose of debinding is to avoid cracking or collapsing of the composite during sintering due to thermal expansion and vapour pressure attributable to the polymer rapidly decomposing. Therefore, it is an important step in a powder injection moulding process, especially for parts that require a great precision of geometry. In order to preserve the geometric integrity of the moulded part, the binder must be removed without disturbing the powder particles. The binder must be removed from the green compact in liquid or vapour form.

A single polymeric or wax component was originally used for the injection moulding process, therefore a straightforward operation based upon thermal evaporation was used. However, the debinding process required up to 300 hours for complete binder removal [German, 1990]. Such a time consuming debinding period was uneconomical and inefficient. Therefore, modern binder systems,

which contain multiple components, such as polymers and waxes, were developed to accelerate the debinding process. Anwar [1995] has developed a combination binder system such that complete removal of the binder components can be achieved in two hours. However, these techniques were considered too complicated, since fine control of processing is required to attain such a rapid binder removal process. A binder system that provides simplicity combined with rapid debinding would have a major impact on the development of an economical production process for powder injection moulding.

Generally, there are two approaches to debinding: solvent debinding and thermal debinding. The choice of the debinding method depends up on the properties of the binder, e.g. thermal properties, and also the geometry of the compact. The solvent debinding method involves immersing the green compact in a specific chemical fluid that would dissolve some of the binder. This reaction leaves an open pore structure between the remaining powder particles. Consequently, an 'exit' is created for subsequent removal of the remaining binder by thermal evaporation at an elevated temperature.

The alternative approach of debinding is to remove the binder without assistance of chemicals, using a thermal method. The thermal debinding method involves several stages [Mutsuddy and Ford, 1995]. During the early stage of heating, thermal expansion of the binder induces hydraulic pressure in the fully saturated part. The binder then begins to evaporate from the compact surface due to the increase in temperature. When the saturation level of the binder is reduced to a certain level, the remaining binder liquid in the mix would be driven to the compact's surface by capillary pressure, and then evaporated. As the binder removal by liquid transfer continues, 'gas pockets' in the compact begin to

connect together and form a 'network' of interconnected pores. Eventually, the binder liquid flows through this internal structure, where diffusion takes place. Chemical reactions could happen if the debinding takes place in air. *Figure 2.6* illustrates the debinding process.

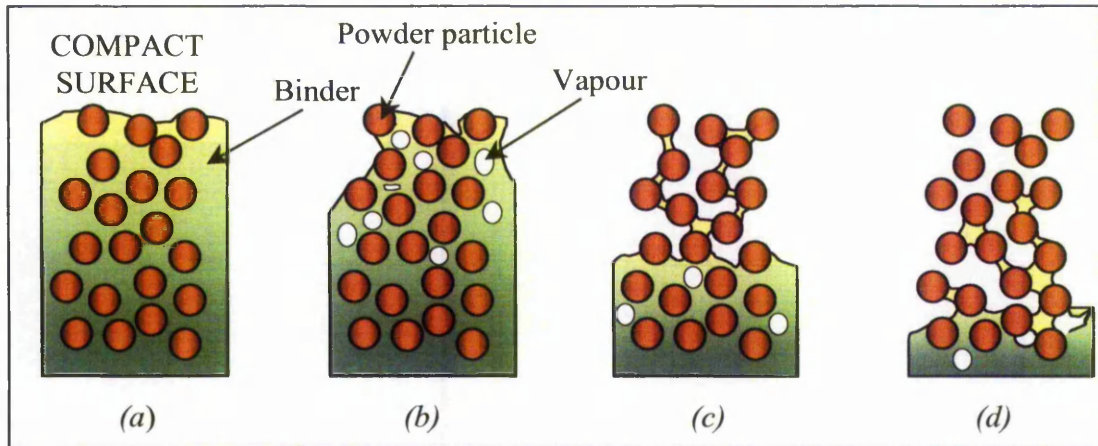


*Figure 2.6: Stages of binder removal by evaporation. (a) Evaporate from the compact surface. (b) Binder liquid being driven to surface by a capillary pressure. (c) Forming a 'network' of interconnected pores. (d) Final stage of evaporation with complete evaporation [Source: Ridgway, 2000].*

## 2.8 Sintering

Sintering is a process in which the debonded compact is heated to a temperature that is sufficiently high to give bonding of the powder particles together. It is a subsequent heat treatment process to the debinding and bonds the powder particles into a solid mass. Therefore, it is often combined with the debinding cycle so that the compacts are heated in the one furnace for debinding, and followed by sintering. However, a two stage process can also be used, i.e. debinding the compacts in a low temperature oven and transferring the compacts to a furnace for sintering.



Sintering densification usually take place close to the melting temperature of the ceramic powder. The bonds between particles develop by the motion of the atoms. For each single material, the level of atomic motion scales with the melting temperature, e.g. faster motion if the temperature increases [German and Bose, 1997]. Therefore, the sintering process can be speeded up by processing close to the melting point of the material.

### **2.8.1 Polymorphic Transformation**

Materials which have the same chemical composition but a different crystal structure, caused by change of temperature or pressure, are called polymorphs. The change of the structures is called polymorphic transformation. Such transformations usually do not cause problems during sintering, but may do so during the cooling down after sintering, since a sudden volume change is involved. It is a common problem in ceramic materials and normally affects the properties of the original structure and further affects the useful limits of application [Richerson, 1992].

### **2.8.2 Sintering stages**

The sintering stages and primary physical changes that occur in each stage are as follows:

- **Initial Stage**
  - Particle rearrangement
  - Bonding
  - Neck formation

- **Intermediate Stage**

- Neck growth
- Grain growth
- High shrinkage
- Pore phase continuous

- **Final Stage**

- More grain growth
- Pore phase discontinuous
- Grain boundary pores eliminated

The initial sintering stage involves rearrangement of the powder particles, which increases the contact points between particles, then initial neck formation. The rearrangement process includes slight movement or rotation of adjacent particles to increase the contact points. Material transport occurs at the contact points, where the surface energy is highest, to build up bonding between particles. *Figure 2.7* illustrates the changes that occur during the initial stage of sintering.

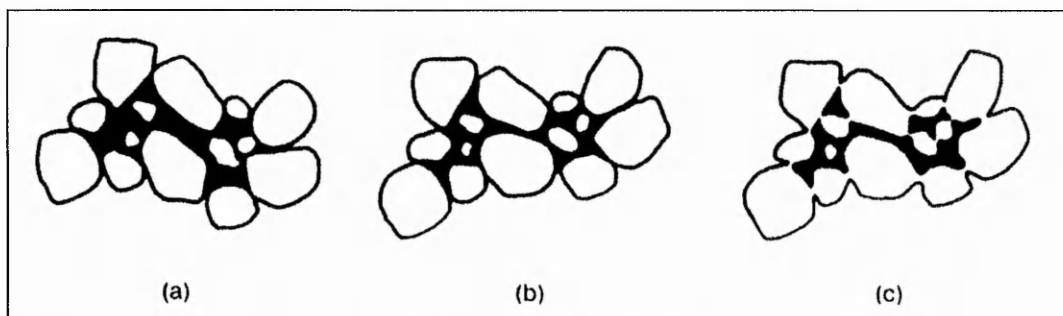


*Figure 2.7: Physical changes during initial stage of sintering. (a) Starting particles arrangement. (b) Rearrangement. (c) Bonding/Neck formation [Source: Richerson, 1992].*

The intermediate stage of sintering involves growth of the neck bonding between particles and reduction of porosity, which results in shrinkage. The bonding particles are now called grains. In this stage, the grain boundaries are mobile and allow further grain growth. The geometry of the compact changes to accommodate further neck growth and reduction in porosity. Most of the shrinkage of the compact occurs during this stage of sintering. *Figure 2.8* illustrates the physical changes that occur during the intermediate stage of sintering.

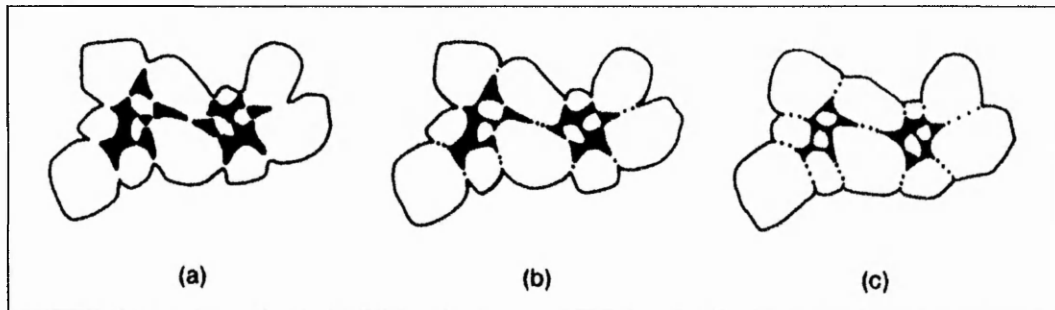


*Figure 2.8: Physical changes during intermediate stage of sintering. (a) Neck growth and compact volume shrinkage. (b) Lengthening of grain boundaries. (c) Further neck and grain growth, and volume shrinkage [Source: Richerson, 1992].*

The final sintering stage involves further grain growth and final reduction of porosity. In fact, the pores are removed by the aid of grain boundary movement and grain growth. Therefore, grain growth must be controlled to achieve the maximum porosity removed and also to avoid pores not being eliminated as a result of too rapid grain growth. *Figure 2.9* illustrates the mechanisms in the final stage of sintering.

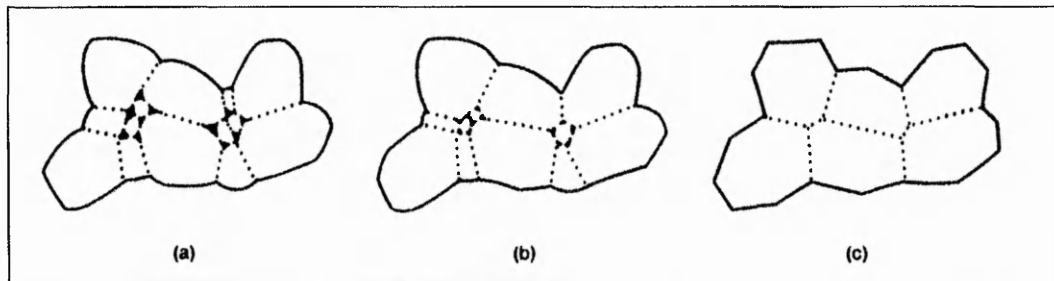


Figure 2.9: Physical changes during the final stage of sintering. (a) and (b) Continuous grain growth and porosity reduction. (c) Porosity eliminated [Source: Richerson, 1992].

## 2.9 Powder Injection Moulding (PIM)

Injection moulding (IM) is a widely used technique for shaping plastics. It was initially applied to polymers that melt on heating. However, ceramics and metals have certain property advantages over polymers, such as higher strength, higher stiffness, higher operating temperatures, and exhibit electrical and thermal properties that cannot be achieved by polymers.

Consequently, a new technology known as Powder Injection Moulding (PIM) uses the shaping advantage of the injection moulding technique, but is applicable to metals and ceramics. These processes are called Metal Injection Moulding (MIM) and Ceramics Injection Moulding (CIM). MIM and CIM combine a small quantity of polymer with a metal or ceramic powder to form a feedstock that can be moulded. After shaping, the polymeric binder is extracted and the powder is sintered.

A major difference between IM and PIM is that the production of a moulded compact is only an intermediate step for PIM, whilst it is the finishing step in the fabrication process for IM [Holme, 1993]. PIM has many options in developing the final product of the process. Different powders, binders and process environments can be used to produce an engineering part [McCabe and

Chang, 2002]. Accordingly, PIM delivers structural materials in a shaping technology that was previously restricted to polymers [German and Bose, 1997].

Figure 2.10 is a schematic diagram of PIM.

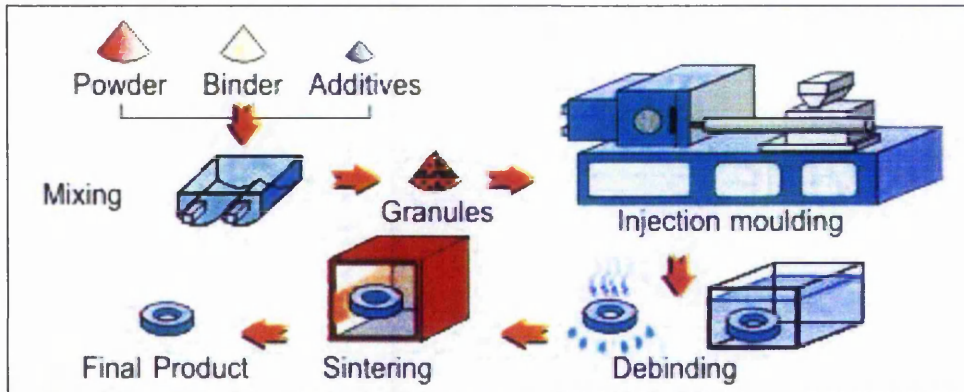


Figure 2.10: Schematic diagram of PIM [Jeffrey and David, 1996].

### 2.9.1 Ceramics Injection Moulding (CIM)

Injection moulding was first used in a ceramic fabrication process in the 1930s and became a production process for the manufacture of spark plug insulators in 1937 [Rak, 1999]. Ceramic Injection Moulding is a technology capable of producing a new range of components from ceramic powders. It allows high shape complexity, wide range of compact sizes and can achieve high density and other high performance attributes of ceramics [Mutsuddy and Ford, 1995].

In this technique, the ceramic powder is initially mixed with a binder to form a homogeneous mixture with rheological properties compatible with mould filling [Nogueira et al., 2001]. The process starts with the selection of ceramic powder and binder, followed by mixing, injection moulding, debinding, and finally sintering. Each stage is considered critical with regard to the success of the process.

The properties that give ceramics their desirable characteristics of strength and hardness also contribute to their brittleness and low toughness (or resistance to fracture). These properties must always be taken into consideration for every stage in the process to successfully produce compacts for commercial applications.

### **2.9.2 Metal Injection Moulding (MIM)**

Metal Injection Moulding (MIM) is the process used to manufacture complex components from ultra fine metal powders. The technology can be used to produce any small metal component, but it is of most value when the part is complex and difficult or expensive to machine using conventional techniques [Barriere et al., 2003]. In theory, any metal or metal alloy that can be produced in powder form can be MIM. MIM is a development of the traditional Powder Metallurgy (PM) process and it is regarded as a branch of that technology [Brown, 1998].

MIM is essentially a technology for producing complex shaped parts in large quantities. If the shape allows the production of the part by a conventional process, such as conventional pressing and sintering, MIM would in most cases be too expensive.

Theoretically there is no limit to the maximum size of part that could be produced by MIM, but economic considerations restrict the sizes that are currently practicable. There are two important factors in this connection: (1) the larger the part, the greater is the proportion of the overall cost that is attributable to the raw material, which is costly, and (2) the thicker the section the longer the debinding

time, and thus the higher the cost of that part of the process. At the present time, the limiting thickness seems to be about 30 mm. [German and Bose, 1997]

### **2.9.3 Feedstock**

Feedstock is a term for the mixture of powder (ceramic or metal) and binder. The most crucial concern when mixing is homogeneity of the feedstock, since uniform quantities of the binder and powder are required throughout the mixture. Three generalised rules of mixing feedstock for the powder injection process are:

- Coat the particles of powder with binder
- Break up agglomerates
- Attain uniform distributions of binder and powder throughout the feedstock

[Ridgway, 2000]

## **2.10 Powder Reaction Injection Moulding Engineering**

In 1996, Hull et al. were granted a patent on a novel PIM called Powder Reaction Injection Moulding Engineering (PRIME), which is a technique that involves mixing a reactive binder with a particulate material, moulding, debinding and finally sintering to near net density. This process, which utilises cyanoacrylate fluid (superglue) as the powder binder or carrier, has proved to be successful for developing conduit articles out of ceramic. Investigation of coating using the PRIME feedstock is also being undertaken in Nottingham Trent University by Kashefi et al. [2004]. The PRIME coating technique is an alternative technique to

those time-consuming traditional coating processes, provided the desired coating qualities could be achieved.

Compacts produced by the PRIME technique appeared to have good mechanical properties in the 'green' unfired state. It seemed that the binder could provide adequate strength for green machining, which would provide the possibility of making parts to a high tolerance before being sintered. For articles where surface finish is a prime concern, such as the heart valve, this method is of significant benefit. *Figure 2.11* illustrates the PRIME processes.

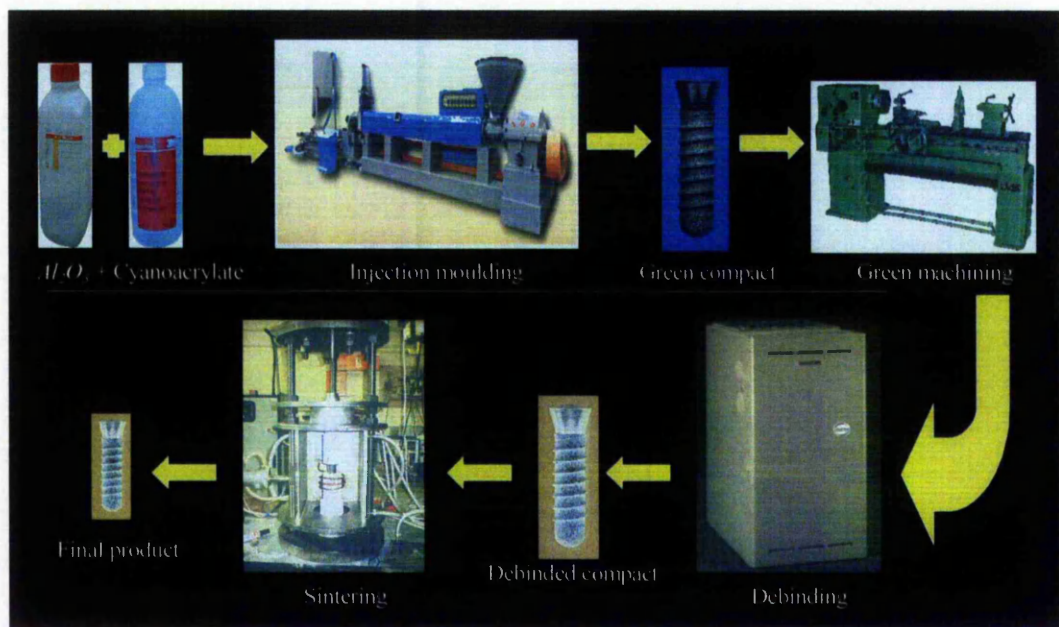


*Figure 2.11: PRIME processes [Hull and Ridgway, 2001].*

PRIME is a unique solution to the problems associated with the debinding of conventional waxes or polymeric binders used in powder moulding, since the cyanoacrylate binder (superglue) employed in PRIME de-polymerises back to a monomer. Traditionally, debinding of waxes and polymeric binders used in powder moulding is a very costly part of the process. Thermal degradation and



solvent wicking of polymeric binders can take hours or even days, but cyanoacrylate has major advantages because of its ability to unzip in minutes when exposed to temperatures greater than  $\sim 180^{\circ}\text{C}$ . Also, it can be collected for reuse. This enables a simple approach to powder moulding and a significantly decreased processing time.

### **2.10.1 Cyanoacrylate as Binder**

The binder is described as a temporary vehicle for homogeneously packing a powder to a desired shape and holding the powder particles in that shape until the start of sintering. It gives sufficient strength to the compact by causing the particle to stick together. It has great influence on the success of any PIM process [Bast, 1993].

In PRIME, the binder cyanoacrylate is a reactive monomer, which has the potential to simplify the moulding process and increase the efficiency of the process by eradicating the need for complex controls [Ridgway, 2000]. Cyanoacrylates are commonly known as superglue or instant glue because of their ability to form strong, permanent bonds almost instantaneously, although it is just a single component product. Cyanoacrylate adhesives are available in a wide range of viscosities and are curable at room temperature on a wide range of common surfaces and substrates. They are typically fixed within 1 minute and achieve full bond strength in 24 hours [Lee, 1981]. Cyanoacrylate adhesives are cyanoacrylate esters, in which methyl and ethyl cyanoacrylate are the most commonly used adhesive formulations. *Figure 2.12* shows some common cyanoacrylate adhesive monomer formulations [Courtney and Verosky, 1999].

Cyanoacrylate undergoes anionic polymerisation in contact with a weak base and is stabilised through the addition of a weak acid [Courtney and Verosky, 1999], see *Figure 2.13*. For example, when cyanoacrylate contacts a surface, where trace amounts of water or other substrate species present on the surface dilute or neutralize the acidic stabilizer in it, then rapid polymerisation occurs.

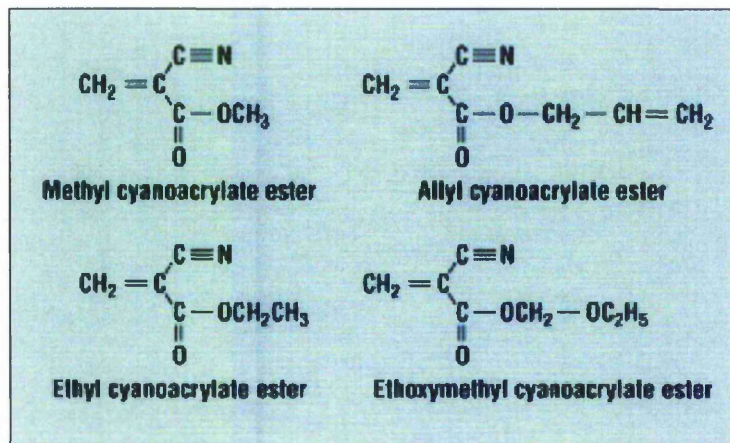


*Figure 2.12: Cyanoacrylate adhesive monomer formulations [Source: Courtney and Verosky, 1999].*

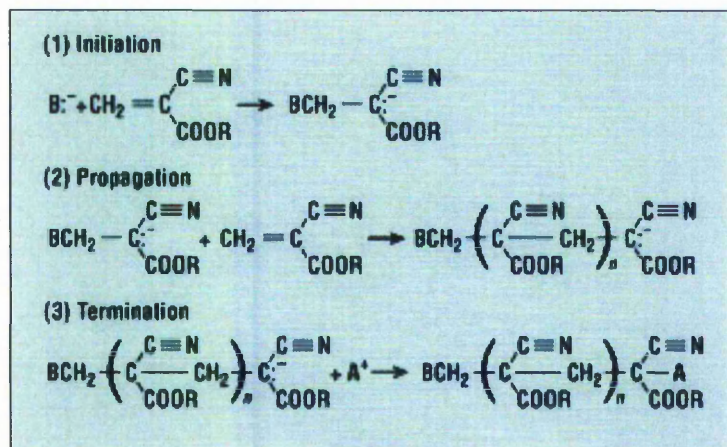


*Figure 2.13: Cyanoacrylate anionic polymerisation [Source: Courtney and Verosky, 1999].*

In recent times, there are only two research groups developing techniques employing cyanoacrylate as a binder for a CIM feedstock. They are butyl-

cyanoacrylate in PRIME [Hull et al., 1996] and ethyl-cyanoacrylate in Powder Reaction Moulding Technology [Birkinshaw et al., 1996]. Results from both investigations are sufficiently encouraging to justify further research.

### **2.10.2 Inhibition and Initiation of Polymerisation**

The main advantages of the PRIME technique stem from the use of a reactive binder, i.e. cyanoacrylate, that has the capability to rapidly solidify and can also be removed from the compact in a short period by thermal depolymerisation. However, the highly reactive cyanoacrylate monomer reacts almost immediately with a catalyst to initiate the rapid polymerisation process, which may not always be desirable.

Control of the polymerisation is a primary concern and the use of chemical inhibitors has been developed. A balanced mixture of inhibitor(s) and initiator(s) can be mixed into the monomer to delay the polymerisation and provide an adequate mixing period. Effective inhibitors for cyanoacrylate monomers are strong acids, such as para-toluene sulphonic acid, which effectively completely inhibit the polymerisation reaction, enabling cyanoacrylates to be stable for significant lengths of time [Birkinshaw et al., 1996].

On the other hand, an initiator is needed to initiate the polymerisation after the monomer and ceramic powder have mixed. The initiation, in this case, increases the flexibility and effectiveness of the process and also the possibility of achieving commercialisation. Typical initiators which have been successfully employed for the initiation of cyanoacrylate polymerisation are water, steam [Ridgway, 2000] and caffeine [Birkinshaw et al., 1996].

### **2.10.3 Key Properties of Cyanoacrylate as Reactive Binder**

The advantages of employing cyanoacrylate as a binder are:

- Availability of low viscosity cyanoacrylate that enables the feedstock to be transported through the moulding cycle while it remains fluid.
- Capability of initiating the curing process of cyanoacrylate by adding initiator or accelerator to increase the efficiency of the process in terms of curing time.
- Reasonable tensile and shear strength can be achieved, which will increase the machinability of the green compact [Courtney and Verosky, 1999].
- Reasonable resistance to humidity, moisture and solvents that enable the compact to be machined with coolant.

## **2.11 Summary**

This chapter discusses the existing literature in the relevant fields of work and also provides a description of the basic PRIME process cycle. This information has provided a sound basis for the present research project, particularly those aspects concerning:

- The situation and problems of the current ceramic fabrication industry.
- Machinability of ceramic compacts manufactured by traditional methods.
- Advantages of green machining in ceramic fabrication.
- Advantages of PRIME.
- Previous research in PRIME.

## **Chapter 3 Compact Moulding Techniques**

### **3.1 Introduction**

Ceramic powder moulding is a process of mixing a binder, ceramic powder and other additives, and forming it into a shape. There are a number of methods available for forming compacts. In PRIME, the forming process involves mixing a reactive binder/carrier with a ceramic powder, together with an inhibitor and an initiator. Finally, the resultant mixture is cured and moulded to shape concurrently.

Machining of a green ceramic compact is primarily influenced by the properties of the compact, and hence, the preparation of the compact and the properties of the raw materials are crucial factors.

In this chapter the selection and properties of the chemicals to be used in preparing the feedstock, mixing process, mould material and investigation of the green compact's properties are discussed. The layout is as follows:

- **Selection of Binder**

Using a cyanoacrylate binder is a novel technique in powder injection moulding. Therefore, investigation of the cyanoacrylate is very important to ensure that the process can be successful. This section describes the binder requirements, and includes the investigation of several cyanoacrylates that could be appropriate for PRIME.

- **Selection of Ceramic Powder**

The ceramic powder is another crucial factor that could directly affect the quality of the final product of the process. In this section, the characteristics of two ceramic powders that would be suitable for PRIME are described, with reference to particle size and chemical reaction with other additives. An investigation was undertaken to determine the maximum volume fraction of the two ceramic powders that could be used satisfactorily.

- **Mixing**

In PRIME, the binder cyanoacrylate is a reactive monomer, which has the potential to simplify the moulding process, but which undergoes extremely rapid anionic polymerisation in the presence of moisture or a weak base. This poses a problem in relation to producing a homogeneous feedstock. The interactions of the main parameters relevant to the production of high quality ceramic products are described. The interactions are generally concerned with the preparation processes of the compact, i.e. inhibition, initiation and method of mixing, whilst ensuring that concomitant problems such as blooming are obviated.

- **Mould materials**

Since cyanoacrylates are strong adhesives that adhere quickly and strongly to most materials, an investigation was carried out to obtain

an appropriate mould material. The process required a simple mould that would allow release of the green compact without damage.

- **Material properties**

The properties of the green compact would provide basic understanding for further processes such as green machining.

### **3.2 Selection of Binder**

The binder can be described as a vehicle for placing ceramic or metallic powders into a desired shape and then holding the powder particles in that shape until the initiation of sintering. Selection of the binder is crucial in all typical ceramics processing because the binders can significantly affect the strength of the green compact. A good binder for ceramic applications should provide high green strength at a low usage level.

Various binders can be used for ceramic processing, including waxes, polymers, alginates, gums and synthetic materials [German and Bose, 1997, Mutsuddy and Ford, 1995, Reed, 1995]. PVA and PEG are strong binders, which are frequently used as a binder/ carrier in traditional processing. PVA is a highly effective and versatile formulating tool because of its solution stability, its compatibility with many of the chemicals used as additives, and its availability in a wide range of grades. PVA produces high green strength, whereas PEG produces high green density. A disadvantage of both of these materials is that they have a hydrophilic nature [Bassner and Klingenberg, 1998]. However, it has been suggested that acrylic binders could be the preferred option, compared to PVA

and PEG, due to the acrylic's hydrophobic nature [Kumar et al., 2000]. Kumar et al. have studied acrylic co-polymer emulsion binders with very high strength. They claim that their green compacts can be machined, but they provide very little evidence and discussion of the green machining of their compacts. The comparative green strengths of compacts produced using PVA, PEG or acrylic are shown in *Table 3.1*.

*Table 3.1: Comparison of green strengths using traditional binders [King, 2002].*

| <b><i>Binder</i></b>  | <b><i>Strength (MPa)</i></b> |
|-----------------------|------------------------------|
| <b><i>PVA</i></b>     | 0.7                          |
| <b><i>PEG</i></b>     | 0.4                          |
| <b><i>Acrylic</i></b> | 6.5                          |

It is virtually impossible to obtain the optimum properties, if the reactive binder does not have the right characteristics.

The choice of binder/ carrier is also influenced by parameters such as flow characteristics, powder interaction, debinding and manufacturing. *Table 3.2* details these parameters and the requirements of an optimal binder to develop successful ceramic processing using the PRIME approach.

In most cases, a combination of a main binder material, in conjunction with other chemicals, which modify its properties in a particular desired manner, would be used to satisfy the requirements throughout an injection moulding process. For example, a binder might provide ideal rheological properties for mixing and processing, but take days to cure.



Table 3.2: Parameters and requirements of an optimal binder [German and Bose, 1997].

|   |  |
|---|--|
| <b>Flow characteristics</b>             | <ul style="list-style-type: none"> <li>● Viscosity below 10 Pa.s at the moulding temperature</li> <li>● Low viscosity change with temperature during moulding</li> <li>● Strong and rigid after curing</li> <li>● Small molecule to fit between particles</li> </ul>   |
| <b>Powder and additives interaction</b> | <ul style="list-style-type: none"> <li>● Low contact angle and good adhesion with powder</li> <li>● Have no, or a very low, 'blooming' effect</li> <li>● Chemically passive with respect to powder</li> </ul>  |
| <b>Manufacturing</b>                    | <ul style="list-style-type: none"> <li>● Inexpensive and available</li> <li>● Safe and environmentally acceptable</li> <li>● Not degraded by cyclic heating (reusable)</li> <li>● High strength and stiffness</li> <li>● High thermal conductivity</li> <li>● Low thermal expansion coefficient</li> <li>● Be stable under mixing and moulding conditions</li> <li>● Soluble in common solvents</li> <li>● Short chain length, no orientation</li> </ul> |
| <b>Green Strength</b>                   | <ul style="list-style-type: none"> <li>● Provide sufficient green strength</li> </ul>  |
| <b>Debinding</b>                        | <ul style="list-style-type: none"> <li>● Non-corrosive, non-toxic decomposition product(s)</li> <li>● Impart adequate strength to the moulded parts after binder removal</li> <li>● Leave a minimal residue after binder removal</li> <li>● Decomposition temperature above moulding and mixing temperature</li> </ul>   |

If the feedstock is highly viscous during the moulding process, complete mould filling is not possible; on the other hand, if the viscosity is too low, then uniform filling becomes difficult and results in segregation [German, 1993]. The understanding of the rheological behaviour of the feedstock is a complete subject in itself because it is governed by a number of properties of both the powder and binder, and their quantities [Reddy, 2001]. From experience, it has been proposed that the maximum useful viscosity of feedstock is  $10^3$  Pa.s at the moulding temperature. Powder additions to the binder raise the viscosity by 10 to 10000 times; thus the initial viscosity for an appropriate binder for PIM should be less

than  $\sim 10$  Pa.s [German and Bose, 1997]. This should allow good flow and packing of the ceramic powder and binder into a mould or die cavity.

### 3.2.1 Blooming

Blooming, or bubble formation, in the feedstock during polymerisation poses a significant problem. In this case, any gases released during processing result in voids within the final compact. Blooming increases the apparent porosity level and reduces the final sintered density of the compact.

Four different grades of cyanoacrylate with different characteristics were selected for the present investigation. The main properties that were evaluated were the viscosities of the binders and the 'blooming' effect during polymerisation. Caffeine was used as the initiator in all cases.

The procedure used was that 4 g of cyanoacrylate monomer liquid was dispensed into a polypropylene beaker, using a polypropylene syringe, followed by the addition of 0.001 g of caffeine. The solution was stirred with a polypropylene mixing-stick for 1 minute. The compacts were cured under ambient conditions to give cylinders of approximate dimensions 15.5 mm diameter x 19.5 mm high. A timer was used to record the curing period for the samples.

As shown in *Table 3.3*, it was observed that sample *Cya A* cured in 3 minutes with little blooming effect. Sample *Cya B* also cured in 3 minutes, but with blooming. For the other two binders, *Cya C* and *Cya D* took longer to cure, with significant and limited blooming respectively. The greater the degree of blooming, the more likely it is that there would be an increase in the porosity level, which could adversely affect the properties of the final compact. It was

found that the extent of blooming could be well observed visually using backlighting of the samples as demonstrated in *Figure 3.1*.

In conclusion, sample *Cya A*, alkoxy-ethyl cyanoacrylate, appeared to be the most suitable for making alumina/cyanoacrylate compacts, since it has a viscosity within the acceptable range and a relatively low blooming effect.

*Table 3.3: Effect of cyanoacrylate type on curing time and degree of blooming.*

| <b>Sample</b>       | <b>Cyanoacrylate</b>                           | <b>Viscosity of Cyanoacrylate (mPa.s)</b> | <b>Cyanoacrylate (g)</b> | <b>Caffeine added (g)</b> | <b>Observations</b>  |
|---------------------|--|---|--------------------------|---------------------------|--|
| <b><i>Cya A</i></b> | Alkoxy-ethyl cyanoacrylate, <i>Loctite 408</i> | 7   | 1.0                      | 0.1g                      | <ul style="list-style-type: none"> <li>● Cured within 3 minutes</li> <li>● Small amount of blooming</li> </ul> |
| <b><i>Cya B</i></b> | Alkoxy-ethyl cyanoacrylate, <i>Loctite 460</i> | 45  | 1.0                      | 0.1g                      | <ul style="list-style-type: none"> <li>● Cured within 3 minutes</li> <li>● Blooming</li> </ul>                 |
| <b><i>Cya C</i></b> | Alkoxy-ethyl cyanoacrylate, <i>Loctite 403</i> | 1100~1600                                 | 1.0                      | 0.1g                      | <ul style="list-style-type: none"> <li>● Cured within 15 minutes</li> <li>● Blooming</li> </ul>                |
| <b><i>Cya D</i></b> | Ethyl-cyanoacrylate, <i>Loctite 4062</i>       | 2   | 1.0                      | 0.1g                      | <ul style="list-style-type: none"> <li>● Cured within 5 minutes</li> <li>● Blooming</li> </ul>                 |

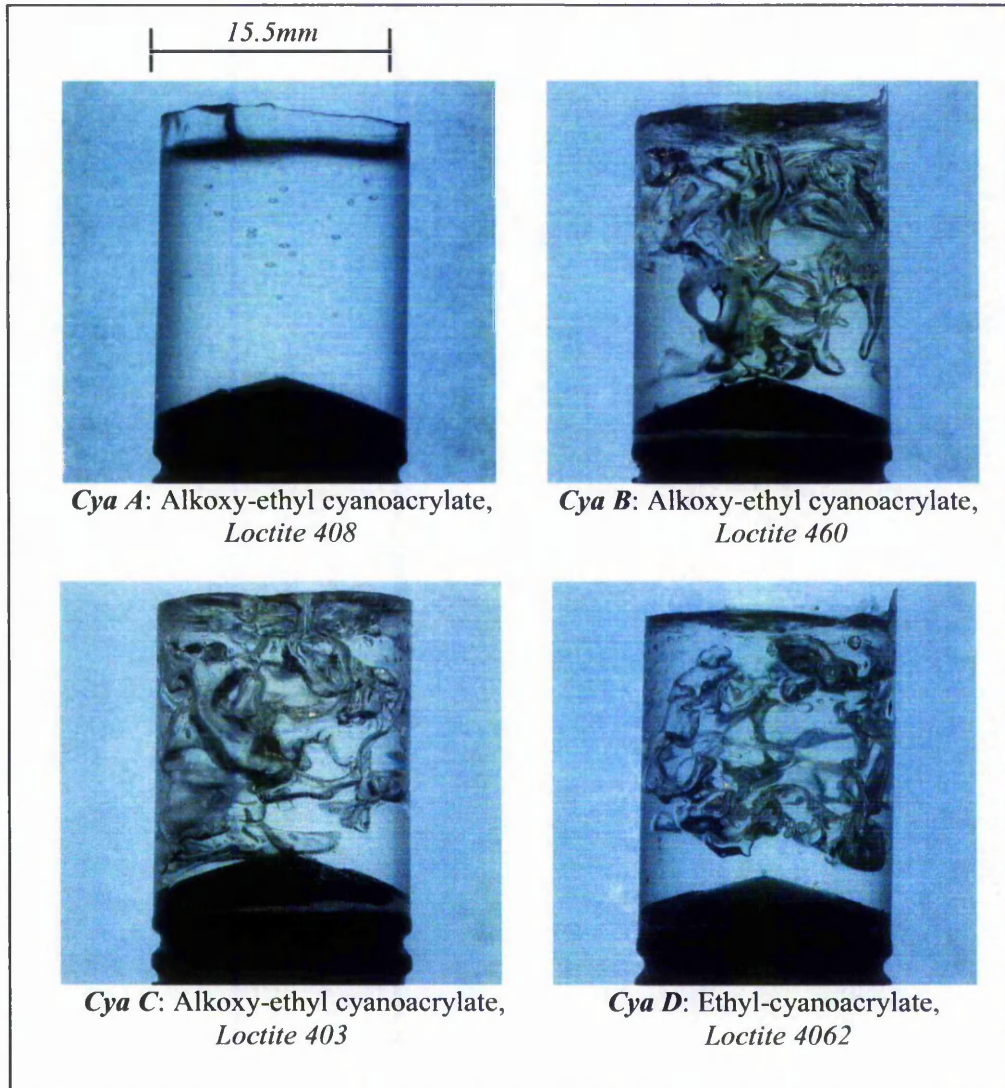


Figure 3.1: Examples of blooming in pure cyanoacrylate (99.9%) compacts.

### 3.3 Selection of Ceramic Powder

In the experimental investigations described in this thesis, the quantities of binder, powder and additives were measured by weight. However, in the literature, the proportions of the different phases are often described by their volume fraction, in order to simplify comparison of the data. It has been proposed by German [1997] that the range of powder volume fraction,  $V_f$ , should be between 0.45 and 0.85 so that the compacts can be successfully sintered. It also

has been proposed that for satisfactory ceramic injection moulding, there is a basic requirement that the powder particle size should be less than 20  $\mu\text{m}$  [Vervoort, 1996], and an ideal mean particle size is between 2  $\mu\text{m}$  and 8  $\mu\text{m}$  [German, 1991].

Two different grades of calcined alumina powder, reactive grade calcined alumina (*Alcan RAC45B*) and low soda grade calcined alumina (*Alcan MA2LS*), were selected for the investigation with different characteristics, e.g. purity, density, and median particle size. *Table 3.4* details the characteristics of the powders and *Figure 3.2* shows SEM images of the alumina powders *MA2LS* and *RAC45B*. The *MA2LS* grade particles appear to be angular with a mixture of dimensions, i.e. mainly cuboidal, rhombohedral and some platelets, *Figure 3.2(a)*. The *RAC45B* grade, *Figure 3.2(b)*, shows the particles appear to be regular cuboidal with some platelets.

The maximum particle dimensions of the *MA2LS* appear to be  $\sim 10 \mu\text{m}$  and the *RAC45B* appear to be less than 1  $\mu\text{m}$ , which is consistent with the information provided by the manufacturer.

*Table 3.4: Characteristics of the Alumina powders (from manufacturer's data)*

|  | <b>Low soda grade<br/>calcined alumina<br/>(Alcan MA2LS)</b> | <b>Reactive grade<br/>calcined alumina<br/>(Alcan RAC45B)</b> |
|--|--|---|
| <b>Purity (%)</b>                                      | 99.7   | >99.8   |
| <b>Density (<math>\text{g/cm}^3</math>)</b>            | 3.97   | 3.85  |
| <b>Median particle size (<math>\mu\text{m}</math>)</b> | 8  | <1  |
| <b>Chemical analysis (%)</b>                           |  |   |
| <i>Na<sub>2</sub>O</i>                                 | 0.05   | 0.04  |
| <i>SiO<sub>2</sub></i>                                 | 0.05   | 0.01  |
| <i>Fe<sub>2</sub>O<sub>3</sub></i>                     | 0.02   | 0.01  |
| <i>CaO</i>   | 0.02   | 0.01  |
| <i>MgO</i>   | -  | 0.05  |

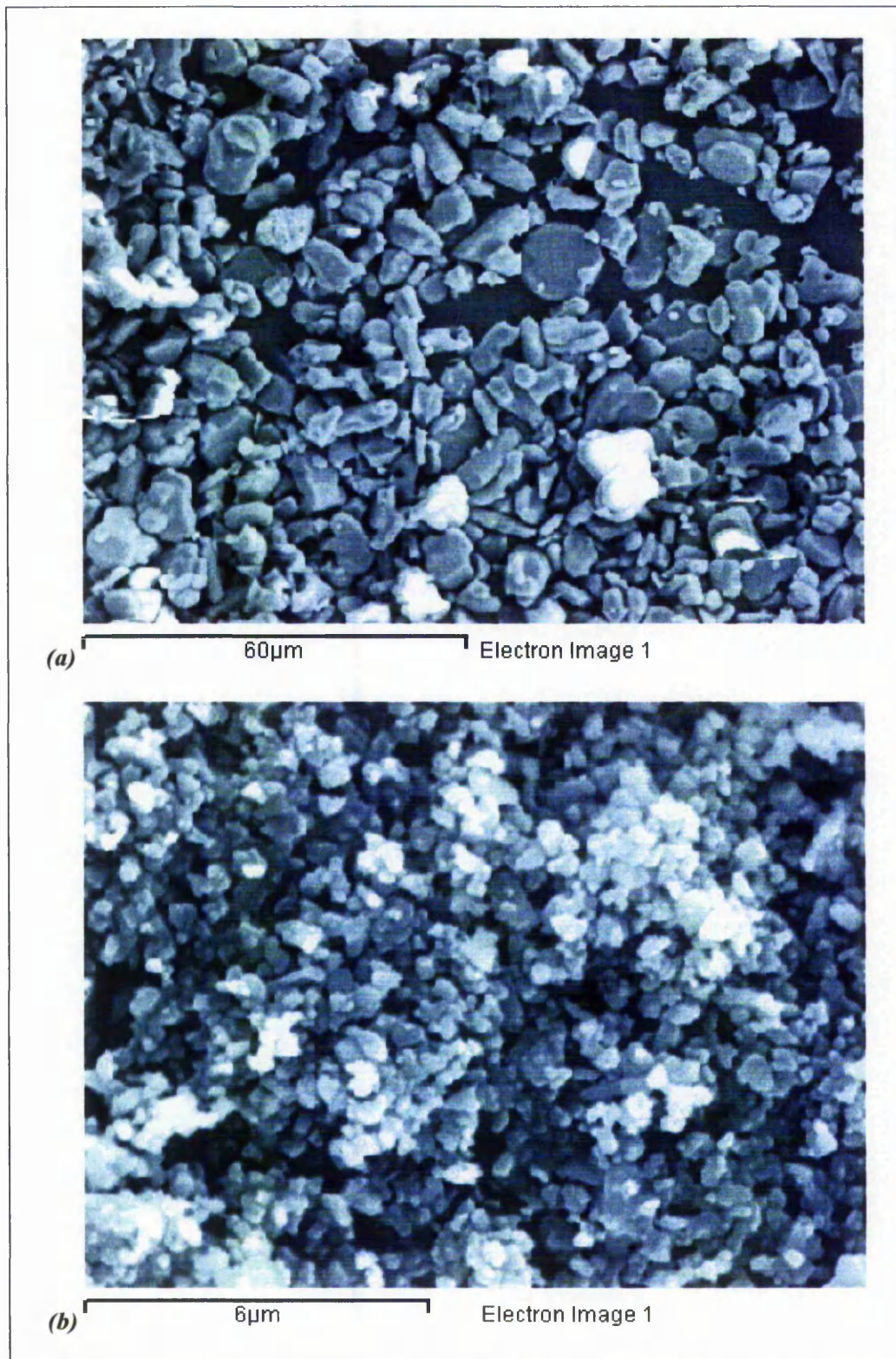


Figure 3.2: SEM image of the alumina powders. (a) MA2LS. (b) RAC45B.

The following experimental procedure was used for the mixing process:

- A measured quantity (by weight) of cyanoacrylate was dispensed into a polypropylene beaker, using a polypropylene syringe
- A measured quantity (by weight) of para-toluene-sulphonic acid crystals (or powder) was mixed into the cyanoacrylate
- The mixture was heated at 50°C in a water bath for 100 minutes, whilst the acid dissolved into the cyanoacrylate monomer
- The alumina powder was pre-dried in an oven for 30 minutes, at a temperature of 250°C; the purpose of this procedure is to reduce the surface moisture content
- The solution was removed from the heated water bath, and alumina was added (in small quantities) into the binder, whilst continuously mixing until no further powder could be mixed into the binder

*Table 3.5* details the amount of each material used as well as any observations regarding the uniformity of the mixture.

It was observed that the *RAC45B* grade alumina could not be mixed into the binder in as high a proportion as the *MA2LS* grade. This may be due to two reasons; firstly, the powders have slightly different chemical composition, e.g. *MgO* is present in the *RAC45B* grade, which might particularly affect their surface properties, e.g. alkalinity, and secondly they also have different particle size distributions. The *MA2LS* grade powder can be mixed with the binder up to a maximum volume fraction of 49%. This is sufficient to satisfy the powder volume fraction range for compacts that should be able to be sintered successfully.

Table 3.5: Results and observations of preliminary mixing trials.

| <b>Powder grade</b>                              | <b>Binder cyanoacrylate (g)</b> | <b>Maximum powder mixable weight (g)</b> | <b>Powder volume fraction (%)</b> | <b>Acid level* (%)</b> | <b>Observations</b>      |
|--|---------------------------------|--|-----------------------------------|------------------------|--------------------------|
| <b>Reactive grade calcined alumina, (RAC45B)</b> | 9.8                             | 24.0                                     | ~40                               | 2 (0.2g)               | ● Did not mix well       |
| <b>Low soda grade calcined alumina, (MA2LS)</b>  | 9.8                             | 34.0                                     | ~49                               | 2 (0.2g)               | ● No problems for mixing |

\* Note: the acid level percentage is expressed as a proportion by weight of the binder, not the total mixture.

### 3.4 Mixing

The purpose of mixing is to generate a uniform distribution of particles. The mixing method is key in achieving a homogeneous mix, which is free from agglomerates and contains the optimum content of powder and binder, while still maintaining sufficient fluidity for moulding [Mutsuddy and Ford, 1995].

The “feedstock” is the product of the mixing process, and it is a suspension of ceramic particles in a binder. The feedstock may also contain other chemicals such as pH modifiers.

The binder cyanoacrylate is a reactive monomer, which undergoes extremely rapid anionic polymerisation in the presence of moisture or a weak base. This poses a problem in relation to premature polymerisation and obtaining a homogeneous feedstock. Therefore, inhibition and initiation were investigated to determine if these could be used to facilitate the preparation process.



### 3.4.1 Inhibition

In the PRIME process, inhibition of the cyanoacrylate polymerisation is one of the most important factors in ensuring that there is enough time for thorough mixing, thus preventing premature polymerisation. Cyanoacrylate is a highly reactive monomer that reacts almost immediately with a catalyst, such as water or pyridine to initiate the rapid polymerisation process. In addition, alumina is an alkaline powder and as such promotes rapid polymerisation of the cyanoacrylate. Hence, when mixing the alumina powder into the *Loctite 408* cyanoacrylate, polymerisation occurred very rapidly as a result of reaction with surface moisture, and also because of the alkalinity of the powder. This meant that it was not possible to prepare and process a mixture of just cyanoacrylate and *MA2LS* grade alumina powder.

Para-toluene-sulphonic acid has previously been used successfully as an inhibitor with cyanoacrylate monomers. An additional aspect involves the alumina powder being dried in an oven to reduce its surface moisture content [Ridgway, 2000].

The procedure used was the same as outlined in the previous *section 3.3*. A comparison was undertaken using either para-toluene-sulphonic acid or glacial acetic acid as the inhibitor. The amount of inhibitor added was varied between 1% and 10% (by weight) to determine which would be most suitable for effective mixing and moulding. The samples were cured in polypropylene moulds, which were 27 mm in internal diameter. The results are shown in *Table 3.6*.

It was observed that samples *Inhi 4* and *Inhi 5* took more than 24 hours to cure, indicating that the added acid levels were too high. Samples *Inhi 1* and *Inhi 2* could not be successfully mixed because of insufficient inhibitor. Sample *Inhi 3*

was well behaved in that it was possible to thoroughly mix the powder into the binder and it cured several hours after mixing.

Table 3.6: Comparison of Para-toluene-sulphonic acid and Glacial acetic acid as inhibitors in cyanoacrylate-alumina mixtures

| Sample No                          | Cyanoacrylate (g) | Powder volume fraction (%) | Acid level* (%) | Observations   |
|------------------------------------|-------------------|----------------------------|-----------------|--|
| <b>Para-toluene-sulphonic acid</b> |                   |                            |                 |  |
| <i>Inhi 1</i>                      | 9.9               | 40                         | 1<br>(0.1g)     | <ul style="list-style-type: none"> <li>● Could not mix well</li> <li>● Polymerised whilst mixing</li> </ul>                      |
| <i>Inhi 2</i>                      | 9.8               | 40                         | 2<br>(0.2g)     | <ul style="list-style-type: none"> <li>● Could not mix well</li> <li>● Cured within 1 day</li> </ul>                             |
| <i>Inhi 3</i>                      | 9.7               | 40                         | 3<br>(0.3g)     | <ul style="list-style-type: none"> <li>● No problems with mixing</li> <li>● Cured within 1 day</li> </ul>                        |
| <i>Inhi 4</i>                      | 9.5               | 40                         | 5<br>(0.5g)     | <ul style="list-style-type: none"> <li>● No problems with mixing</li> <li>● Cured after 3 days</li> </ul>                        |
| <i>Inhi 5</i>                      | 9.0               | 40                         | 10<br>(1.0g)    | <ul style="list-style-type: none"> <li>● No problems with mixing</li> <li>● Not cured after 5 days (test terminated).</li> </ul> |
| <b>Acetic acid glacial</b>         |                   |                            |                 |  |
| <i>Inhi A</i>                      | 9.8               | 45                         | 2<br>(0.2g)     | <ul style="list-style-type: none"> <li>● Could not mix well</li> <li>● Polymerised whilst mixing</li> </ul>                      |
| <i>Inhi B</i>                      | 9.4               | 45                         | 6<br>(0.6g)     | <ul style="list-style-type: none"> <li>● Could not mix well</li> <li>● Polymerised whilst mixing</li> </ul>                      |
| <i>Inhi C</i>                      | 9.2               | 45                         | 8<br>(0.8g)     | <ul style="list-style-type: none"> <li>● No problems with mixing</li> <li>● Cured within a few minutes</li> </ul>                |
| <i>Inhi D</i>                      | 9.0               | 45                         | 10<br>(1.0g)    | <ul style="list-style-type: none"> <li>● No problems with mixing</li> <li>● Cured within a few minutes</li> </ul>                |

\* Note: the acid level percentage is expressed as a proportion by weight of the binder, not the total mixture.

For samples with glacial acetic acid as inhibitor, these were inhibited from polymerisation for a certain time, depending on concentration level of the acetic acid in the solution. Glacial acetic acid has a weaker inhibiting effect on alkoxy-ethyl-cyanoacrylate polymerisation compared to para-toluene-sulphonic acid, i.e. more acid (in terms of weight fraction) is needed to inhibit the alkoxy-ethyl-

cyanoacrylate from polymerisation for a short period to enable the powder to be mixed into the binder.

### **3.4.2 Initiation**

One of the factors that controls the usefulness of PRIME is the initiation of the cyanoacrylate polymerisation, since long, or inconsistent, times lead to poor process efficiency. Consequently, initiation experiments were carried out to establish an efficient method of polymerising an alumina/cyanoacrylate feedstock contained in a polypropylene beaker.

The aim of these experiments was to determine a safe and simple medium that can polymerise cyanoacrylate effectively after the feedstock has been well mixed and moulded. As a few hours for polymerisation was considered too long for an efficient process, a study of the feedstock polymerisation time using water vapour/steam as the initiator was undertaken. Three samples have been prepared using the procedure described in *section 3.4.1*; followed by placing the samples in a 100°C steam atmosphere in a steam cooker, see *Figure 3.3*. In such an environment, the cyanoacrylate binder undergoes anionic polymerisation by contact with the water molecules, which reduce the concentration of the acidic stabilizer, thus resulting in rapid polymerisation (see *section 2.10.1*). The results are shown in *Table 3.7*.

These results indicated that water vapour, nominally at 100°C, promoted the curing process of the inhibited cyanoacrylate/powder feedstock in comparison to the results in *section 3.4.1*, where the samples were maintained under ambient conditions. Although water vapour is a safe and economic catalyst for

cyanoacrylate polymerisation, and one which could be easily integrated into a processing method, this approach is considered to be insufficiently effective as it took up to 5 hours to complete the polymerisation stage.



*Figure 3.3: Steam Cooker used for Initiation.*

An alternative option was to curtail the polymerisation time by adding an additive into the binder, such as a small amount of caffeine. Caffeine has been successfully employed as an initiator for polymerisation of cyanoacrylate monomer [Birkinshaw, 1996]. The procedure used was the same as described in *section 3.4.1*, except that a measured quantity of caffeine was dissolved in the cyanoacrylate, after the para-toluene-sulphonic acid inhibitor had been added, by stirring at 50°C until fully dissolved. The results are shown in *Table 3.8*.

Table 3.7: Samples cured using water vapour as the initiator

| <b>Sample</b> | <b>Cyanoacrylate (g)</b> | <b>Powder volume fraction (%)</b> | <b>Acid level* (%)</b> | <b>Observations</b>  |
|---------------|--------------------------|-----------------------------------|------------------------|--|
| <b>Init 1</b> | 9.9                      | 48                                | 1 (0.1g)               | <ul style="list-style-type: none"> <li>● Did not mix well</li> <li>● Only a thin layer from the surface cured after 3 hours</li> <li>● Completely cured after 5 hours</li> </ul>                                       |
| <b>Init 2</b> | 9.8                      | 48                                | 2 (0.2g)               | <ul style="list-style-type: none"> <li>● No problems for mixing</li> <li>● Only a thin layer from the surface cured after 3 hours</li> <li>● Was not completely cured after 5 hours</li> </ul>                         |
| <b>Init 3</b> | 9.7                      | 48                                | 3 (0.3g)               | <ul style="list-style-type: none"> <li>● No problems for mixing</li> <li>● Had not polymerised within the investigation period of 3 hours</li> <li>● Only a thin layer from the surface cured after 5 hours</li> </ul> |

\* Note: the acid level percentage is expressed as a proportion by weight of the binder, not the total mixture.

It was observed that sample *Init A* has the lowest alumina powder volume fraction and agglomerated particles appeared whilst mixing. This could be because the caffeine level has neutralised the acid to such an extent that it was possible for polymerisation to be initiated at the surface of the alumina. Samples *Init B*, *Init C* and *Init D* could be mixed thoroughly, with curing occurring within a reasonable time. The caffeine concentration had no perceptible influence on the ease of mixing, but the curing times increased with decreasing caffeine concentration. Sample *Init E* produced a high-purity-cyanoacrylate compact with the highest powder volume fraction, but which took a significant length of time to cure.

Table 3.8: Samples produced with caffeine as initiator

| Sam-<br>-ple      | Binder solution    |                 |                 | Powder        |                              | Observations  |
|-------------------|--------------------|-----------------|-----------------|---------------|------------------------------|---|
|                   | Cyanoa-<br>crylate | Acid            | Caffeine        | Alumi-<br>-na | Powder<br>volume<br>fraction |   |
| <b>Init<br/>A</b> | 5.0 g<br>98.8%w    | 0.02 g<br>0.4%w | 0.04 g<br>0.8%w | 15.0 g        | 0.451                        | <ul style="list-style-type: none"> <li>• Acid dissolved within 15min</li> <li>• Caffeine dissolved within 35min</li> <li>• Agglomerated particles in mixture while mixing</li> <li>• Could not mix well</li> <li>• Polymerised whilst mixing</li> </ul> |
| <b>Init<br/>B</b> | 5.0 g<br>99.0%w    | 0.02 g<br>0.4%w | 0.03 g<br>0.6%w | 17.0 g        | 0.483                        | <ul style="list-style-type: none"> <li>• Acid dissolved within 15min</li> <li>• Caffeine dissolved within 25min</li> <li>• No problems with mixing</li> <li>• Cured within 30min</li> </ul>   |
| <b>Init<br/>C</b> | 5.0 g<br>99.2%w    | 0.02 g<br>0.4%w | 0.02 g<br>0.4%w | 17.0 g        | 0.483                        | <ul style="list-style-type: none"> <li>• Acid dissolved within 15min</li> <li>• Caffeine dissolved within 25min</li> <li>• No problems with mixing</li> <li>• Cured within 1hrs</li> </ul>  |
| <b>Init<br/>D</b> | 5.0 g<br>99.4%w    | 0.02 g<br>0.4%w | 0.01 g<br>0.2%w | 17.0 g        | 0.484                        | <ul style="list-style-type: none"> <li>• Acid dissolved within 15min</li> <li>• Caffeine dissolved within 15min</li> <li>• No problems for mixing</li> <li>• Cured within 2hrs 30min</li> </ul>   |
| <b>Init<br/>E</b> | 5.0 g<br>99.6%w    | 0.02 g<br>0.4%w | 0 g<br>0%w      | 17.0 g        | 0.484                        | <ul style="list-style-type: none"> <li>• Acid dissolved within 15min</li> <li>• No problems for mixing</li> <li>• Cured after 10 hrs</li> </ul>   |

### **3.5 Mould materials**

Cyanoacrylate is a strong adhesive that adheres to most materials within seconds. This ruled out the use of metallic moulds normally employed in traditional injection moulding processes. However, cyanoacrylate does not adhere to some polymeric materials.

An investigation was carried out to establish the appropriateness of a suitable polymeric mould material. The mould material for PRIME was expected to be:

- Low cost
- Readily available
- Would allow easy release of the green compact without damage to the compact

The mould materials used for this investigation were: polyethylene (PE), polypropylene (PP), polytetrafluoroethylene (PTFE) and Ultra High Molecular Weight Polyethylene (UHMWPE).

A feedstock containing 99.2%w cyanoacrylate (*Loctite 408*), 0.4%w para-toluene-sulphonic acid, 0.4%w caffeine and 48% $V_f$  of alumina was prepared using the procedures described in *sections 3.4.2*. The feedstock was applied in small amounts onto the surface of each test piece and left in ambient conditions for 24 hours to cure. The cured feedstock was then removed by hand. The feedstock on all the test materials, PE, PP, PTFE and UHMWPE could be removed with ease.

Although all the materials were useable as an appropriate mould material for the manufacture of PRIME compacts, cost and availability were considered. Polypropylene was cheap and accessible in terms of shape. Hence, polypropylene syringes were employed as the moulds and polypropylene mixing-sticks were

used to mix the alumina/cyanoacrylate feedstock during manufacture of the green compacts. A new syringe and mixing-stick were used each time.

### **3.6 Material properties**

It is generally considered to be important for the future development and application of a material that some data on the relevant material properties should be determined, as is the common practice in many processing industries.

Consistency of material properties refers to the reproducibility of the feedstock and its stability as a function of time. The feedstock must be easily reproduced, and preferably should not be excessively sensitive to slight variations in chemical composition or to storage conditions, such as temperature and humidity.

#### **3.6.1 Reproducibility**

The cyanoacrylate polymerisation reaction is exothermic. Consequently, the temperature of the binder can be used to monitor the progress of the curing reaction. A thermocouple (type K) data logger, *Figure 3.4*, was used with a PC to record the temperature profile after mixing. The aim of this exercise was to investigate the reproducibility of the curing process for the alumina/cyanoacrylate compacts.

A mixture containing 5 g (99.2%w) cyanoacrylate (*Loctite 408*), 0.02 g (0.4%w) para-toluene-sulphonic acid, 0.02 g (0.4%w) caffeine and 17 g (48%*V<sub>f</sub>*) of alumina was prepared using the procedures described in *sections 3.4.2*. The data logger was used to record the temperature and time profile for 3 hours.





Figure 3.4: Thermocouple Data Logger

The graphs in *Figure 3.5* show the temperature distributions for three batches of feedstock, which were prepared using the same procedures, but at different times. All of the profiles have similar characteristics. The peak temperatures occurred after the mixture had initially cooled down to around room temperature. The values of these peak temperatures are relatively low compared with conventional ‘pure’ cyanoacrylate curing [Birkinshaw, 1996]. The profiles indicate that the polymerisation process in the compact took approximately 2 hours to complete, which is much longer than the curing time for non-powder containing cyanoacrylates [Birkinshaw, 1996]. The slight variations in the timings for the start and end of the polymerisation could arise from variations in the dissolving and mixing times or slightly different ambient conditions. The curing of these compacts clearly exhibits good reproducibility.

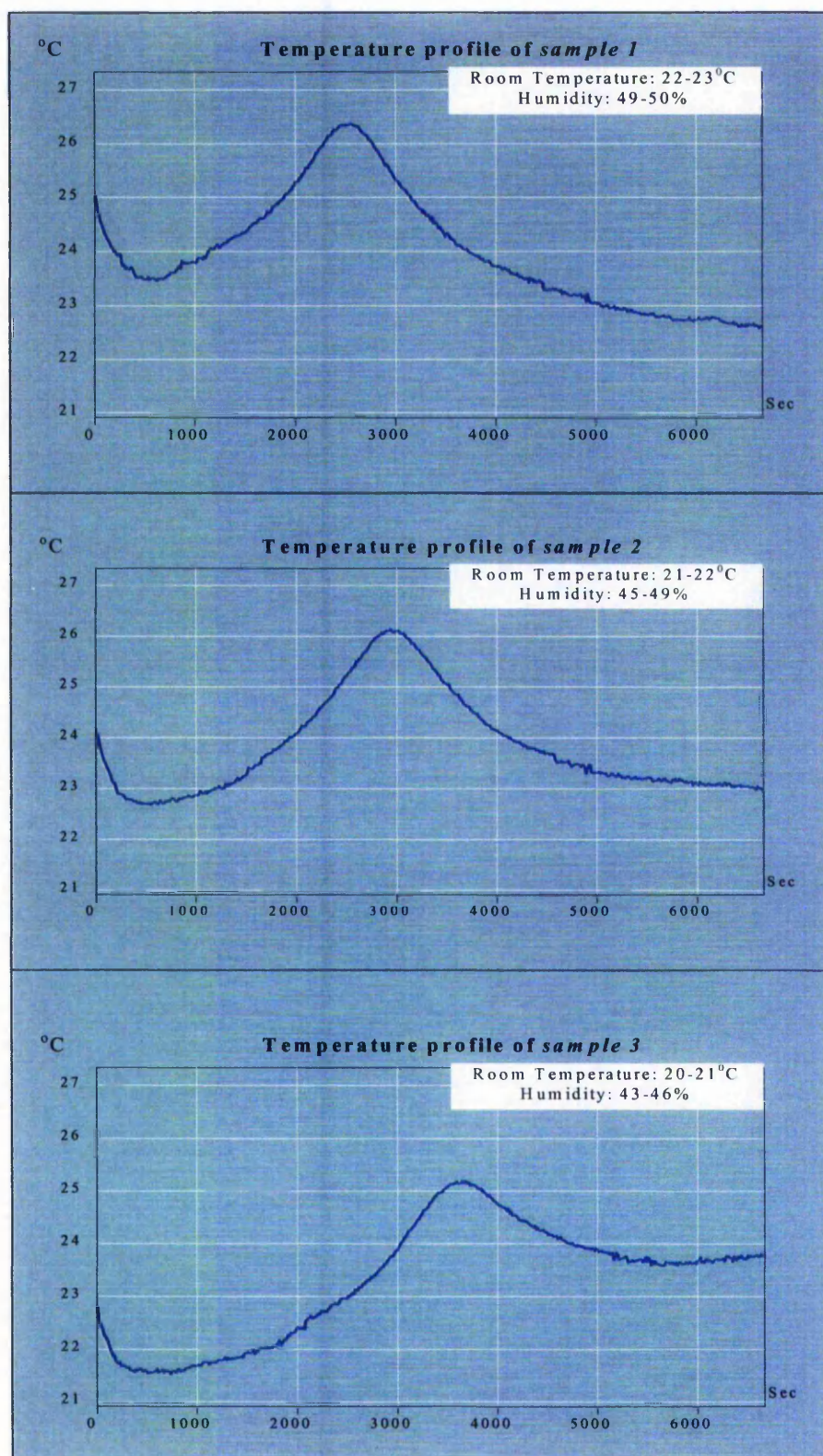


Figure 3.5: Variation of temperature ( $^{\circ}\text{C}$ ) with time (sec) after mixing and cooling to room temperature for para-toluene-sulphonic acid inhibited alkoxy-ethyl cyanoacrylate/alumina initiated with caffeine (all concentrations are the same).

### 3.6.2 Hardness

Although cyanoacrylate monomers are capable of rapid polymerisation with typical reaction times of a few seconds, resulting in a polymer with a high degree of polymerisation, it is very unlikely that complete polymerisation of the monomer takes place during manufacture of the compacts. The polymerisation process is dependant on diffusion of the initiator, and this, in turn, will affect local concentrations of initiator, inhibitor and monomer, which will affect the polymerisation process. Arguably, this may be an advantage in compact machining, since any residual monomer will plasticise, and assist both powder cohesion and compact shape retention under shear loading

In order to determine the level of stability of manufactured compacts, hardness tests were made on an alumina/cyanoacrylate compact and a 'pure' cyanoacrylate compact using a Vickers Pyramid Hardness Testing Machine. *Table 3.9* details the constituent components of the compacts.

*Table 3.9: Compositions of samples used for hardness tests*

|                                    | <i>Alumina/cyanoacrylate compact</i> | <i>'Pure' cyanoacrylate compact</i> |
|------------------------------------|--------------------------------------|-------------------------------------|
| <i>Cyanoacrylate</i>               | 99.2%w                               | 99.9%w                              |
| <i>Para-toluene-sulphonic acid</i> | 0.4%w                                | -                                   |
| <i>Caffeine</i>                    | 0.4%w                                | 0.01%w                              |
| <i>Alumina powder</i>              | 48.3% V <sub>f</sub>                 | -                                   |

A weight of 1 kilogram was used for the hardness testing. The samples were tested 7 hours after the mixing process. Black marker ink was applied on the surface of the samples to improve the visibility of the indentations under the microscope of the test machine. The standard test procedure was used. An average of 5 readings was taken for each sample.

From the results shown in *Table 3.10*, the hardness of the alumina-containing compact was more than double that of the 'pure' cyanoacrylate (from 8.76 to 19.84). The black marker ink was found to be very effective in assisting the measurement of the diagonal lengths of the hardness indentations. A comparison of hardness values taken with and without black ink on the surface showed that it did not influence the actual hardness, but simply made the readings easier and more reproducible to measure.

*Table 3.10: The hardness of 'pure' cyanoacrylate compact and alumina/cyanoacrylate compact at 7 hours after mixing.*

| <i>Sample</i>                        | <i>Vickers Pyramid Numerals Mean</i> | <i>*Hardness in SI unit (MPa)</i> |
|--------------------------------------|--------------------------------------|-----------------------------------|
| <i>'Pure' Cyanoacrylate compact</i>  | 8.76                                 | 85.9                              |
| <i>Alumina/cyanoacrylate compact</i> | 19.84                                | 194.6                             |

\*To convert HV to MPa multiply by 9.807.

In this case, the lower bound estimate 'rule of mixtures' was in reasonable agreement with the practical result, i.e.

$$\frac{1}{H_{Comp}} = \frac{V_M}{H_M} + \frac{V_P}{H_P}$$

where  $H_M$  = Hardness of the matrix = 85.9 MPa.

$H_P$  = Hardness of the particles = 194.6 MPa.

$V_M$  = Volume fraction of the matrix = 0.55.

$V_P$  = Volume fraction of the particles = 0.45.

This gives an estimated value of 152 MPa. The sample containing alumina was subjected to further testing after a period of time. The test was carried out to examine the development of the compact's hardness, which can be used as an indication of the long term stability of the green compact. An average of 5

readings was taken for each final reading. The same compact was tested with the same procedure to maintain the accuracy of the result.

Figure 3.6 shows the variation of the compact hardness with time. From the graph, the maximum hardness of the alumina-containing compact was developed over a period of 27 hours after mixing. It can also be noted that the compact is very stable, with there being no change in the hardness even more than 18 months after mixing.

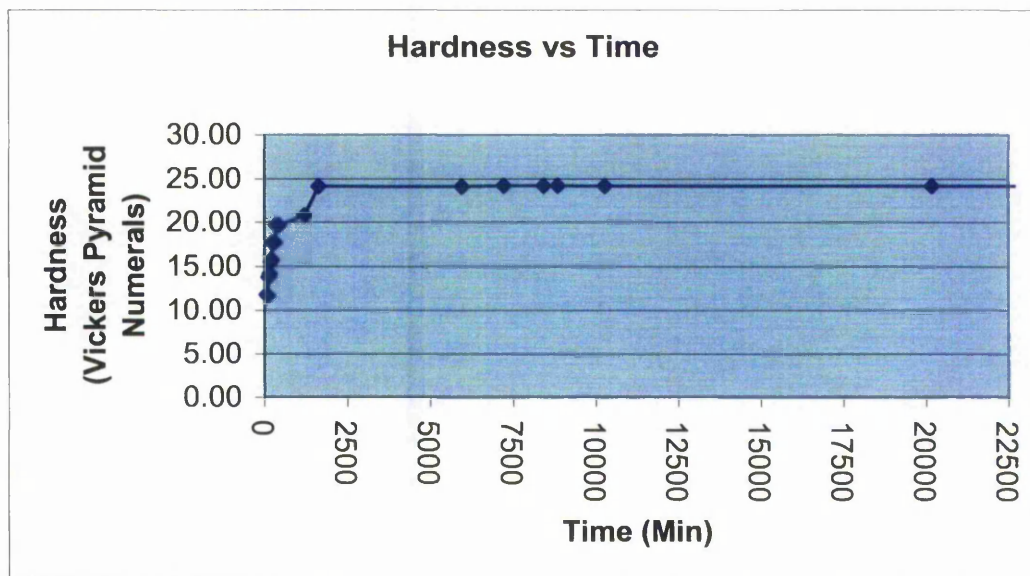


Figure 3.6: The variation of compact hardness with time.

### 3.6.3 Summary

This chapter describes and discusses the experimental procedures that have been developed for the moulding of green compacts using cyanoacrylate as the binder. From the results for each stage, i.e. mixing, inhibition, initiation, and mould material selection, a reproducible and appropriate moulding technique based on the PRIME process has been identified. This comprises the following aspects:

- Alkoxy-ethyl cyanoacrylate had the lowest blooming level and an appropriate viscosity within the target range.
- Low soda grade calcined alumina powder could be mixed with the cyanoacrylate binder up to a maximum volume fraction of 0.49.
- Para-toluene-sulphonic acid has been confirmed to be an effective inhibitor, with only as little as 3%w of binder required, while glacial acetic acid required up to 8%w for effective inhibition of the polymerisation.
- Caffeine was used as an initiator for the cyanoacrylate polymerisation since its inclusion at the identified concentrations had no perceptible influence on the ease of mixing, but the curing times decreased with increasing caffeine concentration.
- Polypropylene was selected as the first choice mould material because of its low cost and good availability.
- The hardness of the compact developed quickly, followed by a more gradual increase to be a maximum 27 hours after processing, and was then stable for at least 18 months.
- The polymerisation temperature profiles for three separate batches of nominally identical materials, concentrations and mixing procedure were matched very closely and were considered to exhibit good reproducibility.

In summary, a moulding technique has been successfully developed to produce green compacts. The use of controlled procedures has enabled a reproducible and effective process to be achieved.

## **Chapter 4 Green Machining**

### **4.1 Introduction**

The alumina/cyanoacrylate mixtures produced as described in *Chapter 3* had good mechanical properties in that they were chemically stable over a period of time and could be handled without difficulty. These factors indicated that there was a reasonable probability that the cyanoacrylate binder would provide sufficient strength and stability to permit green machining using appropriate conventional tools and machining conditions, to provide parts with good tolerances prior to sintering.

Thus, in this chapter, green machining of the compacts using conventional machining operations and tools has been investigated. The main objectives of this phase of the research were to:

- **Determine the machinability of the alumina/cyanoacrylate green compact**

Conventional machining operations, *viz.* drilling, turning and milling were applied to the green compacts.

- **Investigate the influence of tool material**

The tool material is one of the important aspects that has a direct influence on the quality of the machined part, as well as the efficiency of the machining operation. Four common tool materials were selected

to establish a suitable tool material for the machining of the green compact.

- **Investigate the type of support**

Clamping or holding of a ceramic compact for machining is generally a problem because of its fragility. For precise machining however, the work piece must be held rigidly and without distortion or stress concentration. Investigation of the support methods for the machining of the alumina/cyanoacrylate blanks was carried out.

## **4.2 Machinability of Alumina/Cyanoacrylate compacts**

The machinability of a material is usually defined in terms of three factors:

- Surface finish and integrity of the machined part
- Tool life obtained
- Force and power requirements

As a result, good machinability indicates good surface finish and integrity, long tool life, and low force and power requirements [Kalpakjian, 1997].

Since the PRIME process is relatively new, there has been very little research into the properties of the green compacts. Consequently, given the unusual nature of these compacts, it was considered that the machining of them might be quite dissimilar to the machining of other ceramic compacts.



#### 4.2.1 Preliminary Machining Exercises

Generally when machining a material, there is at least a reasonable body of experience that can be used to guide the selection of the tools and operating conditions. Since this is not the case with the present material, it was decided to undertake some preliminary trials to determine if a suitable machining regime could be identified which would be appropriate for more detailed evaluation trials. The PRIME green compacts used for the preliminary study had the composition as detailed in *Table 4.1*. The compacts were manufactured as cylinders 30 mm diameter and 20 mm high.

*Table 4.1: Composition of alumina/cyanoacrylate compacts.*

|               |  |        |             |
|---------------|--|--------|-------------|
| <b>Binder</b> | Cyanoacrylate ( <i>Loctite 408</i> )           | 99.2%w | 51.7% $V_f$ |
|               | Para-toluene-sulphonic acid ( <i>Aldrich</i> ) | 0.4%w  |             |
|               | Caffeine ( <i>Aldrich</i> )                    | 0.4%w  |             |
| <b>Powder</b> | Alumina powder ( <i>Alcan MA2LS</i> )          | 76.0%w | 48.3% $V_f$ |

For the preliminary drilling exercise, a pedestal precision drill (*Ajax Precision Drill, type B-16L*) was employed, in which a vacuum vice with soft rubber jaw was used to hold the compact firmly, and without fracture, on the machine table. A spindle speed of 700 rpm was used with no coolant fluid. A new 4 mm diameter high-speed steel (HSS) drill bit was used. It was found that using these conditions enabled the samples to be drilled successfully, indicating that the cyanoacrylate binder has appropriate mechanical and thermal properties for green machining. These results enabled a range of drilling parameters to be identified such that they could be systematically evaluated.

Establishing quantitative relationships to define the machinability of a material is relatively expensive because of the number of variable parameters.

Therefore the objective of these initial experiments was to determine the feasibility of machining alumina/cyanoacrylate compacts.

#### 4.2.2 Machining of Cyanoacrylate Binder

The binder phase in a green ceramic compact is not only a temporary vehicle for homogeneously packing the powder particles to the desired shape, but it should also provide sufficient strength to withstand the applied forces during a machining process. In this section the results and observations on the turning of a sample of polymerised cyanoacrylate are described and discussed. These machining trials employed a *Colchester Student 1800 Series* lathe. The compacts were made of 99.9%w alkoxy-ethyl cyanoacrylate (*Loctite 408*) and 0.1%w caffeine (*Aldrich*). Polypropylene (PP) syringes were used to mould the compact to a cylindrical shape of dimensions 13 mm diameter and 50 mm long. Samples were machined with the machining conditions listed in *Table 4.2* for various combinations of cutting speeds and depths of cut at feed rates of 0.1 mm/rev using a carbide tool. Continuous swarf was produced when cutting the pure cyanoacrylate compact, see *Figure 4.1*.

An important result from these trials was that the cyanoacrylate compacts have enough strength to withstand the cutting forces. The surface finish of the compacts became increasingly rougher as the cutting speed increased. This was not regarded as significant since the primary objective of these trials was focused on ensuring that there was a reasonably good expectation that the cyanoacrylate would provide the necessary support as the binder phase during machining of the powder/binder compacts.

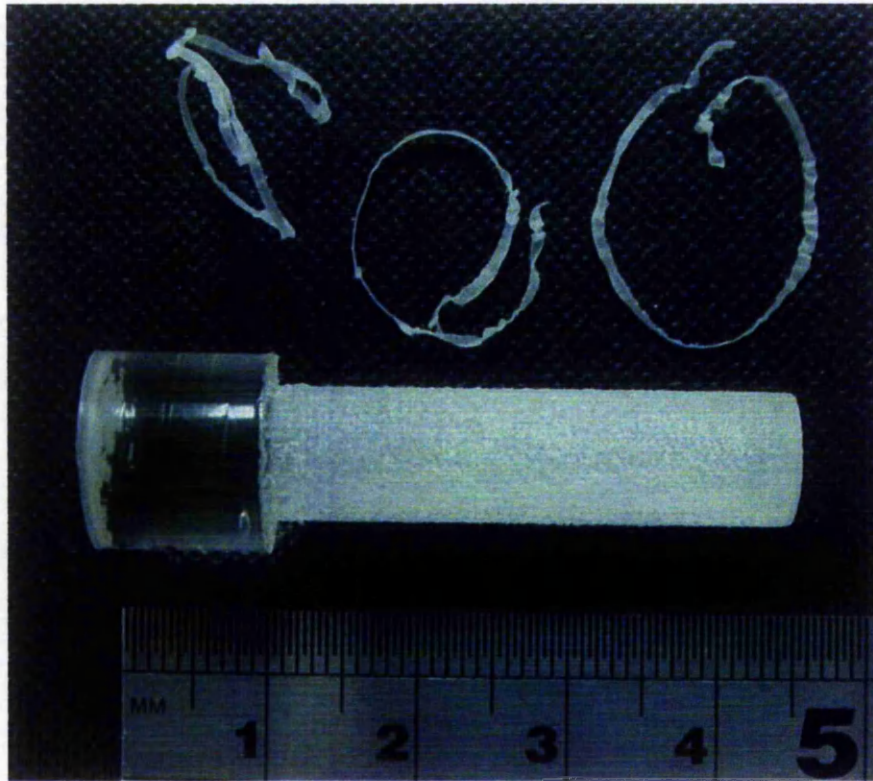


Figure 4.1: Continuous swarf was formed when cutting pure cyanoacrylate compacts with cutting speed 2000 rpm, cut depth 1.0 mm, and feed rate 0.1 mm/rev using a carbide tool.

Table 4.2: Combinations of cutting speeds and cut depths for turning cyanoacrylate cylinders.

| Sample | Cutting speed (rpm) | Depth of cut (mm) | Observations   |
|--------|---------------------|-------------------|--|
| 4.2A   | 1000                | 0.5               | <ul style="list-style-type: none"> <li>● Turned with ease, without fracture</li> <li>● Continuous swarf were formed</li> </ul>                                 |
| 4.2B   | 1000                | 1.0               | <ul style="list-style-type: none"> <li>● Turned with ease, without fracture</li> <li>● Continuous swarf were formed</li> </ul>                                 |
| 4.2C   | 1500                | 0.5               | <ul style="list-style-type: none"> <li>● Turned with ease, without fracture</li> <li>● Continuous swarf were formed</li> </ul>                                 |
| 4.2D   | 1500                | 1.0               | <ul style="list-style-type: none"> <li>● Turned with ease, without fracture</li> <li>● Continuous swarf were formed</li> </ul>                                 |
| 4.2E   | 2000                | 0.5               | <ul style="list-style-type: none"> <li>● Turned with ease, without fracture</li> <li>● Continuous swarf were formed</li> </ul>                                 |
| 4.2F   | 2000                | 1.0               | <ul style="list-style-type: none"> <li>● Turned with ease, without fracture</li> <li>● Continuous swarf were formed</li> <li>● Rough surface finish</li> </ul> |

The results of the preliminary machining trials presented in *sections 4.2.1* and *4.2.2*, i.e. drilling alumina/cyanoacrylate mixtures and turning 'pure' cyanoacrylate, both demonstrated that machining of the green compacts could be performed using conventional machines and tooling with good success.

### **4.3 Tool Materials**

The green ceramics produced in this research are broadly similar to those produced by Ceramic Injection Moulding, rather than the more conventional dry pressing or slip casting processes. They also have some similarities with glass particle reinforced thermosetting polymer matrix composites. These types of materials are generally very abrasive to the cutting tools in machining [Kim et al., 1992]. Consequently, it is probable that a cutting tool for the green machining of the present compacts should have the following characteristics in order to produce well-machined products at a reasonable cost:

- **Hardness**

A high hardness would normally be taken as a good guide to a tool material having good resistance to abrasive wear.

- **Toughness**

A reasonable value of toughness would probably contribute to good wear resistance since it would provide improved resistance to chipping (or microchipping) by the abrasive ceramic particles in the green compact.

- **Wear resistance**

A good wear resistance is likely to be of importance in the present case to not only ensure that good dimensional tolerances are maintained and the cutting forces are minimised, but also to limit any temperature rises due to friction from the rubbing of a rough surface against the work piece.

- **Thermal Conductivity**

Since the depolymerisation temperature of the cyanoacrylate binder is relatively low, the flow of heat, and resultant temperature distributions, must be appropriate to ensure that the newly cut surface of the work piece does not get too hot. The thermal conductivity of the tool material will affect the heat flow. It is most likely that a good thermal conductivity would be advantageous.

- **Chemical stability**

The tool material needs to have sufficient chemical stability to effectively resist attack by any of the chemicals in the compact mixture. For the materials used in the present mixtures, it is very unlikely that there would be any significant chemical reactions between the commonly used tool materials and the compacts.

#### **4.3.1 Tool Material Trials**

The objective of this series of trials was to determine a suitable tool material for machining the green compact. Drilling was chosen as the most appropriate machining operation on which to base the assessment of the

performance of the tool materials that were considered to be most suitable, using the criteria outlined above. The main reasons for this are that a single drilling operation actually covers a range of cutting conditions, and it will also generally be an important part of the machining sequence for green compacts when producing operational components.

The drilling operation was performed on a *Bridgeport Interact 720X* Computer Numerical Control (CNC) machine, *Figure 4.2*, with four 4 mm diameter drill bits of 4 different materials: high-speed steel (HSS) jobber drill, tungsten carbide tipped masonry drill, HSS *TiN* coated drill and solid carbide drill.

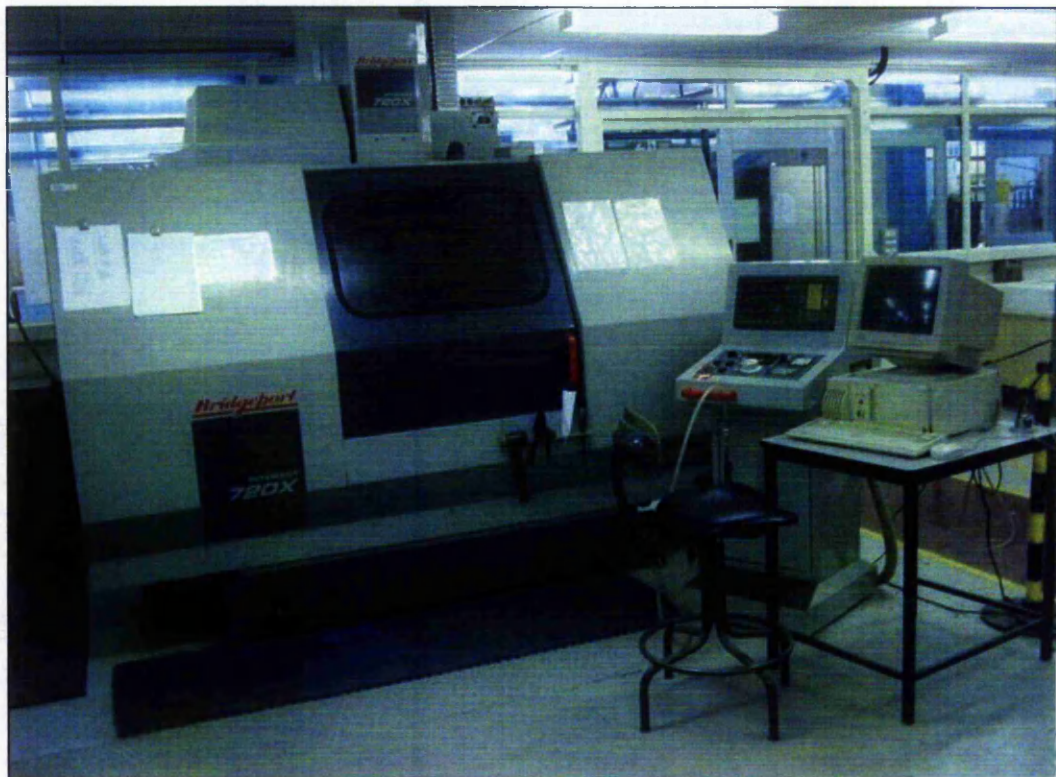


*Figure 4.2: Bridgeport Interact 720X Computer Numerical Control (CNC) machine.*

Each drill was used to drill 4 holes in the compact at a constant rotational speed of 120 rpm, 370 rpm, 1100 rpm and 2000 rpm. The samples were green

compacts containing binder of 99.2%w cyanocrylate (*Loctite 408*), 0.4%w para-toluene-sulphonic acid, 0.4%w caffeine and ceramic powder of 48% $V_f$  alumina. The samples were firmly gripped in position in the CNC using a collet. The used drills were inspected in a microscope to compare to an unused drill of the same type. *Table 4.3* details the relevant observations made during these trials.

*Table 4.3: Observations made during the drilling of the green compacts.*

| <b>Drill type</b>                            | <b>Spindle Speed (rpm)</b> | <b>Observation</b>  |
|--|----------------------------|---|
| <b>HSS jobber drill</b>                      | 120                        | <ul style="list-style-type: none"> <li>● Swarf stuck to drill while drilling</li> <li>● Continuous swarf</li> </ul>     |
|  | 370                        | <ul style="list-style-type: none"> <li>● Swarf stuck to drill while drilling</li> <li>● Continuous swarf</li> </ul>     |
|  | 1100                       | <ul style="list-style-type: none"> <li>● Swarf did not stick to drill</li> <li>● Continuous swarf</li> </ul>            |
|  | 2000                       | <ul style="list-style-type: none"> <li>● Swarf did not stick to drill</li> <li>● Continuous swarf</li> </ul>            |
| <b>Tungsten carbide tipped masonry drill</b> | 120                        | <ul style="list-style-type: none"> <li>● Swarf stuck to drill while drilling</li> <li>● Non continuous swarf</li> </ul> |
|  | 370                        | <ul style="list-style-type: none"> <li>● Swarf stuck to drill while drilling</li> <li>● Non continuous swarf</li> </ul> |
|  | 1100                       | <ul style="list-style-type: none"> <li>● Swarf stuck to drill while drilling</li> <li>● Non continuous swarf</li> </ul> |
|  | 2000                       | <ul style="list-style-type: none"> <li>● Swarf stuck to drill while drilling</li> <li>● Non continuous swarf</li> </ul> |
| <b>HSS TiN coated drill</b>                  | 120                        | <ul style="list-style-type: none"> <li>● Swarf stuck to drill while drilling</li> <li>● Continuous swarf</li> </ul>     |
|  | 370                        | <ul style="list-style-type: none"> <li>● Swarf stuck to drill while drilling</li> <li>● Continuous swarf</li> </ul>     |
|  | 1100                       | <ul style="list-style-type: none"> <li>● Swarf did not stick to drill</li> <li>● Continuous swarf</li> </ul>            |
|  | 2000                       | <ul style="list-style-type: none"> <li>● Swarf did not stick to drill</li> <li>● Continuous swarf</li> </ul>            |
| <b>Solid carbide drill</b>                   | 120                        | <ul style="list-style-type: none"> <li>● Swarf did not stick to drill</li> <li>● Continuous swarf</li> </ul>            |
|  | 370                        | <ul style="list-style-type: none"> <li>● Swarf did not stick to drill</li> <li>● Continuous swarf</li> </ul>            |
|  | 1100                       | <ul style="list-style-type: none"> <li>● Swarf did not stick to drill</li> <li>● Continuous swarf</li> </ul>            |
|  | 2000                       | <ul style="list-style-type: none"> <li>● Swarf did not stick to drill</li> <li>● Continuous swarf</li> </ul>            |

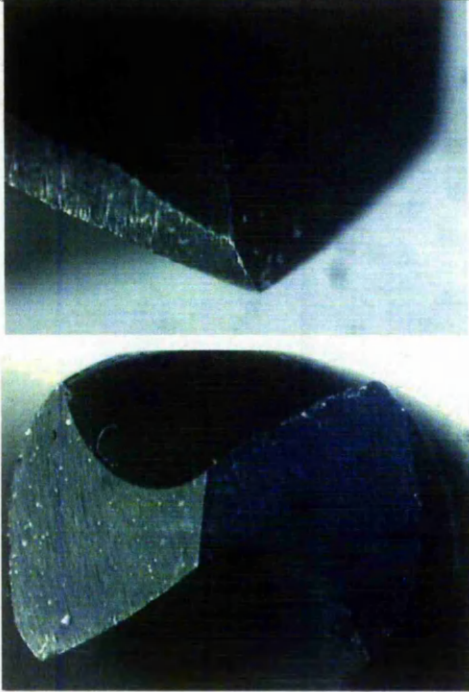
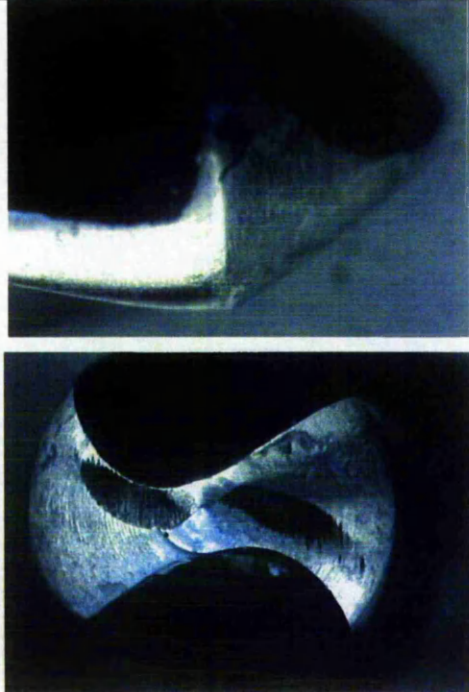
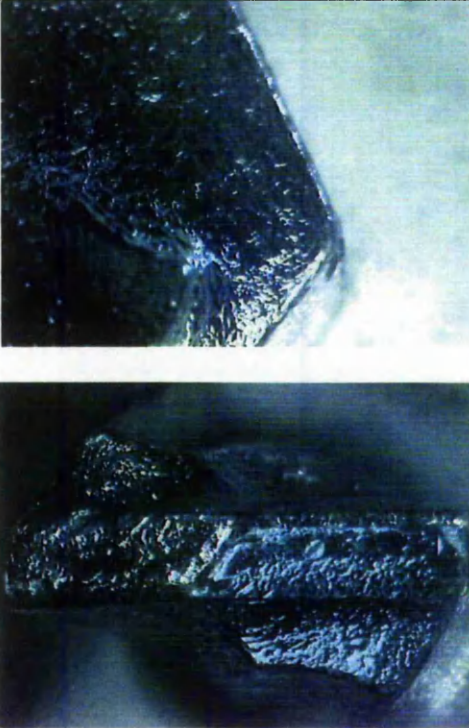
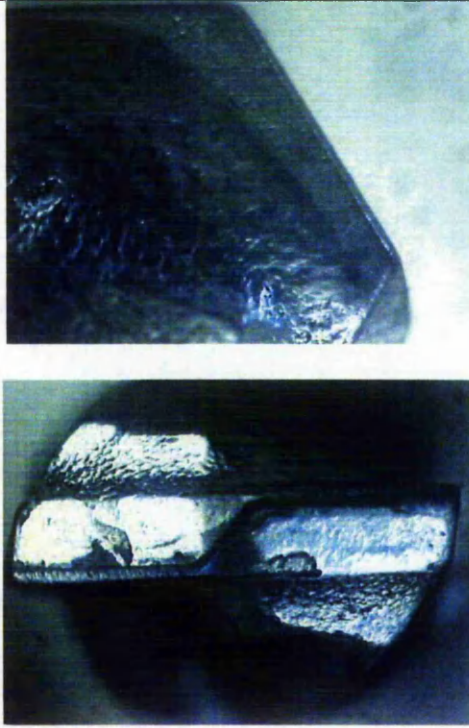
| <b>Drill type</b>               | <b>Unused drill</b>   | <b>Used drill<br/>(Spindle Speed 2000 rpm)</b>                                       |
|---------------------------------|---|--|
| <b>HSS<br/>jobber<br/>drill</b> |   |   |
| <b>Masonry<br/>drill</b>        |  |  |

Figure 4.3: Comparison of new and used drills. Note all the drills are approximately 4 mm in diameter.



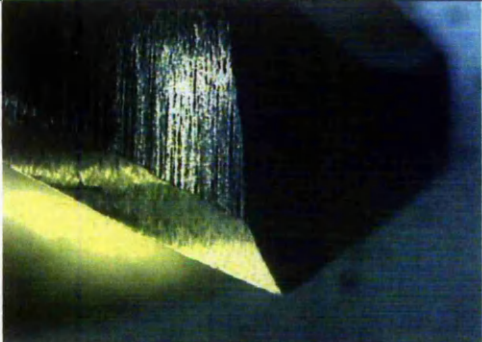
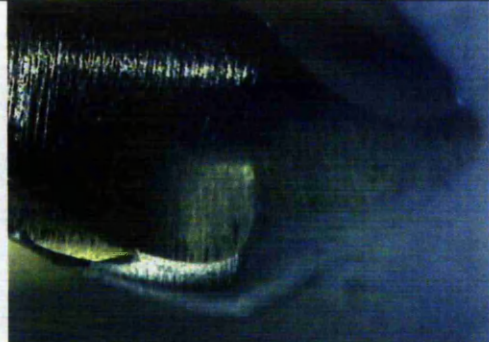
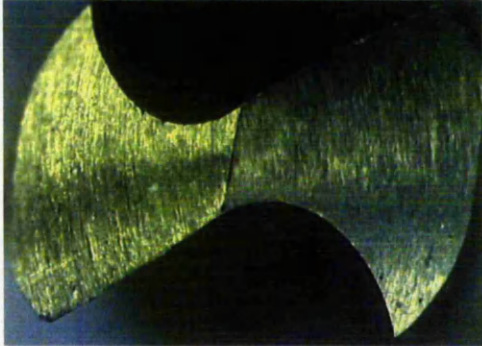
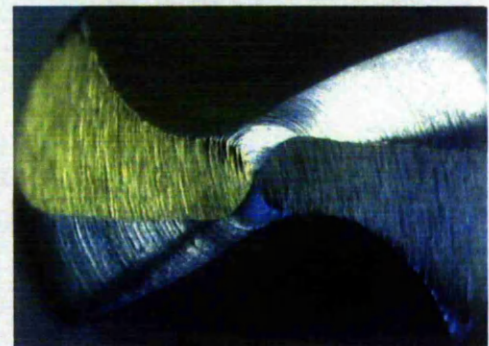
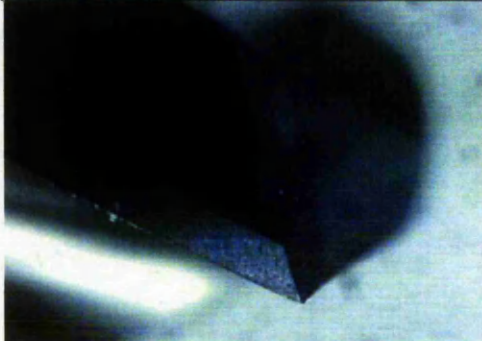
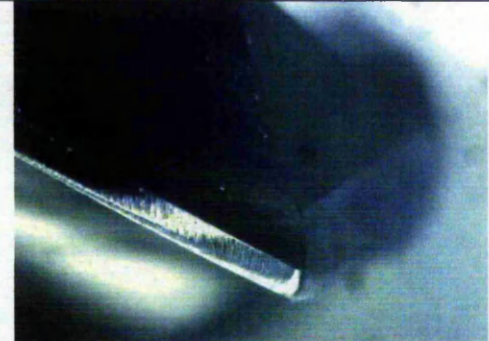
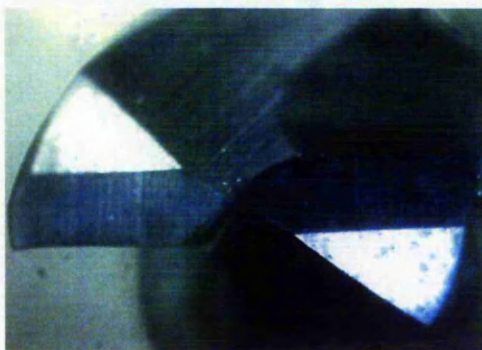
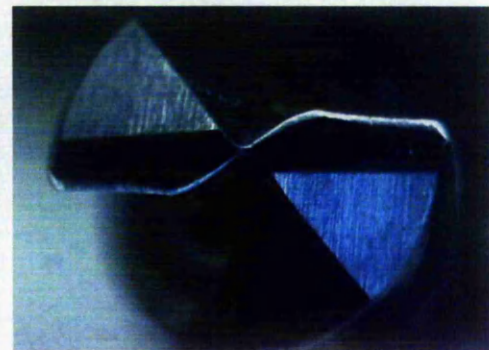
| <b>Drill type</b>                       | <b>Unused drill</b>   | <b>Used drill<br/>(Spindle Speed 2000 rpm)</b>                                       |
|---|---|--|
| <b>HSS<br/>TiN<br/>coated<br/>drill</b> |    |    |
|   |   |   |
| <b>Solid<br/>carbide<br/>drill</b>      |  |  |
|   |  |  |

Figure 4.3(continued): Comparison of new and used drills.

From the observations shown in *Table 4.3*, the general characteristics of the green compact machining were obtained. The HSS jobber drill, masonry drill and HSS *TiN* coated drill clearly exhibited significant wear at their tips, although the flutes were not as badly worn. This degree of wear would affect the effectiveness of the cutting process, and also the surface finish of the compact, because of the interaction between the worn tool surface and the work piece having a 'rubbing' component as well as the cutting action. The solid carbide drill showed almost no signs of wear after drilling 4 holes in the compact. Therefore it was used to drill a further 19 holes, i.e. 23 holes in total to cause the wear shown in *Figure 4.3*.

Swarf was stuck to the HSS and *TiN* coated HSS drills at low speeds, i.e. 120 rpm and 370 rpm, and also strongly attached to the masonry drill at all speeds, see *Figure 4.4*, whereas it did not stick to the carbide drill at any speed.



*Figure 4.4: Swarf stuck to the masonry drill surface*

The factors which are most likely to influence the adherence of the swarf to the drill are (a) chemical interaction between the drill material and the

cyanoacrylate binder, (b) pressure induced welding of the swarf to the drill, (c) temperature, (d) rotational centrifugal forces, and (e) flute geometry. It would be expected that the temperature of the swarf would increase with increasing cutting speed. Since it was observed for the HSS and *TiN* coated HSS drills that the swarf did not adhere at the higher spindle speeds, this would indicate that in this range the temperature has negligible effect. The flute geometries are generally similar, which would indicate that this is not a significant factor in the present case. Therefore it is most likely that there is a chemical interaction between the binder and the drill material, probably assisted by the applied pressure arising during cutting, which is not sufficiently strong to counteract the centrifugal forces at the higher spindle speeds.

The solid carbide drill exhibited relatively little wear after drilling 23 holes at 2000 rpm. Therefore, it was considered to be a highly suitable candidate tool material for the machining of the alumina/cyanoacrylate compacts.

#### **4.4 Drilling**

A CNC programme for drilling the green compact was developed, so that the speed and feed rate can be rapidly adjusted and reproducibly applied. Thirty mm diameter cylindrical samples of nominal lengths 20 mm were cast in cylindrical polyethylene moulds (*METASERV Moulds*) since the cyanoacrylate did not adhere to this mould surface (*Figure 4.5*). The composition of the mixture and the preparation procedure were as specified in *section 3.4.2*. After mixing, the feedstock was poured into the polyethylene moulds, and cured in ambient conditions overnight. Samples were removed from the moulds without difficulty.

From the results presented in *section 3.6.2*, it was known that the feedstock would effectively completely polymerise after 27 hours.

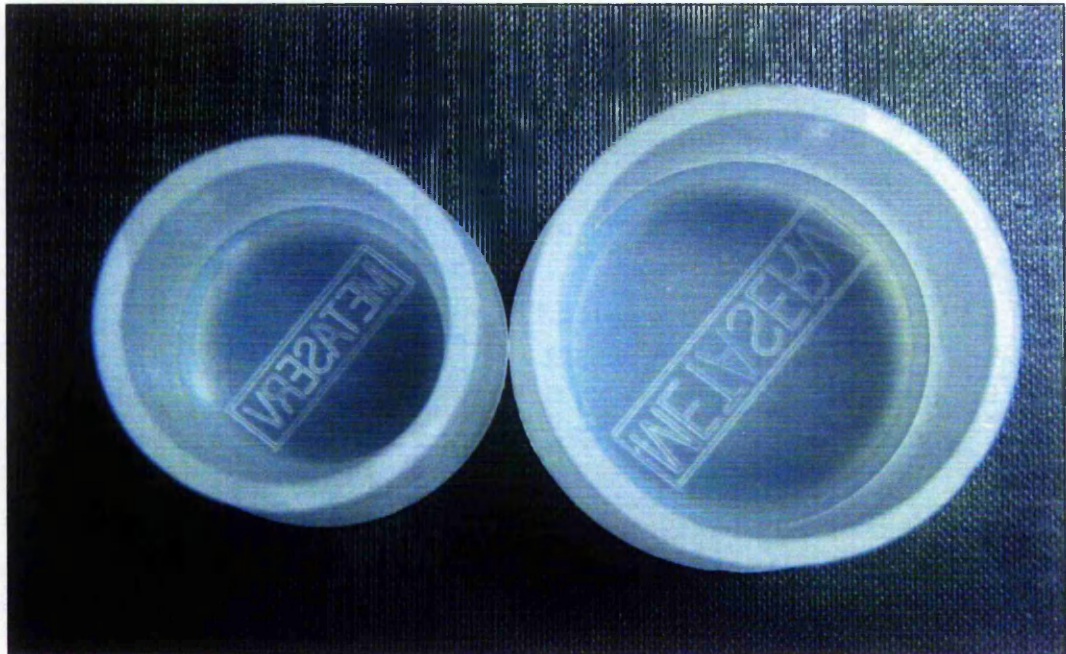


Figure 4.5: METASERV 30 mm (left) and 40mm (right) diameter cylindrical polyethylene moulds

Drilling of the compacts was performed on the *Bridgeford* CNC machine using a 4 mm diameter solid carbide drill. Four holes were drilled in each case at a cutting speed of 1000 rpm, 1500 rpm or 2000 rpm, with a feed rate of 100 mm/min in all cases. *Figure 4.6(a)* shows a schematic diagram of the machined compact, in which those holes labelled as *Group 1* were machined at 1000 rpm, *Group 2* were machined at 1500 rpm and *Group 3* at 2000 rpm; while *Figure 4.6(b)* shows the actual drilled compact.

It can be seen in *Figure 4.6(b)* that the drilled holes are regular with no cracking or chipping. The green compact machined well without any need for unusual precautions. This is a clear demonstration that the strength and rigidity of the mixture composition and preparation procedure are appropriate. It was also

possible to position the holes relatively closely together without affecting the machining behaviour.

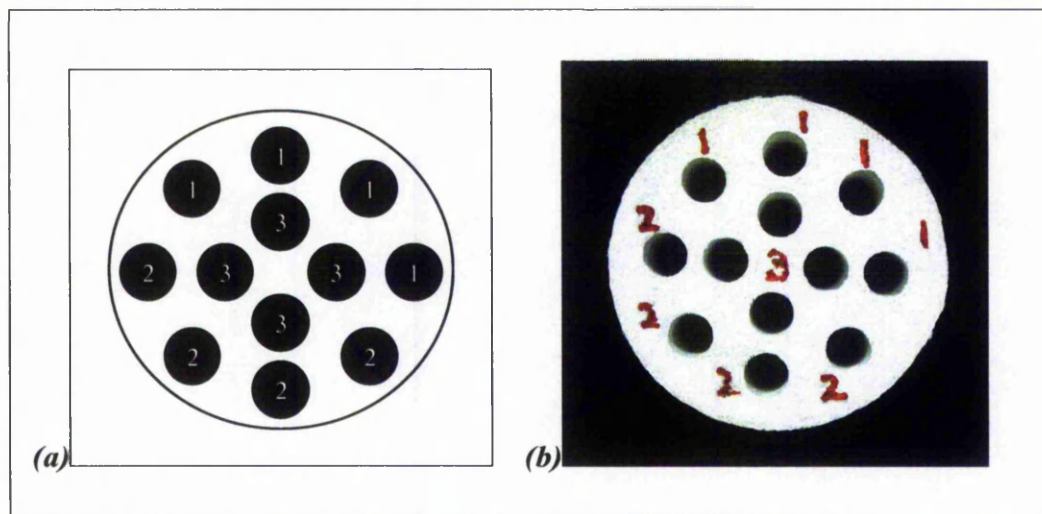


Figure 4.6: (a) Schematic diagram of the machined compact, in which those holes labelled as Group 1 was machined at 1000 rpm, Group 2 was machined at 1500 rpm and Group 3 at 2000 rpm (b) Actual drilled compact.

The swarf that were produced at all speeds were continuous and not discoloured. This latter factor indicated that there was a relatively small amount of heat generated during the cutting process, and that the temperatures during drilling were below the debinding point of the cyanoacrylate. Therefore, coolant was not required when machining the green compact, as there were no signs of any thermal degradation of the cyanoacrylate binder.

## 4.5 Turning

The basic operation of turning is probably the most commonly used technique in experimental research on material cutting. The advantage of turning is that the cutting conditions are relatively constant, unlike drilling where the cutting speed at the tip will vary with radius. For the turning of the green compact,

a single-point cutting tool was used on a *Colchester Student 1800 Series* lathe (see *Figure 4.7*). The green compact samples were prepared using the mixture composition and preparation procedure described in *section 3.4.2*. The specimens were prepared using a polypropylene mould to be cylinders of nominal dimensions 15 mm diameter and 65 mm long.



*Figure 4.7: Colchester Student 1800 Series lathe*

The following factors were considered with regard to the selection of tools and machining conditions to be used:

- **Tool Material and Tool Type**

As discussed above, *section 4.3*, a solid carbide drill was successfully used for the drilling trials. However, it was noted that the tip still underwent some abrasive wear, albeit relatively limited. Grzesik et al. [2003] have studied the cutting mechanics of various coated carbide tools. Although not directly comparable to the present situation, it was noted in their study that coated carbide tool tips generally performed better than uncoated carbide. Therefore, a coated carbide turning insert was selected for use in the present series of turning trials.

- **Tool Geometry**

The various tool angles used have important functions in cutting operations [Kalpakjian, 1997]. Rake angle plays an important role in controlling the direction of swarf flow and the strength of the tool tip. In this present study it must be ensured that the temperature increase during turning must be kept sufficiently low to avoid thermal degradation effects, such as depolymerisation. Thus, a positive rake angle tool was selected, since a positive angle improves the cutting operation by reducing forces and temperatures [Kalpakjian, 1997]. Consequently, a multi-layer coated carbide turning insert (*HERTEL*) was selected for these trials. The insert is claimed to be ideal for medium machining applications and is suitable for a range of feed

rates from 0.15 to 0.4 mm/rev and a depth of cut range from 1.0 to 4.2 mm [Kalpakjian, 1997]. The geometry and dimensions of the coated carbide turning insert, with  $+5^\circ$  rake angle and swarf breaker, are shown in *Figure 4.8*.

- **Feed Rate and Cutting speed**

The trials were carried out at three chuck speeds: 1000 rpm, 1340 rpm and 1800 rpm (or cutting speeds: 47.1 m/min, 63.1 m/min and 84.8 m/min respectively, for a 15 mm diameter cylindrical compact), at a feed rate of 0.1 or 0.2 mm/rev and depth of cut of 0.5 or 1.0 mm.

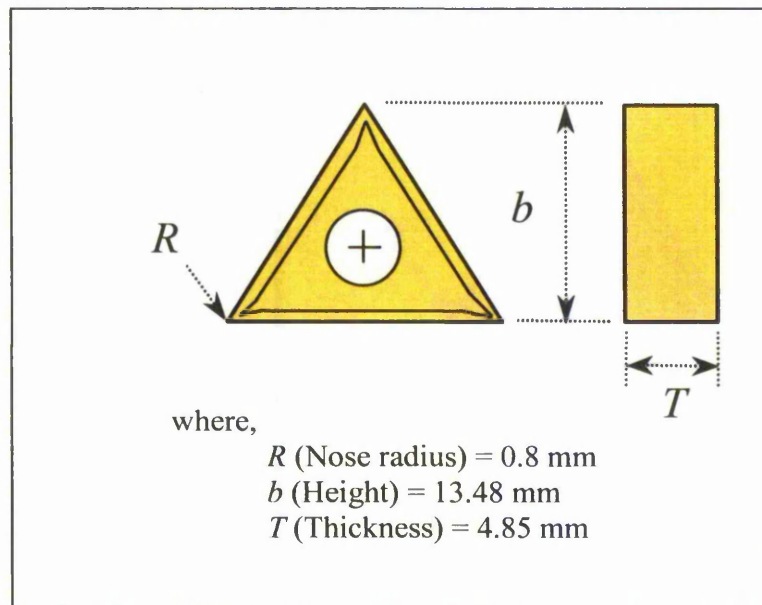


*Figure 4.8: Geometry of coated carbide cutting tool insert.*

*Table 4.4* details the observations from the turning operations. A new tool tip was used for each different cutting condition for a total length of cut of about 30 m. One of the notable observations in this trial is that continuous swarf was



formed during all the operations, see *Figure 4.9*. This type of swarf is normally present in the turning of a ductile material. The work pieces were examined using a SEM for characteristics such as microstructure of the particles. The SEM images of the machined surface (*Figure 4.10*) also show the particles were still bonded together by the cyanoacrylate after the turning operation. This indicates that the tool-work piece interface temperature did not reach the debinding point of the cyanoacrylate.

*Table 4.4: Results and observations of alumina/cyanoacrylate turning operations.*

| <b>Sample</b> | <b>Cutting Speed (m/min)</b> | <b>Depth of cut (mm)</b> | <b>Feed rate (mm/rev)</b> | <b>Observations</b>  |
|---------------|------------------------------|--------------------------|---------------------------|--|
| <b>4.5a</b>   | 47.1                         | 0.5                      | 0.1                       | <ul style="list-style-type: none"> <li>● Turned with ease</li> <li>● Continuous swarf</li> </ul>                               |
| <b>4.5b</b>   |                              |                          | 0.2                       | <ul style="list-style-type: none"> <li>● Turned with ease</li> <li>● Continuous swarf</li> </ul>                               |
| <b>4.5c</b>   |                              | 1.0                      | 0.1                       | <ul style="list-style-type: none"> <li>● Turned with ease</li> <li>● Continuous swarf</li> </ul>                               |
| <b>4.5d</b>   |                              |                          | 0.2                       | <ul style="list-style-type: none"> <li>● Turned with ease</li> <li>● Continuous swarf</li> </ul>                               |
| <b>4.5e</b>   | 63.1                         | 0.5                      | 0.1                       | <ul style="list-style-type: none"> <li>● Turned with ease</li> <li>● Continuous swarf</li> </ul>                               |
| <b>4.5f</b>   |                              |                          | 0.2                       | <ul style="list-style-type: none"> <li>● Turned with ease</li> <li>● Continuous swarf</li> </ul>                               |
| <b>4.5g</b>   |                              | 1.0                      | 0.1                       | <ul style="list-style-type: none"> <li>● Turned with ease</li> <li>● Continuous swarf</li> </ul>                               |
| <b>4.5h</b>   |                              |                          | 0.2                       | <ul style="list-style-type: none"> <li>● Turned with ease</li> <li>● Continuous swarf</li> </ul>                               |
| <b>4.5i</b>   | 84.8                         | 0.5                      | 0.1                       | <ul style="list-style-type: none"> <li>● Turned with ease</li> <li>● Continuous swarf</li> <li>● Insert fairly worn</li> </ul> |
| <b>4.5j</b>   |                              |                          | 0.2                       | <ul style="list-style-type: none"> <li>● Turned with ease</li> <li>● Continuous swarf</li> <li>● Insert fairly worn</li> </ul> |
| <b>4.5k</b>   |                              | 1.0                      | 0.1                       | <ul style="list-style-type: none"> <li>● Turned with ease</li> <li>● Continuous swarf</li> <li>● Insert fairly worn</li> </ul> |
| <b>4.5l</b>   |                              |                          | 0.2                       | <ul style="list-style-type: none"> <li>● Turned with ease</li> <li>● Continuous swarf</li> <li>● Insert fairly worn</li> </ul> |

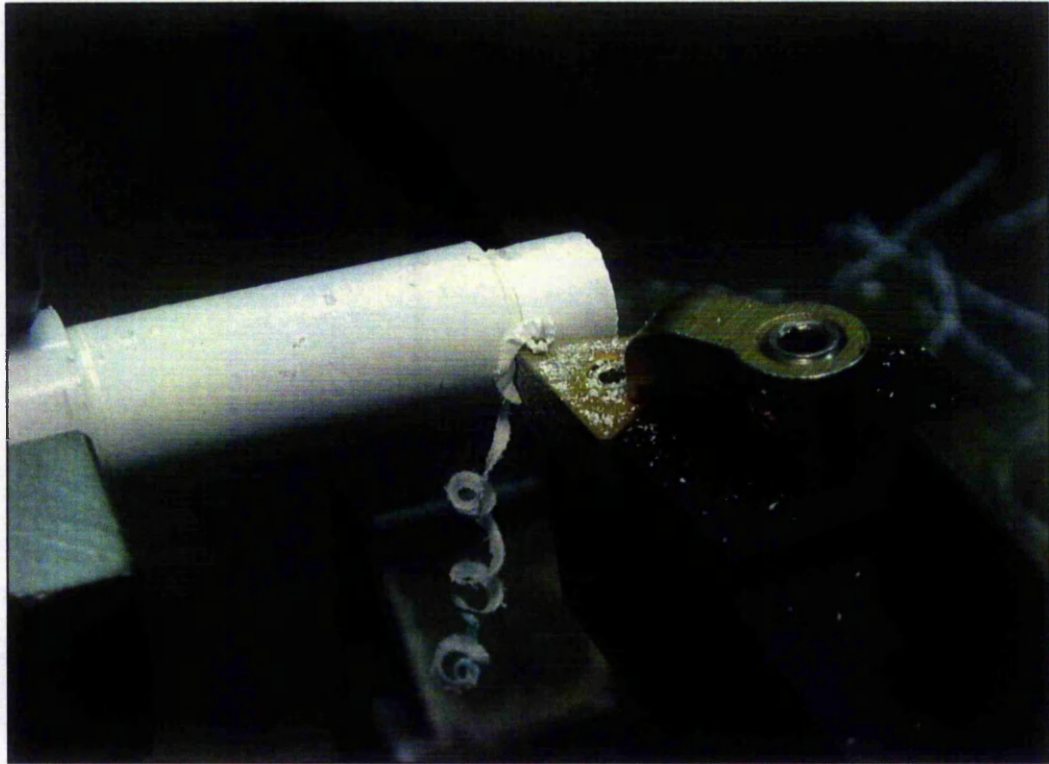
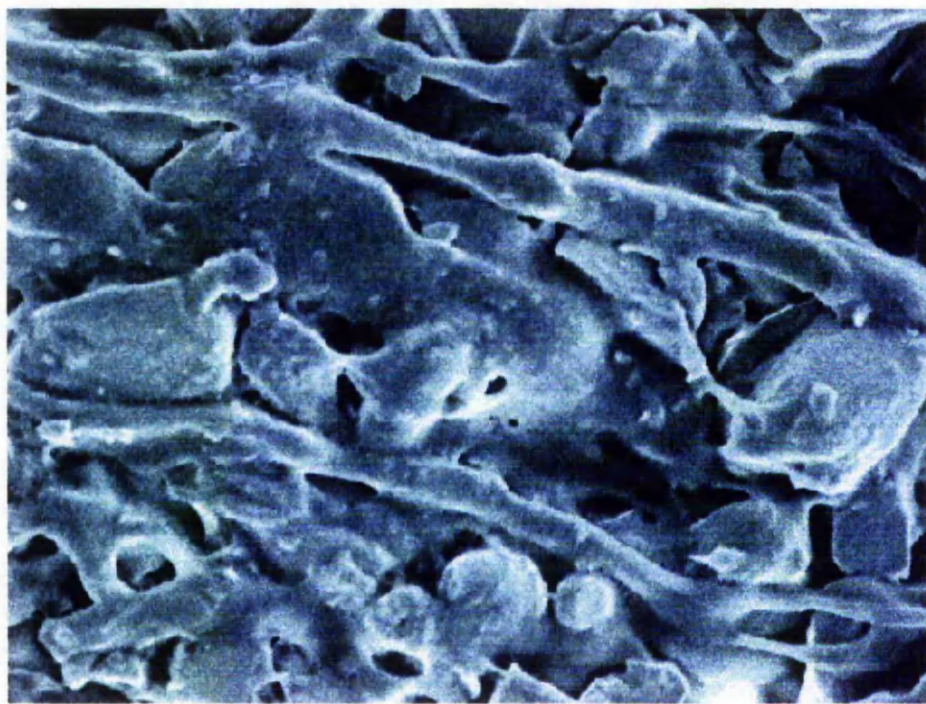


*Figure 4.9: Production of continuous swarf during turning.*



10 $\mu$ m

*Figure 4.10: SEM image on machined surface shows the particles were still bonded together by the cyanoacrylate after machining at a cutting speed of 1800 rpm, feed rate of 0.2 mm/rev, and depth of cut of 1.0 mm.*

A used and a new carbide tool tip were compared in an electron microscope for wear evaluation, *Figure 4.11*. The gold coloured *TiN* coating had worn away, but there was relatively limited wear of the carbide substrate. The wear on the flank face appears to be more significant with respect to tool life than that on the top surface. Further investigation of the tool wear in machining of the compact is discussed below, *section 4.7*.

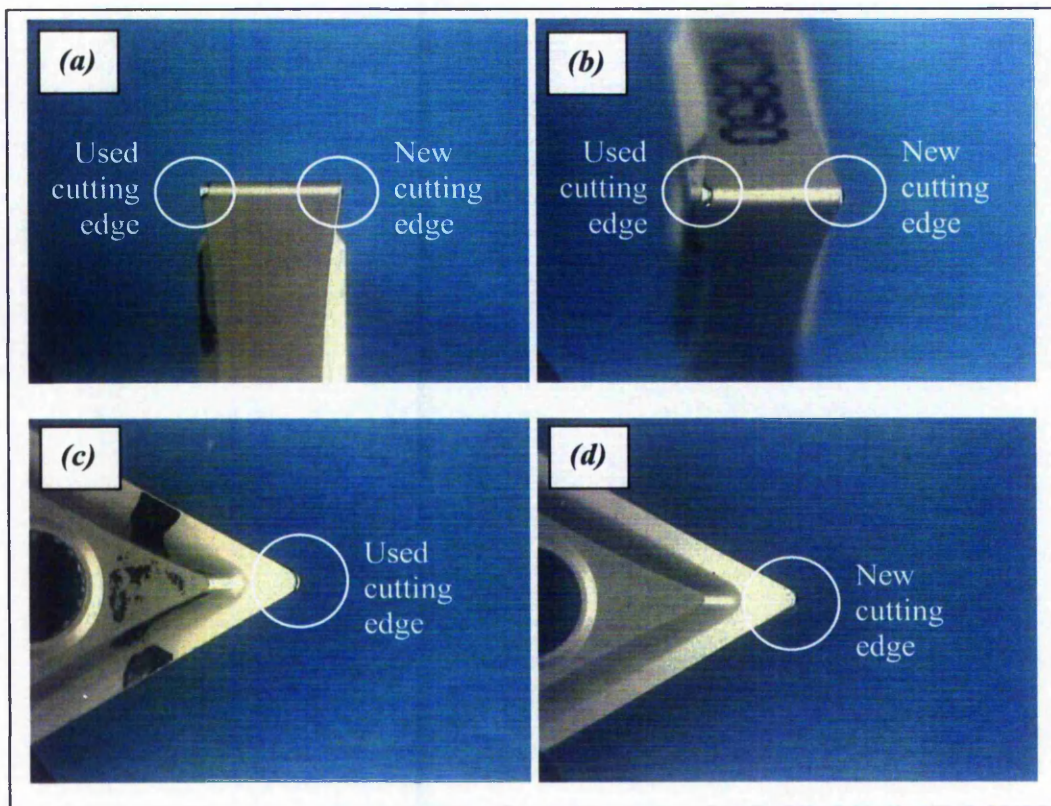


*Figure 4.11: Microscope images on the used and unused cutting edges. (a) Side view (b) End view, (c) and (d) Top view. The cutting edge used to turn the compact for ~100 m, at a cutting speed of 1800 rpm, feed rate of 0.2 mm/rev and depth of cut of 1.0 mm.*

The swarf that was produced during the turning trials can provide some indication of the machining mechanisms and conditions. The swarf were collected and examined using both optical and electron microscopy for characteristics such

as colour and microstructure of the particles. *Figure 4.12(a)* is an electron microscope image of the machined surface of a section of swarf. The swarf was not discoloured, indicating that there was relatively little deformation/friction induced heating during the process. *Figure 4.12(b)* is a higher magnification SEM image of the swarf, which shows that the ceramic particles are still well bonded in the matrix. There was also no loss of cyanoacrylate from the matrix due to the temperature generated during machining causing depolymerisation, which indicates that the temperatures generated are well below 160°C. Furthermore, this also demonstrates that coolant was not required, as the compacts did not show any sign of thermal degradation.

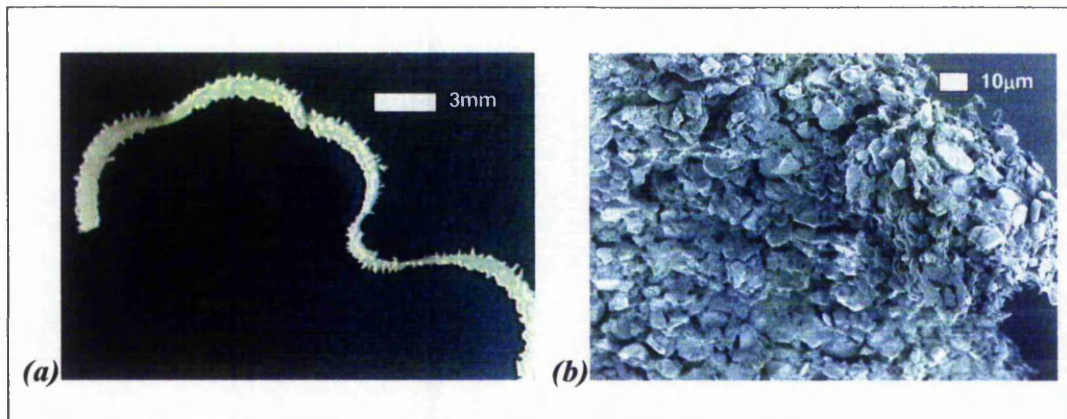


*Figure 4.12: Collected swarf from turning operation with a cutting speed of 1800 rpm, feed rate of 0.2 mm/rev, and depth of cut of 1.0 mm. (a) Continuous swarf (b) SEM image on the swarf from the turning of a compact.*

## 4.6 Milling

Milling is a commonly used conventional machining process in which the cutting action is achieved by rotating the milling tool while the work piece is clamped to a table, and the feed action is obtained by moving the work piece under the cutter. An important feature of all milling operations is that the action of

each cutting edge is intermittent. Therefore, discontinuous swarf is normally produced in a milling process. Each tooth of the milling cutter is cutting less than half of a revolution of the cutter. Thus it is stressed and heated during the cutting part of the cycle, followed by a period when it is not stressed and cools during the non-cutting part of the cycle.

A CNC programme for milling the green compact was developed, so that the speed and feed rate can be well controlled. Cuboidal (45 mm x 34 mm x 10 mm) green compacts, made with the binder consisting of 99.2%w cyanocrylate (*Loctite 408*), 0.4%w para-toluene-sulphonic acid, 0.4%w caffeine containing 48% $V_f$  of alumina ceramic powder (*MA2LS*) were prepared. A 4 mm diameter solid carbide end mill was employed for the machining. 5 mm deep slots were milled at four spindle speeds of 1000 rpm, 1500 rpm, 1800 rpm or 2000 rpm, with three feed rates of 100 mm/min, 150 mm/min or 200 mm/min.

The results showed that the green compacts were machined well by the intermittent cutting process over a reasonable range of cutting speeds and feed rates. Discontinuous swarf were generated in all cases. The compact could be milled satisfactorily without requiring any special procedures or precautions. The gap between two slots was machined to be as close as 1 mm, see *Figure 4.13*. Over the whole machining range, there were no macroscopic signs of degradation of the work piece, i.e. no discolouration, chipping, cracking, or permanent deformation.

The 1 mm gap between slots proved that the compact has high enough strength to withstand the forces applied during the machining process. These observations showed that the compact could also be milled, as well as turned and drilled. This demonstrates that the alumina/cyanoacrylate green compacts

prepared as described herein can be machined with a variety of conventional machining operations. This means that complex shapes can be produced at this stage, which would both reduce the cost of production for relatively simple parts, e.g. tiles or disks, and enable relatively large sized complex shapes to be manufactured.

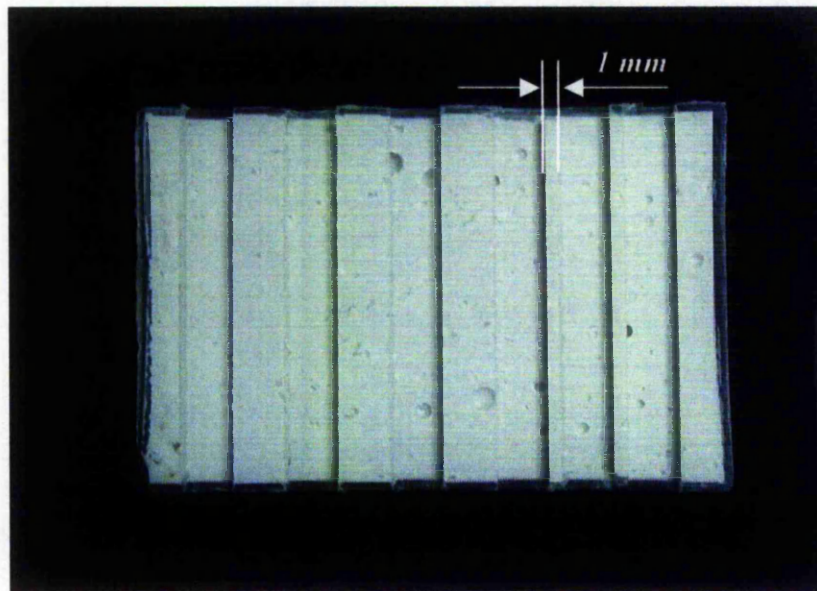


Figure 4.13: Milled green compact. (Note: the large scale porosity that can be seen on some of the surfaces was present prior to the machining trials)

#### 4.7 Tool Wear

The advanced multi-layer ( $Al_2O_3$ ) coated carbide turning insert (*HERTEL*), which was used for turning in *section 4.5*, was investigated with regard to the turning of the alumina/cyanoacrylate compacts. The insert was used to turn the compact *4.5i* in *section 4.5* for a total cutting length of  $\sim 30$  m at 1800 rpm, feed rate of 0.1 mm/rev and depth of cut of 0.5 mm. The insert was then examined in a SEM. *Figure 4.14(a)* shows the SEM images on the rake face of the insert. Abrasive wear was found on the nose edge and flank surface of the insert.

Abrasive wear of a tool generally requires the presence in the work piece material of particles harder than the matrix structure of the tool material. Thus, these observations indicate that abrasion by the alumina particles probably plays the dominant role in the wear of the insert. As can also be seen from *Figure 4.14(a)*, there was no adhesion of material transferred from the alumina/cyanoacrylate work piece.

The used tool tip was also analysed using energy dispersive x-ray analysis in the SEM. It can clearly be seen in *Figure 4.14* that as the carbide tool was coated with two layers, with an outer layer of aluminium oxide and an inner layer of titanium nitride. *Figure 4.14(a)* is a SEM image on the flank surface of the multi-layer coated carbide turning insert. The image indicates the coating layers were in part worn through and the tungsten carbide rich substrate was exposed. *Figure 4.14(b)* and *(c)* indicate that carbon and tungsten are the main base material of the tool, while *Figure 4.14(d)* shows that the inner coating layer contains titanium. Further EDX investigation showed the presence also of nitrogen in this region. *Figure 4.14(e)* and *(f)* indicates the outer coating layer of the tool is made of  $Al_2O_3$ . This coating layer appeared as two different shades in *Figure 4.14(a)*. This might be principally caused by the wear on the darker part, or possibly the different angle that it presents to the electron collector tube. The wear that can be observed in the substrate and coating layers clearly shows the presence of ploughing tracks (which run approximately from 11:30 to 5:30 in *Figure 4.14(a)*), which are very characteristic of abrasion wear. The tracks are very clear in the worn part of the  $Al_2O_3$  layer, less so in the carbide substrate, and much less frequently obvious in the  $TiN$  layer.

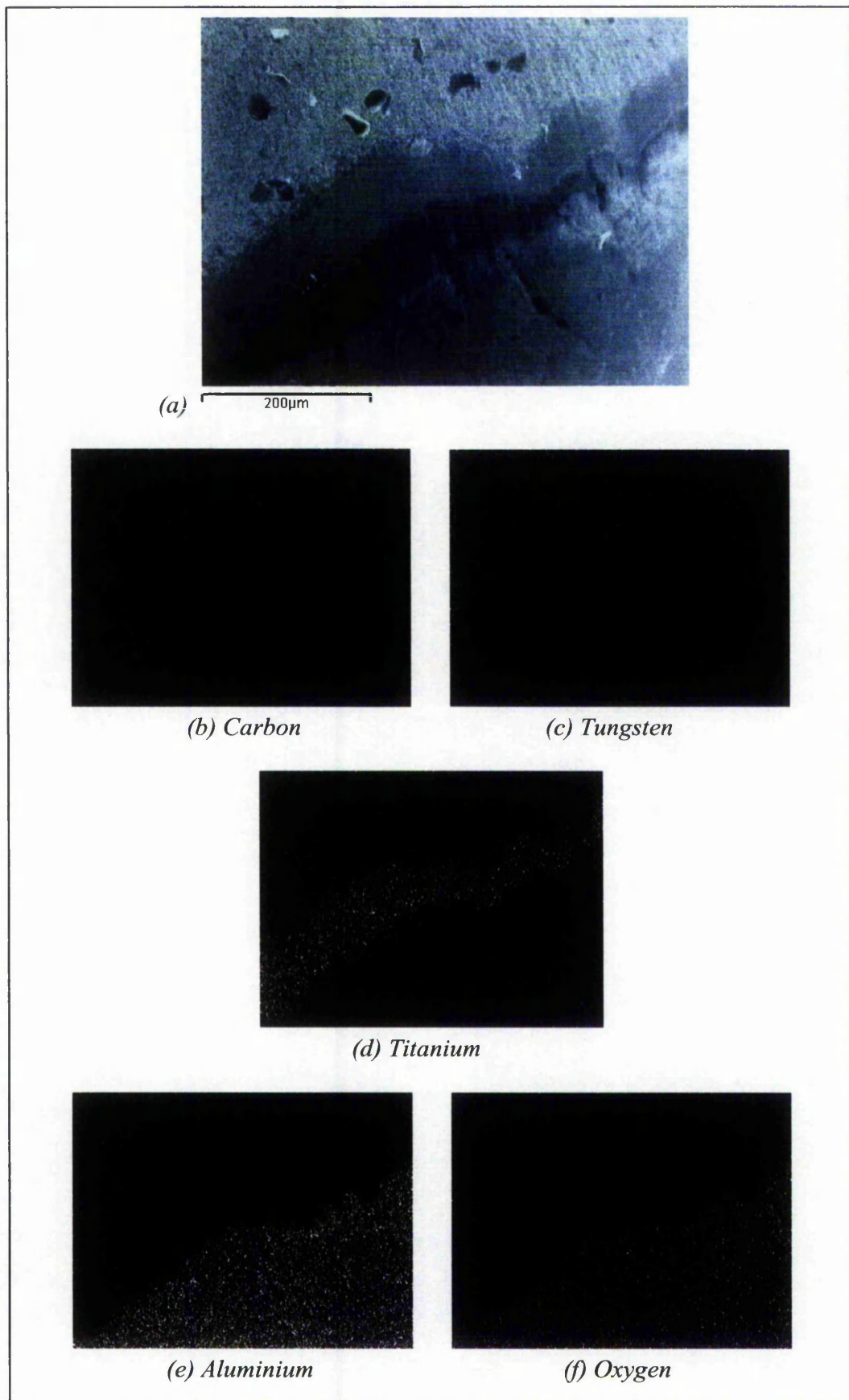


Figure 4.14: Tool coating analysis (a)SEM image of the insert (b,c)Tool substrate material: Tungsten carbide (d)Inner coating: TiN (e, f)Outer coating:  $Al_2O_3$ .



## **4.8 Handling of the Green Compact for Machining**

Unfired green ceramics are normally relatively fragile and great care is necessary in the design and fabrication of fixing and clamping devices, so that the parts can be accurately and uniformly held during the various machining operations. In addition, the machining parameters must be carefully controlled to avoid overstressing the fragile material and producing, cracks, breakage or poor surface finish. Clamping or holding of a ceramic compact for machining is typically a problem because of its fragility. For precise machining, however, the work piece must be held rigidly and without distortion or stress concentration.

As stated in previous sections in this chapter, several manually operated work-holding devices, such as the chuck on the lathe for turning, the vice on the bench for sawing, *Figure 4.15*, and the collet on the CNC for milling and drilling, see *Figure 4.16*, have been used to hold the green compacts for the present machining operations. These devices were capable of accommodating, and firmly holding, a range of compact sizes without the necessity of modifying or extensively adjusting the devices.

In actual implementation, none of these work-holding methods was found to affect the quality of the green compact and productivity of the machining processes. This shows that the strength of the green compact is easily sufficient to withstand the stresses from the holding mechanisms as well as the machining processes.

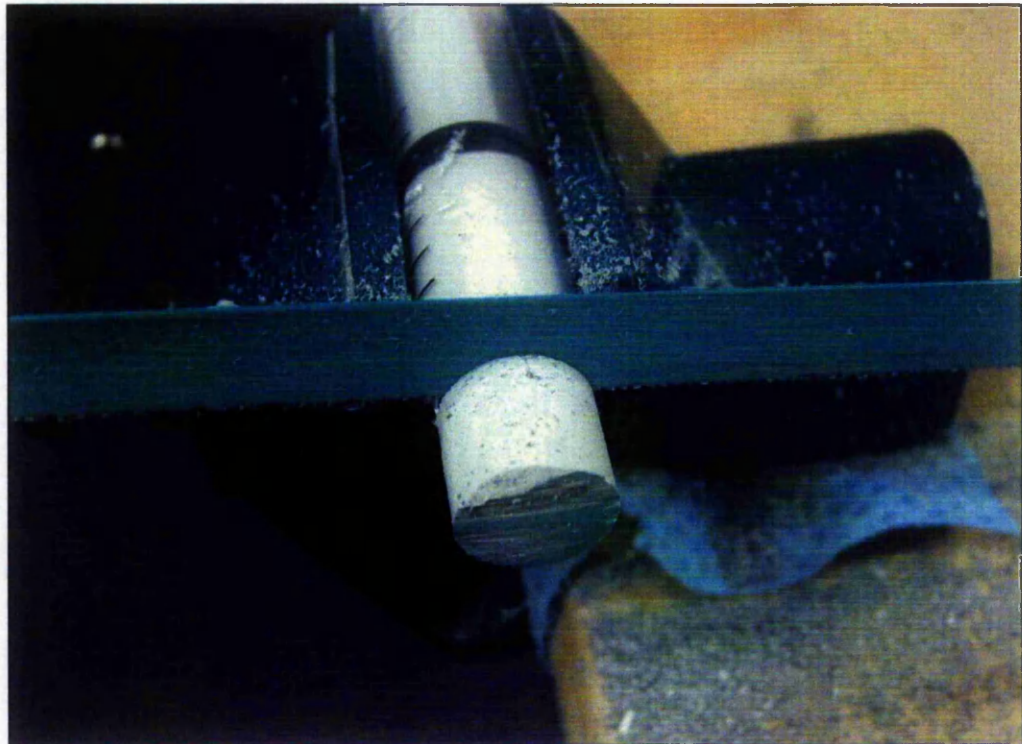


*Figure 4.15: Bench vice used to hold the compact for sawing for preparation of samples.*

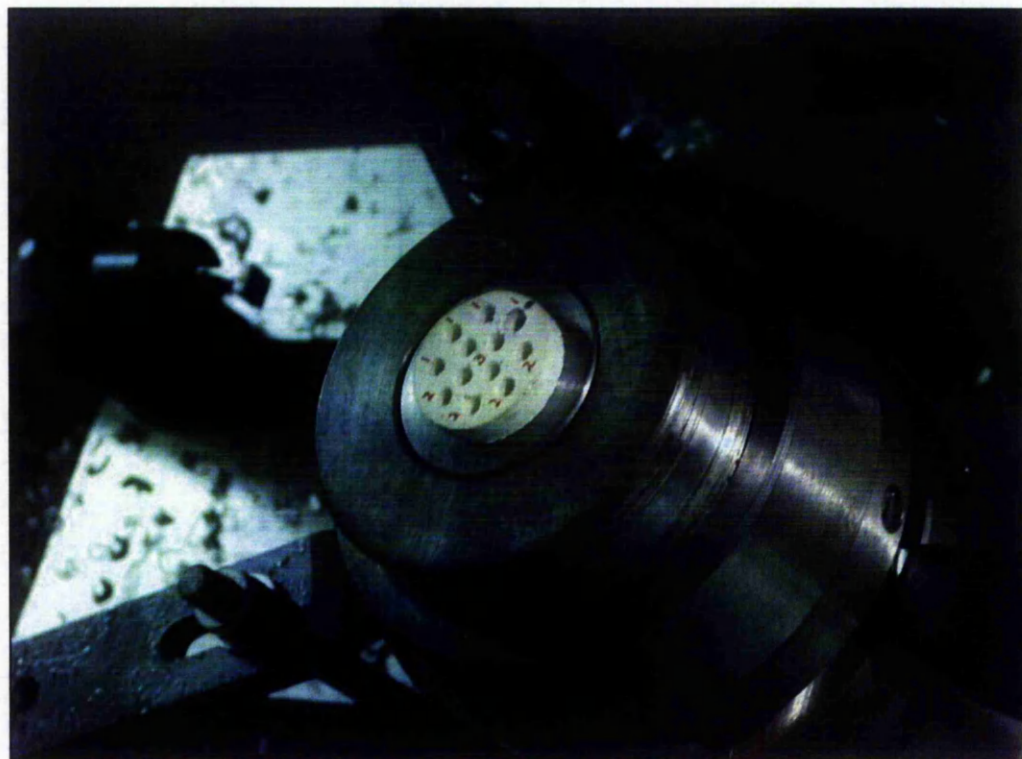


*Figure 4.16: Collet fixed on the CNC table to hold the compact for drilling.*

## **4.9 Summary**

In this chapter, the green compacts were observed to have a sufficiently high strength to enable them to be shaped using conventional machining methods. An investigation of appropriate tool materials for machining of the green compact was also carried out.

The key findings from the compact green machining can be summarised as follows:

- Carbide tools are considered to be highly suitable for the machining of the green compacts with good dimensional tolerances achieved.
- Continuous swarf was formed during the turning of the compact. The swarf were not discoloured.
- Further inspection of the swarf using a SEM showed no signs of debinding or thermal degradation.
- SEM images of the machined surface of a section of swarf show that no debinding effect occurred due to the temperature generated during machining.
- Tool wear of the carbide-based tools used in the machining of the green compact was relatively limited with no material transfer from the alumina/cyanoacrylate affecting the tool tip.

In summary, the green compacts of this new material have been satisfactorily machined using a variety of conventional machining methods.

## **Chapter 5 Finite Element Analysis of Green Machining**

### **5.1 Introduction**

From the investigations described in the previous chapter, it was clear that machining of the new material developed in this research could be satisfactorily undertaken for a variety of machining operations and over a range of operating conditions. However, in general, it is relatively time consuming, and thus expensive, to investigate a range of different compositions for the ceramic/cyanoacrylate mixtures and machining conditions. Hence, it was decided to investigate the possibility of using numerical methods, in this case finite element analysis (FEA), to simulate the cutting operation. This has the advantages of being able to model a wider range of variables than would generally be available on a single tool machine, and at significantly lower cost. It should also be able to provide quantitative estimates for parameters such as the temperatures achieved during machining. The FEA results and the findings from the experimental studies in the previous chapter can then be compared for consistency.

This chapter details the development of the FEA models for single point turning, and the results obtained are discussed. The key steps in the investigation were:

- The development of FEA models to analyse the relative influence of the main material parameters in the composite, e.g. Young's modulus, thermal conductivity, heat capacity, yield stress and strain hardening constant.

- The development of FEA models for different tool material parameters, e.g. tool materials and tool coating.
- The development of FEA models to investigate the influence of the operational parameters, e.g. cutting speed.
- The validation of these models by comparing the FEA results to the observations from the experimental study, e.g. formation of the swarf and work piece/tool interface temperature(s).
- The investigation of temperature distribution and maximum work piece/tool interface temperatures, which were not directly observable in the machining trials.

In the simulation of the green compact machining, DEFORM 2D Cutting (Version 8.1), a commercial self-contained FEM code, developed by SFTC, was used to conduct all the cutting simulations. The geometries, cutting conditions and material properties used were based on the experimental parameters reported in the previous chapter. As with all FEA programs, DEFORM 2D provides estimated values for a variety of parameters. Those of most interest in this study were: temperature, strain and stress.

## **5.2 Creation of Models**

The geometries of the work piece and the insert were created with the geometry primitive template within the DEFORM 2D Cutting programme. The plastic type work piece was created with dimensions of 3 mm in length ( $x$  direction) x 1 mm in height ( $y$  direction). A rigid type tool insert was created with

the dimensions shown in *Figure 5.1*. These insert and work piece geometries were used in all the modelling studies in this chapter.

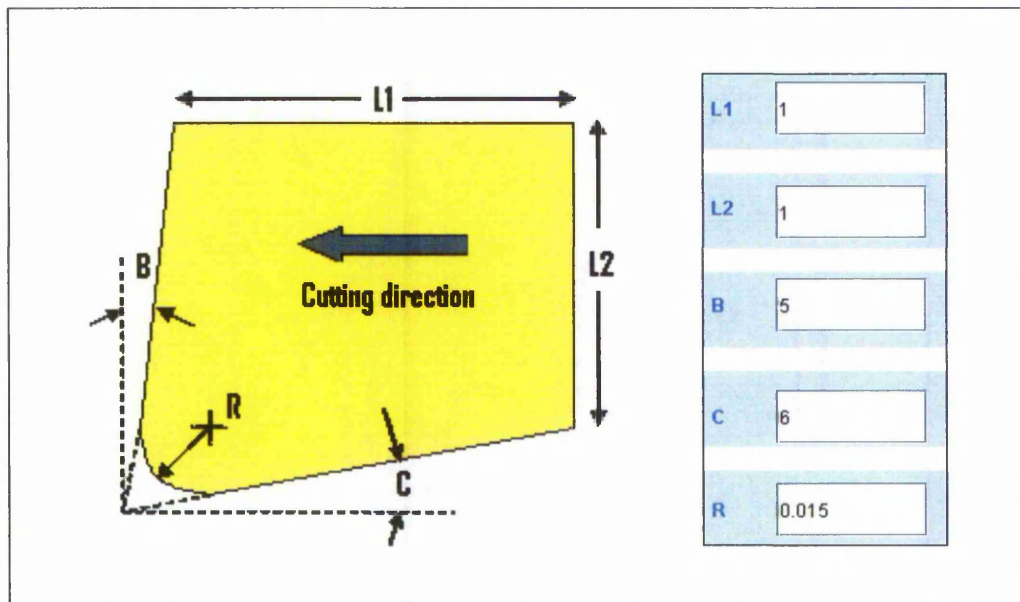


*Figure 5.1: Insert geometry (All dimensions in mm).*

### 5.3 Boundary Conditions

*Figure 5.2* shows the displacement and boundary conditions for the work piece and tool used in the simulations. The models were all 2D plane strain. The tool was rigidly fixed in position. The boundaries A-B, B-C and A-G were all constrained to have zero displacement in the y direction. The boundary A-G-F-E was initially planar and parallel to B-C, as shown in *Figure 5.2*. A constant velocity was applied to the work piece along the boundary C-B-A-G. The boundary C-D-E-F-G represents a free surface.

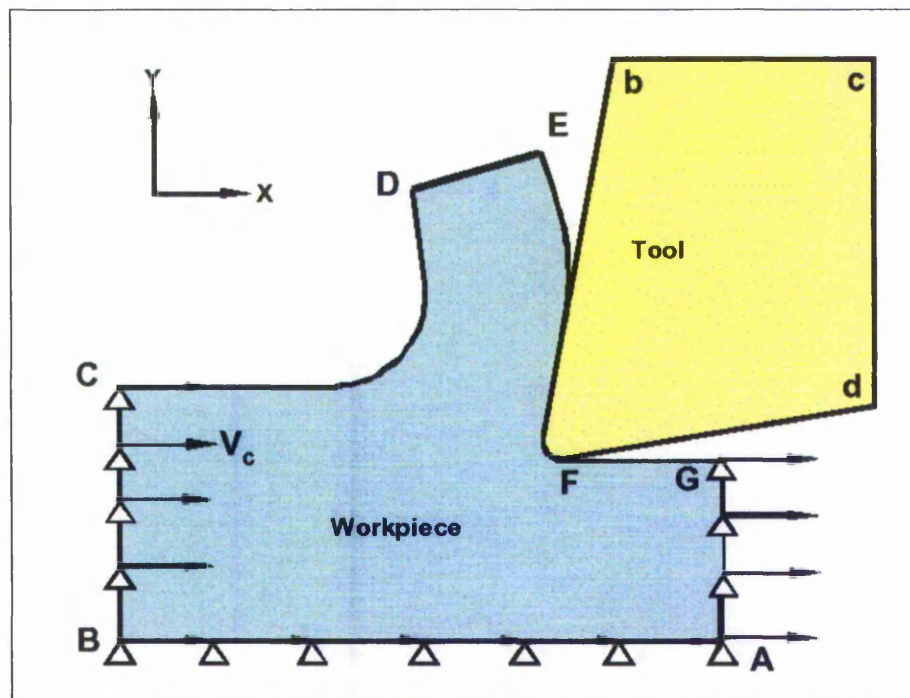


Figure 5.2: Boundary conditions for simulations.

#### 5.4 Model of Tool/Work Piece Contact Interface

An analysis was initially carried out to establish the sensitivity of the shear friction factor based on the default value of the cutting template of 0.6. It was observed that the value did not significantly affect the simulation results, and thus it was used in all the simulations.

The heat transfer conditions used were those contained within the program as default values, since it was stated that these provided a satisfactory representation under most conditions.

#### 5.5 Object Meshing

The mesh density refers to the size of the elements that will be generated within an object boundary. It is defined by the number of nodes per unit length. A

higher mesh density for an object would generally confer enhanced accuracy, and resolution of geometry and field variables such as strain and temperature. However, more time is required for the computer to solve the problem as the number of nodes increases, and also local convergence problems may arise in contact situations. However, it is generally desirable to have a large number of small elements in a region where large gradients in strain or temperature values are present.

*Figure 5.3* shows the initial position of the work piece together with the cutting insert. In this figure, the insert was meshed with 100 elements; whilst the work piece was meshed with 1000 elements with a 1/3 size ratio for the mesh elements placed around the contact point of the tool and the work piece.

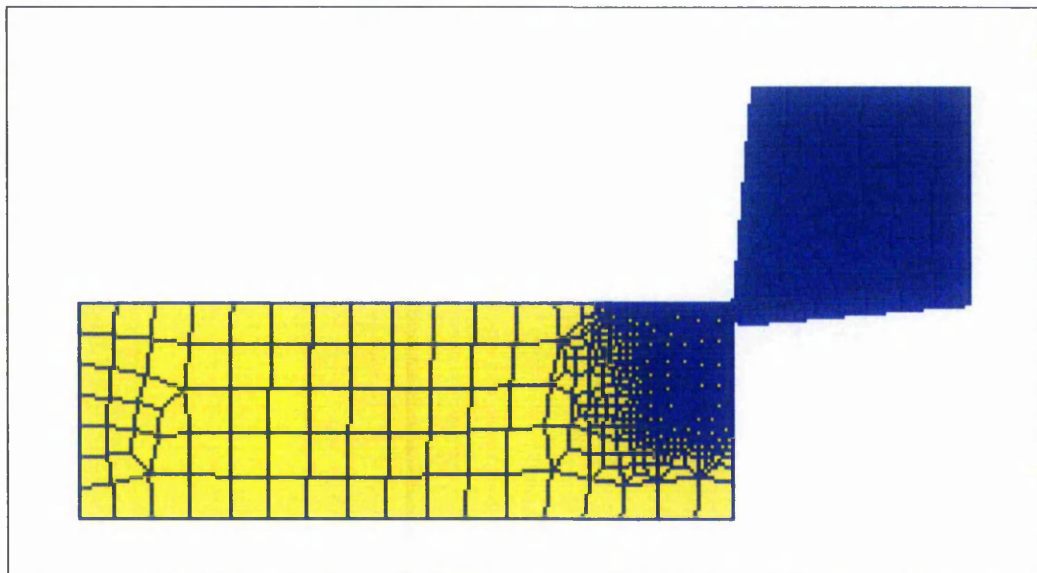


*Figure 5.3: Initial position of the work piece together with the cutting insert.*

Preliminary trial simulations were performed to determine the number of elements required in the simulations. The trial simulation was for orthogonal lathe cutting at a constant speed of 85 m/min, feed rate of 0.1 mm/rev, cutting depth of



1 mm and cutting length of 1.5 mm. The tool material was a 15% cobalt carbide insert. The relevant work piece properties are given in *Table 5.3*. It was noted that as the work piece was translated in the +x direction, swarf was developed as shown in *Figure 5.2*, and also that the swarf geometry and the calculated field parameters, particularly temperature, were found to reach steady state within the initial 0.5 to 1 mm of movement.

Three values were used for the number of elements in the work piece, viz. 500, 1000 and 1500. The meshes were generated automatically by the program, with the element sizes around the contact point of the tool to the work piece being considerably smaller than those at the free boundaries. *Figure 5.4* shows a selection of the results for the three different mesh densities. It can be noted that there was little difference between the 1000 and 1500 meshed models in terms of the stress and temperature contours, and also the ranges for both parameters. However, the 500 element model was less sensitive and exhibited a lower maximum temperature.

It is also appropriate to note from the results for the temperature distributions that the temperature was always a maximum in the work piece material at the swarf/tool interface. The temperatures experienced by the new work piece surface are considerably lower. This observation is consistent with those for the orthogonal cutting of metals, and with the Piispanen's card model for the mechanics of orthogonal cutting [Matthew and Timothy, 2001]. It is particularly desirable in this instance that the machined work piece should not experience any thermal degradation of the cyanoacrylate binder. The temperature criterion for the swarf however is less stringent and only really requires that

sufficient cyanoacrylate remains in place to prevent the swarf disintegrating into a powder, which would be environmentally disadvantageous.

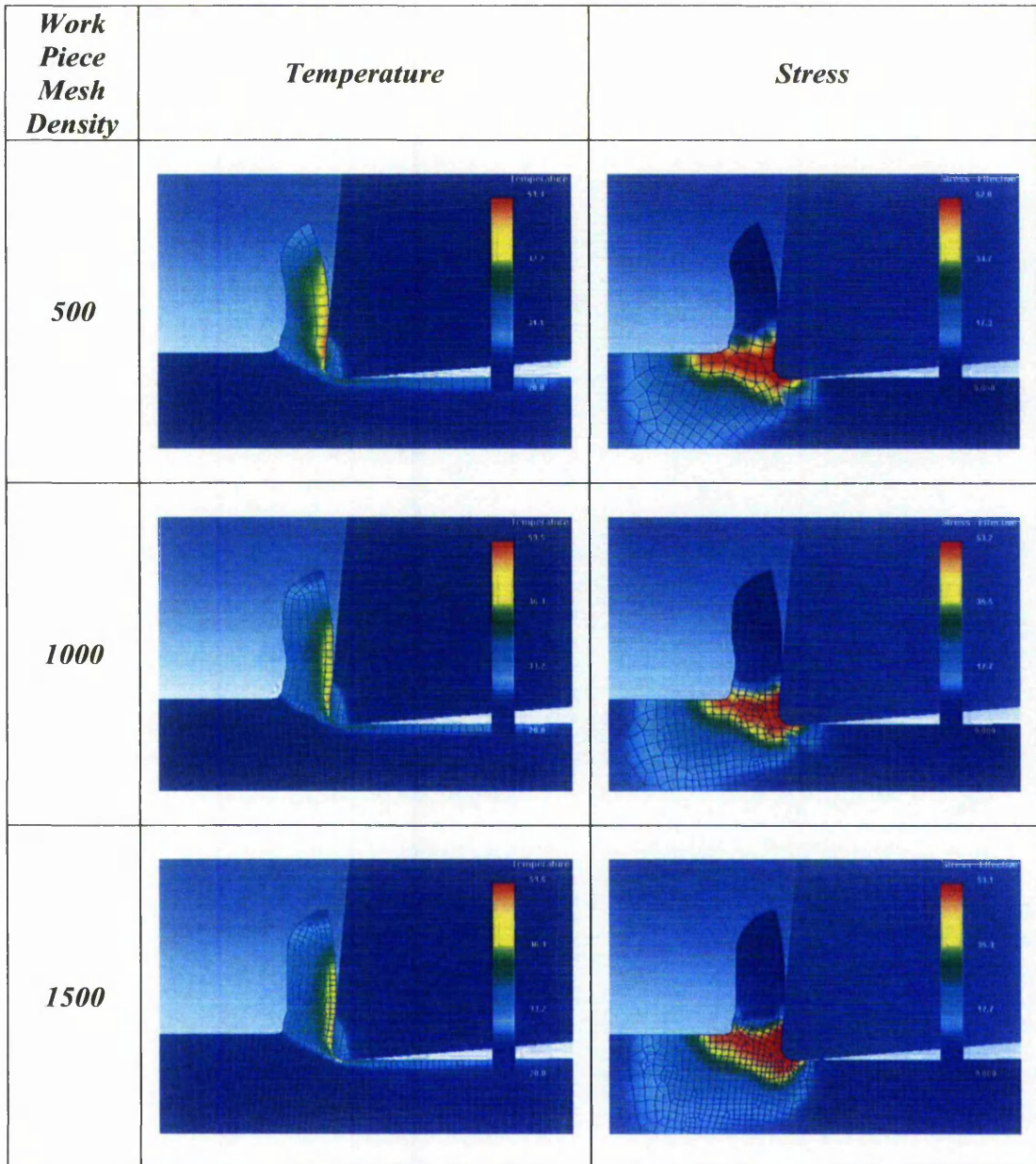


Figure 5.4: Comparison of temperature and equivalent stress results for different mesh densities: (a) 500 elements (b) 1000 elements and (c) 1500 elements.

Based on the observations presented in this section it was therefore decided that the work pieces in all the modelling simulations in this chapter should be meshed with 1000 elements. Also, a standard cutting length of 1.5 mm was used for all the results presented in this chapter, which represents the values under steady state conditions.

## 5.6 Tool Materials

Simulation models for three different tool material arrangements, as listed in *Table 5.1*, were carried out using cutting conditions based on the orthogonal turning experiments described in the previous chapter. The work piece material properties as presented in *Table 5.3* were used in these simulations. *Figure 5.5* shows a schematic diagram of the coated carbide tool.

*Table 5.1: Tools and process conditions for simulation of orthogonal cutting.*

| <b>Tool material</b>                                    |   | <b>HSS<br/>(AISI-D3)</b> | <b>Carbide<br/>(15% cobalt)</b> | <b>Coated Carbide<br/>(15% cobalt)</b> |
|---|---|--------------------------|---------------------------------|--|
| <b>Coating<br/>Thickness (<math>\mu\text{m}</math>)</b> | <b><math>\text{Al}_2\text{O}_3</math></b> | -                        | -                               | 5                                      |
|   | <b>TiC</b>                                | -                        | -                               | 5                                      |
|   | <b>WC</b>                                 | -                        | -                               | 5                                      |
| <b>Cutting speed (m/min)</b>                            |   | 85                       | 85                              | 85                                     |
| <b>Feed rate (mm/rev)</b>                               |   | 0.1                      | 0.1                             | 0.1                                    |

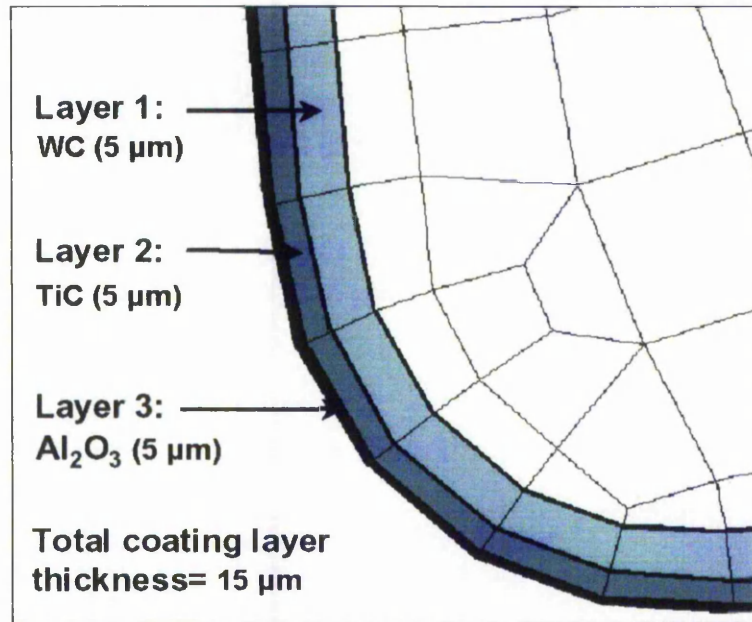


Figure 5.5: Schematic diagram of the coated carbide tool.

Figure 5.6 shows the simulation results for the predicted steady state interface temperatures for the three different tool material arrangements. It can be seen from the figure that temperatures developed in the simulations with an AISI-D3 HSS insert or 15% cobalt carbide insert were comparable. These both estimated a maximum cutting temperature of 62.8°C. However, the coated carbide tool had a slightly higher calculated maximum temperature of 65.7°C. The most likely explanation for the higher temperatures in the swarf, and lower temperature in the coated tool, is the lower thermal conductivity of the coating layers, particularly the Al<sub>2</sub>O<sub>3</sub>, resulting in less of the frictionally generated heat at the tool/swarf interface being transferred into the tool, thus resulting in higher temperatures at the interface and in the swarf.

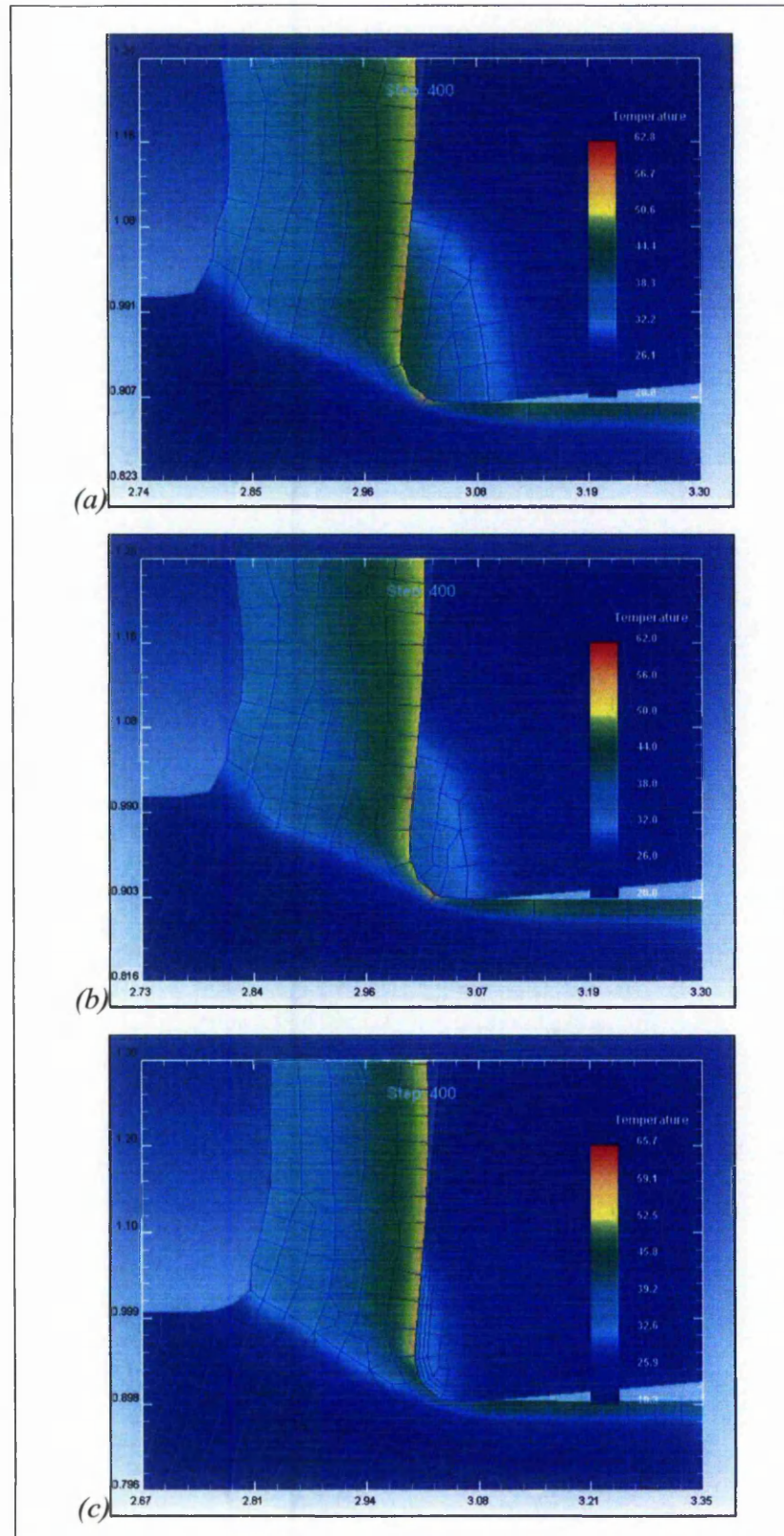


Figure 5.6: Temperature contours in work piece, tool and swarf for three different tool materials (a) AISI-D3HSS (b) 15% cobalt carbide (c) Coated carbide (15% cobalt).

## 5.7 Material Properties of the Alumina/cyanoacrylate

One of the difficulties in the modelling of a new material is to obtain accurate and reliable mechanical and thermal properties for the material. Furthermore, in this case, information about some of the relevant properties of the cyanoacrylate was not available from the suppliers. The mechanical, and to a lesser extent thermal, properties of cyanoacrylates do not appear to have been studied anywhere near as much as their chemistry and adhesive behaviour. For example, it was not possible to locate data for the elastic constants of cyanoacrylate in the literature. It would be expected that the values of such constants would depend upon the composition of the polymer and the degree of polymerisation etc. Since there would be expected to be some variations, it was considered appropriate to use elastic constant data for epoxy as a first estimate. The properties of the composite were estimated using the conventional ‘rule of mixtures’, which is based on the individual properties of the alumina and cyanoacrylate in proportion to their volume fraction in the composite [Konopka et al., 2004].

Since the composite consists of alumina particles in a cyanoacrylate matrix, it was considered that the lower bound estimate for the Young’s modulus was likely to be the appropriate equation to use, i.e.

- **Young’s modulus of the composite,  $E_C$**

$$\frac{1}{E_C} = \frac{V_M}{E_M} + \frac{V_P}{E_P}$$

where  $E_M$  = Young’s modulus of the matrix = 2 GPa.

$E_P$  = Young’s modulus of the particles = 300 GPa.

$V_M$  = Volume fraction of the matrix = 0.55.

$V_P$  = Volume fraction of the particles = 0.45.

It was considered most appropriate to use the upper bound estimate for the thermal expansion, i.e.

- **Thermal expansion of the composite,  $\alpha_C$**

$$\alpha_C = \alpha_M \cdot V_M + \alpha_P \cdot V_P$$

where  $\alpha_M$  = Thermal expansion coefficient of the matrix =  $80 \times 10^{-6} / ^\circ\text{C}$ .

$\alpha_P$  = Thermal expansion coefficient of the particles =  $8 \times 10^{-6} / ^\circ\text{C}$ .

The thermal conductivity of the alumina/cyanoacrylate compacts was measured using a standard Cussons Technology thermal conductivity apparatus. This technique is a standard method, which uses thin flat discs of material and measures the temperature gradient with a known heat flux across the specimen. The average value measured using this method was  $5.5 \times 10^{-3} \text{ N/s} \cdot ^\circ\text{C}$  (or  $1.5 \text{ N/s} \cdot \text{K}$ ).

It was considered most appropriate to use the upper bound estimate for the heat capacity, i.e.

- **Heat capacity of the composite,  $C_C$**

$$C_C = C_M \cdot V_M + C_P \cdot V_P$$

where  $C_M$  = Heat capacity of the matrix =  $1464 \text{ J/kg} \cdot ^\circ\text{C}$ .

$C_P$  = Heat capacity of the particle =  $850 \text{ J/kg} \cdot ^\circ\text{C}$ .

A series of simulations was performed to establish the effect of the approximated properties of the composite using a range of values for the relevant material properties. The orthogonal lathe cutting simulation was performed at a constant speed of 85 m/min, feed rate of 0.1 mm/rev, cutting depth of 1 mm and cutting length of 1.5 mm. The tool material was a 15% cobalt carbide insert. Table 5.2 shows the comparison of extracted values from the results for a range of values for the Young's modulus and thermal conductivity.

Table 5.2: Comparison of the simulation results of the estimated value range.

| Young's modulus of the composite, $E_C$ (GPa) | Thermal conductivity of the composite, $K_C$ (N/sK) | Simulation Results                  |                             |                    |                                  |
|---|---|-------------------------------------|-----------------------------|--------------------|----------------------------------|
|   |   | Maximum temperature ( $^{\circ}C$ ) | Maximum stress ( $N/mm^2$ ) | Maximum strain (%) | Maximum strain rate ( $s^{-1}$ ) |
| 2   | 1.5   | 61.9                                | 52.7                        | 2.68               | 50200                            |
| 4*  | 1.5   | 61.9                                | 52.7                        | 2.68               | 50200                            |
| 8   | 1.5   | 64.9                                | 52.7                        | 2.69               | 50200                            |
| 4   | 0.75  | 66.8                                | 52.7                        | 2.68               | 50200                            |
| 4   | 1.5 <sup>+</sup>                                    | 61.9                                | 52.7                        | 2.68               | 50200                            |
| 4   | 3.0   | 58.2                                | 52.5                        | 2.51               | 50200                            |

\* Estimated using Lower Bound Equation

+ Measured experimentally

It can be observed from the results shown in Table 5.2 that the values for maximum stress, strain and strain rate did not significantly depend on the material constants over the ranges used. The variation in Young's modulus has a slight effect on the maximum temperature, and the thermal conductivity variations have a slightly more pronounced effect on the maximum temperatures, as shown in Figure 5.7 and Figure 5.8. However, the variations of  $\pm 5^{\circ}C$  would not be expected to result in a significant difference in the behaviour. The calculated results are consistent with qualitative physical reasoning since it would be



anticipated that the Young's modulus of the material would have a limited effect to the cutting process and a decrease in the thermal conductivity would be expected to result in an increase in the maximum temperature in the swarf. It should also be noted that the estimated maximum temperatures generated by the machining process, particularly in the machined work piece, were all well below the degradation temperature of the cyanoacrylate. *Table 5.3* summarizes the mechanical and thermal properties of the composite used in the remaining simulations in this chapter.

*Table 5.3: Summary of alumina/cyanoacrylate material properties generally used in simulations in this chapter.*

|  |   |
|--|---|
| <b><i>Young's modulus, E</i></b>                     | 4 GPa   |
| <b><i>Poisson's ratio, <math>\nu</math></i></b>      | 0.35  |
| <b><i>Thermal expansion, <math>\alpha</math></i></b> | $47.6 \times 10^{-6} / ^\circ\text{C}$          |
| <b><i>Thermal conductivity, K</i></b>                | $5.5 \times 10^{-3} \text{ N/s.}^\circ\text{C}$ |
| <b><i>Heat capacity, C</i></b>                       | 1188 J/kg $^\circ\text{C}$                      |
| <b><i>Initial yield stress, Y</i></b>                | 50 MPa  |
| <b><i>Strain hardening constant, H</i></b>           | 1 MPa   |

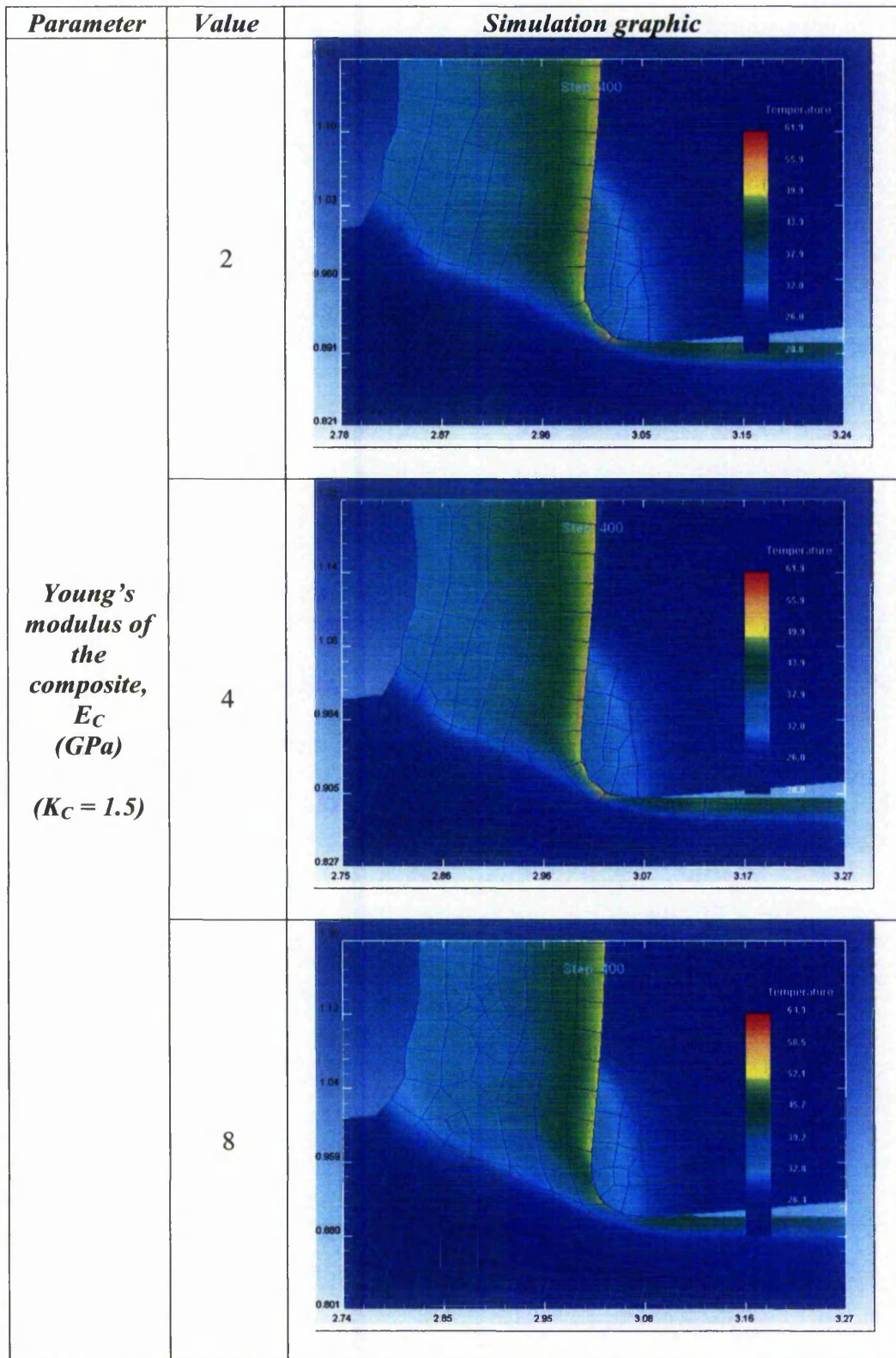


Figure 5.7: Comparison of the temperature distributions for the different values of Young's modulus.

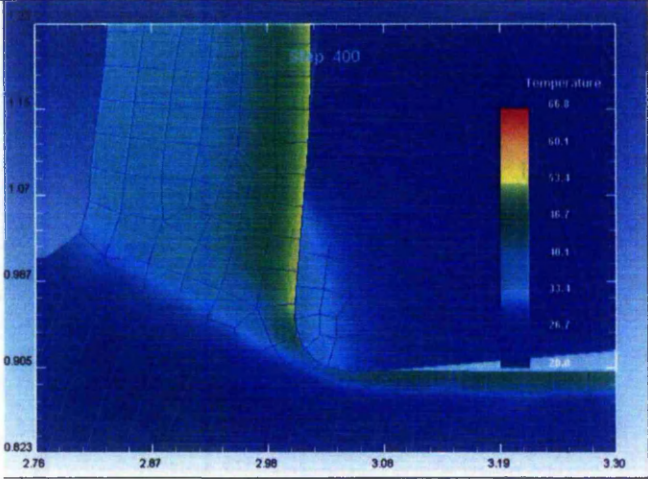
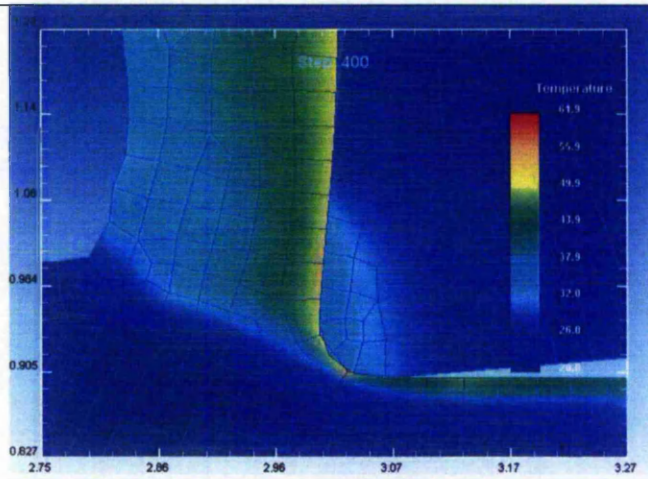
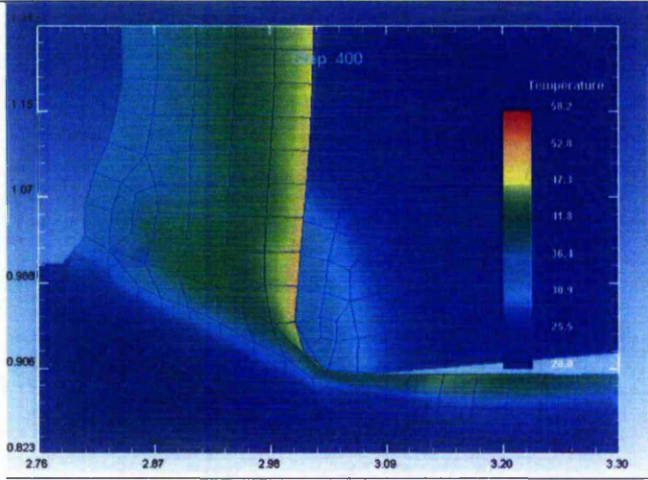
| Parameter   | Value                       | Simulation graphic   |
|---|-----------------------------|--|
| <p style="text-align: center;"><i>Thermal conductivity of the composite, <math>K_C</math> (N/sK) (<math>E_c = 4</math>)</i></p> | 0.75                        |    |
|   | 1.5<br>(Experimental value) |   |
|   | 3.0                         |  |

Figure 5.8: Comparison of the calculated temperature distributions for the different values in thermal conductivity.

## 5.8 Flow Stress Model for the Composite

The flow stress of a material is the stress required to continue plastic deformation of the material at a particular true strain [Kalpakjian, 1997]. A linear hardening flow stress model was assumed for the work piece material in the simulations. The mathematical model for the flow stress data of the composite can be expressed by

$$\bar{\sigma} = Y(T, A) + H(T, A)\bar{\varepsilon}$$

where  $A$  = Atom content

$T$  = Temperature

$\bar{\varepsilon}$  = Effective plastic strain

$\bar{\sigma}$  = Flow stress

$Y$  = Initial yield stress

$H$  = Strain hardening constant

[Source: DEFORM 2D manual, 2004]

In these simulations of the green machining, the initial yield stress,  $Y$ , was estimated based on hardness data of the green material, i.e.  $Y = \text{Hardness}/3.1$  [Hu, 2005]. Estimating a value for the strain hardening constant,  $H$ , is more problematical, although it is commonly observed (at least for thermoplastic polymers) that the strain hardening coefficient is low. In the present case, its value has been varied over the range that is most physically likely. Simulations were carried out to establish the effect of the approximated properties of the composite on the simulation results, *Table 5.4*.

Table 5.4: Comparison of the simulation results of the estimated value range.

| Initial yield stress, $Y$ (MPa) | Strain hardening constant, $H$ (MPa) | Simulation Results*                        |                                    |                    |   |
|---------------------------------|--------------------------------------|--|------------------------------------|--------------------|---|
|                                 |                                      | Maximum temperature ( $^{\circ}\text{C}$ ) | Maximum stress ( $\text{N/mm}^2$ ) | Maximum strain (%) | Maximum strain rate ( $\text{s}^{-1}$ ) |
| 25                              | 1                                    | 41.3                                       | 27.6                               | 2.51               | 49600                                   |
| 50                              | 1                                    | 61.9                                       | 52.7                               | 2.68               | 50200                                   |
| 75                              | 1                                    | 79.3                                       | 78.6                               | 3.65               | 50300                                   |
| 50                              | 0.1                                  | 57.1                                       | 50.3                               | 2.51               | 50500                                   |
| 50                              | 10                                   | 90.6                                       | 84.8                               | 3.10               | 44900                                   |

\* Note: These values are all taken from the detached material, i.e. swarf.

It can be observed from the results shown in Table 5.4 that the values for maximum temperature, stress, and strain show a reasonable degree of variation, but the maximum strain rate did not significantly depend on the yield stress or strain hardening rate of the material over the ranges used. As the yield stress (for constant  $H$ ) or strain hardening coefficient (for constant  $Y$ ) is increased, then the maximum stress is increased approximately in proportion, as would be expected. Since the amount of energy generated by plastic deformation is also increased, there is a resultant increase in the maximum temperature. The maximum temperature calculated of  $90.6^{\circ}\text{C}$  occurred with  $Y = 50$  MPa and  $H = 10$  MPa. This value for  $H$  is likely to be an overestimate of the true value. Overall, a consideration of these results would indicate that for these cutting conditions and tool material that the most likely maximum temperature in the swarf would be in the range  $60^{\circ}\text{C}$  to  $70^{\circ}\text{C}$ . The corresponding maximum temperatures in the machined work piece are only  $40^{\circ}\text{C}$  to  $50^{\circ}\text{C}$ , which were all well below the degradation temperature of the cyanoacrylate.

## 5.9 Cutting speeds

Orthogonal cutting simulations with the designated material properties for the work piece as presented in *Table 5.3* were carried out to investigate the machining of the composite at different cutting speeds. A 15% cobalt carbide insert with geometry as shown in *Figure 5.1* was assigned to the simulation. The cutting simulation was performed for three cutting speeds, i.e. 28 m/min, 85 m/min and 255 m/min, at a feed rate of 0.1 mm/rev and a depth of cut of 1 mm. *Table 5.5* shows the simulation results for the different cutting speeds.

*Table 5.5: Orthogonal cutting simulations at different cutting speeds.*

| <b>Cutting speed (m/min)</b> | <b>Simulation Results</b>       |  |                           |   |
|------------------------------|---------------------------------|--|---------------------------|---|
|                              | <b>Maximum temperature (°C)</b> | <b>Maximum stress (N/mm<sup>2</sup>)</b> | <b>Maximum strain (%)</b> | <b>Maximum strain rate (s<sup>-1</sup>)</b> |
| 28                           | 43.2                            | 52.9                                     | 2.85                      | 15900                                       |
| 85                           | 61.9                            | 52.7                                     | 2.68                      | 50200                                       |
| 255                          | 66.3                            | 52.5                                     | 2.51                      | 150000                                      |

The results shown in *Table 5.5* indicate that the values for maximum stress and strain were not significantly affected by the cutting speed over the ranges used. However, there was a noticeable effect on the maximum temperature and the maximum strain rate. The temperature difference of 23°C between the lowest and highest cutting temperatures occurred in the swarf, with the corresponding calculated maximum temperatures in the machined work piece, being 32°C to 56°C, which are well below the degradation of the cyanoacrylate binder.

*Figure 5.9* shows swarf formation in the simulation at a cutting speed of 85 m/min. This figure indicates that the energy consumed in the compact cutting would appear to be mainly converted into heat in the swarf and the cutting edge of

the tool. In this case, the swarf acts as a heat carrier, with the heat remaining in the swarf after it breaks contact being carried out of the system.

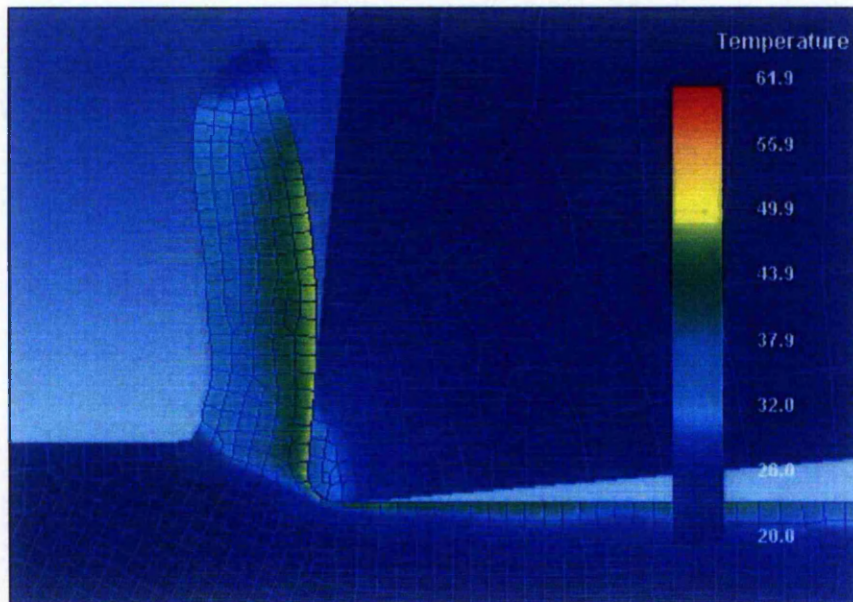


Figure 5.9: Swarf formation in the simulation at cutting speed of 85 m/min.

## 5.10 Swarf Formation

Continuous swarf were produced in all the simulations, e.g. *Figure 5.9*. This actually represents how the swarf was produced in the machining trials described and discussed in *Chapter 3*. However, once the swarf is clear of the tool, and its temperature has decreased, then it does not matter with regard to the simulations, if the swarf remains continuous or breaks up into smaller chips. During machining, the main deformation of the material should take place in the primary and secondary shear zones. *Figure 5.10* shows a narrow high strain zone that corresponds to the primary shear zone. The energy dissipated in the secondary shear zone is not apparent as a high strain zone, although the fact that the maximum temperatures are generated at the swarf/tool interface indicates that

there is significant energy expended therein. The relatively low thermal conductivity of the green compact ensures that the heat does not greatly conduct into the newly machined work piece surface. Thus, the maximum temperatures experienced by the new work piece surface are relatively low.

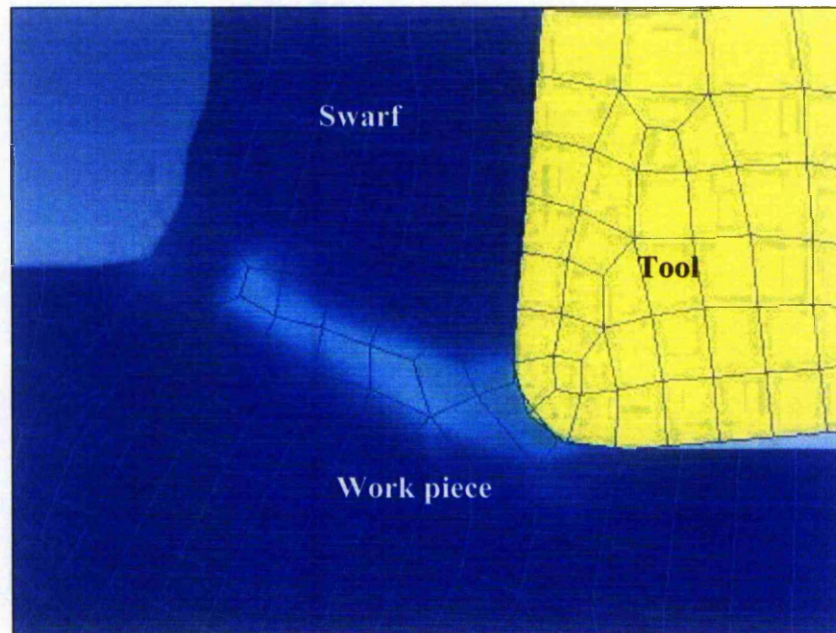


Figure 5.10: Primary shear zone in the machining simulation.

## 5.11 Summary

A FEM simulation model of orthogonal cutting for alumina/cyanoacrylate green composite was developed based on the orthogonal cutting machining trials described and discussed in *Chapter 4*. The key findings from the simulations can be summarised as follows:

- It is possible to use the DEFORM 2D FEA software to model the machining of the green compact.
- The simulations were also successfully performed using different tool materials and cutting speeds.



- The maximum temperatures calculated using the most likely material parameter values were  $\sim 60^{\circ}\text{C}$ , with the range varying between  $41^{\circ}\text{C}$  and  $91^{\circ}\text{C}$  at the swarf/tool interface. The maximum temperature attained at the new machined work piece surface was only  $\sim 50^{\circ}\text{C}$ .
- Continuous swarf were produced in the simulations.

## **Chapter 6 Debinding and Sintering**

### **6.1 Introduction**

Debinding and sintering are the main final stages in a ceramic fabrication process, with the preferred goal of any significant shaping of the final product being very limited, since this is usually a costly step. Therefore, the ceramic compact should be able to be handled, with appropriate care, during these processes to avoid distortion or failure in the final product.

In this chapter, the investigation of green compact debinding and sintering are discussed. A debinding process that can completely debind the compact, followed by a suitable sintering process for the compact has been developed. The main objectives of this phase of the research were to:

- **Investigate handling methods for compact debinding**

Holding of a green compact for debinding can cause problems because free surfaces for consistent heating are required to avoid distortion. An investigation of suitable handling methods for the debinding of the alumina/cyanoacrylate was undertaken.

- **Determine the efficient temperature range and heating rate for the debinding of the green compact**

Depolymerisation of the cyanoacrylate binder in the compact was first investigated using a Differential Scanning Calorimeter (DSC) and Thermogravimetric Analyser (TGA). In addition, experimental trials at

various heating rates were performed to determine the most effective debinding temperatures and times for the compact.

- **Determine the effective sintering temperature for the compact**

An aim of the present research was to produce fully dense monolithic ceramic blocks. The purpose of this phase of the research was not so much as to investigate the sintering mechanism in depth, but to demonstrate that the sintering of a machined green compact could be performed without the machining generating major defects, such as cracks or localised severe distortion. Sintering densification usually take place close to the melting temperature of the ceramic powder. Therefore, in this case sintering temperatures in the range 1550°C to 1750°C were used. The influence of time at the sintering temperature was also investigated.

## **6.2 Debinding**

In typical powder injection moulding industries, a two-step debinding sequence is typically adopted to remove the low molecular weight components, e.g. wax, then subsequently the high molecular weight components, e.g. polymer, of the binder system [German, 1987]. However, the reactive binder used in alumina/cyanoacrylate compacts can be debonded in a single process since the cyanoacrylate debinds by a chain end initiated unzipping reaction. Small molecules of cyanoacrylate monomer are released during the debinding.

In this case, the debinding was commenced with gradual heating of the compact in an oven. The cyanoacrylate binder started to depolymerise and evaporate from the compact surface when the surrounding temperature reached the degradation temperature of the cyanoacrylate. This is followed by the remaining monomer vapourising and flowing through the open pores to the surface. The monomer could be collected and re-used [Birkinshaw, 1996], however, it was decided that this was not practicable given the relatively limited volume of binder used throughout this investigation.

### 6.2.1 Differential Scanning Calorimeter (DSC) and Thermogravimetric Analyser (TGA)

The thermal sensitivity of the alumina/cyanoacrylate compact was established using a *DuPont 2000 Thermal Analysis* at the University of Limerick (Birkinshaw, 2003). Both DSC and TGA methods were used. Green compacts used for the analysis had the composition as detailed in *Table 6.1*. The key objective of the analysis was to determine the effective debinding temperature(s) for the cyanoacrylate binder depolymerisation. The results from the TGA and DSC analysis are shown in *Figure 6.1* and *Figure 6.2* respectively.

*Table 6.1: Composition of alumina/cyanoacrylate compacts*

|               |  |        |             |
|---------------|--|--------|-------------|
| <b>Binder</b> | Cyanoacrylate ( <i>Loctite 408</i> )           | 23.8%w | 51.7% $V_f$ |
|               | Para-toluene-sulphonic acid ( <i>Aldrich</i> ) | 0.1%w  |             |
|               | Caffeine ( <i>Aldrich</i> )                    | 0.1%w  |             |
| <b>Powder</b> | Alumina powder ( <i>Alcan MA2LS</i> )          | 76.0%w | 48.3% $V_f$ |

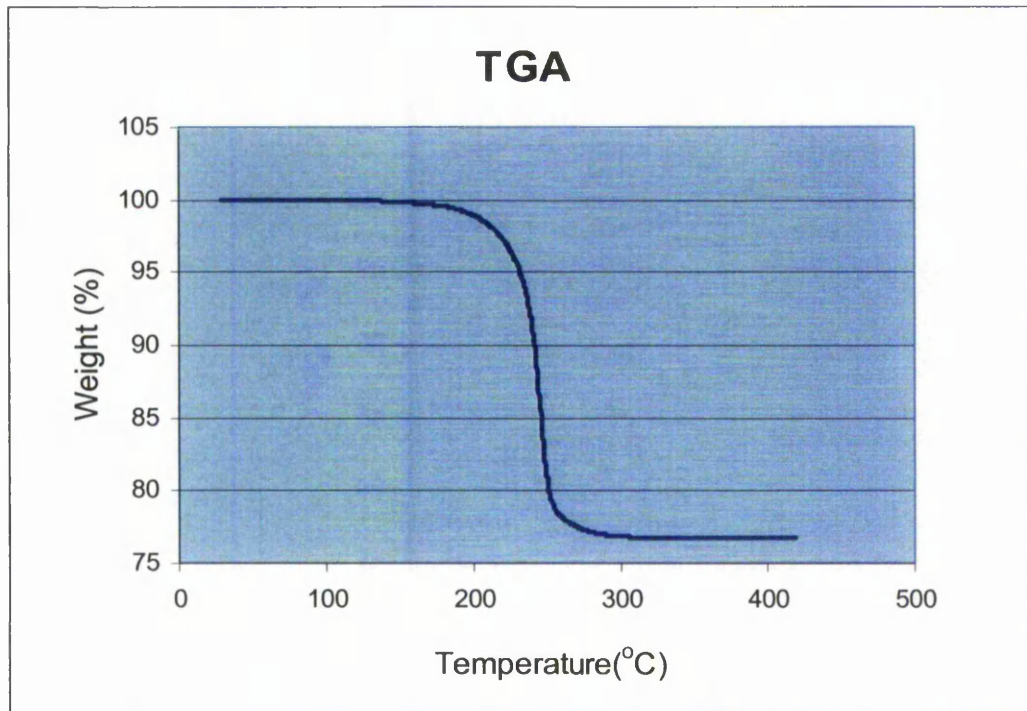


Figure 6.1: Thermogravimetric analysis of degradation of cyanoacrylate in the compact [Birkinshaw, 2003].

A small green compact piece of weight 20.504 mg was used for the TGA. Heating was carried out at constant ramp rate of 10°C/min. From *Figure 6.1*, it is apparent that the compact had completely debonded when the temperature reached approximately 300°C. There was a total weight loss of 23.01% (4.718 mg). This demonstrated that the cyanoacrylate could be unzipped rapidly. However, the green compact would be distorted or collapsed if too high a heating rate were used due to uneven thermal expansion and vapour pressure caused by the temperature difference between the surface and inside of the compact, and also decomposition of the cyanoacrylate polymer.

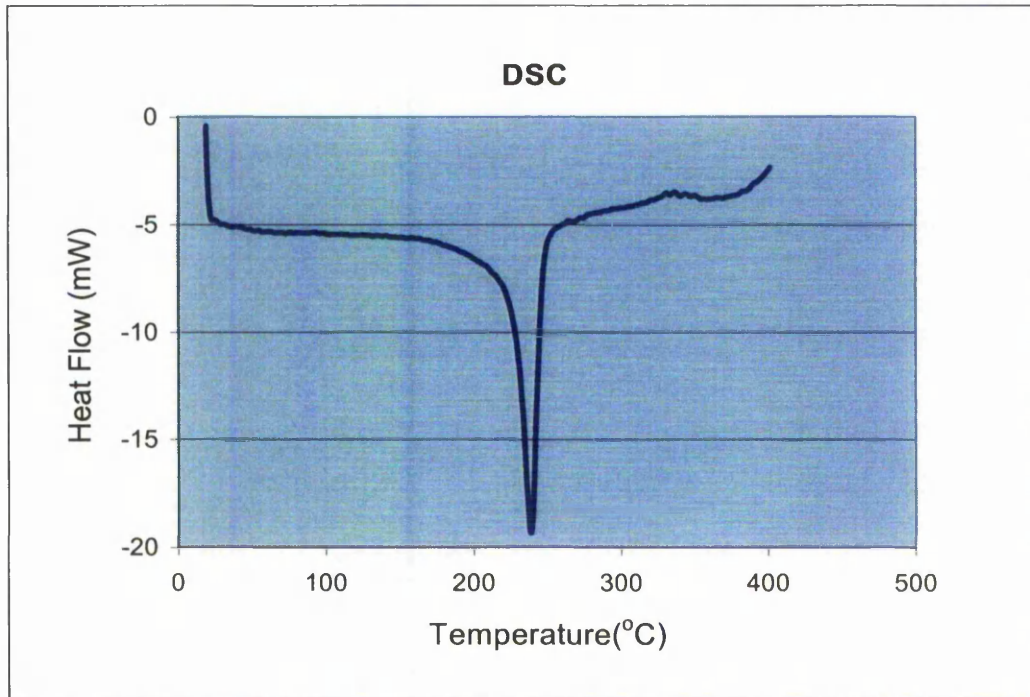


Figure 6.2: DSC analysis of degradation of cyanoacrylate in the compact [Birkinshaw, 2003].

A compact with the same composition as that used for the TGA of weight 13.93 mg was used to investigate the degradation properties of the compact using DSC analysis. The main objectives of this investigation were to determine the start and finish temperatures for the depolymerisation and the effect of the heating rate on the debinding of the compacts. It can be seen from the *Figure 6.2* that the debinding of the compact initiated actively at a temperature of approximately 170°C and the maximum endothermic heat flow occurred at approximately 240°C. These results provided useful information on the effective temperature range for debinding the compacts.

### 6.2.2 Debinding of Alumina/Cyanoacrylate compacts

The data from the TGA and DSC analysis in the previous section indicated an estimated temperature range for debinding. A practical trial was carried out to

establish an effective temperature/time profile when shape retention is the primary concern, e.g. avoidance of distortion, non-uniform shrinkage or cracking.

The green compacts used in these trials had the composition as detailed in *Table 6.1*. The compacts were manufactured as cylinders 40 mm diameter and 7 mm in height. All the debinding trials were performed in a sealed oven (*WTB FED-53*) with an extractor fan, which ensured that the monomer vapour of the cyanoacrylate was dispersed into the open atmosphere. *Figure 6.3* shows the debinding oven.

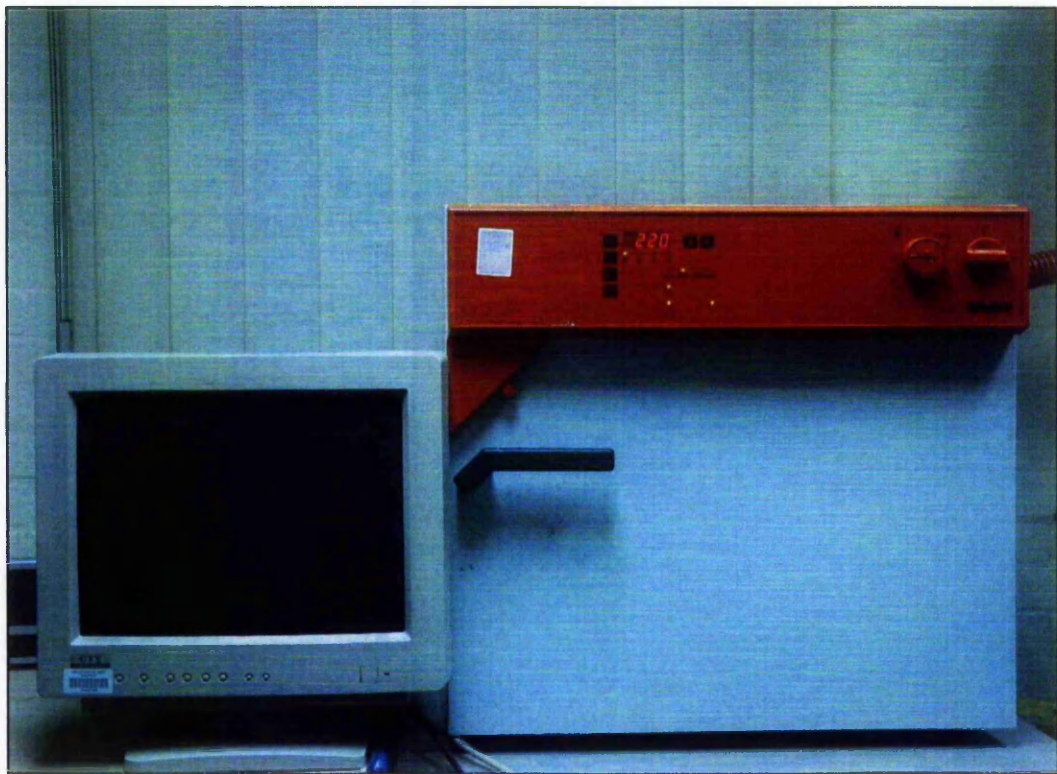


*Figure 6.3: Debinding oven with PC programmable temperature control and extractor fan facility.*

### 6.2.3 Handling Methods for Debinding

Four compacts were separately placed on an aluminium plate, vitreosil basin, wire mesh, or firebrick. The oven was preheated to 80°C before the prepared samples were placed into it. The oven was heated up to 220°C at an average heating rate of 10°C/min. *Table 6.2* details the observations of this trial.

*Table 6.2: Debinding set up and observations.*

| <b>Sample set up</b>   | <b>Weight loss (%)</b> | <b>Observations</b>   |
|--|------------------------|---|
| <b><i>Deb-A</i></b><br><b><i>(seated on aluminium plate)</i></b> | 18.33                  | <ul style="list-style-type: none"> <li>● Surface cracks</li> <li>● Compact stuck to the plate surface</li> <li>● Bubbled effect at the bottom surface of the compact</li> </ul> |
| <b><i>Deb-B</i></b><br><b><i>(seated in vitreosil basin)</i></b> | 18.98                  | <ul style="list-style-type: none"> <li>● Surface cracks</li> <li>● Compact stuck to the basin surface</li> <li>● Bubbled effect at the bottom surface of the compact</li> </ul> |
| <b><i>Deb-C</i></b><br><b><i>(seated on wire mesh)</i></b>       | 22.64                  | <ul style="list-style-type: none"> <li>● Small cracks in the surface</li> <li>● Warping due to uneven surface</li> </ul>  |
| <b><i>Deb-D</i></b><br><b><i>(seated on firebrick)</i></b>       | 22.62                  | <ul style="list-style-type: none"> <li>● Small cracks in the surface</li> <li>● No warping</li> </ul>   |

A bubbled effect occurred on the bottom surfaces of the compacts *Deb-A* and *Deb-B* that were placed on the metal plate and vitreosil basin respectively during the debinding procedure, see *Figure 6.4*. This effect is most probably caused by the solid metal plate and the vitreosil basin not allowing the evolved monomer gases to flow through. Compact *Deb-C*, *Figure 6.5(a)*, was distorted as a result of the relatively coarse spacing of the uneven surface of the net, but 95.1% of the cyanoacrylate was debonded. Compact *Deb-D* seated on the firebrick, *Figure 6.5 (b)*, was well debonded, i.e. >95% of the cyanoacrylate was debonded.



Therefore, further debinding investigations were performed using this method to reduce the distortion to a minimal level, whilst still enabling reasonable debinding results to be obtained.

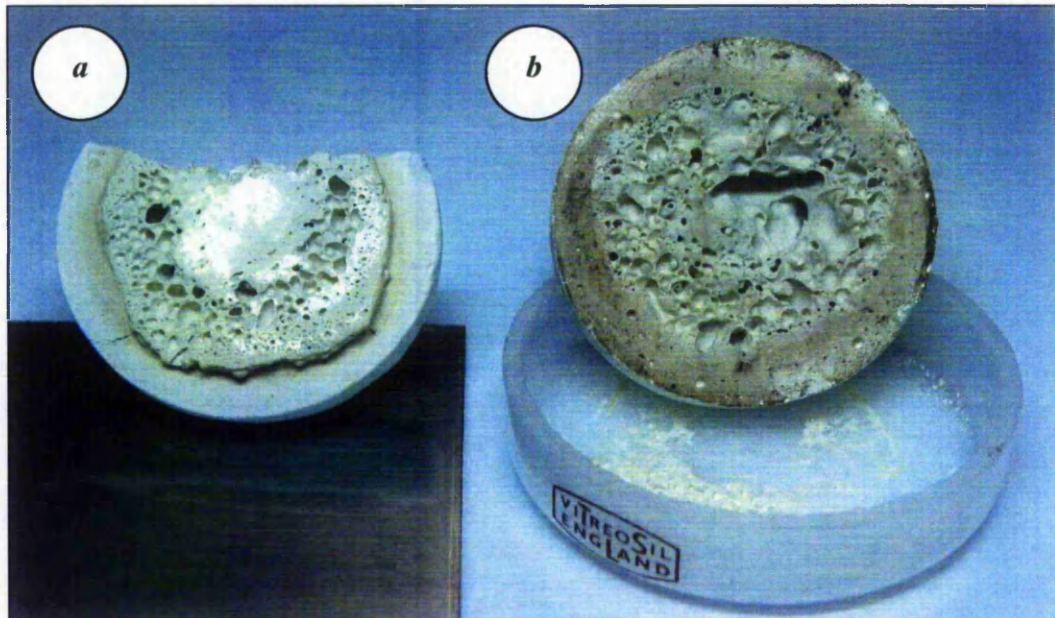


*Figure 6.4: Bubbled effect in the bottom surface of the compact that were deboned on a metal plate (a) and vitreosil basin (b).*

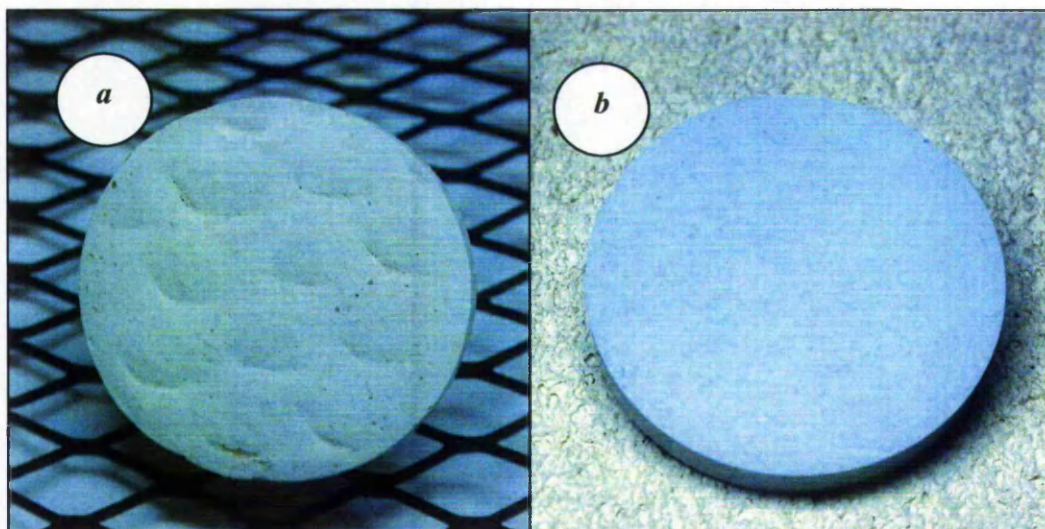


*Figure 6.5: Distortion in the bottom surface of the compact that was deboned on a metal net (a) and defect free compact that was deboned on a firebrick (b).*

#### 6.2.4 Heating Rate

As a result of the preliminary trial described in the previous section, it was considered that a heating rate of 10°C/min was too rapid to allow the debinding of the compact to be performed successfully. The cracks which appeared in the compacts at this heating rate probably arose from differential thermal expansion within the compact as it heated up from the surface inwards.

The temperature within the compact will increase relatively slowly compared to the increase in temperature of the air in the oven. Consequently an estimate has been made of the change in average temperature of the compact using basic [Eastop and McConkey, 1993]. The relevant equation can be written as:

$$\frac{t_f - \bar{t}}{t_f - t_i} = e^{-BiFo}$$

where  $t_f$  = oven temperature

$t_i$  = initial compact temperature

$\bar{t}$  = average compact temperature

$Bi$  = Biot number

$Fo$  = Fourier number

If the temperature of the oven is increased in ten degree Centigrade steps then the time taken for the average compact temperature to rise to within one degree Centigrade of the set oven temperature can be estimated as:

$$\frac{t_f - \bar{t}}{t_f - t_i} = \frac{1}{10} = 0.1$$

$$\therefore e^{-BiFo} = 0.1$$

or  $e^{BiFo} = 10$

i.e.  $BiFo = \ln 10$

or  $BiFo = 2.303$

The Biot number and Fourier number can be written as:

$$Bi = \frac{h.L}{k} \text{ and } Fo = \frac{k.\tau}{\rho.C.L^2}$$

where  $h$  = heat transfer coefficient = 30 J/m<sup>2</sup>.s.°C [NZIFST Inc., 2005].

$L$  = mid-plane distance within the compact = 0.005 m.

$k$  = thermal conductivity of the compact.

$\rho$  = density of the compact = 2392 kg/m<sup>3</sup>.

$C$  = heat capacity of the compact = 1188 J/kg.°C (*section 5.7*).

$\tau$  = time

therefore  $BiFo = \frac{h.\tau}{\rho.C.L}$

and  $\therefore \tau = \frac{\rho.C.L}{h}.BiFo$

i.e.  $\tau = \frac{2392 \times 1188 \times 0.005 \times 2.303}{30}$

i.e.  $\tau = 1091$  seconds or ~18 minutes

The calculation ignores heat absorbed by the depolymerisation of the cyanoacrylate. The result indicates that for the average temperature in a compact to be within 1 degree Centigrade of the furnace temperature, then the oven temperature should be increased in steps of about 10 degrees Centigrade and held at that temperature for 18 minutes, or more.

An oven-to-PC communication software, APT-COM (version 2.01), was used to develop control temperature programs. The oven was connected to a PC with a RS232 interface cable. This enabled the oven to be programmed and controlled using the PC.

Several oven temperature programmes were tested in order to establish an efficient heating rate to draw the binder out, whilst obtaining a defect free pre-sintering ceramic compact. The extent of debinding was determined by weighing the compact beforehand and then rapidly removing the compact from the oven every 30 minutes and re-measuring its weight. *Table 6.3* details the debinding temperatures and measurements, and observations for a series of compacts heated at different constant rates from the insertion temperature to the final temperature. *Figure 6.6* is a percentage debonded vs temperature profile for sample *DebII-E*.

*Table 6.3: Debinding temperature profiles and observations.*

| <i>Sample</i>  | <i>Total time at temperature (min)</i> | <i>Temperature (°C)</i> |            | <i>Heating rate (°C/min)</i> | <i>Compact weight loss (%)</i> | <i>Cyanoacrylate weight loss (%)</i> | <i>Observation</i>  |
|----------------|--|-------------------------|------------|------------------------------|--------------------------------|--------------------------------------|---------------------|
|                |  | <i>Start</i>            | <i>End</i> |                              |                                |                                      |                     |
| <i>DebII-A</i> | 28                                     | 80                      | 220        | 5                            | 22.2                           | 93.28                                | ● Surface cracks    |
| <i>DebII-B</i> | 40                                     | 100                     | 220        | 3                            | 22.4                           | 94.12                                | ● Surface cracks    |
| <i>DebII-C</i> | 120                                    | 100                     | 220        | 1                            | 22.7                           | 95.38                                | ● Surface cracks    |
| <i>DebII-D</i> | 240                                    | 100                     | 220        | 0.5                          | 23.0                           | 96.64                                | ● Surface cracks    |
| <i>DebII-E</i> | 480                                    | 100                     | 220        | 0.25                         | 22.65                          | 99.78                                | ● Negligible cracks |

Based on the observations from these trials, it was apparent that defects in the compact could be reduced by decreasing the heating rate. However, the reduction in the heating rate would prolong the debinding period. In addition, the

weight vs temperature profile indicated that rapid debinding only occurred after the temperature reached 170°C. Therefore, a two-stage-heating programme was developed. The debinding oven was heated from 100°C to 160°C at a heating rate of 0.5°C/min and held at 160°C for slow debinding.

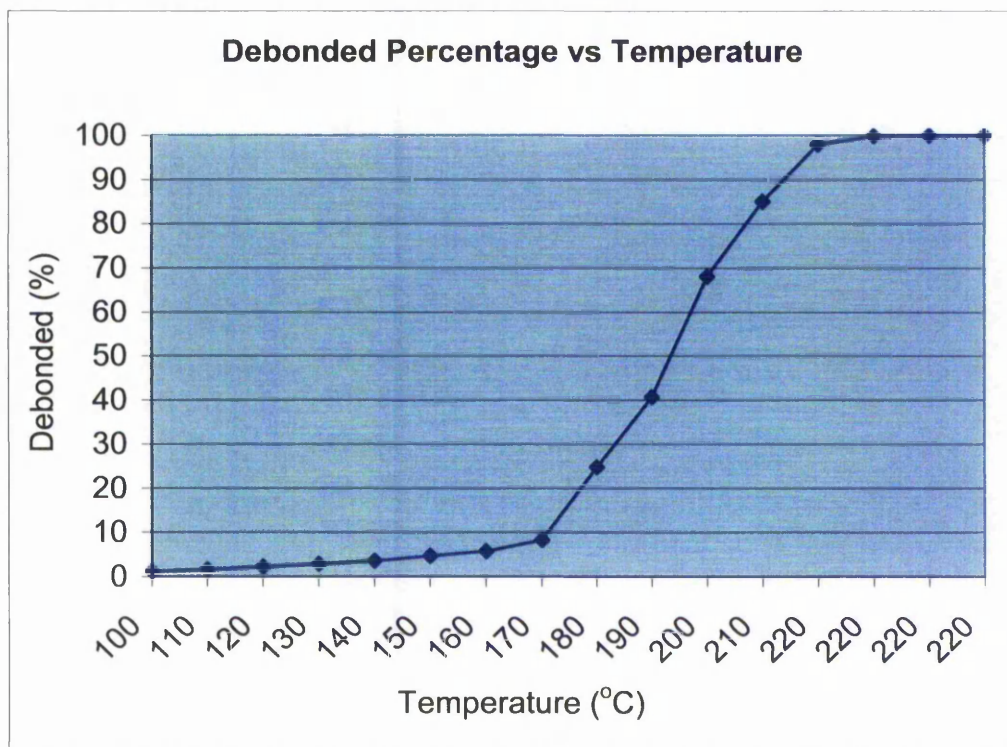


Figure 6.6: Percentage debonded vs temperature profile for sample DebII-E.

The compact was seated on a firebrick cube (approximate dimensions: 35 mm x 40 mm x 25 mm). The weight of the compact with the firebrick was measured before heating and thereafter removed from the oven using tongs and re-weighed every 30 minutes using a digital weighing machine, as shown in Figure 6.7. The compact was stopped from heating after a period where the rate of weight loss had reduced to zero. The purpose of the further heating period was to ensure that all binder had evaporated. It was noted that the compact weight

remained constant when observed after the cooling period of 30 minutes. This indicated that the binder was completely removed within the period at temperature and that the debonded compact did not change during the cooling period, e.g. by the absorption of water from the atmosphere.



*Figure 6.7: Digital weighing machine used to weigh the compact with the firebrick.*

*Figure 6.8* shows the results for this two-stage-debinding process of the compact. The debinding process profile was comparatively constant without any abrupt and rapid debinding. This more uniform rate of debinding was considered to be more appropriate and would be anticipated to assist with the preparation of a crack and distortion free compact.

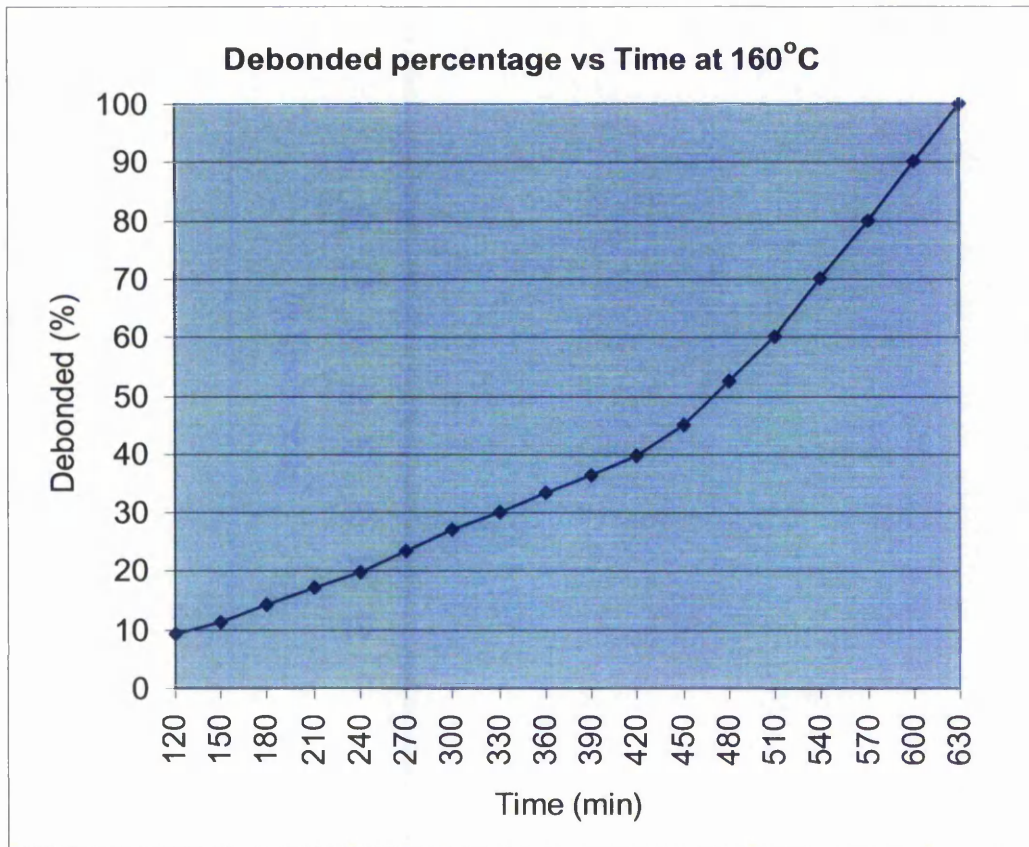


Figure 6.8: Debinding profile of cyanoacrylate.

The compact was cooled in the oven from its final temperature. Figure 6.9 is an SEM image of a debonded compact, showing the uniform small pore structure between the particles.

These observations demonstrate that the compact could be well debonded using the two-stage heating method. The cyanoacrylate was effectively completely removed using a gradual heating rate of  $0.5^{\circ}\text{C}/\text{min}$  from  $100^{\circ}\text{C}$  to  $160^{\circ}\text{C}$  for 2 hours, followed by 7.5 hours at  $160^{\circ}\text{C}$ , i.e. a total heating period of 9.5 hours.

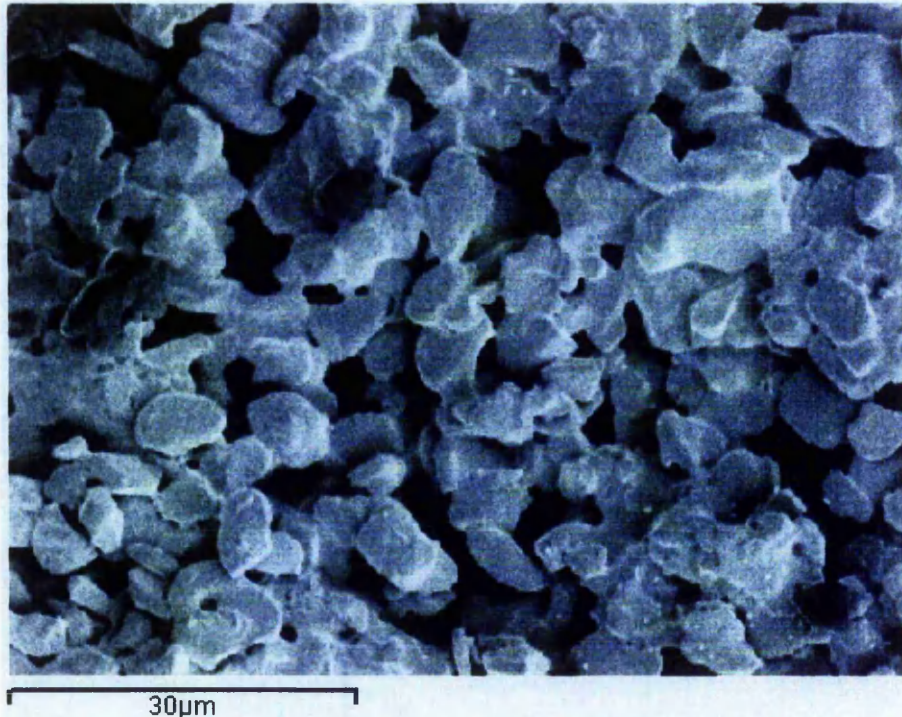


Figure 6.9: Microstructure of a debonded compact.

### 6.2.5 Debinding of Machined Compact

The debinding arrangement and the effective debinding temperature from the observations in previous sections were applied to a machined compact. The green compact used for the investigation had the composition as detailed in *Table 6.1*. The compact was prepared using a polypropylene mould to be a cylinder of dimensions 16 mm diameter and approximately 65 mm long. The compact was then sawed into shorter lengths of approximately 12 mm, turned down to a diameter of 15 mm, and then the faces turned to give 10 mm lengths using a carbide insert. This was followed by drilling through the centre using a 4 mm diameter carbide drill. The compact was seated on the firebrick cubic and placed in the debinding oven. The weight of the compact with the firebrick was measured before heating and thereafter re-weighed every 30 minutes.



The debinding process profile was very similar to *Figure 6.8*, which shows a comparatively constant debinding rate. The compact was debonded without any cracking or distortion.

## **6.3 Sintering**

In practice, ceramic compacts manufactured using a PIM technique are formed from a moulding process and pressure is not required to create the shape of the compacts during sintering. Consequently, the sinterability of the PRIME compact was investigated in a furnace without externally applied pressure.

### **6.3.1 Sintering Procedure**

An initial study of sintering of the PRIME compacts that had been debonded effectively, as reported above, is described in this section. An induction heating furnace, with a maximum frequency capability of 50 kHz and maximum power of 15 kVA, was employed for the investigation. The compact was heated inside a cylindrical hollow two-part graphite die. The compact was placed in a bed of loose boron nitride powder to minimise potential interaction between the compact and the graphite at high temperature, *Figure 6.10*.

The graphite is used as the susceptor and to transfer heat to the compact through conduction. The furnace was flushed with argon gas for 5 minutes to eliminate oxygen and other gases in the air before the heating cycle commenced. The temperatures were measured using an optical pyrometer sited on the side of the furnace. The data from the pyrometer were monitored using an analogue to digital data logger, *Figure 6.11*.

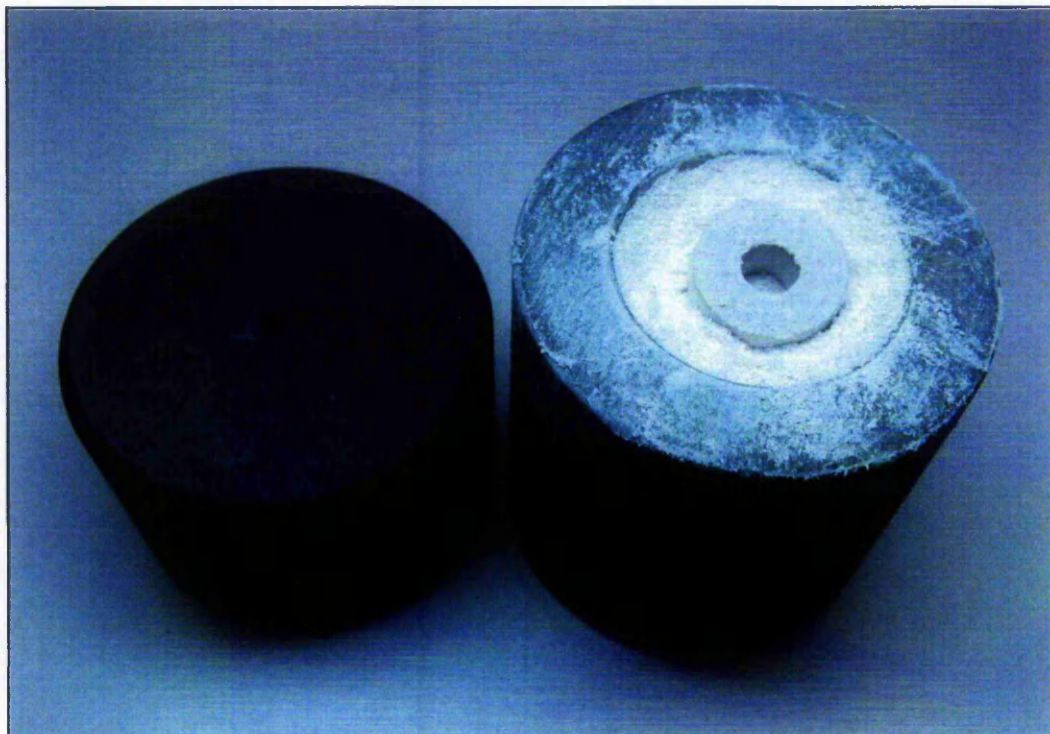


*Figure 6.10: A hollow cylindrical alumina debonded compact placed in a bed of loose boron nitride powder in a two part hollow cylindrical graphite die.*

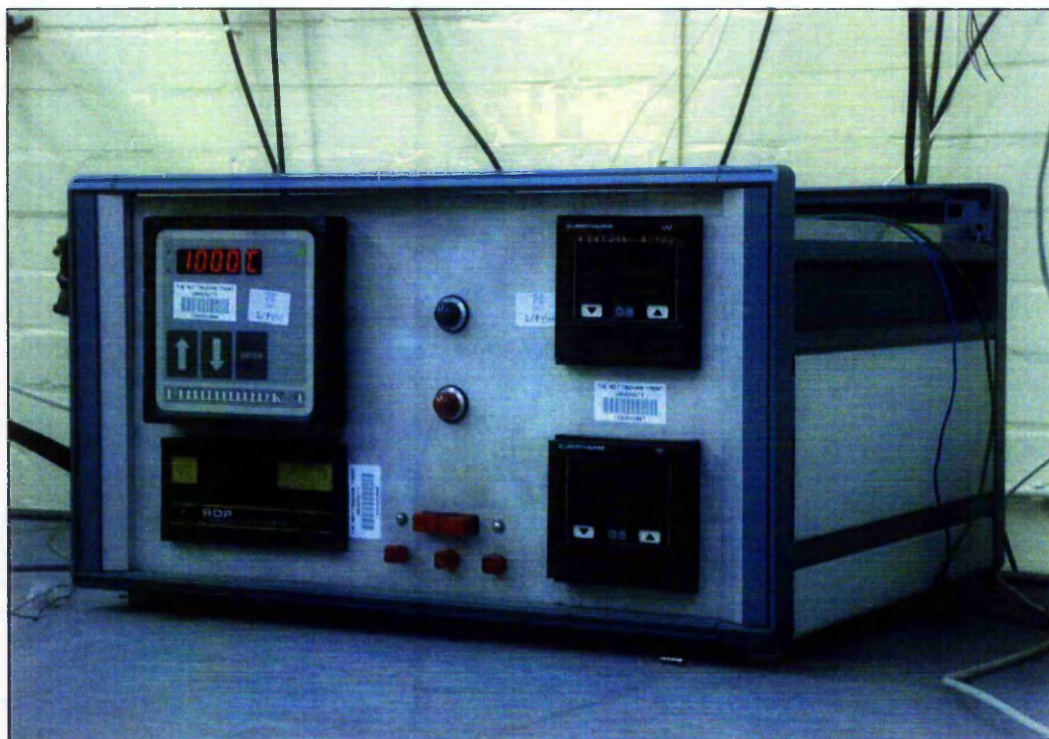


*Figure 6.11: Analogue to digital data logger used for temperature reading.*

*Figure 6.12* shows the arrangement of the sintering for the compact, with the front cover of the furnace removed, showing the graphite die within the induction-heating coil. The coil was covered with thermal insulating tape during the process to minimise heat losses due to the water-cooling system in the furnace, *Figure 6.13*. The heating rate and temperature were controlled manually. It was considered that the heating rate for the ceramic up to the sintering temperature would not be too critical, since the binder had already been removed from the compact. Therefore a reasonably high rate was used so that the time for the overall sintering cycle could be as short as practicable. All the compacts were heated to the final sintering temperature at a rate of approximately 150°C/min.

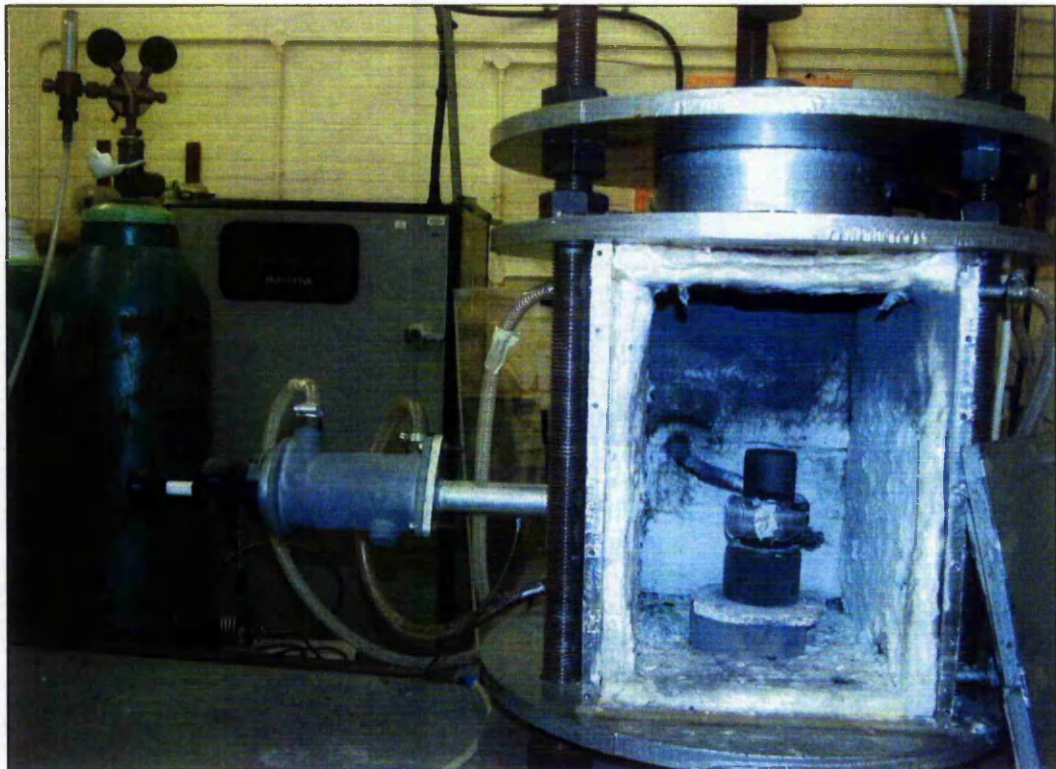


*Figure 6.12: Arrangement used for sintering*



*Figure 6.13: Induction coil covered with thermal insulating tape.*

Alumina compacts manufactured using traditional methods can be sintered at temperatures up to 1750°C for times between 60 minutes and 100 minutes [Ridgway, 2000]. Consequently, the debonded alumina compacts were heated to a sintering temperature of 1550°C, 1650°C or 1750°C, for a time of either 60 or 100 minutes. The compacts were cooled to room temperature in the furnace. *Table 6.4* details the parameters and observations on the compact sintering.

Table 6.4: Parameters and observations of the compact sintering.

| <b>Sample</b> | <b>Sintering temperature<br/>(°C)</b> | <b>Hold period<br/>(minute)</b> | <b>Observations</b>  |
|---------------|---------------------------------------|---------------------------------|--|
| <b>Si-A</b>   | 1550 °C                               | 60                              | <ul style="list-style-type: none"> <li>● Sintered</li> <li>● Fragile- collapsed</li> </ul>     |
| <b>Si-B</b>   | 1550 °C                               | 100                             | <ul style="list-style-type: none"> <li>● Sintered</li> <li>● Fragile- not handlable</li> </ul> |
| <b>Si-C</b>   | 1650 °C                               | 60                              | <ul style="list-style-type: none"> <li>● Sintered</li> <li>● Rigid</li> </ul>                  |
| <b>Si-D</b>   | 1650 °C                               | 100                             | <ul style="list-style-type: none"> <li>● Sintered</li> <li>● Rigid</li> </ul>                  |
| <b>Si-E</b>   | 1750 °C                               | 60                              | <ul style="list-style-type: none"> <li>● Sintered</li> <li>● Rigid</li> </ul>                  |
| <b>Si-F</b>   | 1750 °C                               | 100                             | <ul style="list-style-type: none"> <li>● Sintered</li> <li>● Rigid</li> </ul>                  |

The results from the *Table 6.4* demonstrated that the compact could be sintered without any problem at temperatures of 1650°C and above. Compacts *Si-A* and *Si-B*, which were sintered at 1550°C, were bonded but were very fragile. The time at the sintering temperature did not appear to have a significant influence on the macrostructure of the compact. In all cases there was no gross distortion, or any macroscopically visible cracks or other defects.

Shrinkage of the compacts *Si-C*, *Si-D*, *Si-E* and *Si-F* was measured by comparing the change in diameter before and after the sintering process using a micrometer. The compacts appeared to have reduced in diameter by less than 5%. This is a low shrinkage rate comparing to typical 15-20% linear shrinkage of green compacts with maximum dimensions of ~1 cm [Rice, 2003]. In addition, they did not appear to be any slumping or distortion, noted by their internal diameter not being distorted when it was measured. This suggested that the feedstock had mixed homogeneously and that uniform sintering took place in the whole compact.

### 6.3.2 Microstructure of the Sintered Compacts

Compact *Si-C* was examined in the SEM. *Figure 6.14* is an SEM image of the compact, indicating that small necks had formed between particles, which corresponds to the initial stage of sintering. There is also a small reduction in porosity from ~50% in the debonded green compact to ~45% in the sintered specimens. It would appear from the micrographs that sintering had occurred by joining of the initial particles, without the formation of a significant volume fraction of liquid phase. Further sintering would reduce the porosity and densify the compact further.

The compact was fractured and a small piece of the resultant sample was used for grain size measurement using the linear intercept method based on a series of SEM micrographs. A mean grain size of 3  $\mu\text{m}$  was obtained, which falls into the typical grain size of 2-4  $\mu\text{m}$  for commercial aluminas [Richerson, 1992, He and Ma, 2002].

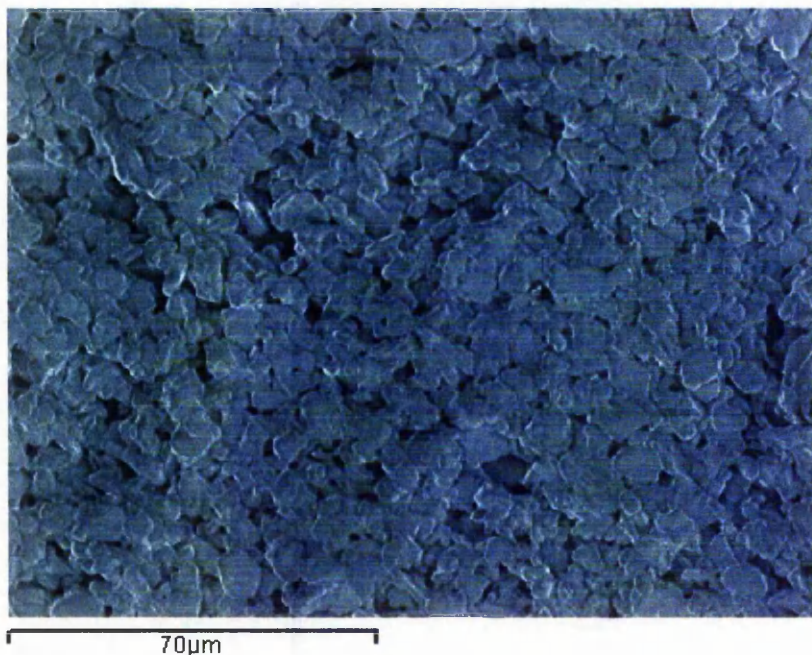


*Figure 6.14: SEM image of a sintered compact fractured surface.*

### 6.3.3 Sintering of Machined Compact

The sintering method and the effective sintering temperature of 1600°C for 60 minutes in the induction furnace were applied to the machined compact that was debonded successfully as reported in *section 6.2.5*. The compact sintered well without any cracking or significant shape distortion, see *Figure 6.15*.



*Figure 6.15: The sintered machined compact.*

### 6.3.4 Hardness of the Sintered Compact

Hardness tests were carried out on the sintered alumina/cyanoacrylate compact using a Vickers Pyramid Hardness Testing Machine. A weight of 1 kilogram was used for the hardness test. The sample was tested after it had cooled down to room temperature. Black marker ink was applied on the surface of sample to improve the visibility of the indentations under the microscope of the test machine. An average of 5 readings was taken for the final reading.

The average Vickers Pyramid Number of the compact was 12.0 VHN. The hardness of the sintered compact was about half of the green compact, which had an average hardness of 19.84 VHN.

## **6.4 Summary**

In this chapter, the ability of the green compact to be debonded and sintered was investigated. The key findings from the green compact debinding and sintering can be summarised as follows:

- The cyanoacrylate/alumina compacts could be debonded well using the two-stage heating method developed in this study. The two-stage heating method was developed for slow debinding.
- The cyanoacrylate was completely removed after gradually heating at a rate of 0.5°C/min from 100°C to 160°C and 7.5 hours heating at 160°C. The total heating period was 9.5 hours.
- The investigation of the compact sintering process showed that the compact could be sintered to form a porous load bearing body at a temperature 1650°C for 60 minutes.
- The sintered compacts could be handled by hand and could withstand reasonable forces applied to the surface.
- The sintered compact had a relatively low hardness, which was only about half of the hardness of the green compact (from 19.84 to 12.0 VHN).



## **Chapter 7 Summary and Discussion**

### **7.1 Introduction**

This project was designed to investigate a complete cycle of a new ceramic fabrication method, i.e. from selection of materials, mixing, moulding, green machining, debinding to sintering, with particular emphasis given to the experimental and modelling of the machining of the green compacts. The reactive cyanoacrylate binder imparted sufficient strength to the green compact for green machining to be performed using conventional machining techniques and tools. The reactive binder also played the main role in improving the situation with regard to two common problems occurring in the current ceramic industry: (1) time consuming, high temperature, complex debinding processes, and (2) expensive investment in non-conventional green machining facilities [Allor and Jahanmir, 1996, Inoue, 2003]. However, the properties of the reactive binder required that a non-traditional, although still relatively straightforward, fabrication process had to be developed. The highly reactive binder meant that considerable care had to be taken when mixing and handling the feedstock containing unpolymerised binder.

In this chapter, the salient features of the present study are summarised and discussed.

### **7.1.1 Compact Moulding Techniques**

The investigation of the compact moulding techniques studied the interaction of parameters and conditions required to produce high quality green ceramic compacts.

One of the novel ideas of this ceramic fabrication method is the reactive binder, cyanoacrylate, used in the feedstock. Cyanoacrylate has major advantages because of its ability to debind in a short period when exposed to relatively modest temperatures. However, the very active reaction of the cyanoacrylate during mixing produced gases that resulted in voids and increased the apparent porosity level, which also further reduced the final sintered density of the compact. Four different grades of cyanoacrylate were investigated. The cyanoacrylates were selected with a range of characteristics, including certain features that were known to assist in the success of the fabrication technique, such as viscosity and blooming level. It was found that alkoxy-ethyl cyanoacrylate had the lowest blooming level and an appropriate viscosity for the manual moulding method used in this study.

Alumina ( $Al_2O_3$ ), the most commonly used advanced engineering ceramic, was selected for the investigation because of its useful properties, such as biocompatibility, resistance to wear, high temperature strength, and resistance to corrosion. Each of these properties is typical for the class of advanced structural ceramics, and thus the present study on green machining, which was the main aim of this research, should be able to be applied successfully to green compacts containing any of these ceramic powders. Two different grades of calcined alumina powder were investigated. It was established that the *MA2LS* grade powder could be mixed with the cyanoacrylate binder up to a maximum volume

fraction of 0.49. This is sufficient to satisfy the powder volume fraction range proposed by German [1997], such that the compacts can be successfully sintered. The particle size of the powder also fulfilled the basic requirement for successful ceramic processing that it should be less than 20  $\mu\text{m}$  [Vervoort, 1996], with an ideal mean particle size being between 2  $\mu\text{m}$  and 8  $\mu\text{m}$  [German, 1991].

The major factors, in addition to the selection of an appropriate ceramic powder and binder, connected with the preparation processes of the compact were inhibition, initiation and mixing. For inhibition of the polymerisation during the mixing process, para-toluene-sulphonic acid has been confirmed to be an effective inhibitor, since only a small amount was required (as low as 3%w of binder), while glacial acetic acid required up to 8%w for effective inhibition of the polymerisation. The alumina powder was heated at 200°C before mixing to remove surface moisture, and possibly also other contaminants, which might affect the polymerisation process. Following Birkinshaw et al. [1996], caffeine was added to act as an initiator for the cyanoacrylate polymerisation. It was observed that the caffeine concentration had no perceptible influence on the ease of mixing, but the curing times decreased with increasing caffeine concentration. The inhibition and initiation of the binder are crucial to the control of the polymerisation of the cyanoacrylate, and thus the reproducibility and usefulness of the technique. These simplify the mixing process by circumventing the melting of a thermoplastic or wax based binder while mixing the feedstock in a traditional PIM technique, such as a binder system comprising of wax and polyethylene [Harranz et al., 2002], paraffin wax and polypropylene [Suri et al., 2002], or Poly Vinyl Alcohol (PVA) [Bassner and Klingenberg, 1998] which would need to be heated at mixing temperatures of 150°C to 170°C.

PE, PP, PTFE and UHMWPE were useable as appropriate mould materials for the manufacture of the compacts. Polypropylene was selected as the first choice because of its low cost and good availability.

The properties of the green compact were investigated to establish the curing or hardening period of the feedstock after mixing. The polymerised compact surface was tested with a Vickers Pyramid Hardness test. It was observed that the hardness of the compact developed quickly, followed by a more gradual increase to be a maximum 27 hours after processing, and was then stable for at least 18 months. The strength and rigidity of the green compacts were found to be more than adequate to be able to use conventional machining procedures.

Reproducibility of the compact was also investigated by examining the polymerisation temperature profile of three samples after mixing. The temperature profiles of these samples matched very closely and were considered to be sufficiently reproducible.

Overall, a moulding technique has been developed to produce green compacts with dimensions up to 15 mm diameter and 19.5 mm high, which have relatively good stability, strength and rigidity. The use of controlled procedures has enabled a reproducible and effective process to be achieved.

### **7.1.2 Green Machining**

After moulding, the green compact was observed qualitatively to have a sufficiently high strength such that it could withstand manual handling and appeared to be amenable to shaping using conventional machining methods, including drilling, turning, milling, in addition to grinding and sawing which were

used to shape the green compacts into the desired shape for the machining trials. The machining of cyanoacrylate-only compacts demonstrated that the cyanoacrylate binder has a sufficiently high strength for green machining.

As a whole, carbide tools are considered to be highly suitable materials for the machining of the alumina/cyanoacrylate compacts. Good dimensional tolerances were achieved. It is possible to machine the compact, e.g. drilling holes and milling slots, in close proximity, i.e. less than 1 mm apart.

Swarf formation in the green compact was detailed for the understanding of the behaviour of the binder and property of the material. It was noted that continuous swarf was formed during the turning operation. This type of swarf is normally present in the machining of a ductile material. This indicates that the compacts effectively behave in a macroscopically ductile manner.

From a manufacturing standpoint, this type of swarf is much preferred to the usual very fine particulate swarf generated during the machining of other green ceramic compacts [Klocke et al., 1997], for the reasons referred to in *section 2.6.2*, and also the potential adverse health effects of fine air-borne particles. The swarf were not discoloured, indicating that there was relatively little deformation/friction induced heating during the process. Further inspection of the swarf using a SEM showed no signs of debinding or thermal degradation. Therefore, coolant is not required, even for high speed machining (up to 848 m/min) based on the results of the present research.

SEM images of the machined surface of a section of swarf show that no debinding effect occurred due to the temperatures generated during machining. The ceramic particles are well bonded by the cyanoacrylate, which indicates that the temperatures generated are well below 160°C, which would result in the

depolymerisation of the cyanoacrylate binder. The machining speed did not affect the structure of the compact.

Overall, tool wear of carbide-based tools used in the machining of the green compact was relatively limited and no material transfer from the alumina/cyanoacrylate affecting the tool tip. Abrasive wear was found on the tools, due to the fact that the presence of high hardness alumina particles in the work piece material. Abrasion by the alumina particles most probably plays the dominant role in the wear of the tool.

In summary, the green new material compacts have been machined by various conventional machining methods. This means that the green material has sufficient mechanical strength to withstand the shearing action produced by the machine tool in these operations. This is the main advantage of the PRIME compact as compared to traditional green compacts that consist of a wax or polymer mixture binder and have low mechanical strength such that they cannot be easily machined.

### **7.1.3 FEA of the Green Machining**

A FEM simulation model of orthogonal cutting for the alumina/cyanoacrylate green composites was developed and evaluated with reference to the available experimental results on green machining.

The mechanical and thermal properties of the new material, where not known or measured, were estimated using either an Upper Bound or Lower Bound Estimate as considered appropriate. The key findings from the simulations can be summarised as follows:

- It is possible to use the DEFORM 2D FEA software to model the machining of the green compact, which is in effect a particulate reinforced composite with high solid volume fraction. The appropriate geometry and mesh density were determined.
- Given that the required material property data, particularly at the high strain rates involved in machining, are not known, the simulations were performed for a range of material properties, which were considered to cover the probable actual material values. It was possible in all cases to obtain solutions, which were generally qualitatively consistent with the variations expected using physical reasoning.
- The simulations were also successfully performed using different tool materials and cutting speeds based on the experimental study.
- The maximum temperatures calculated using the most likely material parameter values were  $\sim 60^{\circ}\text{C}$ , with the range varying between  $41^{\circ}\text{C}$  and  $91^{\circ}\text{C}$  at the swarf/tool interface. The maximum temperature attained at the new machined work piece surface was only  $\sim 50^{\circ}\text{C}$ . These temperatures are relatively low, and would not be expected to result in thermal degradation of the cyanoacrylate, particularly for the short times involved. Also, although the temperature dependence of the green compact's material properties is not known, it is expected that there will be only a relatively modest variation within such a limited temperature range.
- The simulation results were in good agreement with the observations of the experimental study, e.g. continuous swarf were produced, and

cutting temperatures were below the degradation temperature of the cyanoacrylate binder.

- The modelling of the green composite gave consistent results for a wide range conditions.

#### **7.1.4 Debinding and Sintering**

The moulded and the machined cyanoacrylate/alumina compacts could be debonded with a two-stage heating method. Although the results from the DSC analysis of the compact indicated that the cyanoacrylate binder would debind most efficiently between 200°C to 250°C, it was found that the compact would collapse or crack when debonded at the relatively high heating rate used for DSC. Therefore, a two-stage heating method was developed for slow debinding. The cyanoacrylate was completely drawn out after gradually heating from 100°C to 160°C at a ramp rate of 0.5°C/min, and 7.5 hours heating at 160°C. The total heating period was 9.5 hours. Significantly, the debinding period of the alumina/cyanoacrylate compact is much shorter and less complicated than debinding of typical polymeric binders in traditional CIM green compacts [Grohowski and Strauss, 2002 and Zorzi et al., 2003]. Also the process is sufficiently straightforward such that it could be undertaken using conventional thermal equipment, since it is a single binder system.

The investigation of the moulded and the machined compact sintering process had demonstrated that the compact could be partially sintered at a temperature of 1650°C for 60 minutes when placed in a bed of loose boron nitride powder within a cylindrical hollow two-part graphite die. The sintered compacts



did not crack or significantly distort under these conditions. The reduction in porosity from ~ 50% in the debonded green compact to less than ~ 45% in the sintered specimens was achieved, and joining of the initial particles had occurred without the formation of a significant volume fraction of liquid phase.

The sintered compact could be manually handled without particularly special precautions, and could withstand reasonable forces applied on the surface. The hardness of the sintered compact was very low, i.e. only about half of the hardness of the green compact (from 19.84 to 12.0 VHN).

## **7.2 Discussion**

The development of a new technique for shaping of ceramic green compacts is very important in developing cost effective and environmentally friendly techniques, broadening the potential commercial applications, and increasing the reliability and reproducibility of the product. This project was intended to create a novel ceramic fabrication method that could go some way to alleviating the common problems with conventional ceramic fabrication techniques. In this research, alumina powder and cyanoacrylate liquid were mixed and the green compacts were directly machined using different conventional machining methods.

A comparison of the novel fabrication techniques developed in this study with other more conventional techniques is presented below:

### **7.2.1 Compact Manufacturing Techniques**

The main approaches used in conventional ceramic fabrication techniques include pressing (e.g. cold and hot isostatic pressing), casting (e.g. slip and gel casting), and plastic forming (e.g. injection moulding and extrusion). Cold isostatic pressing has been used in the ceramics industry for several years and has gained wide recognition as many of the first mass produced advanced ceramics were produced using this method. Hot isostatic pressing, and a number of other methods, are rather newer fabrication techniques, which have found some success in the research and development of advanced ceramics, but have not as yet experienced very significant use as manufacturing processes. Ceramic injection moulding has been adapted from the same technique used in the plastics industry for many years, and therefore has the advantage of a base of industrial experiential knowledge. Extrusion has long been a method of manufacturing traditional ceramics, and has been adapted to advanced ceramics for certain appropriate component shapes.

Each technique has its advantages and disadvantages when it comes to the cost, properties of the product, size and geometry of the compact, and efficiency of the processes. The PRIME technique takes advantage of the cyanoacrylate for more efficient processing, e.g. controllable inhibition and initiation of the feedstock, and improved strength of the compact in the green state for conventional machining processes.

Although only certain polymeric materials, e.g. PE, PP, PTFE and UHMWPE, are suitable materials for moulding and handling the PRIME feedstock, these do generally have the advantages of being relatively low cost, high availability and can be reused. This contrasts with the plaster moulds used in

casting techniques which have limited durability [Lyckfeldt et al., 1991]. Furthermore, in the casting methods, the feedstock needs a longer time than PRIME feedstock to set in the mould, and it requires many moulds and a large space for the moulds for mass production.

In this research, the compacts were manually moulded to shape rather than injection moulded by machine. In principle traditional ceramic injection moulding machines could be used, with minor modifications if necessary, to enable the compacts to be injection moulded. The feed materials for injection moulding generally consist of a mixture of the ceramic powder with a thermoplastic polymer plus additives. The mixture is preheated in the heating barrel of the injection moulding machine to a temperature at which the polymer has a low enough viscosity to flow through the system. In PRIME, the cyanoacrylate is mixed prior feeding into the injection moulding machine and no heating is needed in the system. The separate mixing process would probably improve the homogeneity of the feedstock.

Irregular density in the compact or insufficient density or size of the compact due to incorrect die or punch(es) design are often found with pressing methods, especially uniaxial pressing [Richerson, 1992]. This affects the strength of the green compact, and furthermore, its green machineability. Another problem that needs attention is the rapid die wear that results in a progressive change in dimensions. These problems could also occur in the PRIME method but it would be expected that the rate would be slower since the mechanism of injection moulding does not require elevated temperature, and should be achievable with lower applied forces.

### **7.2.2 Green Machining**

Green compacts produced by the conventional ceramic fabrication techniques are comparatively fragile, therefore great care is necessary in the design and fabrication of tooling and handling for green machining. Attempts at improving tooling for green machining have been made [Inoue et al., 2003, Jia et al., 1996]. However, many of them focus on non-conventional methods and diamond tooling, which can be very expensive.

In this project, the green compacts produced by the PRIME method were successfully machined using conventional machining operations. The carbide tools used for the green machining of PRIME compacts are standard commercially available products, and thus relatively much cheaper than diamond tools or specialised purpose-made non-conventional tooling. It was found that long ribbon like swarf was obtained with the green machining of PRIME compacts, instead of the dust-like particles that are normally produced in the green machining of conventional ceramic compacts [Klocke, 1997]. Thus the green machining of PRIME compacts has several technological advantages for ceramic fabrication in a commercial environment.

The tool wear mechanism occurring in the machining of the alumina/cyanoacrylate green compacts is similar to that observed in an investigation of oxide ceramics green machining by Klocke et al. [2000], in which the wear behaviour of the tools is dominated by abrasion and surface damage. Abrasion wear occurring in the form of micro machining of the hard ceramic particles, and the particle phase is the primary cause of the wear on the flank face of the tool.

### **7.2.3 Debinding**

Debinding is one of the most crucial steps in any ceramic fabrication method. From the results in *section 6.2.4*, it is clear that the debinding rate is not a constant in the high debinding rate period for a powder/polymeric binder compact. German [1987] and Ying et al. [2002] have shown that the debinding rate is different from the constant drying rate period in drying theory.

It is important that debinding does not introduce any defects into the compact prior to sintering. However, there still exists a need to improve the efficiency of the debinding process by shortening the debinding period. In the current PIM industries, a two step debinding protocol is usually adopted, since combined binders are commonly required for successful moulding. Low molecular component(s), e.g. wax and stearic acid, are normally removed prior to high molecular component(s), e.g. polymer. The removal of the low molecular components by thermal debinding can result in the formation of cracks and distortion in the compact, and it is generally time-consuming. The cycle time for the debinding process depends on the binder composition, particle packing, and also on the cross sectional thickness of the compact. For compacts with a thickness of less than 10 mm, these may be debonded in 8 hours, whereas thicker sections, e.g. >1 cm, may require 20 hours, or even a complete week cycle, at high temperatures, typically above 500°C [Richerson, 1992]. In contrast, debinding of PRIME compacts only requires a simpler single step and a shorter period, *cf* 9.5 hours for compacts with diameters up to 40 mm and thicknesses up to 10 mm. Debinding of the alumina/cyanoacrylate was able to be completed at a relatively low temperature, i.e. a maximum of 160°C.

In comparison to other plastic forming methods, PRIME has a shorter debinding period. However, the shrinkage, distortion, and cracking due to too rapid binder extraction may also exist in the debinding of the PRIME compacts, but the problem(s) can be resolved by using an appropriate heating rate.

#### **7.2.4 Sintering**

The debonded particulate compacts could be transformed into ceramic articles with adequate strength during sintering. In this study, PRIME compacts were sintered using a pressureless induction furnace. Although the compacts sintered to >55% of full density without any problems, they only had a relatively low hardness. The apparent porosity is appropriate for certain applications such as in prosthetic devices, which required pores for tissue growth on the compact surface, and thermal shock sensitive engineering components.

### **7.3 Summary**

This study has shown that a cyanoacrylate binder could be employed to set up a novel injection moulding process with advantages in comparison to the traditional powder injection moulding cycles. The complete fabrication process has demonstrated that cyanoacrylate can be used as an effective reactive binder with alumina powder to produce compacts that can be machined using conventional carbide tools in order to manufacture engineering parts.

## **Chapter 8 Conclusions**

The aim of this project was to investigate the application of conventional machining techniques for green ceramic compacts produced by the PRIME method. The results from the research have shown that the aim has been achieved with reasonable success. The additional objectives of determining a complete fabrication route, including for the production of high quality sintered compacts has also been achieved.

### **8.1 Compact Moulding Techniques**

- It was determined that alkoxy-ethyl cyanoacrylate was the most appropriate binder with a low viscosity and low gaseous blooming.
- Low soda grade calcined alumina powder mixed well with alkoxy-ethyl-cyanoacrylate to combine as an appropriate feedstock.
- Alumina powder mixed with the cyanoacrylate binder to a volume fraction as high as 48%  $V_f$ , which is acceptable for injection moulding investigation.
- Polypropylene was found to be an appropriate container material for mixing and moulding of the green compacts.
- Para-toluene-sulphonic acid has been determined as an effective inhibitor, which only required a small amount of binder (as low as 3%w).
- Caffeine could contribute to the initiation of cyanoacrylate polymerisation more efficiently than water/steam.

- The hardness of the green compact increased to a maximum value within 27 hours of processing, and remained constant thereafter.
- The reaction temperature after mixing the feedstock materials increased by less than 10°C.
- The processing conditions for the green compacts were reproducible.

## **8.2 Green Machining**

- The green compacts could be drilled, turned, milled, grinded and sawn with conventional tools, indicating that the cyanoacrylate binder has a suitable combination of properties for green machining.
- Continuous swarf formation while turning indicated that the compacts behave in a macroscopically ductile manner.
- Good dimensional tolerances can be achieved, e.g. drilling holes and milling slots, in close proximity, i.e. less than 1 mm apart.
- SEM images of the machined surface of a section of swarf showed that ceramic particles were well bonded by the cyanoacrylate, which indicated that the temperatures generated during machining are probably below 160°C.
- The machining speed did not affect the structure of the compact.
- Coolant was not required for the machining operation, as the compacts did not show any signs of thermal degradation.
- Carbide, and coated carbide, tools exhibited limited wear in the machining of the green compact, with no material transfer from the alumina/cyanoacrylate affecting the tool tip.



- Abrasive wear was found on the tools, probably due to the presence of high hardness alumina particles in the work piece material.

### **8.3 FEA of the Green Machining**

- A FEM simulation model of orthogonal cutting for the alumina/cyanoacrylate green composite was developed using DEFORM 2D.
- The simulation results were in good agreement with the observations of the experimental investigation, e.g. continuous swarf were produced, and cutting temperatures were below the degradation temperature of the cyanoacrylate binder.
- The modelling of the green composite gave consistent results for a wide range conditions.

### **8.4 Debinding and Sintering**

- The cyanoacrylate/alumina compacts could be well debonded using a two-stage heating procedure.
- The cyanoacrylate was completely removed after heating from 100°C to 160°C at a ramp rate of 0.5°C/min, followed by 7.5 hours at 160°C.
- The compact could be partially sintered at a temperature of 1650°C for 60 minutes.
- The sintered compacts did not crack or appear to have any signs of distortion and could withstand reasonable forces applied to the surface.

## **Chapter 9 Further work**

The further research that could be undertaken would generally be to extend the range of ceramic and metal materials that could be manufactured by this technique. The proposed future work for further investigation can be broken down into six major areas of study:

### **9.1 Improvement in the Reactive Binder System**

- Determine the possibility of using ultraviolet or visible light curing cyanoacrylate, such as photo-initiated-ethyl cyanoacrylate, which would initiate the polymerisation after moulding by an external influence. This could simplify the mixing process and improve the efficiency of the curing process.

### **9.2 Mixing and Moulding System**

- Design a mixing and moulding machine that can avoid the cyanoacrylate binder and the powder being exposed to air. This would minimise the polymerisation caused by humidity in the surrounding air.

### **9.3 Computational Analysis**

- Develop a computational analysis for the mixing and moulding processes that includes parameters such as inhibition and initiation of the polymerisation as well as the particle's conditions.

### **9.4 Analysis of Green Machining Parameters**

- Develop a quantitative relationship between feed rate, cutting speed and surface finish. The use of profileometer or a non-contact laser scanning method to measure surface finish should be investigated.

### **9.5 Sintering Process**

- Investigate a sintering process that will sinter the PRIME compact to a denser level in order to widen the applications potential of the sintered compacts. This may involve sintering aids.

### **9.6 Application of the Technique**

- Determine the possibility of applying the technique to other ceramic powders, including the incorporation of sintering aids.
- Determine the possibility of manufacturing metal compacts using this technique.

## References

- Allor R. L. and Jahanmir S., 1996**, “*Current Problems and Future Directions for Ceramic Machining*”, The American Ceramic Society Bulletin, Vol. 75, No.7, Pp. 40-43.
- Arola D. and Rumulu M., 1997**, “*Orthogonal Cutting of Fibre-Reinforced Composites: A Finite Element Analysis*”, International Journal of Mechanical Sciences, Vol. 39, Pp. 597-613.
- Ashby M. and Jones D., 1998**, “*Engineering Materials 2*”, Butterworth Heinemann.
- Baker M., Rosler J. and Siemers C., 2002**, “*Finite Element Simulation of Segmented Chip Formation of Ti-6Al-4V*”, ASME Journal of Manufacturing Science and Engineering, Vol. 124, No. 2, Pp. 485-488.
- Barriere T., Liu B. and Gelin J. C., 2003**, “*Determination of the Optimal Process Parameters in Metal Injection Molding from Experiments and Numerical Modeling*”, Journal Materials Processing Technology, Vol. 143-144, Pp. 636-644.
- Bassner S. L. and Klingenberg E. H., 1998**, “*Using Poly(Vinyl Alcohol) as a Binder*”, The American Ceramic Society Bulletin, Pp. 71-75.
- Bast R., 1993**, “*Organic Additives for Ceramics- An Overview*”, British Ceramic Transactions, Vol. 92, No.5, Pp 217-218.
- Birkinshaw C., Buggy M., and O’Neill A., 1996**, “*Reaction Moulding of Metal and Ceramic Powders*”, Journal of Chemical Technology & Biotechnology, Vol. 66, 19-24.
- Brown J., 1998**, “*Advanced Machining Technology Handbook*”, McGraw-Hill.
- Campbell J., 1997**, “*Opportunities for Ceramics Industry*”, British Ceramic Transactions, Vol. 96, No. 6, Pp. 237-246.
- Ceretti E., 1998**, “*FEM Simulations of Segmented Chip Formation in orthogonal cutting: Further Improvements*”, Proc. of the CIRP International Workshop on Modelling of Machining Operations, Pp. 257-263.

**Ceretti E., Lazzaroni C., Menegardo L. and Altan T., 2000,** *“Turning Simulations using a Three-Dimensional FEM Code”*, J. Mater. Process. Technol., Vol. 98, Pp. 99–103.

**Chand R. and Guo C., 1996,** *“A New Concept in Cost-Effective Machining”*, The American Ceramic Society Bulletin, Vol. 75, No. 6, Pp.58-59.

**Courtney P. J. and Verosky C., 1999,** *“Advances in Cyanoacrylate Technology for Device Assembly”*, Medical Device & Diagnostic Industry, Pp. 62-77.

**Deng J. and Lee T., 2002,** *“Ultrasonic Machining of Alumina-Based Ceramic Composites”*, Journal of the European Ceramic Society, Vol. 22, No. 8, Pp. 1235-1241.

**Desai C. S. and Abel J. F., 1972,** *“Introduction to the Finite Element Method- A Numerical Method for Engineering Analysis”*, Van Nostrand Reinhold Company.

**Eastop T. D. and McConkey A., 1993,** *“Applied Thermodynamics for Engineering Technologist”*, Fifth Edition, Longman Scientific & Technical.

**Engineering Fundamentals, eFunda, 2005,** Home Page at <http://www.efunda.com/processes/machining/chip.cfm> [Accessed: 9<sup>th</sup> February 2005]

**Filser F., Lüthy H., Schärer P. and Gauckler L., 1998,** *“All Ceramic Dental Bridges by Direct Ceramic Machining (DCM)”*, Journal of Materials Science: Materials in Medicine, Vol. 7, Pp. 165-189.

**Fischer C. E. and Chigurupati P. 2003,** *“Using Computer Simulation to Understand and Optimize High-Speed Machining”*, SME High Speed Machining Conference, Chicago, Illinois.

**Foresight Report, 2000,** *“Shaping our Society- Materials Panel consultation recommendations”*, The UK Office of Science and Technology.

**Freitag D.W. and Richerson D.W. 1998,** *“Opportunities for Advanced Ceramics to Meet the Needs of the Industries of the Future”*, US Department of Energy Report DOE/ORO 2076.

**Fujishima S., 2000**, "*The History of Ceramic Filter*", IEEE Transactions on Ultrasonic, Ferroelectrics and Frequency Control, Vol. 47, No. 1, Pp. 1-7.

**Glaw V., Hahn R., Paredes A., Hein U., Ehrmann O. and Reichl H., 1997**, "*Laser Machining of Ceramics and Silicon for MCM-D Applications*", International Symposium on Advanced Packaging Materials, Pp. 173-177.

**German R. M., 1987**, "*Theory of Thermal Debinding*", International Journal of Powder Metallurgy, Vol. 23, Pp. 237-245.

**German R. M., 1990**, "*Powder Injection Moulding*", Metal Powder Industries Federation, Princeton, NJ.

**German R. M. and Bose A., 1997**, "*Injection Molding of Metals and Ceramics*", Metal Powder Industries Federation.

**Grzesik W. and Nieslont P., 2003**, "*A Computational Approach to Evaluate Temperature and Heat Partition in Machining with Multilayer Coated Tools*", International Journal of Machine Tools & Manufacture, Vol. 43, Pp. 1311-1317.

**Grohowski J. A. and Strauss J. T., 2002**, "*Effect of Atmosphere Pressure on Thermal Debinding Rate Behaviour*", Advances in Powder Metallurgy & Particulate Materials, Vol. 10, Pp.101-116.

**Hannink R. H. J., Green D. J. and Swain M. V., 1989**, "*Transformation Toughening of Ceramics*", Boca Raton, Fla.:CRC Press.

**Harranz G., Levenfeld B., Varez A. and Torralba J.M., 2002**, "*Effect of Binder Composition on Rheological Behaviour of M2-HSS Powder-Polymer Mixtures for PIM Tech*", Advances in Powder Metallurgy & Particulate Materials, Vol. 10, Pp.366-378.

**He Z. and Ma J., 2002**, "*Grain-Growth Law during Stage 1 Sintering of Materials*", Journal of Physics D: Applied Physics, Vol. 35, Pp. 2217-2221.

**Holme J. D., 1993**, "*Powder Injection Moulding: Still Waiting in the Wings*", Materials World, Vol. 1, No. 10, Pp. 552-554.

**Hu J., 2005**, "*Computational Modelling of Hardness and Soft Impresser Testing of Materials*", Nottingham Trent University, PhD Thesis.

**Hua J. and Shivpuri R., 2002,** *"Influence of Crack Mechanics on the Chip Segmentation in Machining of Ti-6Al-4V"*, Proc. of the Ninth ISPE International Conference on Concurrent Engineering, Pp. 375-365.

**Hull J. B., Birkinshaw C. and Buggy M., 1996,** *"Novel Binder/Carrier System: Powder Reaction Injection Moulding Engineering (PRIME)"*, Patent No.9615698.9.

**Hull J. B. and Ridgway J., 2001,** *"Green Machining of Powder/Carrier Feedstock used in the Manufacture of Ceramic Heart Valves"*, New Trent in Design and Manufacture, Aswan, Egypt.

**Inoue T., Tsuchida Y., Suzuki T. and Aoki W. 2003,** *"Alumina Ceramics Cutting by Self-Sharpening Edge Technique of Diamond"*, Journal of Materials Processing Technology, Vol. 143, Pp. 657-661.

**Jia Z., Guo Y. F., Liu Y., Zhang J. H., Ai X., Ai Z. and Liu J., 1996,** *"The State of the Machining of Ceramic Materials in China"*, Journal of Materials Processing Technology, Vol. 62, Pp. 20-23.

**Jeffrey A. and David S., 1996,** *"The Powder Injection Moulding Process"*, Materials World, Materials World, Vol. 16 No., Pp. 629-30.

**Kalpakkjian S., 1997,** *"Manufacturing Processes for Engineering Materials"*, Addison Wesley Longman, Inc..

**Kashefi M., Henshall J. L. and Hull J. B., 2004,** *"PRIME Surface Coating- A Novel Technique of Applying Thick Ceramic Coatings"*, 3<sup>rd</sup> ASM International Surface Engineering congress, Orlando, USA.

**Kashefi M., Henshall J. L. and Hull J. B., 2004,** *"PRIME Surface Coatings"*, International Congress for Particle Technology, PARTEC 2004, Nuremberg, Germany.

**Kim K. S., Lee D.G., Kwak Y. K. and Suk N., 1992,** *"Machinability of Carbon Fiber-Epoxy Composite Materials in Turning"*, Journal of Materials Processing Technology, Vol. 32, No. 3, Pp. 553-570.

**King A. G., 2002,** *"Ceramic Technology and Processing- a practical working guide"*, William Andrew publishing.

**Klocke F., Gerent O., Schippers C. and Aachen D., 1997**, "*Machining of Advanced Ceramics in the Green State*", Ceramic Forum International, Vol. 74, Pp. 288-290.

**Klocke F., Pähler D., Schippers C. and Schmidt C., 2000**, "*Green Machining of Oxide Ceramics with a Defined Cutting Edge*", Production Engineering, Vol. VII/2, Pp. 35-40.

**Kobayashi A., 1989**, "*Precision Machining Methods for Ceramics*", Advanced Technical Ceramics, Pp. 261-313.

**Konopka K., Boczkowska A., Batorski K., Szafran M. and Kurzydyowski K.J., 2004**, "*Microstructure and Properties of Novel Ceramic-Polymer Composites*", Materials Letters, Vol. 58, Pp. 3857-3862.

**Kumar D. B. R., Reddy M. R., Mulay V. N. and Krishnamurti N., 2000**, "*Acrylic Co-polymer Emulsion Binders for Green Machining of Ceramics*", European Polymer Journal, Vol. 36, Pp. 1503-1510.

**Lee H., 1981**, "*Cyanoacrylate Resins- The Instant Adhesives*", Paradena Technology Press.

**Lee W. E. and Rainforth W. M., 1994**, "*Ceramics Microstructures- Property Control by Processing*", Chapman & Hall.

**Lin Z. C. and Lin S. Y., 1992**, "*A Coupled Finite Element Model of Thermoelatic- Plastic Large Deformation for Orthogonal Cutting*", Journal of Engineering Materials Technology, Vol. 114, Pp. 218-226.

**Lyckfeldt O., Bostedt E., Persson M., Carlsson R. and Bergström L., 1991**, "*Stabilization and Slip Casting of Silicon and Silicon Nitride in a Non-Aqueous Medium*", Proceedings 7<sup>th</sup> CIMTEC, Pp. 1073-1082.

**Maier H. R. and Michaeli N., 1997**, "*Green Machining of Alumina*", Key Engineering Materials, Vol. 132-136, Pp. 436-439.

**Marusich T. D. and Ortiz M., 1995**, "*Modelling and Simulation of High Speed Machining*", Int. J. Numer. Math. Eng., Vol. 38, Pp. 3675-3694.



**Matthew A. D. and Timothy J. B., 2001,** “*Thermomechanical Oscillation in Material Flow during High-Speed Machining*”, *Philosophical Transactions: Mathematical, Physical and Engineering Sciences*, Vol. 359, Pp. 821-846.

**McCabe T. and Chang D., 2002,** “*Mechanical Properties Differences in PIM Materials*”, *Advanced in Powder Metallurgy & Particulate Materials*, Vol. 10, Pp. 234-239.

**Mills B. and Redford A. H., 1983,** “*Machinability of Engineering Materials*”, Applied Science Publishers.

**Mutsuddy B. C. and Ford R. G., 1995,** “*Ceramic Injection Molding*”, Chapman & Hall.

**Nakagawa T., Ohmori H., Suzuki K., Uematsu T., Hamano Y., Kamigaito O., Kishi T. and Sakai M., 1988,** “*Novel Efficient and Precise Grinding Technology for Structural Ceramics*”, *MRS International Meeting on Advanced Materials-Structural Ceramics/Fracture Mechanics*, Vol. 5, Pp. 159–169.

**Newby R. A., Lippert T. E., Bruck G. J., Alvin M. A. and Smeltzer E. E., 1999,** “*Development of Advanced Hot Gas Ceramic Filter Systems*”, *Proceedings of the 15th International Conference on Fluidized Bed Combustion*, Paper No. FBC99-0132.

**Ng E. G. and Aspinwall D. K., 2002,** “*Modelling of Hard Part Machining*”, *Journal of Materials Processing Technology*, Vol. 127, Pp. 222-229.

**Nogueira R. E., Bezerra A. C., Santos F. C., Sousa M. R. and Acchar W., 2001,** “*Low-Pressure Injection Moulding of Alumina Ceramics Using a Carnauba Wax Binder: Preliminary Results*”, *Key Engineering Materials*, Vol. 189-191, Pp.67-72.

**NZIFST Inc.,** Home Page at <http://www.nzifst.org.nz> [Accessed: 10<sup>th</sup> March 2005].

**Obikawa T., Sasahara H., Shirakashi T. and Usui E., 2002,** “*Application of Computational Machining Method to Discontinuous Chip Formation*”, *ASME Journal of Manufacturing Science and Engineering*, Vol. 119, No. 4b, Pp. 667-674.

**Okushima K. and Kakino Y., 1971,** “*The Residual Stress Produced by Metal Cutting*”, *Annual CIRP* 20, Vol. 1, Pp. 13-14.

**Oxley P. L. B., 1989**, "*An Analytical Approach to Assessing Machinability*", Ellis Horwood Limited.

**Pao Y. C., 1986**, "*A First Course in Finite Element Analysis*", Allyn and Bacon, Inc.

**Puertas I. and Luis C. J., 2004**, "*A Study on the Electrical Discharge Machining of Conductive Ceramics*", Journal of Material Processing Technology, Vol. 153-154, Pp. 1033-1038.

**Rak Z. S., 1999**, "*New Trends in Powder Injection Moulding*", Powder Metallurgy and Metal Ceramics, Vol. 38, No. 3-4, Pp.126-132.

**Reddy J. J., and Vijayakumar M., 2001**, "*Combined Model for Prediction of Viscosity of Powder Injection Moulding Mixes*", Powder Metallurgy, Vol. 44, No. 2, Pp. 128-132.

**Reed J. S., 1995**, "*Principles of Ceramics Processing*", Second Edition, John Wiley & Sons, Inc.

**Rice R. W., 2003**, "*Ceramic Fabrication Technology*", Marcel Dekker Inc.

**Richerson D. W., 1992**, "*Modern Ceramic Engineering- Properties, Processing, and Use in Design*", Second Edition, Revised and Expanded, Marcel Dekker, Inc.

**Ridgway J. S., 2000**, "*Development of Novel Ceramic Processing Techniques for Manufacture of Heart Valves*", Nottingham Trent University, PhD Thesis.

**Ridgway J. S., Hull J. B. and Gentle C. R. 1999**, "*Machining of Green Ceramic Compacts Produced by Powder Reaction Moulding*", Proc. Conf. TECOS, Rogaska Slatina, Slovenia.

**Ridgway J. S., Hull J. B. and Gentle C. R., 2001**, "*Development of a Novel Binder System for Manufacture Of Ceramic Heart Valve Prostheses*", Journal of Materials Processing Technology, Vol. 109, No. 1-2, Pp. 161-167.

**Rohini K. D. B., Rami R. M., Mulay V. N. and Krishnamurti N., 2000,** “*Acrylic Co-Polymer Emulsion Binders for Green Machining of Ceramics*”, *European Polymer Journal*, Vol. 36, Pp. 1503-1510.

**Roberts J. T. A., 1979,** “*Ceramic Utilization in the Nuclear Industry: Current Status and Future Trends*”, *Powder Metallurgy International*, Vol.11, No 1, Pp. 24-29.

**Russo F. P. and Partis D. A., 2000,** “*Advanced Materials & Powders*”, *The American Ceramic Society Bulletin*, Pp. 45-56.

**Shet C. and Deng X., 2002,** “*Finite Element Analysis of the Orthogonal Metal Cutting Process*”, *J. Mater. Process. Technol.*, Vol. 105, Pp. 95-109.

**Stevens R., 1986,** “*Zirconia and Zirconia Ceramics*”, *Magnesium Electron Ltd*, Second Edition.

**Sohner J., Weule H., Biesinger F., Schulze V. and Vohringer O., 2001,** “*Examinations and 3D-Simulations of HSC Face Milling Process*”, *Proceedings of the Fourth CIRP International Workshop on Modelling of Machining Operations*, Pp. 111–115.

**Sōmiya S., 1984,** “*Ceramics: Definitions*”, *Advanced Technical Ceramics*, Academic Press Limited.

**Suri P., Atre S. A. and German R. M. 2002,** “*Effect of Mixing on the Rheology of Alumina Feedstock*”, *Advances in Powder Metallurgy & Particulate Materials*, Vol. 10, Pp. 23-32.

**Tay A. O., Stevenson M. G. and Davis G. de V., 1974,** “*Using the Finite Element Method to Determine Temperature Distributions in Orthogonal Machining*”, *Proc. Inst. Mech. Eng.*, Vol. 188, No. 55, Pp. 681-683.

**Thoe T. B., Aspinwall D. K. and Killey N., 1999,** “*Combined Ultrasonic and Electrical Discharge Machining of Ceramic Coated Nickel Alloy*”, *Journal of Material Processing Technology*, Vol. 92-93, Pp. 323-328.

**Tirloq J. and Cambier F., 1989,** “*An Overview of the Movements in the Engineering Ceramics Area 1985-1987*”, *2nd European Symposium on Engineering Ceramics*, Elsevier Applied Science, Pp. 31-43.

**Trent E. M. and Wright P. K. W., 2000, "Metal Cutting",** Fourth Edition, Butterworth Heinemann.

**Tsai C. H. and Ou C. H., 2004, "Machining a Smooth Surface of Ceramic Material by Laser Fracture Machining Technique",** Journal of Material Processing Technology, Vol. 155-156, Pp. 1797-1804.

**Vervoort P. J., Vetter R. and Duszczyc J., 1996, "Overview of Powder Injection Molding",** Advanced Performance Materials, Vol. 3, Pp. 121-151.

**Wachtman J. B. and Haber R. A., 1993, "Ceramic Films and Coatings",** William Andrew Publishing.

**Wakuda M., Yamauchi Y. and Kanzaki S., 2003, "Material Response to Particle Impact during Abrasive Jet Machining of Alumina Ceramics",** Journal of Material Processing Technology, Vol. 132, Pp. 177-183.

**Wang R., Pan W., Chen J., Fang M., Jiang M. and Cao Z., 2003, "Microstructure and Mechanical Properties of Machinable  $Al_2O_3/LaPO_4$  Composites by Hot Pressing",** Ceramics International, Vol. 23, Pp. 83-89.

**Weller E.J. and Haavisto M., 1984, "Nontraditional Machining Processes",** Society of Manufacturing Engineers, Second Edition.

**Yen Y. C., Jain A., Chigurupati P., Wu W. T. and Altan T., 2003, "Computer Simulation of Orthogonal Cutting Using a Tool with Multiple Coatings",** Journal of Machining Science & Technology, Vol. 8, Pp. 305-326.

**Ying S., Lam Y. C., Yu S. C. M. and Tam K. C., 2002, "Simulation of Thermal Debinding",** Advances in Powder Metallurgy & Particulate Materials, Vol. 10, Pp. 117-128.

**Zhang B., Zheng X. L., Tokura H. and Yoshikawa M., 2002, "Grinding Induced Damage in Ceramics" Journal of Materials processing Technology, Vol. 132, Pp. 353-364.**

**Zorzi J. E., Perotoni C. A. and Jornada J. A. H. Da, 2003, "A New Partially Isostatic Method for Fast Debinding of Low-Pressure Injection Molded Ceramic Parts",** Materials Letters, Vol. 57, Pp. 3784-3788.

# Appendix A Technical Data Sheet of Loctite 408



Loctite UK Limited, Watchmead,  
 Welwyn Garden City, Herts, AL7 1JH  
 Technical Services Tel: (01707) 358888  
 Customer Services Tel: (01707) 358844

## Technical Data Sheet Product 408

January 1995

### PRODUCT DESCRIPTION

LOCTITE® Product 408 is a very low viscosity cyanoacrylate adhesive with low odour and non-blooming characteristics.

### TYPICAL APPLICATIONS

Bonding applications where vapour control is difficult.

### PROPERTIES OF UNCURED MATERIAL

|                                    | Value                                | Typical | Range   |
|------------------------------------|--------------------------------------|---------|---------|
| Chemical Type                      | Alkoxy-ethyl cyanoacrylate           |         |         |
| Appearance                         | Water white to straw coloured liquid |         |         |
| Specific Gravity @ 25°C            | 1.1                                  |         |         |
| Viscosity @ 25°C, mPas (cP)        |                                      |         |         |
| Brookfield LVF Spindle #1 @ 60 rpm | 7                                    |         | 4 to 10 |
| Flash Point (TCC), °C              | >82                                  |         |         |

### TYPICAL CURING PERFORMANCE

Under normal conditions, the surface moisture initiates the hardening process. Although full functional strength is developed in a relatively short time, curing continues for at least 24 hours before full chemical/solvent resistance is developed.

### Cure speed vs. substrate

The rate of cure will depend on substrate used. The table below shows the fixture time achieved on different materials at 22°C, 50% relative humidity. This is defined as the time to develop a shear strength of 0.1 N/mm<sup>2</sup> (14.5 psi) tested on specimens according to ASTM D1002.

| Substrate          | Fixture Time, seconds |
|--------------------|-----------------------|
| Steel (degreased)  | 30 to 70              |
| Aluminium          | 5 to 20               |
| Neoprene           | <5                    |
| Nitrile rubber     | <5                    |
| ABS                | 20 to 60              |
| PVC                | 20 to 50              |
| Polycarbonate      | 20 to 60              |
| Phenolic materials | 30 to 60              |

### Cure speed vs. bond gap

The rate of cure will depend on the bondline gap. High cure speed is favoured by thin bond lines. Increasing the bond gap will slow down the rate of cure.

### Cure speed vs. activator

Where cure speed is unacceptably long due to large gaps, applying activator to the surface will improve cure speed. However, this can reduce the ultimate strength of the bond, therefore testing is recommended to confirm effect.

### TYPICAL PROPERTIES OF CURED MATERIAL

#### Physical Properties

|   |                     |
|---|---------------------|
| Coefficient of thermal expansion, ASTM D696, K <sup>-1</sup>                      | 80x10 <sup>-6</sup> |
| Coefficient of thermal conductivity, ASTM C177, W.m <sup>-1</sup> K <sup>-1</sup> | 0.1                 |
| Glass Transition temperature, ASTM E228, °C                                       |                     |

#### Electrical Properties

Dielectric constant & loss, 25°C, ASTM D150:

| measured at                           | Constant | Loss                 |
|---------------------------------------|----------|----------------------|
| at 50Hz:                              | 2.3      | <0.02                |
| 1kHz:                                 | 2.3      | <0.02                |
| 1MHz:                                 | 2.3      | <0.02                |
| Volume resistivity, ASTM D257, Ω.cm:  |          | 1 x 10 <sup>16</sup> |
| Dielectric strength, ASTM D149, KV/mm |          | 25                   |

### PERFORMANCE OF CURED MATERIAL

(After 24 hr at 22°C)

|   | Value       | Typical Range           |
|---|-------------|-------------------------|
| Shear Strength, ASTM D1002, DIN 53283       |             |                         |
| Grit Blasted Steel, N/mm <sup>2</sup> (psi) | 18 (2610)   | 14 to 22 (2030 to 3190) |
| Etched Aluminium, N/mm <sup>2</sup> (psi)   | 12 (1740)   | 9 to 15 (1305 to 2175)  |
| ABS, N/mm <sup>2</sup> (psi)                | >6 (>870)   |                         |
| PVC, N/mm <sup>2</sup> (psi)                | 5 (725)     | 2 to 8 (290 to 1160)    |
| Polycarbonate, N/mm <sup>2</sup> (psi)      | >3 (>435)   |                         |
| Phenolic, N/mm <sup>2</sup> (psi)           | 10 (145)    | 5 to 15 (700 to 2200)   |
| Neoprene rubber, N/mm <sup>2</sup> (psi)    | >10 (>1450) |                         |
| Nitrile rubber, N/mm <sup>2</sup> (psi)     | >10 (>1450) |                         |
| Tensile Strength, ASTM D2095, DIN 53282     |             |                         |
| Grit Blasted Steel, N/mm <sup>2</sup> (psi) | 17.5 (2538) | 10 to 25 (1450 to 3600) |

NOT FOR PRODUCT SPECIFICATIONS.

THE TECHNICAL DATA CONTAINED HEREIN ARE INTENDED AS REFERENCE ONLY.  
 PLEASE CONTACT LOCTITE CORPORATION QUALITY DEPARTMENT FOR ASSISTANCE AND RECOMMENDATIONS ON SPECIFICATIONS FOR THIS PRODUCT.  
 ROCKY HILL, CT FAX: +1 (203)-571-5473 DUBLIN, IRELAND FAX: +353-(1)-451-9494

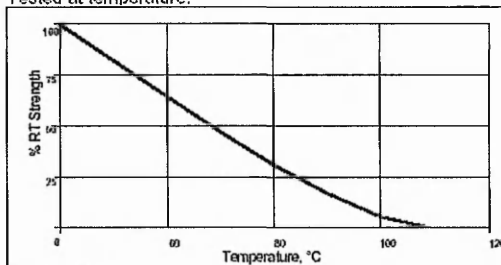
TDS 408 January 1995

**TYPICAL ENVIRONMENTAL RESISTANCE**

Test Procedure : Shear Strength ASTM-D1002/DIN 53283  
 Substrate: Grit blasted mild steel laps  
 Cure procedure: 1 week at 22°C

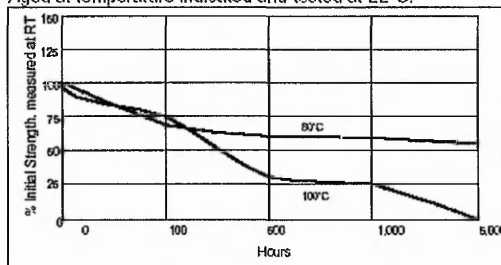
**Hot Strength**

Tested at temperature.



**Heat Aging**

Aged at temperature indicated and tested at 22°C.



**Chemical / Solvent Resistance**

Aged under conditions indicated and tested at 22°C.

| Solvent                       | Temp. | %Initial strength retained at |        |         |
|-------------------------------|-------|-------------------------------|--------|---------|
|                               |       | 100 hr                        | 500 hr | 1000 hr |
| Motor Oil                     | 40°C  | 75                            | 75     | 65      |
| Gasoline                      | 22°C  | 100                           | 90     | 75      |
| Isopropanol                   | 22°C  | 90                            | 90     | 90      |
| Industrial Methylated Spirits | 22°C  | 90                            | 90     | 90      |
| 1,1,1 Trichloroethane         | 22°C  | 100                           | 100    | 100     |
| Freon TA                      | 22°C  | 100                           | 100    | 100     |
| Humidity 95% RH               | 40°C  | 20                            | 0      | 0       |

**GENERAL INFORMATION**

This product is not recommended for use in pure oxygen and/or oxygen rich systems and should not be selected as a sealant for chlorine or other strong oxidising materials.

For safe handling information on this product, consult the Material Safety Data Sheet, (MSDS).

**Directions for use**

For best performance surfaces should be clean and free of grease. This product performs best in thin bond gaps, (0.05mm). Excess adhesive can be dissolved with Loctite clean up solvents, nitromethane or acetone.

**Storage**

Products shall be ideally stored in a cool, dry location in unopened containers at a temperature between 8-21°C (46-70°F) unless otherwise labelled. Optimal storage conditions for unopened containers of cyanoacrylate products are achieved with refrigeration: 2-8°C (36-46°F). Refrigerated packages shall be allowed to return to room temperature prior to use. The refrigerated shelf-life for a 500gm container is 18 months based upon date of manufacture. To prevent contamination of unused product, do not return any material to its original container. For further specific shelf-life information on other package sizes, contact your local Technical Service Centre.

**Data Ranges**

The data contained herein may be reported as a typical value and/or range (based on the mean value ±2 standard deviations). Values are based on actual test data and are verified on a periodic basis.

**Note**

The data contained herein are furnished for information only and are believed to be reliable. We cannot assume responsibility for the results obtained by others over whose methods we have no control. It is the user's responsibility to determine suitability for the user's purpose of any production methods mentioned herein and to adopt such precautions as may be advisable for the protection of property and of persons against any hazards that may be involved in the handling and use thereof. In light of the foregoing, Loctite Corporation specifically disclaims all warranties expressed or implied, including warranties of merchantability or fitness for a particular purpose, arising from sale or use of Loctite Corporation's products. Loctite Corporation specifically disclaims any liability for consequential or incidental damages of any kind, including lost profits. The discussion herein of various processes or compositions is not to be interpreted as representation that they are free from domination of patents owned by others or as a license under any Loctite Corporation patents that may cover such processes or compositions. We recommend that each prospective user test his proposed application before repetitive use, using this data as a guide. This product may be covered by one or more United States or foreign patents or patent applications.

# Appendix B Technical Data Sheet of Loctite 460



Loctite UK Limited, Watchmead,  
Welwyn Garden City, Herts, AL7 1JB  
Technical Services Tel: (01707) 358888  
Customer Services Tel: (01707) 358844

## Technical Data Sheet Product 460

Worldwide Version, February 1996

### PRODUCT DESCRIPTION

LOCTITE® Product 460 is a low viscosity, fast curing, single component cyanoacrylate adhesive. It is specifically formulated to have low odour.

### TYPICAL APPLICATIONS

Rapid bonding of a wide range of metal, plastic or elastomeric materials with low blooming characteristics for cosmetic applications.

### PROPERTIES OF UNCURED MATERIAL

|                              | Value                      | Typical Range |
|------------------------------|----------------------------|---------------|
| Chemical Type                | Alkoxy-ethyl cyanoacrylate |               |
| Appearance                   | Clear colourless liquid    |               |
| Specific Gravity @ 25°C      | 1.10                       |               |
| Viscosity @ 25°C, mPa.s (cP) |                            |               |
| Brookfield LVT               |                            |               |
| Spindle 1 @ 30 rpm           | 45                         | 30 to 60      |
| Flash Point (TCC), °C        | >80                        |               |

### TYPICAL CURING PERFORMANCE

Under normal conditions, the surface moisture initiates the hardening process. Although full functional strength is developed in a relatively short time, curing continues for at least 24 hours before full chemical/solvent resistance is developed.

### Cure speed vs. substrate

The rate of cure will depend on substrate used. The table below shows the fixture time achieved on different materials at 22°C, 50% relative humidity. This is defined as the time to develop a shear strength of 0.1 N/mm<sup>2</sup> (14.5 psi) tested according to ASTM D1002.

| Substrate          | Fixture Time, seconds |
|--------------------|-----------------------|
| Steel (degreased)  | 30 to 70              |
| Aluminium          | 5 to 20               |
| Zinc dichromate    | 60 to 180             |
| Neoprene           | <5                    |
| Nitrile rubber     | <5                    |
| ABS                | 20 to 60              |
| PVC                | 20 to 50              |
| Polycarbonate      | 20 to 60              |
| Phenolic materials | 30 to 60              |

### Cure speed vs. bond gap

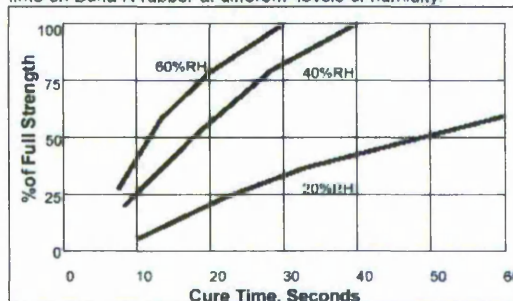
The rate of cure will depend on the bondline gap. High cure speed is favoured by thin bond lines. Increasing the bond gap will slow down the rate of cure.

### Cure speed vs. activator

Where cure speed is unacceptably long due to large gaps or low relative humidity applying activator to the surface will improve cure speed. However, this can reduce the ultimate strength of the bond, therefore testing is recommended to confirm effect.

### Cure speed vs. humidity

The rate of cure will depend on the ambient relative humidity. The graph below shows the tensile strength developed with time on Buna N rubber at different levels of humidity.



### TYPICAL PROPERTIES OF CURED MATERIAL

#### Physical Properties

Coefficient of thermal expansion, ASTM D668, K<sup>-1</sup> 80 x 10<sup>-6</sup>  
Coefficient of thermal conductivity, ASTM C177, W.m<sup>-1</sup>K<sup>-1</sup> 0.1  
Glass transition temperature, ASTM E228, °C 130

#### Electrical Properties

|  | Constant | Loss                 |
|--|----------|----------------------|
| Dielectric constant & loss, 25°C, ASTM D150, measured at |          |                      |
| 100Hz  | 2.65     | <0.02                |
| 1kHz   | 2.75     | <0.02                |
| 10kHz  | 2.75     | <0.02                |
| Volume resistivity, ASTM D257, Ω.cm                      |          | 1 x 10 <sup>18</sup> |
| Surface resistivity, ASTM D257, Ω                        |          | 1 x 10 <sup>18</sup> |
| Dielectric strength, ASTM D149, kV/mm                    |          | 25                   |

### PERFORMANCE OF CURED MATERIAL

(After 24 hr at 22°C)

|   | Value       | Typical Range           |
|---|-------------|-------------------------|
| Shear Strength, ASTM D1002/DIN 53283        |             |                         |
| Grit Blasted Steel, N/mm <sup>2</sup> (psi) | 18 (2600)   | 14 to 22 (2000 to 3200) |
| Etched Aluminium, N/mm <sup>2</sup> (psi)   | 12 (1700)   | 9 to 15 (1300 to 2200)  |
| Zinc dichromate, N/mm <sup>2</sup> (psi)    | 7 (1000)    | 4 to 10 (600 to 1450)   |
| ABS, N/mm <sup>2</sup> (psi)                | 13 (1900)   | 6 to 20 (900 to 3000)   |
| PVC, N/mm <sup>2</sup> (psi)                | 5 (700)     | 2 to 8 (300 to 1200)    |
| Polycarbonate, N/mm <sup>2</sup> (psi)      | 6.5 (900)   | 3 to 10 (400 to 1450)   |
| Phenolic, N/mm <sup>2</sup> (psi)           | 10 (1450)   | 5 to 15 (700 to 2200)   |
| Neoprene rubber, N/mm <sup>2</sup> (psi)    | 10 (1450)   | 5 to 15 (700 to 2200)   |
| Nitrile rubber, N/mm <sup>2</sup> (psi)     | 10 (1450)   | 5 to 15 (700 to 2200)   |
| Tensile Strength, ASTM D2095, DIN 53282     |             |                         |
| Grit Blasted Steel, N/mm <sup>2</sup> (psi) | 17.5 (2600) | 10 to 25 (1450 to 3600) |
| Buna N rubber, N/mm <sup>2</sup> (psi)      | 10 (1450)   | 5 to 15 (700 to 2200)   |

NOT FOR PRODUCT SPECIFICATIONS  
THE TECHNICAL DATA CONTAINED HEREIN ARE INTENDED AS REFERENCE ONLY.  
PLEASE CONTACT LOCTITE CORPORATION QUALITY DEPARTMENT FOR ASSISTANCE AND RECOMMENDATIONS ON SPECIFICATIONS FOR THIS PRODUCT.  
ROCKY HILL, CT FAX: +1 (860) 571-8473 DUBLIN, IRELAND FAX: +353 (1) 461-9868

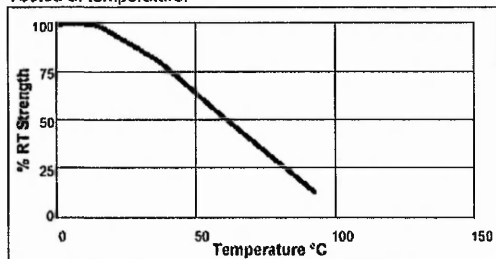
TDS 460 February 1996

**TYPICAL ENVIRONMENTAL RESISTANCE**

Test Procedure : Shear Strength ASTM D1002/DIN 53283  
 Substrate: Grit blasted mild steel laps  
 Cure procedure: 1 week at 22°C

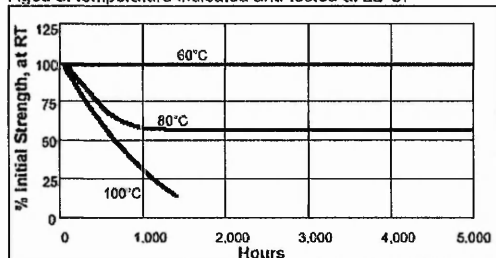
**Hot Strength**

Tested at temperature.



**Heat Ageing**

Aged at temperature indicated and tested at 22°C.



**Chemical / Solvent Resistance**

Aged under conditions indicated and tested at 22°C

| Solvent                       | Temp | %Initial strength retained at |        |         |
|-------------------------------|------|-------------------------------|--------|---------|
|                               |      | 100 hr                        | 500 hr | 1000 hr |
| Motor Oil                     | 40°C | 75                            | 75     | 65      |
| Leaded Petrol                 | 22°C | 100                           | 90     | 75      |
| Ethanol                       | 22°C | 90                            | 90     | 90      |
| Isopropanol                   | 22°C | 90                            | 90     | 90      |
| Freon TA                      | 22°C | 100                           | 100    | 100     |
| Humidity 95% RH               | 40°C | 15                            | 0      | 0       |
| Humidity 95% RH polycarbonate | 40°C | 100                           | 100    | 100     |

**GENERAL INFORMATION**

This product is not recommended for use in pure oxygen and/or oxygen rich systems and should not be selected as a sealant for chlorine or other strong oxidising materials.

For safe handling information on this product, consult the Material Safety Data Sheet, (MSDS).

**Directions for use**

For best performance surfaces should be clean and free of grease. This product performs best in thin bond gaps, (0.05mm). Excess adhesive can be dissolved with Loctite clean up solvents, nitromethane or acetone.

**Storage**

Product shall be ideally stored in a cool, dry location in unopened containers at a temperature between 8°C to 21°C (46°F to 70°F) unless otherwise labelled. Optimal storage conditions for unopened containers of cyanoacrylate products are achieved with refrigeration; 2°C to 8°C (36°F to 46°F). Refrigerated packages shall be allowed to return to room temperature prior to opening and use. To prevent contamination of unused product, do not return any material to its original container. For specific shelf life information contact your local Technical Service Centre.

**Data Ranges**

The data contained herein may be reported as a typical value and/or range (based on the mean value ±2 standard deviations). Values are based on actual test data and are verified on a periodic basis.

**Note**

The data contained herein are furnished for information only and are believed to be reliable. We cannot assume responsibility for the results obtained by others over whose methods we have no control. It is the user's responsibility to determine suitability for the user's purpose of any production methods mentioned herein and to adopt such precautions as may be advisable for the protection of property and of persons against any hazards that may be involved in the handling and use thereof. In light of the foregoing, Loctite Corporation specifically disclaims all warranties expressed or implied, including warranties of merchantability or fitness for a particular purpose, arising from sale or use of Loctite Corporation's products. Loctite Corporation specifically disclaims any liability for consequential or incidental damages of any kind, including lost profits. The discussion herein of various processes or compositions is not to be interpreted as representation that they are free from domination of patents owned by others or as a licence under any Loctite Corporation patents that may cover such processes or compositions. We recommend that each prospective user test his proposed application before repetitive use, using this data as a guide. This product may be covered by one or more United States or foreign patents or patent applications.

Loctite is a Registered Trademark of Loctite Corporation, Hartford, CT 06108



# Appendix C Technical Data Sheet of Loctite 403



Loctite UK Limited, Watchmead,  
Webbys Garden City, Herts, AL7 1JB  
Technical Services Tel: (01707) 358888  
Customer Services Tel: (01707) 358844

## Technical Data Sheet Product 403

January 1990

### PRODUCT DESCRIPTION

LOCTITE® Product 403 is a high viscosity cyanoacrylate adhesive with low odour and non-blooming characteristics.

### TYPICAL APPLICATIONS

Bonding applications where vapour control is difficult.

### PROPERTIES OF UNCURED MATERIAL

|                              | Value                      | Typical Range  |
|------------------------------|----------------------------|----------------|
| Chemical Type                | Alkoxy-ethyl Cyanoacrylate |                |
| Appearance                   | Colourless                 |                |
| Specific Gravity @ 25°C      | 1.1                        |                |
| Viscosity @ 25°C, mPa.s (cP) |                            |                |
| Brookfield LVT               |                            |                |
| Spindle 2-6 rpm              |                            | 1,100 to 1,600 |
| Flash Point (COC), °C        | >80                        |                |
| Vapour pressure mbar         | <1                         |                |
| Shelf life at 20°C, months   | 6                          |                |

### FIXTURING TIME

This is defined as the number of seconds after assembly when a joint develops a tensile shear strength of 0.1 N/mm<sup>2</sup> measured at 22°C, 50% relative humidity according to ASTM D1002 and DIN 53283. This cure speed is affected by the nature of the substrate, ambient humidity and temperature. High cure speed is favoured by thin bond lines and by avoiding excess adhesive.

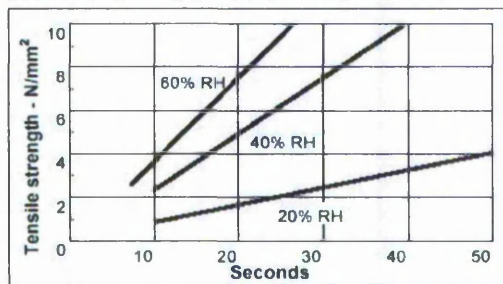
#### Performance of Loctite Product 403 on metallic and non-metallic substrates.

| Substrate              | Fixture Time, seconds |
|------------------------|-----------------------|
| Mild steel (degreased) | 30 to 70              |
| Aluminium (degreased)  | 5 to 20               |
| Zinc bichromate        | 60 to 180             |
| Neoprene rubber        | <5                    |
| Nitrile rubber         | <5                    |
| ABS                    | 20 to 60              |
| PVC                    | 20 to 50              |
| Polycarbonate          | 20 to 60              |
| Phenolic materials     | 30 to 60              |

All surfaces were cleaned by isopropyl alcohol wipe.

Times and strengths can vary considerably for different grades of plastics, rubber and plated metals.

The effect of relative humidity on cure speed is shown in the graph, for a cyanoacrylate adhesive to a Buna N rubber.



Where cure speed is inadequate, due to low relative humidity, or large gaps, a LOCTITE ACTIVATOR may be used. This can, however, lead to a reduction in eventual strength of the bond and careful testing is recommended before use in production.

While full functional strength is developed in a relatively short time, curing continues for at least 24 hours before full chemical and solvent resistance is developed.

### PHYSICAL PROPERTIES OF CURED MATERIAL

|   |                        |
|---|------------------------|
| Full strength achieved after 12 hours at 22°C on most substrates.                 |                        |
| Coefficient of thermal expansion, ASTM D696, K <sup>-1</sup>                      | 100 x 10 <sup>-6</sup> |
| Coefficient of thermal conductivity, ASTM C177, W.m <sup>-1</sup> K <sup>-1</sup> | 0.1                    |
| Softening point, °C   | 150                    |
| Recommended gap, mm   | 0.05                   |
| Maximum gap, mm:  | 0.25                   |
| Cleaning solvent:   | Acetone                |

### Electrical Properties

|                                  |          |
|----------------------------------|----------|
| Dielectric constant, ASTM D150 - |          |
| 100 Hz:                          | 2 to 3.3 |
| 1kHz:                            | 2 to 3.5 |
| 10 kHz:                          | 2 to 3.5 |
| Dissipation factor, ASTM D150 -  |          |
| 100 Hz:                          | < 0.02   |
| 1kHz:                            | < 0.02   |
| 10 kHz:                          | < 0.02   |

|  |          |
|--|----------|
| Volume resistivity, ASTM D257 -            |          |
| ΩCM X 10 <sup>18</sup>                     | 0.2 to 1 |
| Surface resistivity - Ω x 10 <sup>16</sup> | 1 to 8   |
| Dielectric strength, ASTM D149 - kV/mm:    | 25       |

### PERFORMANCE OF CURED MATERIAL

Tensile shear strength, ASTM D1002, DIN 53283, N/mm<sup>2</sup> -

|                 |          |
|-----------------|----------|
| Steel *         | 14 to 22 |
| Aluminium *     | 9 to 12  |
| Zinc bichromate | 4 to 10  |
| ABS             | 6 to 20  |
| PVC             | 2 to 8   |
| Polycarbonate   | 3 to 10  |
| Phenolic        | 5 to 15  |
| Neoprene Rubber | 5 to 15  |
| Nitrile Rubber  | 5 to 15  |

Tensile strength, ASTM D2095, DIN 53288, N/mm<sup>2</sup>:

|               |          |
|---------------|----------|
| Steel         | 10 to 25 |
| Buna N Rubber | 5 to 15  |

Peel strength, ASTM D186, DIN 53282, N/mm<sup>2</sup>

|                 |      |
|-----------------|------|
| Degreased steel | <0.5 |
|-----------------|------|

\* Sand-blasted surface

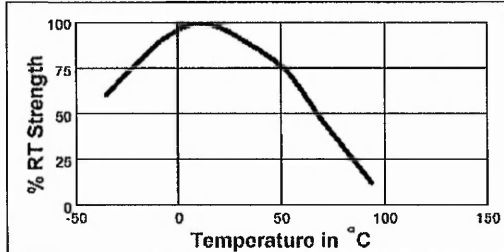
NOT FOR PRODUCT SPECIFICATIONS  
THE TECHNICAL DATA CONTAINED HEREIN ARE INTENDED AS REFERENCE ONLY.  
PLEASE CONTACT LOCTITE CORPORATION, QUALITY DEPARTMENT FOR ASSISTANCE AND RECOMMENDATIONS ON SPECIFICATIONS FOR THIS PRODUCT.  
ROCKY HILL, CT FAX: +1 (860) 571-5473 DUBLIN, IRELAND FAX: +353 (1) 461-9969

TDS 403 January 1990

**TYPICAL ENVIRONMENTAL RESISTANCE**

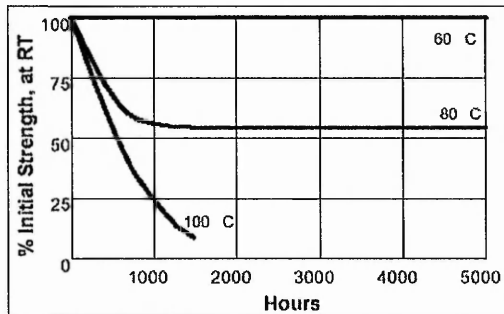
**Hot Strength**

Strength test procedure: ASTM D1002/DIN 53283  
 Substrate: Grit blasted mild steel.  
 Cure procedure: 1 week at 22°C.



**Heat Ageing**

Strength test procedure: ASTM D1002/DIN 53283  
 Substrate: Grit blasted mild steel.  
 Cure procedure: 1 week at 22°C.



**CHEMICAL / SOLVENT RESISTANCE**

Strength test procedure: ASTM D1002/DIN 53283  
 Substrate: Grit blasted mild steel.  
 Cure procedure: 1 week at 22°C

| Solvent                  | Temperature | % Initial strength retained at |        |         |
|--------------------------|-------------|--------------------------------|--------|---------|
|                          |             | 100 hr                         | 500 hr | 1000 hr |
| 95% R.H.                 | 40°C        | 15                             | 0      | 0       |
| 95% R.H. (polycarbonate) | 40°C        | 100                            | 100    | 100     |
| Motor oil                | 40°C        | 75                             | 75     | 65      |
| Leaded petrol            | 22°C        | 100                            | 90     | 75      |
| Isopropanol              | 22°C        | 90                             | 90     | 90      |
| Ethanol                  | 22°C        | 100                            | 97     | 95      |
| Freon TA                 | 22°C        | 100                            | 100    | 100     |
| 1,1,1. Trichloroethane   | 22°C        | 95                             | 95     | 95      |

**GENERAL INFORMATION**

This product is not recommended for use in pure oxygen and/or oxygen rich systems and should not be selected as a sealant for chlorine or other strong oxidising materials.

For safe handling information on this product, consult the Material Safety Data Sheet, (MSDS).

**Directions for use**

For best performance surfaces should be clean and free of grease. This product performs best in thin bond gaps. (0.05mm). Excess adhesive can be dissolved with Loctite clean up solvents, nitromethane or acetone.

**Storage**

Product shall be ideally stored in a cool, dry location in unopened containers at a temperature between 8°C to 21°C (46°F to 70°F) unless otherwise labelled. Optimal storage conditions for unopened containers of cyanoacrylate products are achieved with refrigeration: 2°C to 8°C (36°F to 46°F). Refrigerated packages shall be allowed to return to room temperature prior to opening and use. To prevent contamination of unused product, do not return any material to its original container. For specific shelf life information contact your local Technical Service Centre.

**Data Ranges**

The data contained herein may be reported as a typical value and/or range (based on the mean value ± standard deviations). Values are based on actual test data and are verified on a periodic basis.

**Note**

The data contained herein are furnished for information only and are believed to be reliable. We cannot assume responsibility for the results obtained by others over whose methods we have no control. It is the user's responsibility to determine suitability for the user's purpose of any production methods mentioned herein and to adopt such precautions as may be advisable for the protection of property and of persons against any hazards that may be involved in the handling and use thereof. In light of the foregoing, Loctite Corporation specifically disclaims all warranties expressed or implied, including warranties of merchantability or fitness for a particular purpose, arising from sale or use of Loctite Corporation's products. Loctite Corporation specifically disclaims any liability for consequential or incidental damages of any kind, including lost profits. The discussion herein of various processes or compositions is not to be interpreted as representation that they are free from domination of patents owned by others or as a licence under any Loctite Corporation patents that may cover such processes or compositions. We recommend that each prospective user test his proposed application before repetitive use, using this data as a guide. This product may be covered by one or more United States or foreign patents or patent applications.

Loctite is a Registered Trademark of Loctite Corporation, Hartford, CT

06106

# Appendix D Technical Data Sheet of Loctite 4062



**Research, Development & Engineering**  
 Tallaght Business Park,  
 Dublin, Ireland

## Technical Data Sheet Product 4062

**PRELIMINARY**

**February 1998**

### PRODUCT DESCRIPTION

LOCTITE® Product 4062 is a very low viscosity, very fast curing, single component cyanoacrylate adhesive.

### TYPICAL APPLICATIONS

Rapid bonding of a wide range of metal, plastic or elastomeric materials. The low viscosity is particularly suitable for bonding applications where controlled penetration of adhesive is required.

### PROPERTIES OF UNCURED MATERIAL

|                                   | Value               | Typical Range |
|-----------------------------------|---------------------|---------------|
| Chemical Type                     | Ethyl Cyanoacrylate |               |
| Appearance                        | Clear liquid        |               |
| Specific Gravity @ 25 °C          | 1.05                |               |
| Viscosity @ 25 °C, mPa.s (cP)     |                     |               |
| Brookfield LVF Spindle 1 @ 30 rpm | 2                   | 1 to 3        |
| Flash Point (TCC), °C             | >80                 |               |

### TYPICAL CURING PERFORMANCE

Under normal conditions, the surface moisture initiates the hardening process. Although functional strength is developed in a relatively short time, curing continues for at least 24 hours before full chemical/solvent resistance is developed.

### Cure speed vs. substrate

The rate of cure will depend on substrate used. The table below shows the fixture time achieved on different materials at 22°C, 50% relative humidity. This is defined as the time to develop a shear strength of 0.1 N/mm<sup>2</sup> (14.5 psi) tested on specimens according to ASTM D1002.

| Substrate          | Fixture Time, seconds |
|--------------------|-----------------------|
| Steel (degreased)  | 3 to 20               |
| Aluminium          | 2 to 5                |
| Neoprene           | <5                    |
| Nitrile rubber     | <5                    |
| ABS                | 2 to 5                |
| PVC                | 2 to 5                |
| Polycarbonate      | 3 to 10               |
| Phenolic materials | <5                    |

### Cure speed vs. bond gap

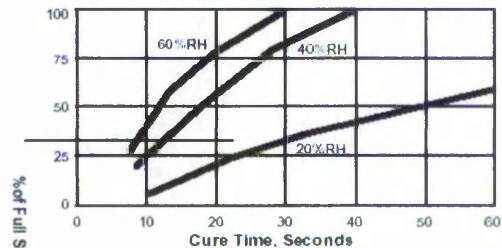
The rate of cure will depend on the bondline gap. High cure speed is favoured by thin bond lines. Increasing the bond gap will slow down the rate of cure.

### Cure speed vs. activator

Where cure speed is unacceptably long due to large gaps or low relative humidity applying activator to the surface will improve cure speed. However, this can reduce the ultimate strength of the bond, therefore testing is recommended to confirm effect.

### Cure speed vs. humidity

The rate of cure will depend on the ambient relative humidity. The graph below shows the tensile strength developed with time on Buna N rubber at different levels of humidity.



### TYPICAL PROPERTIES OF CURED MATERIAL

#### Physical Properties

Coefficient of thermal expansion, ASTM D696, K<sup>-1</sup> 80 x 10<sup>-6</sup>  
 Coefficient of thermal conductivity, ASTM C177, W.m<sup>-1</sup>K<sup>-1</sup> 0.1  
 Glass transition temperature, ASTM E228, °C 120

#### Electrical Properties

|  | Constant | Loss  |
|--|----------|-------|
| Dielectric constant & loss, 25°C, ASTM D150, measured at 100Hz | 2.65     | <0.02 |
| 1kHz   | 2.75     | <0.02 |
| 10 kHz   | 2.75     | <0.02 |

Volume resistivity, ASTM D257, Ω.cm 1 x 10<sup>16</sup>

Surface resistivity, ASTM D257, Ω 1 x 10<sup>16</sup>

Dielectric strength, ASTM D149, kV/mm 25

#### PERFORMANCE OF CURED MATERIAL

(After 24 hr at 22 °C)

|   | Value       | Typical Range             |
|---|-------------|---------------------------|
| Shear Strength, ASTM D1002, DIN 53283   |             |                           |
| Grill Blasted Steel, N/mm (psi)         | 16 (2320)   | 12 to 20 (1740 to 2900)   |
| Grillblasted Aluminium, N/mm (psi)      | 13 (1885)   | 11 to 15 (1595 to 2175)   |
| Zinc dichromate, N/mm (psi)             | 5 (725)     | 3 to 8 (435 to 1160)      |
| ABS, N/mm (psi)                         | 7 (1015)    | 6 to 8 (870 to 1160)      |
| PVC, N/mm (psi)                         | 7 (1015)    | 6 to 8 (870 to 1160)      |
| Polycarbonate, N/mm (psi)               | 10 (1450)   | 8 to 12 (1160 to 1740)    |
| Phenolic, N/mm (psi)                    | 8 (1160)    | 6 to 12 (870 to 1740)     |
| Neoprene rubber, N/mm (psi)             | 0.3* (43.5) | 0.1 to 0.5 (14.5 to 72.5) |
| Nitrile rubber, N/mm (psi)              | 0.3* (43.5) | 0.1 to 0.5 (14.5 to 72.5) |
| Tensile Strength, ASTM D2095, DIN 53288 |             |                           |
| Grill Blasted Steel, N/mm (psi)         | 16 (2320)   | 10 to 20 (1450 to 2900)   |
| Buna N rubber, N/mm (psi)               | 0.3* (43.5) | 0.1 to 0.5 (14.5 to 72.5) |

\* Adhesive exceeds strength of bonded material

NOT FOR PRODUCT SPECIFICATIONS  
 THE TECHNICAL DATA CONTAINED HEREIN ARE INTENDED AS REFERENCE ONLY.  
 PLEASE CONTACT LOCTITE CORPORATION QUALITY DEPARTMENT FOR ASSISTANCE AND RECOMMENDATIONS ON SPECIFICATIONS FOR THIS PRODUCT.  
 ROCKY HILL, CT FAX: +1 (860)-571-5473 DUBLIN, IRELAND FAX: +353(41)-461-9989

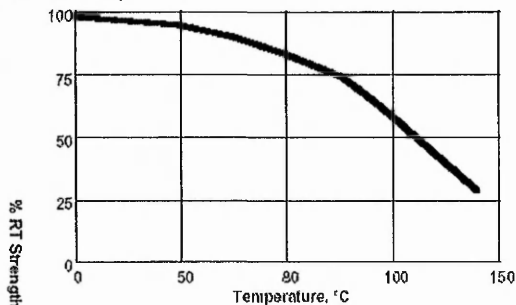


TDS 4062, February 1998

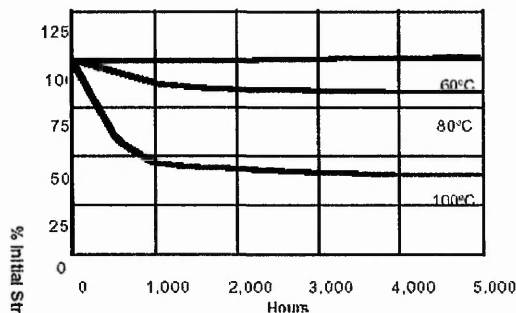
**TYPICAL ENVIRONMENTAL RESISTANCE**

Test Procedure : Shear Strength ASTM D1002/DIN 53283  
 Substrate: Grit blasted mild steel laps  
 Cure procedure: 1 week at 22\_C

**Hot Strength**  
 Tested at temperature.



**Heat Ageing**  
 Aged at temperature indicated and tested at 22 C.



**Chemical / Solvent Resistance**  
 Aged under conditions indicated and tested at 22°C.

| Solvent                       | Temp. | %Initial strength retained at |        |         |
|-------------------------------|-------|-------------------------------|--------|---------|
|                               |       | 100 hr                        | 500 hr | 1000 hr |
| Motor Oil                     | 40 C  | 100                           | 100    | 95      |
| Leaded Petrol                 | 22 C  | 100                           | 100    | 100     |
| Water/Glycol (50%/50%)        | 22 C  | 100                           | 100    | 100     |
| Ethanol                       | 22 C  | 100                           | 100    | 100     |
| Isopropanol                   | 22 C  | 100                           | 100    | 100     |
| Freon TA                      | 22 C  | 100                           | 100    | 100     |
| Humidity 95% RH               | 40°C  | 100                           | 95     | 80      |
| Humidity 95% RH polycarbonate | 40 C  | 100                           | 100    | 90      |

**GENERAL INFORMATION**

This product is not recommended for use in pure oxygen and/or oxygen rich systems and should not be selected as a sealant for chlorine or other strong oxidising materials.

For safe handling information on this product, consult the Material Safety Data Sheet, (MSDS).

**Directions for use**

For best performance surfaces should be clean and free of grease. This product performs best in thin bond gaps. (0.05mm). Excess adhesive can be dissolved with Loctite clean up solvents, nitromethane or acetone.

**Storage**

Product shall be ideally stored in a cool, dry location in unopened containers at a temperature between 8\_C to 21\_C (46\_F to 70\_F) unless otherwise labelled. Optimal storage conditions for unopened containers of cyanoacrylate products are achieved with refrigeration: 2\_C to 8\_C (36\_F to 46\_F). Refrigerated packages shall be allowed to return to room temperature prior to opening and use. To prevent contamination of unused product, do not return any material to its original container. For specific shelf life information contact your local Technical Service Centre.

**Data Ranges**

The data contained herein may be reported as a typical value and/or range (based on the mean value .2 standard deviations). Values are based on actual test data and are verified on a periodic basis.

**Note**

The data contained herein are furnished for information only and are believed to be reliable. We cannot assume responsibility for the results obtained by others over whose methods we have no control. It is the user's responsibility to determine suitability for the user's purpose of any production methods mentioned herein and to adopt such precautions as may be advisable for the protection of property and of persons against any hazards that may be involved in the handling and use thereof. In light of the foregoing, Loctite Corporation specifically disclaims all warranties expressed or implied, including warranties of merchantability or fitness for a particular purpose, arising from sale or use of Loctite Corporation's products. Loctite Corporation specifically disclaims any liability for consequential or incidental damages of any kind, including lost profits. The discussion herein of various processes or compositions is not to be interpreted as representation that they are free from domination of patents owned by others or as a licence under any Loctite Corporation patents that may cover such processes or compositions. We recommend that each prospective user test his proposed application before repetitive use, using this data as a guide. This product may be covered by one or more United States or foreign patents or patent applications.

Loctite is a Registered Trademark of Loctite Corporation, Hartford, CT 06105

## Appendix E Technical Data Sheet of Alcan Reactive Grade Calcined Alumina

**Alcan Chemicals**  
Europe

Data Sheet 570

Issue 6/6/99/570

### Calcined Alumina Alcan Reactive Grades for Ceramics

The three products featured in this data sheet are low soda reactive aluminas. It can be seen from the physical properties overleaf that RAC45B and RA207LS are more reactive than RA203LS.

These Alcan RA grades are white, free flowing crystalline powders with the chemical formula  $Al_2O_3$ .

All grades are recommended for use in the ceramic industry where there is a requirement for high thermal reactivity. Their reactive nature allows low porosity, high density, high alumina ceramic parts to be produced at lower firing temperatures; other benefits include high mechanical strength and good surface finish.

RAC45B and RA207LS also have a controlled magnesia content which assists with the control of grain growth during the firing process.

Another important feature of the products is the low soda content which imparts excellent electrical properties to the finished ceramic products.

Another important feature of the products is the low soda content which imparts excellent electrical properties to the finished ceramic products.

Alcan low soda reactive aluminas can be used with all conventional ceramic fabrication techniques.

#### Summary

- High reactivity
- Low soda content
- Excellent sintering performance
- Reduced firing temperatures
- Controlled grain growth during firing (RAC45B and RA207LS)
- Can be used with all conventional ceramic forming techniques

#### Typical Applications

- Wear resistant ceramics
- Electrical and electronic components
- Engineering components

Every care is taken in compiling this information, but it is supplied without any representations or warranty and Alcan Aluminium UK Limited disclaims all liability for any loss, damage or expense arising from any inaccuracy therein. As the use of the product is beyond our control, the user must accept responsibility for the suitability of the product for any particular application.

**Alcan Chemicals Europe (Part of Alcan Aluminium UK Limited)**  
135 Aberdour Road Burntisland Fife Scotland UK KY3 0EP  
Telephone: +44 (0) 1592 411000 Facsimile: +44 (0) 1592 411111



**Alcan Chemicals**  
Europe

**Specification**  
(Typical values)

**Data Sheet 570**  
Issue 6/6/99/570

**Physical Properties**

| Products  | RA203LS <sup>(6)</sup> | RA207LS | RAC45B |
|---|------------------------|---------|--------|
| Surface area <sup>(1)</sup>   | 3                      | 7.5     | 8      |
| Screen analysis <sup>(2)</sup> Retained on 45µm   | 0.01                   | 0.01    | 0.01   |
| Particle size distribution <sup>(3)</sup> d <sub>10</sub><br>d <sub>50</sub><br>d <sub>90</sub> | 3.3                    | 1.2     | 1.7    |
|   | 1.4                    | 0.5     | 0.45   |
|   | 0.5                    | 0.2     | 0.2    |
| Green density <sup>(4)</sup>  | 2.2                    | 2.1     | 2.12   |
| Fired Density <sup>(5)</sup> 1500°C<br>1550°C<br>1600°C<br>1650°C                               | 2.8                    | 3.76    | 3.85   |
|   | 3.07                   | 3.89    | 3.92   |
|   | 3.58                   | 3.91    | 3.93   |
|   | 3.84                   | 3.92    | 3.94   |

**Packaging**

|                       |        |    |    |    |
|-----------------------|--------|----|----|----|
| Multi-ply paper sacks | kg     | 25 | 25 | 25 |
| Weight per pallet     | tonnes | 1  | 1  | 1  |

Stretchwrapping of paper sacks is standard for deliveries outside the UK. Options available on request include Big-bags, bulk tanker deliveries and stretchwrapping within the UK. All paper sacks are recyclable.

**Chemical analysis (%)**

|  | RA203LS | RA207LS | RAC45B |
|--|---------|---------|--------|
| Al <sub>2</sub> O <sub>3</sub> (by difference) | 99.6    | 99.8    | > 99.8 |
| Na <sub>2</sub> O (total)                      | ≤ 0.1   | 0.07    | 0.04   |
| SiO <sub>2</sub>                               | ≤ 0.1   | 0.04    | 0.01   |
| Fe <sub>2</sub> O <sub>3</sub>                 | 0.03    | 0.03    | 0.01   |
| CaO  | 0.02    | 0.02    | 0.01   |
| MgO  | 0.005   | 0.04    | 0.05   |
| K <sub>2</sub> O                               | 0.01    | 0.01    | -      |
| Loss on Ignition (300°C - 1100°C)              | 0.2     | 0.2     | -      |

**Notes**

1. Micromeritics Floworb
2. Wet sieve
3. Micromeritics Sedigraph
4. Pressed at 21psf
5. Fired at the rate of 5°C/min. (Soak time of 2 hours)
6. 0.1% MgO added for ceramic testing

**Health and safety**

Alcan Reactive Alumina Ceramic grades when properly used do not constitute a health risk, nor do they carry any fire or explosion hazard. It is recommended that ventilation and personal protection measures are taken to meet the requirements of the Guidance Note on Occupational Exposure issued by the UK Health and Safety Executive, and the American Conference of Governmental Industrial Hygienists (ACGIH) total and respirable airborne particulate of 10 and 4 mg/m<sup>3</sup> respectively.

Please refer to Alcan Chemicals Europe 'Material Safety Data Sheet number 2' for more information about use and disposal.

TTCN: 281820-00-9  
CAS-RN: [1344-28-1]



## Appendix F Technical Data Sheet of Alcan Low Soda Grade Calcined Alumina

**Alcan Chemicals**  
Europe

Data Sheet 490

Issue 3;5/97/490

### Calcined Alumina Alcan MA-LS Low Soda Grades

Alcan MA-LS aluminas are milled, low soda grades of calcined alumina for use in high quality refractory and ceramic products. The products are characterised by their high purity and consistent physical properties.

Alcan MA-LS grades are white crystalline powders which are predominantly  $\alpha$ -alumina ( $Al_2O_3$ ). They are of high chemical purity and offer a choice of ultimate crystallite size and surface area.

Being readily milled and of high chemical purity Alcan MA-LS grades are suitable for immediate use in high quality refractory systems such as refractory bricks, sliding gates, prefired shapes and kiln furniture. Alcan MA-LS grades are also used in catalyst supports.

For applications such as electrical porcelain and wear resistant products where more intensive milling is required Alcan MA-LS grades of alumina offer an alternative energy-saving starting material for in-house grinding.

For whiteware Alcan MA-LS grades are an alternative to Alcan MA95 and increase the options for modifications to the rheological properties of the clay mix.

Alcan Low Soda aluminas are also recommended for use where the effects of grain growth may reduce the useful life of the refractory.

#### Applications

##### Refractories

- Sliding gates
- Bricks
- Prefired shapes
- Kiln Furniture

##### Ceramics

- Wear resistant parts
- Electrical porcelain
- Whiteware

##### Miscellaneous

- Fuel treatment in boilers
- Catalyst supports

Every care is taken in compiling this information, but it is supplied without any representations of warranty and Alcan Aluminium UK Limited disclaims all liability for any loss, damage or expense arising from any inaccuracy therein. As the use of the product is beyond our control, the user must accept responsibility for the suitability of this product for any particular application.

**Alcan Chemicals Europe (Part of Alcan Aluminium UK Limited)**  
135 Aberdour Road Burtisland Fife Scotland UK KY3 0EP  
Telephone: +44 (0) 1592 411000 Facsimile: +44 (0) 1592 411111



**Alcan Chemicals**  
Europe

Data Sheet 490

Issue 3:5/97/490

### Specification (Typical values)

| Physical Properties                             | Products          | MA2LS  | MA4LS |
|---|-------------------|--------|-------|
| Surface area <sup>(1)</sup>                     | m <sup>2</sup> /g | 0.4    | 0.7   |
| Screen analysis <sup>(2)</sup> Retained on 45µm | max %             | 0.5    | 0.5   |
| Median Particle size <sup>(3)</sup>             | µm                | 8      | 6.5   |
| Bulk density <sup>(4)</sup> Untamped            | g/cm <sup>3</sup> | 0.8    | 0.7   |
|   |                   | Tamped | 1.5   |
| pH  | 20% w/v           | 8      | 8     |
| Mohs' hardness                                  |                   | 9      | 9     |
| α-alumina content <sup>(5)</sup>                | %                 | 98     | 98    |
| Density   | g/cm <sup>3</sup> | 3.97   | 3.97  |
| <b>Packaging</b>                                |                   |        |       |
| Multi-ply paper sacks                           | kg                | 25     | 25    |
| Weight per pallet                               | tonnes            | 1      | 1     |

Stretchwrapping of paper sacks is standard for deliveries outside the UK. Options available on request include Big-bags, bulk tanker deliveries and stretchwrapping within the UK. All paper sacks are recyclable.

### Chemical analysis (%)

(Typical for all grades)

|  |      |                                |      |
|--|------|--------------------------------|------|
| Al <sub>2</sub> O <sub>3</sub> (by difference) | 99.7 | SiO <sub>2</sub>               | 0.05 |
| Na <sub>2</sub> O (total)                      | 0.05 | Fe <sub>2</sub> O <sub>3</sub> | 0.02 |
| Loss on Ignition                               | 0.1  | CaO                            | 0.02 |

### Notes

1. Micromeritics Flowsoeb
2. Wet sieve
3. Coulter Counter
4. ISO method 903:1976
5. By XRD

### Health and safety

Alcan MA-LS grades when properly used do not constitute a health risk, nor do they carry any fire or explosion hazard. It is recommended that ventilation and personal protection measures are taken to meet the requirements of the Guidance Note on Occupational Exposure issued by the UK Health and Safety Executive, and the American Conference of Governmental Industrial Hygienists (ACGIH) total and respirable airborne particulate of 10 and 4 mg/m<sup>3</sup> respectively.

Please refer to Alcan Chemicals Europe 'Material Safety Data Sheet number 2' for more information about use and disposal.

TTCN: 251820-00-9  
CAS-RN: [1344-28-1]





## Appendix G Programmes for CNC Machining

This section contains the programmes that was written for drilling and milling of the green compacts:

### Programme Listing for Drilling (Section 4.4)

#### PEPS Cut Programme for Drilling:

```
par 3456
win v4 x-50 y-50 z-30 x50 y50 z20
p1=x0 y0
rem p - point; d - dia; b - base; db - dist from base (inc);
rem n - number of points
pat pcd g1 p1 d20 b0 db45 n4
pat pcd g2 p1 d20 b180 db45 n4
pat pcd g3 p1 d9 b0 db90 n4

from x-30 y-30 z30
tool 5 d4 L5 d55 'twist drill
coo FL
spin 1000
fed v50 h50
cle 5
wof 5
rap
got x-20 y0 z10
dri g1 z-20 n6

from x-30 y-30 z30
tool 5 d4 L5 d55 'twist drill
coo FL
spin 1000
fed v100 h100
cle 5
wof 5
rap
got x-20 y0 z10
dri g2 z-20 n6

from x-30 y-30 z30
tool 5 d4 L5 d55 'twist drill
coo FL
spin 1000
fed v150 h150
cle 5
wof 5
rap
got x-20 y0 z10
dri g3 z-20 n6

end
```

BridgePort Programme for Drilling:

O3456  
N1G21G80G49G40G90  
G10 L91 R2  
N2(TWIST DRILL)  
N3T5M6  
N4G0G58G90X-20.0Y0.0S1000M3  
N5G43Z10.0H5M8  
N6X10.0  
N7Z5.0  
N8G83G99Z-20.0R5.0Q4.167F50.0  
N9X7.071Y7.071  
N10X0.0Y10.0  
N11X-7.071Y7.071  
N12G80  
N13(TWIST DRILL)  
N14T5M6  
N15G0G58G90X-20.0Y0.0S1000M3  
N16G43Z10.0H5M8  
N17X-10.0  
N18Z5.0  
N19G83G99Z-20.0R5.0Q4.167F100.0  
N20X-7.071Y-7.071  
N21X0.0Y-10.0  
N22X7.071Y-7.071  
N23G80  
N24(TWIST DRILL)  
N25T5M6  
N26G0G58G90X-20.0Y0.0S1000M3  
N27G43Z10.0H5M8  
N28X4.5  
N29Z5.0  
N30G83G99Z-20.0R5.0Q4.167F150.0  
N31X0.0Y4.5  
N32X-4.5Y0.0  
N33X0.0Y-4.5  
N34G80  
N35G28G91Z0.0  
N36G28X0.0Y0.0  
N37M30  
%

## Programme Listing for Milling (Section 4.6)

### PEPS Cut Programme for Milling:

```
par 3456
win v4 x-50 y-50 z-30 x50 y50 z20
p1=x0 y0
rem p - point; d - dia; b - base; db - dist from base (inc);
rem n - number of points
pat pcd g1 p1 d20 b0 db45 n4

pat pcd g2 p1 d20 b180 db45 n4

pat pcd g3 p1 d9 b0 db90 n4

from x-30 y-30 z30
tool 5 d4 L5 d55 'twist drill
coo FL
spin 1000
fed v50 h50
cle 5
wof 5
rap
got x-20 y0 z10
dri g1 z-5 n6

from x-30 y-30 z30
tool 5 d4 L5 d55 'twist drill
coo FL
spin 1000
fed v100 h100
cle 5
wof 5
rap
got x-20 y0 z10
dri g2 z-5 n6

from x-30 y-30 z30
tool 5 d4 L5 d55 'twist drill
coo FL
spin 1000
fed v150 h150
cle 5
wof 5
rap
got x-20 y0 z10
dri g3 z-5 n6

end
```

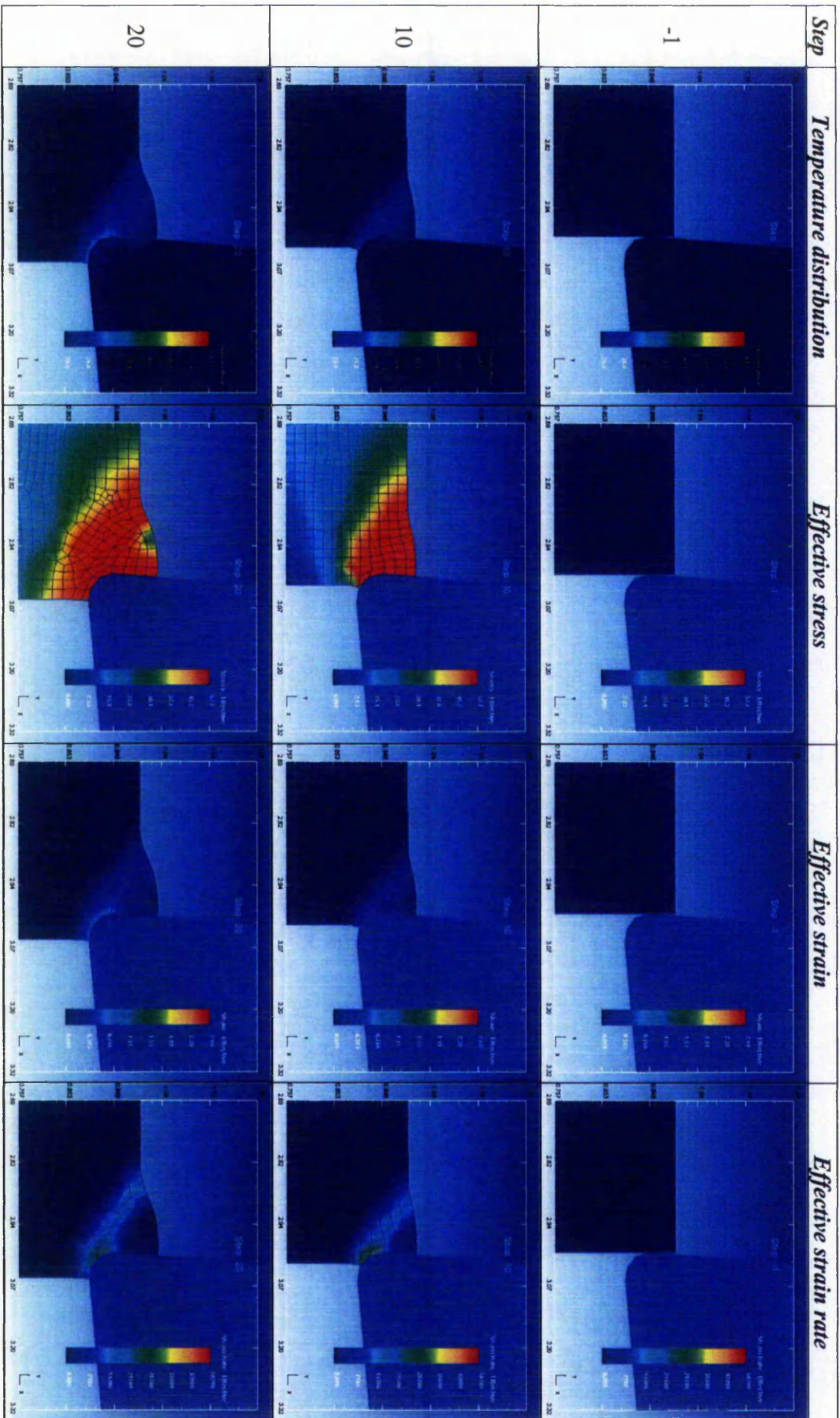
## **Appendix H Finite Element Model of Turning of PRIME Compact**

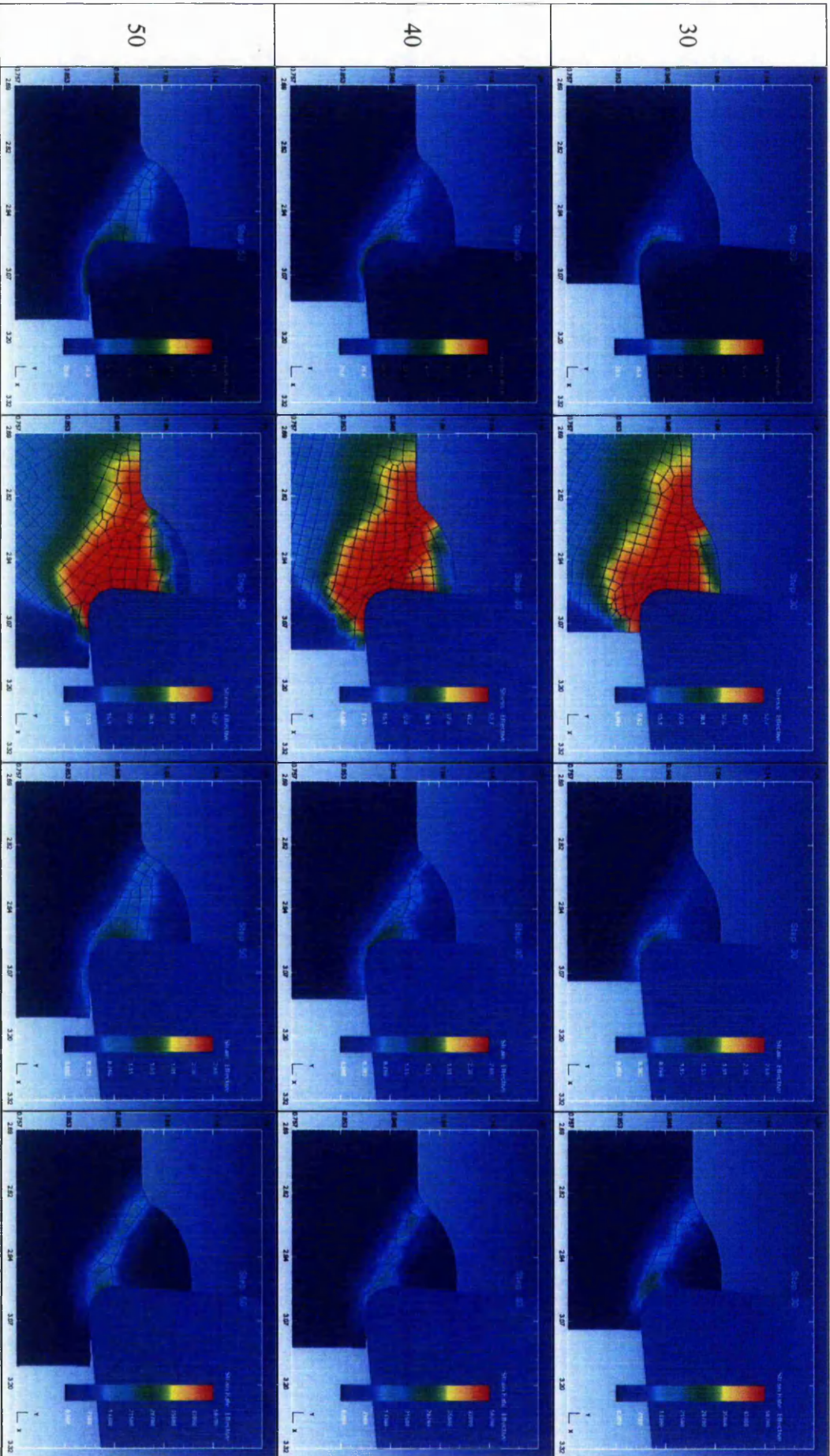
Material parameters:

|   |   |
|---|---|
| <i>Young's modulus, E</i>                     | 4 GPa   |
| <i>Poisson's ratio, <math>\nu</math></i>      | 0.35  |
| <i>Thermal expansion, <math>\alpha</math></i> | $47.6 \times 10^{-6} / ^\circ\text{C}$          |
| <i>Thermal conductivity, K</i>                | $5.5 \times 10^{-3} \text{ N/s.}^\circ\text{C}$ |
| <i>Heat capacity, C</i>                       | 1188 J/kg $^\circ\text{C}$                      |
| <i>Initial yield stress, Y</i>                | 50 MPa  |
| <i>Strain hardening constant, H</i>           | 1 MPa   |

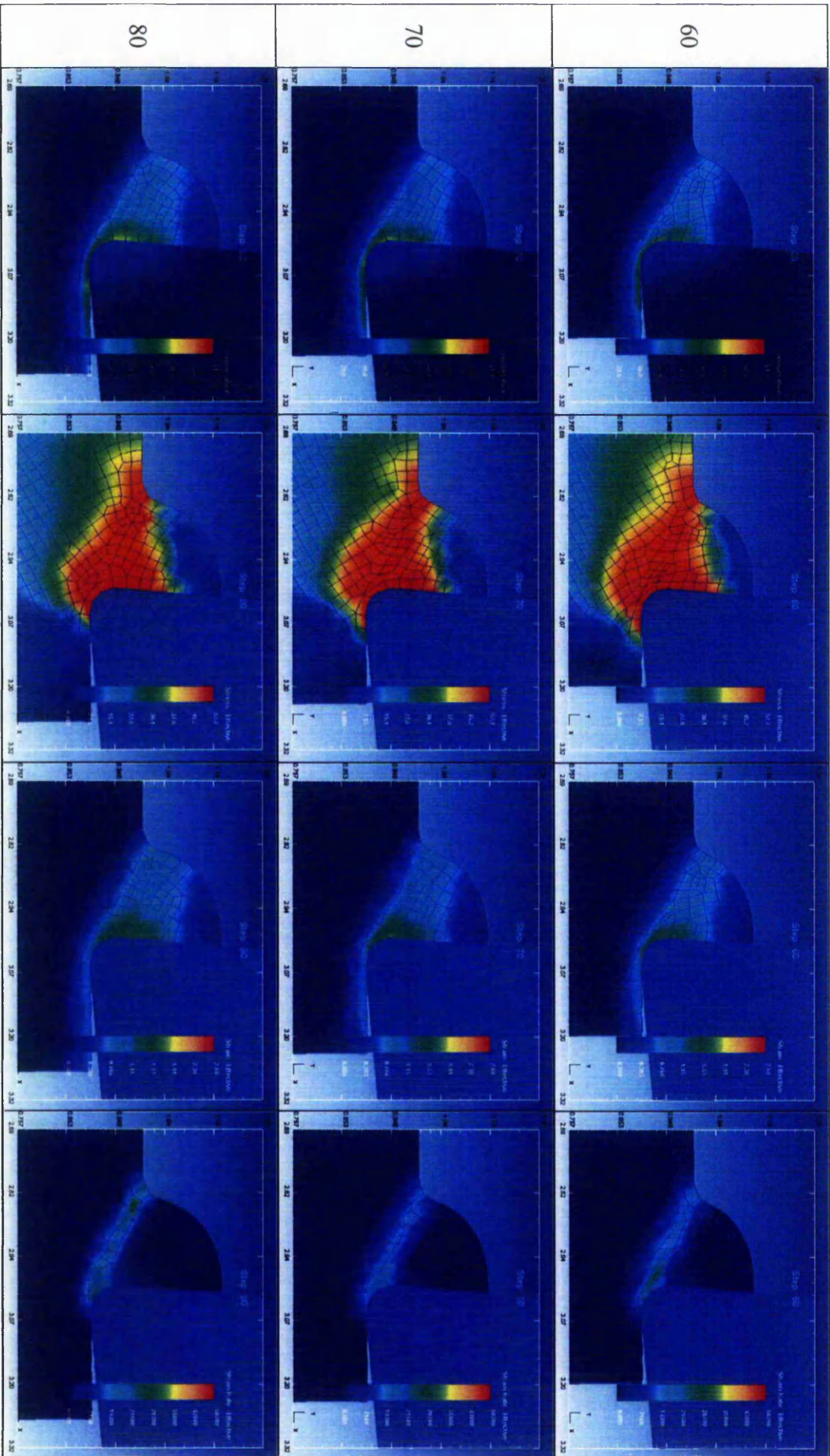
Machining parameters:

|                      |            |
|----------------------|------------|
| <i>Speed</i>         | 85 m/min   |
| <i>Feed rate</i>     | 0.1 mm/rev |
| <i>Depth of cut</i>  | 1 mm       |
| <i>Length of cut</i> | 1.5 mm     |

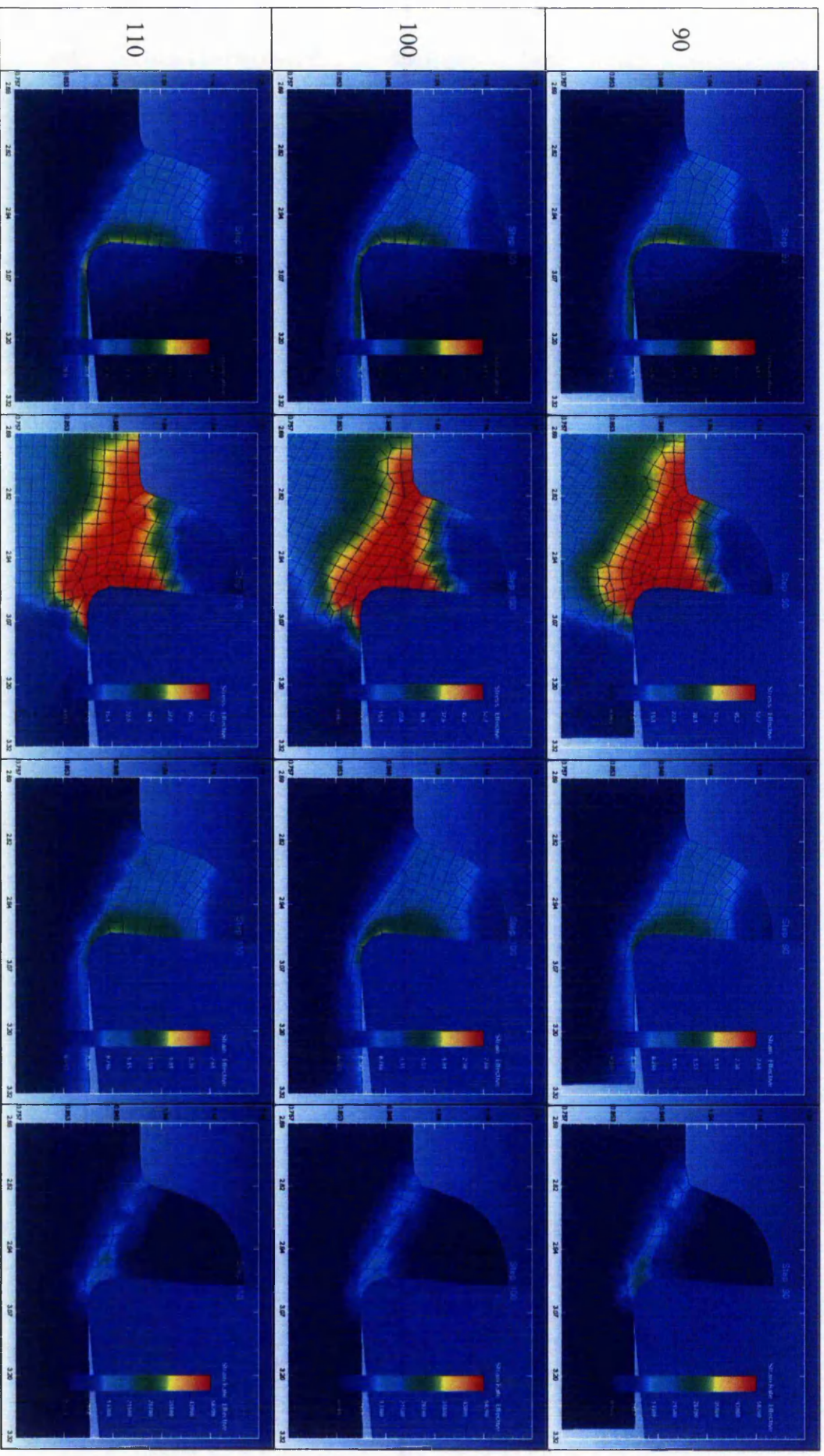




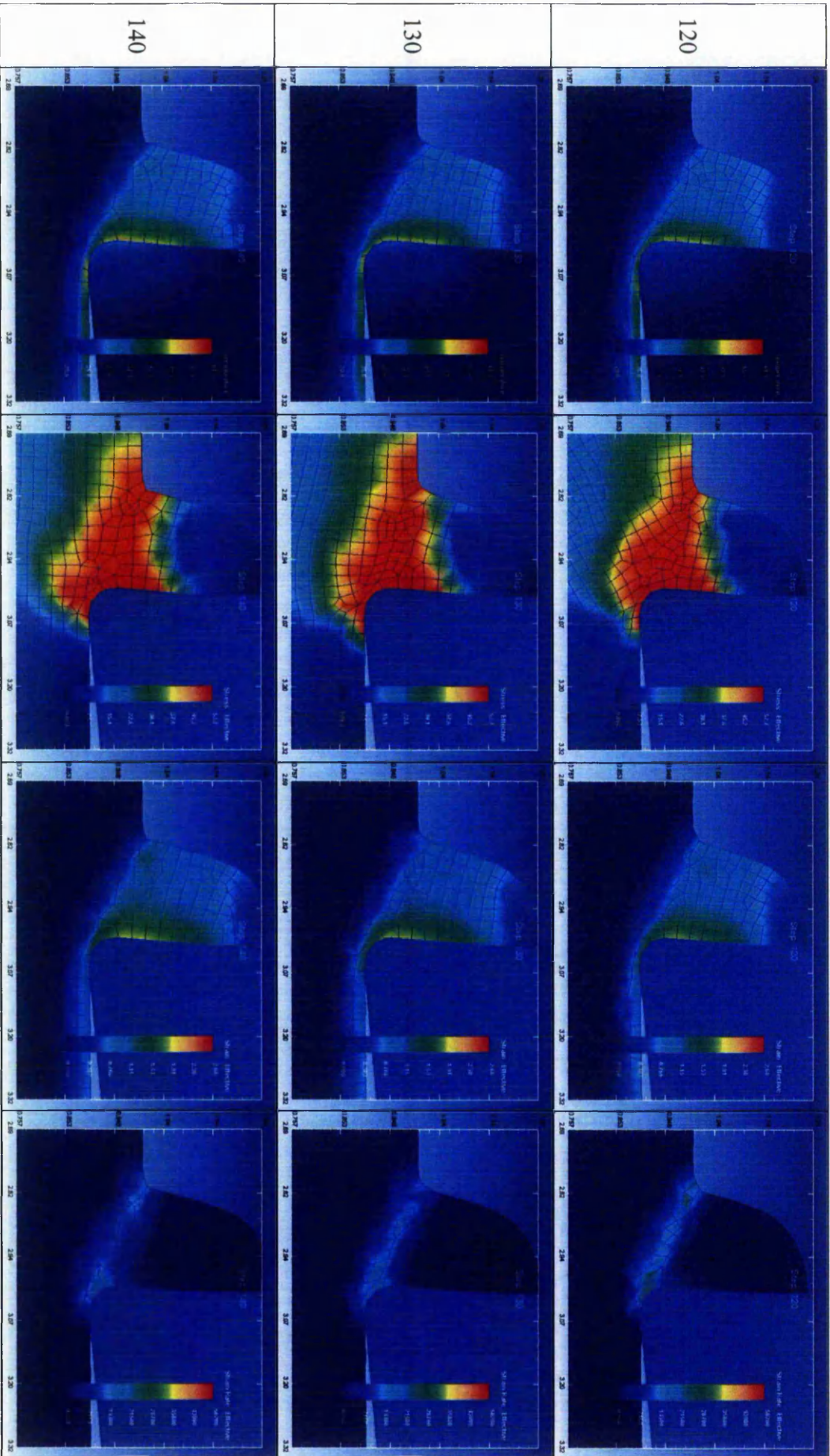
*Application of Conventional Machining Techniques for Green Ceramic Compacts produced by Powder Reaction Moulding*

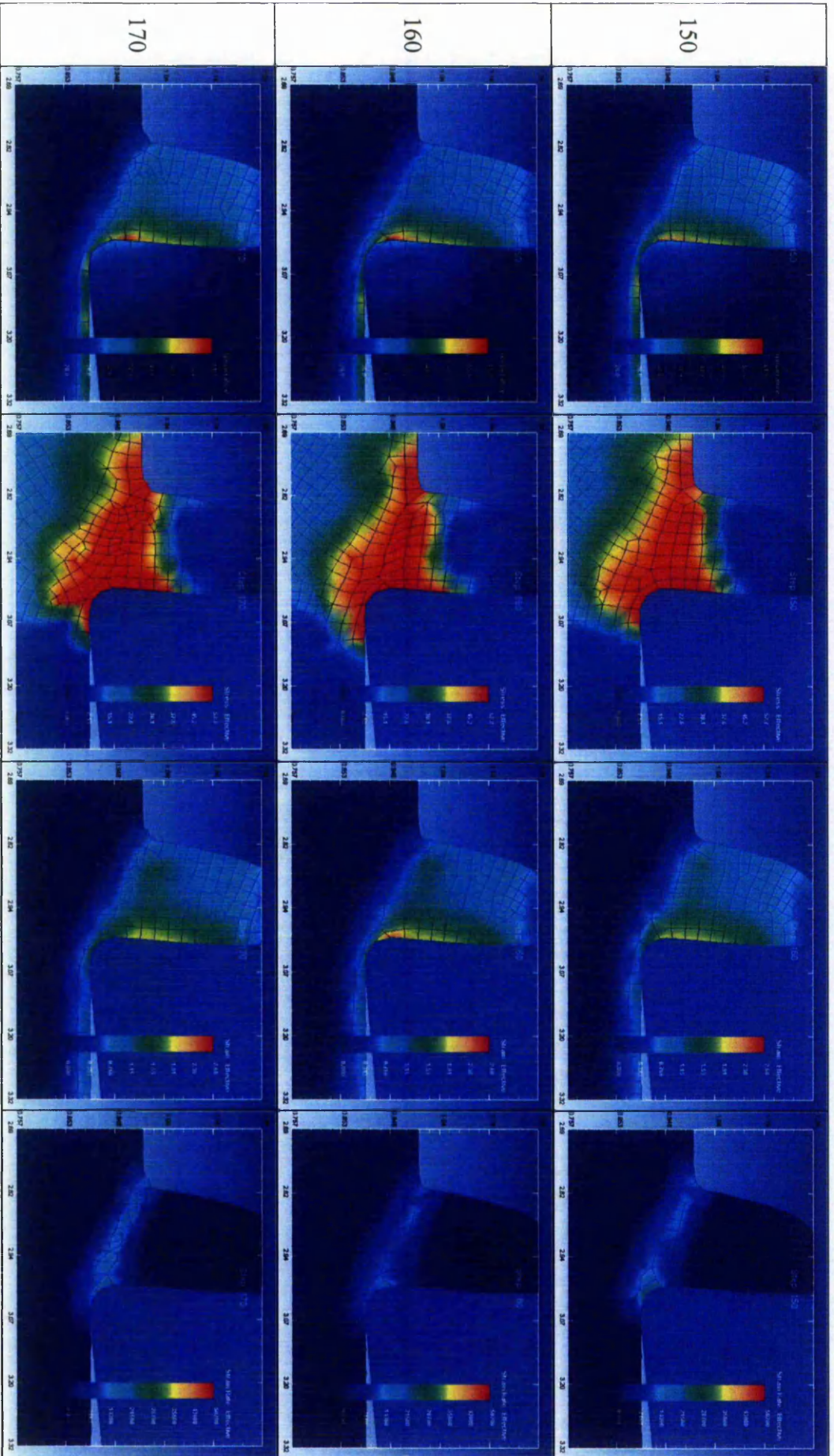


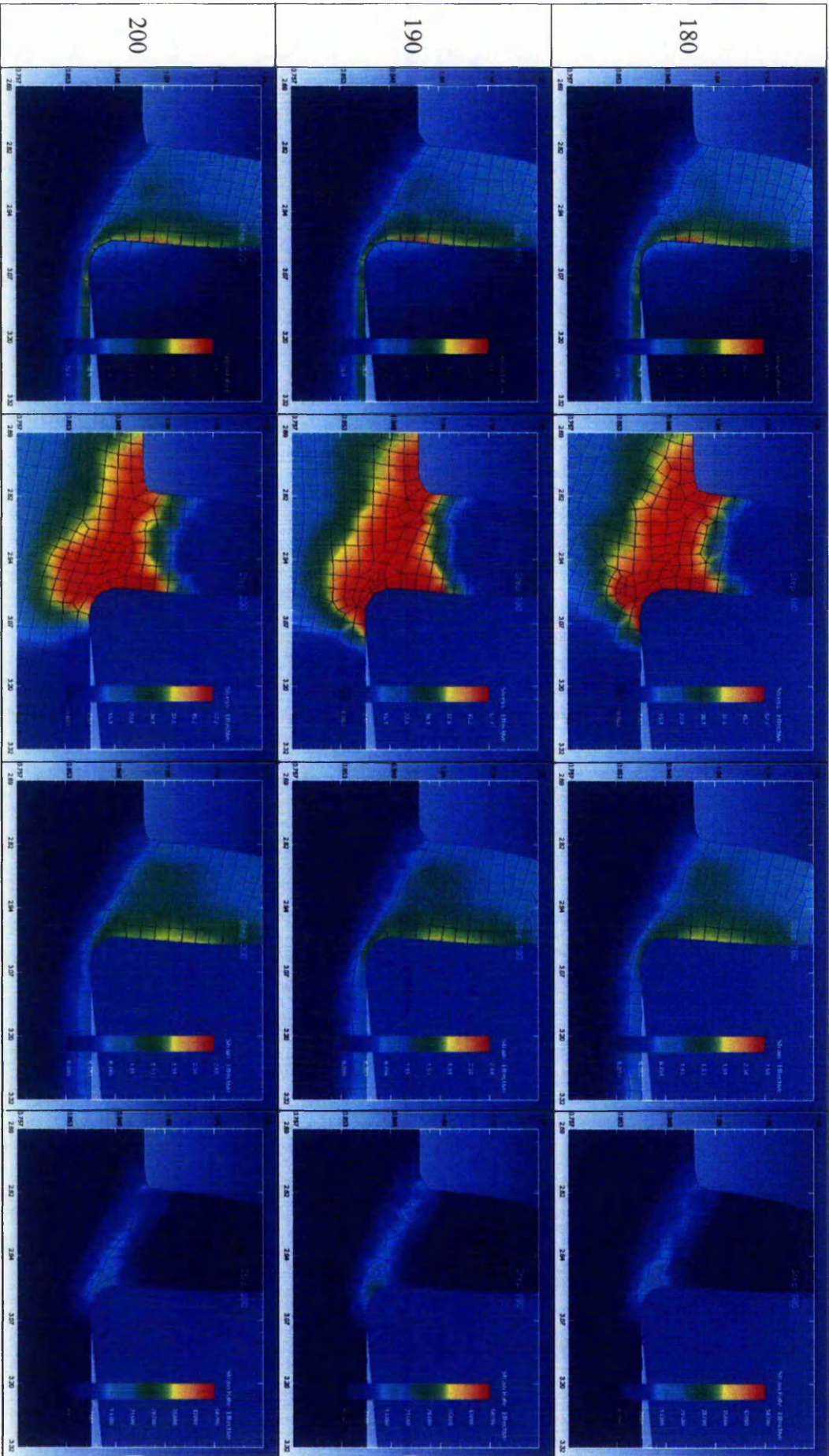
*Application of Conventional Machining Techniques for Green Ceramic Compacts produced by Powder Reaction Moulding*

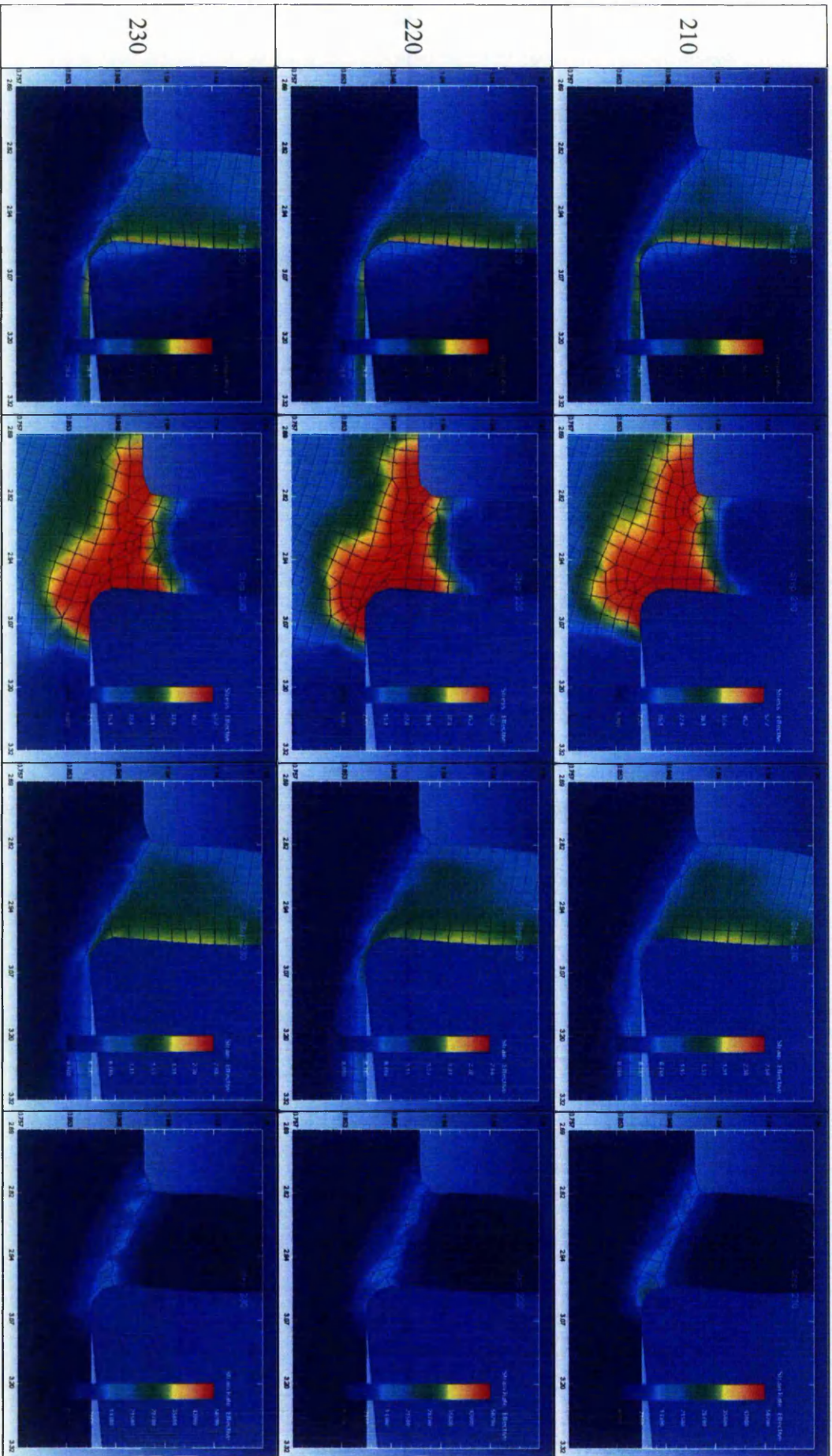


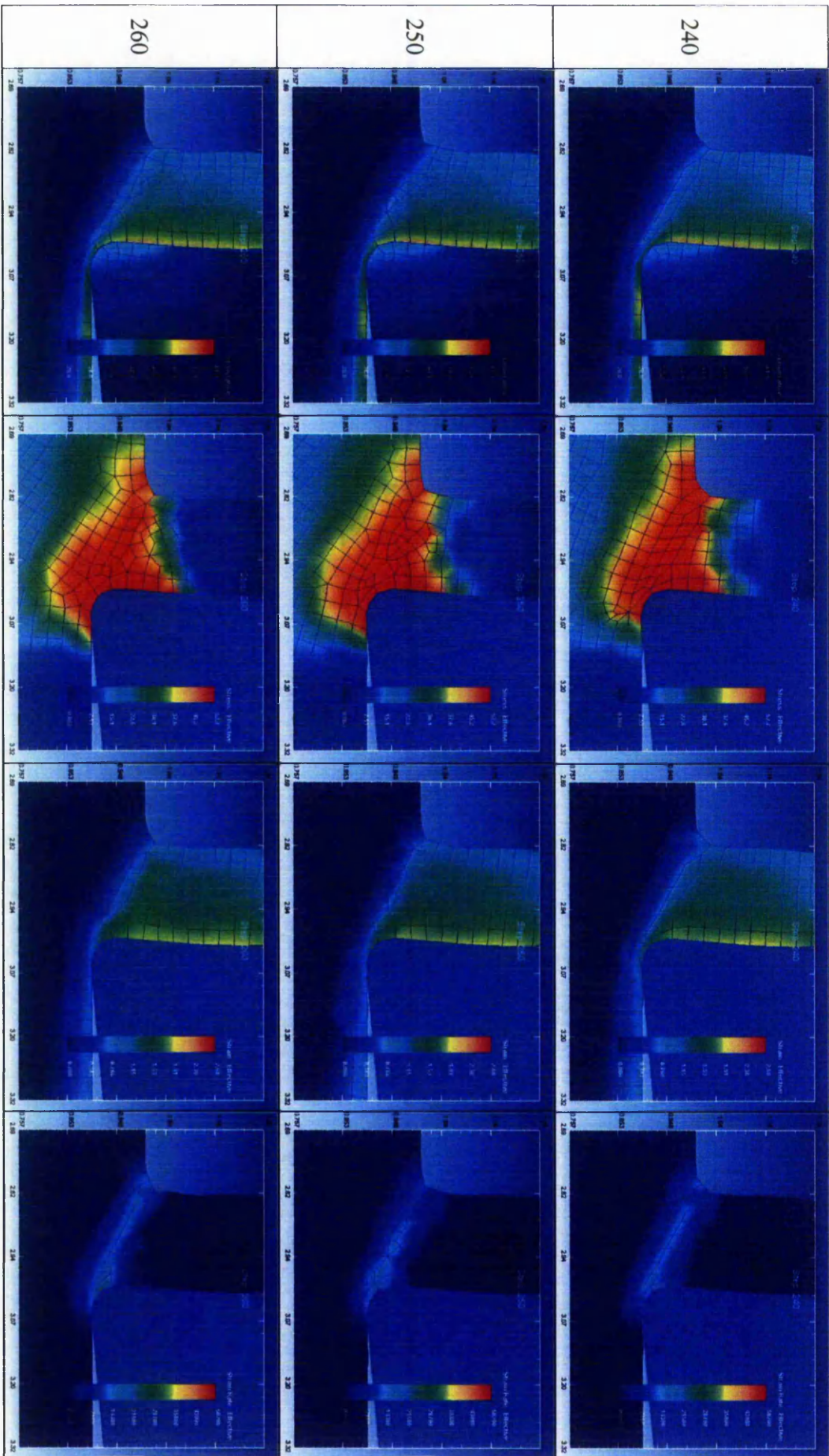


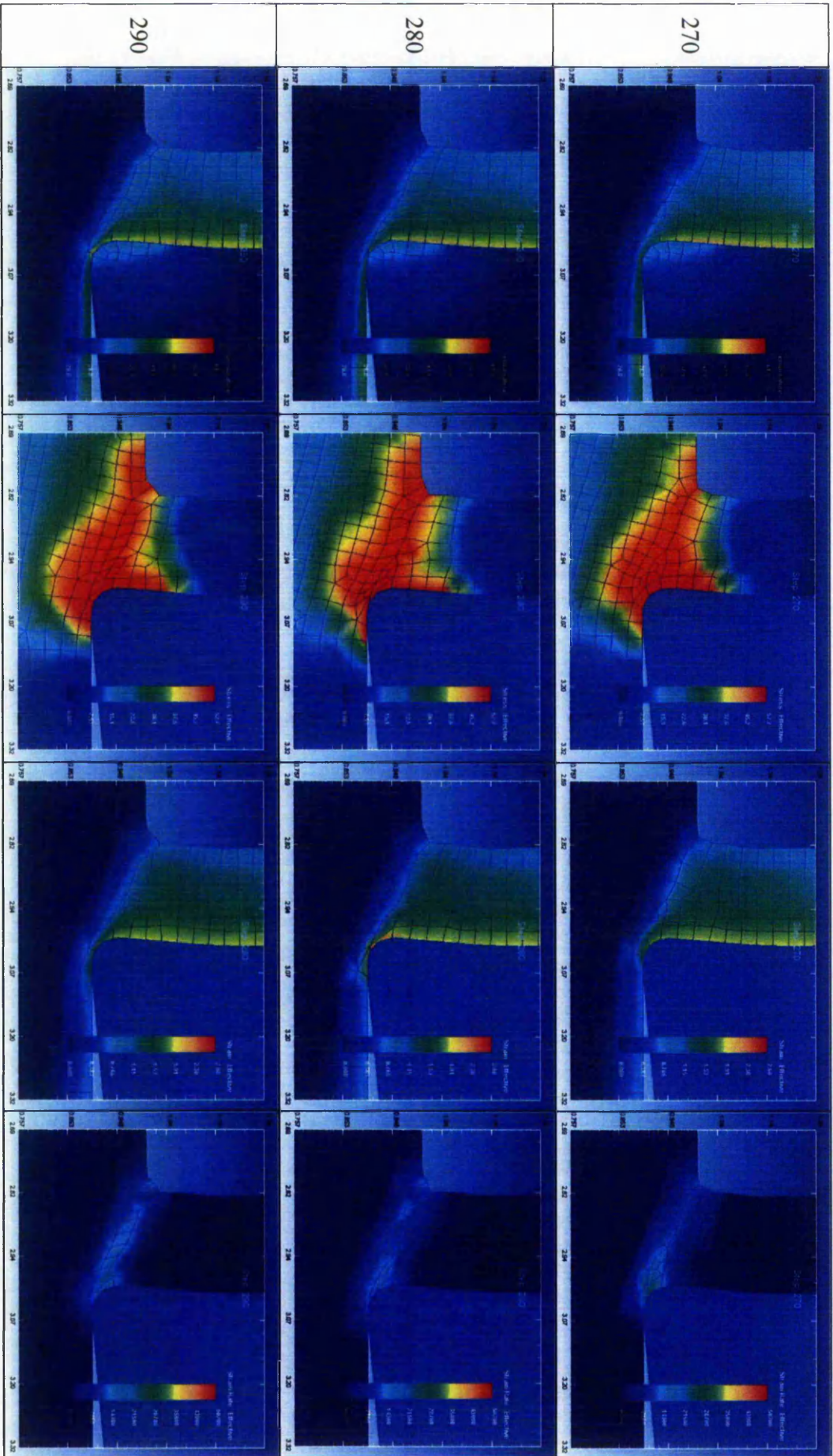


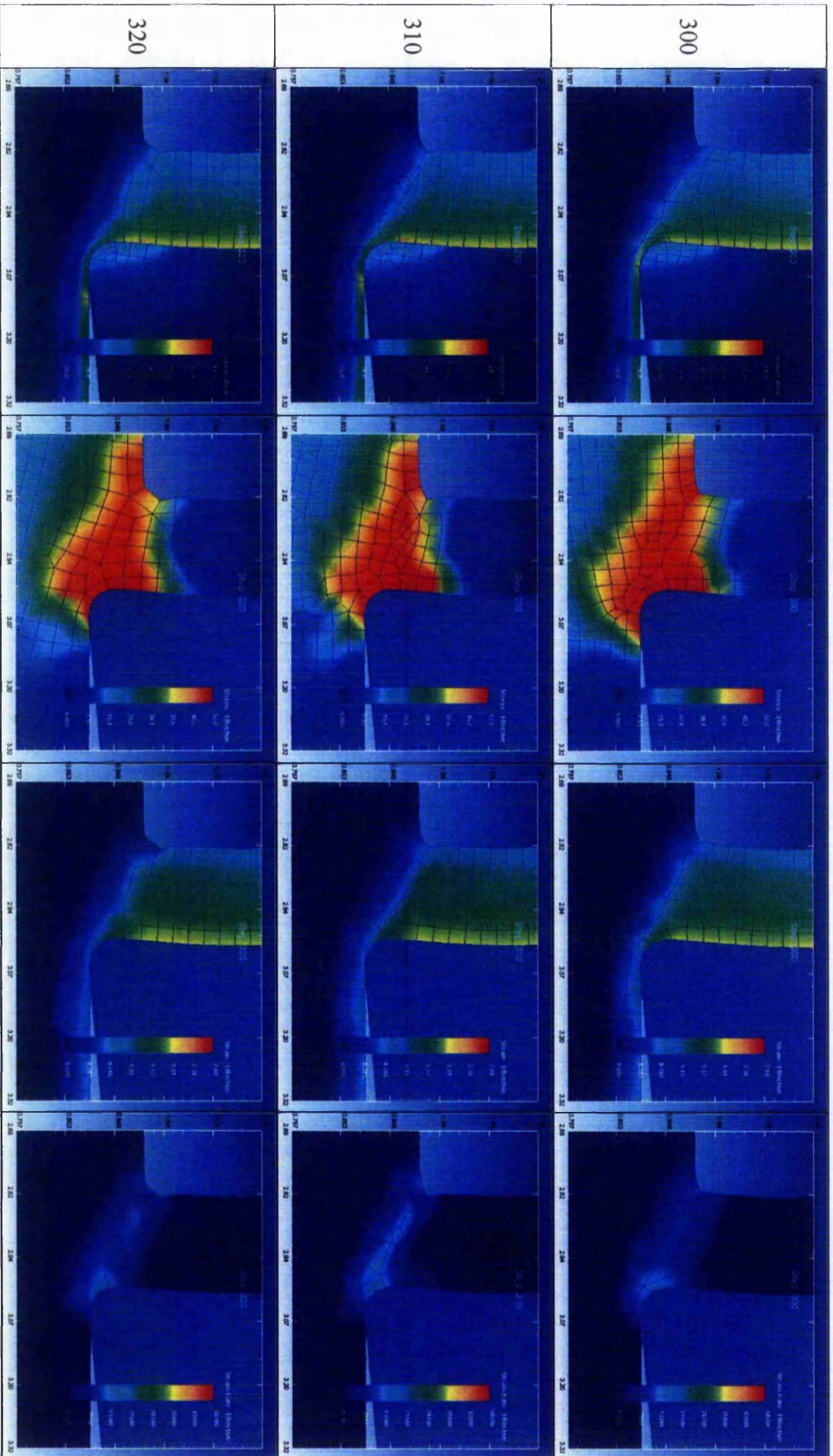


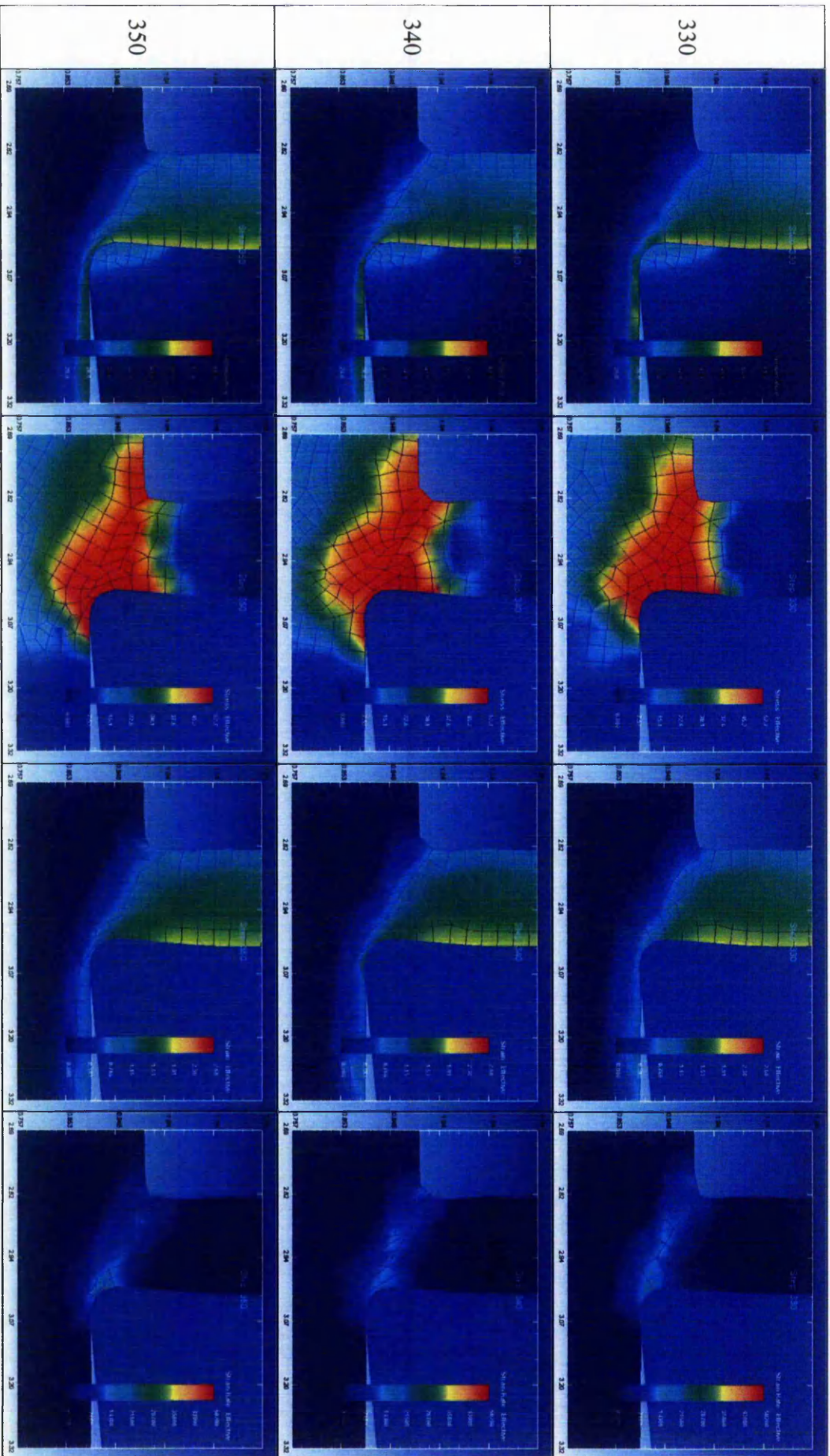






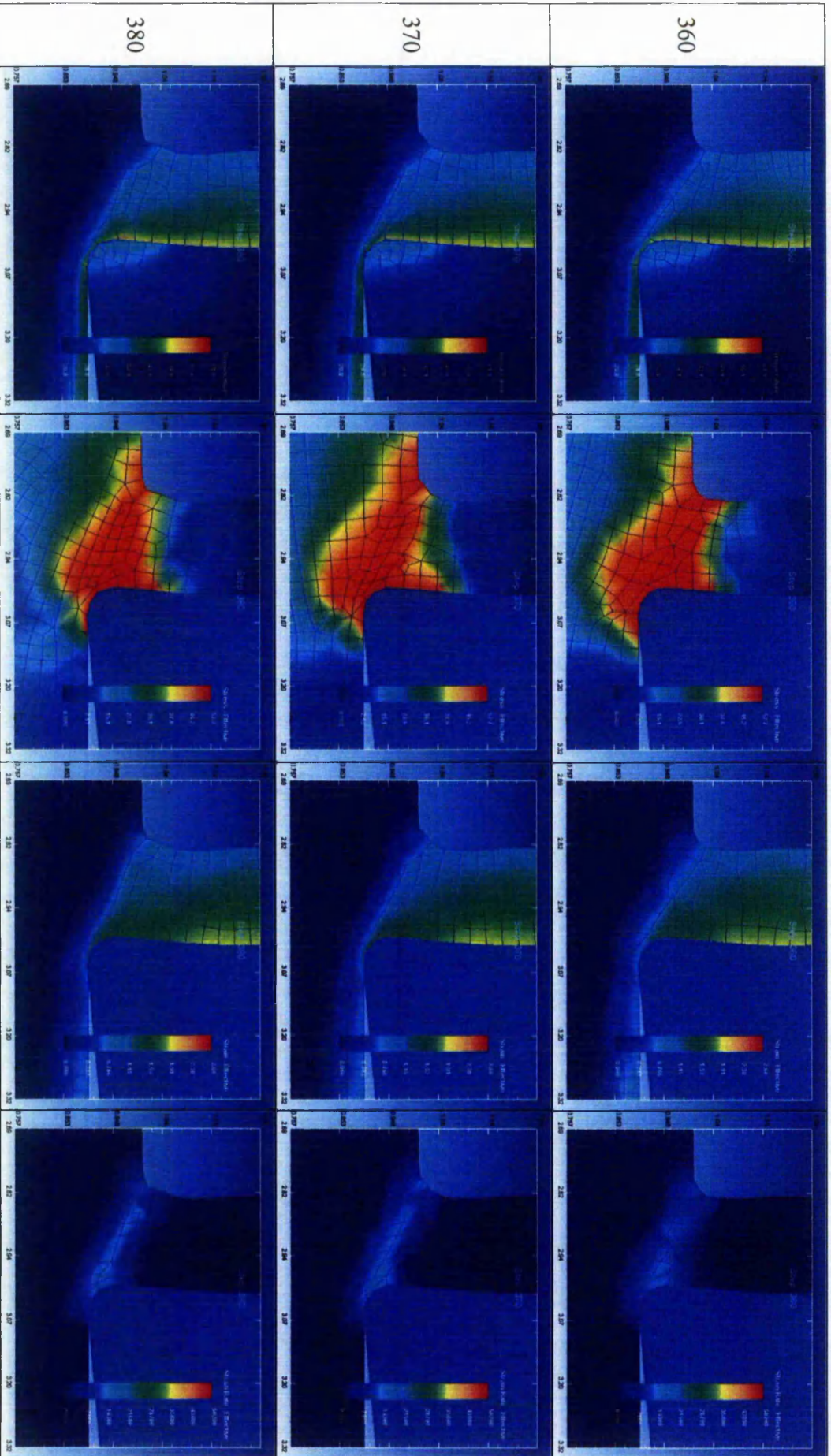








*Application of Conventional Machining Techniques for Green Ceramic Compacts produced by Powder Reaction Moulding*



*Application of Conventional Machining Techniques for Green Ceramic Compacts produced by Powder Reaction Moulding*

